

Durham E-Theses

*Synthesis, characterization and reactivity of
molybdenum and tungsten imido complexes of
relevance to alkene dimerization*

William R.H. Wright

How to cite:

Wright, William R.H. (2009) Synthesis, characterization and reactivity of molybdenum and tungsten imido complexes of relevance to alkene dimerization. Doctoral thesis, Durham University.

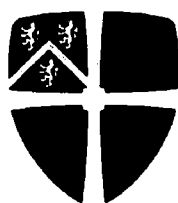
Use policy

The full-text may be used and/or reproduced, and given to third parties in any format or medium, without prior permission or charge, for personal research or study, educational, or not-for-profit purposes provided that:

- a full bibliographic reference is made to the original source
- a <https://etheses.durham.ac.uk/id/eprint/2030/> is made to the metadata record in Durham E-Theses
- the full-text is not changed in any way

The full-text must not be sold in any format or medium without the formal permission of the copyright holders.

Please consult the [full Durham E-Theses policy](#) for further details.



Durham
University

**Synthesis, Characterization and
Reactivity of Molybdenum and
Tungsten Imido Complexes of
Relevance to Alkene Dimerization**

**Thesis submitted for the Degree of Doctor of
Philosophy**

By

William R.H. Wright, M.Chem. (Durham)

**In the Department of Chemistry
Durham University**

The copyright of this thesis rests with the author or the university to which it was submitted. No quotation from it, or information derived from it may be published without the prior written consent of the author or university, and any information derived from it should be acknowledged.

January 2009



20 APR 2009

Statement

This thesis is based on work conducted by the author, in the Department of Chemistry at Durham University, during the period October 2005 to September 2008.

All work described in this thesis is original, unless otherwise acknowledged in the text or in the references. None of this work has been submitted for another degree in this or any other University.

Signed: William Wright

Date: 03/04/2009

William Wright

Abstract

Title: Synthesis, Characterization and Reactivity of Molybdenum and Tungsten Imido Complexes of Relevance to Alkene Dimerization

Author: William Wright

This thesis describes a range of investigations undertaken with the aim of increasing insight into alkene dimerization systems formed *via* reaction of WCl_6 and an aniline.

Chapter 1 introduces alkene dimerization systems based on reaction of WCl_6 with an amine and an Et_xAlCl_{3-x} co-initiator. As imido complexes are postulated to form *in situ* in such WCl_6 -based dimerization systems, the imido chemistry of group VI has briefly been reviewed. Finally the aims of this work are outlined.

Chapter 2 outlines a comparative investigation, examining the capacity of a range of discrete molybdenum and tungsten imido pre-catalysts to initiate ethylene dimerization. This has enabled for the first time direct comparison as to the relative activities of each type of imido complex. With the aim of establishing the nature of the initiator complex formed *in situ*, a range of discrete imido complexes were reacted with the co-initiators $EtAlCl_2$ and $Et_3Al_2Cl_3$ in the absence of any alkenes. Furthermore, the relative capacities of $EtAlCl_2$, $Et_3Al_2Cl_3$ and $EtMgCl$ to activate *mono(imido)* complexes for propylene and ethylene dimerization were assessed. Lastly, WCl_6 was reacted with an aniline using similar conditions to those employed in the preparation of WCl_6 -based initiator solutions.

Chapter 3 outlines the reactions of discrete *bis(imido)* chloride complexes with Me_xAlCl_{3-x} reagents. This study was undertaken with the aim of clarifying the mode by which *bis(imido)* complexes are activated for ethylene dimerization by the co-initiator $EtAlCl_2$. During this investigation a new class of complexes, with the general formula $M(N\{Ar\}AlMe_{(x-1)}Cl_{(3-x)}\{\mu-Cl\})(NAr)Me_2$ ($M = Mo$ or W) were discovered. These dimethyl compounds result from coordination of a Me_xAlCl_{3-x} ($x \geq 1$) fragment to an imido ligand. Furthermore, the reactivity of these new complexes with both Lewis bases and Lewis acids was examined. Finally, a number of ethylene dimerization systems were identified based on *bis(imido)* complexes.

Chapter 4 examines the reactivity of discrete *mono(imido)* chloride complexes with Me_xAlCl_{3-x} reagents. It was determined that in contrast to the *bis(imido)* complexes examined in Chapter 3, coordination of Me_xAlCl_{3-x} groups to *mono(imido)* ligands was disfavoured. Instead, a range of adducts were formed *via* coordination of Me_xAlCl_{3-x} fragments to tungsten chloride ligands. Next, attention turned to assessing the capacity of Me_xAlCl_{3-x} reagents to activate *mono(imido)* complexes for ethylene dimerization.

All the experimental details and supporting information and data for this thesis are presented in Chapter 5. In Chapter 6 further possible investigations are outlined.

Acknowledgements

I wish to thank my supervisor Dr. P.W. Dyer for his help, encouragement and patience. Thanks must also be extended to my collaborators Dr. M.J. Hanton and Professor R.P. Tooze of Sasol Technology UK Ltd for practical input and financial support. I also would like to thank Dr A.K. Hughes and Dr K.B. Dillon for helpful discussions. Furthermore, I must acknowledge Dr. A.S. Batsanov for obtaining molecular structures. I am also grateful for the assistance of Dr. A. Kenwright, Mr I. McKeag and Mrs C. Heffernan (NMR) as well Mrs L. Turner and Dr. M. Jones (MS). In addition I am indebted to Mrs J. Dorstal and Mrs J. Magee for providing combustion analysis.

I am appreciative of everyone I have worked with in Lab 101 during my time within the group. I especially wish to thank Carly, Shelly, Seb, Dan, Pippa and Lise for being great colleges. I am also grateful for the help of all my friends within the department, especially Helena, David and Scott. Furthermore, I am indebted to numerous non-chemistry friends for their encouragement and support. Finally, I wish to thank my family, without their help it would have not been possible for me to have written this thesis.

Contents

Abbreviations used in the text	i-ii
Chapter 1: Introduction	
1.0 The Significance of α -Olefin Manufacture and Dimerization	1
1.1 Alternate Mechanisms of Transition Metal-initiated Olefin Dimerization	3
1.2 Recently Developed Ethylene Dimerization Systems	7
1.3 Ethylene Trimerization Initiated by Homogeneous Chromium-based Initiators	11
1.4 Determining the Mechanism of a Chromium-based Ethylene Trimerization by Reaction of C_2D_4 and C_2H_4	12
1.5 Olefin Dimerization Systems Based on WCl_6	14
1.6 Examining the Selectivity of the WCl_6 Goodyear Dimerization System	17
1.7 Applications and Bonding Modes of Transition Metal Imido Complexes	18
1.8 Attempts to Spectroscopically Distinguish between Imido Bonding Modes	22
1.9 Molecular Orbital Description of Imido Complexes and Resulting Isolobal Relationships	23
1.9.1 Molecular Orbital Description of <i>mono</i> (imido) Complexes	23
1.9.2 Isolobal Relationships Between $[M(NR)_2]^{2-}$ ($M = Mo$ or W) and $[M(Cp)_2]^{2-}$ ($M = Zr$ or Hf) Complexes	25
1.10 Methods of Imido ligand Synthesis	26
1.11 Synthesis and Reactivity of Group VI Imido Complexes	27
1.11.1 Synthesis of Chromium Imido Complexes	27
1.11.2 Synthesis and Reactivity of Molybdenum Imido Complexes	29
1.11.3 Synthesis and Reactivity of Tungsten Imido Complexes	35
1.12 Synthesis and Reactivity of Tungsten and Molybdenum Diamine-chelated Complexes	37
1.13 Aims of this Thesis	44
1.14 References	45

Chapter 2: Evaluating the Ethylene Dimerization Capacity of Discrete Imido Complexes

2.0	Introduction	50
2.1	Synthesis and Characterization of the <i>bis</i> (Imido) Pre-catalysts $W(NAr)_2Cl_2 \cdot DME$ (40) and $Mo(NAr)_2(NH^tBu)_2$ (55)	52
2.1.1	Synthesis and Characterization of the Mixed <i>bis</i> (Imido) <i>bis</i> (Amido) Complex $Mo(NAr)_2(NH^tBu)_2$ (55)	52
2.1.2	Synthesis and Characterization of $W(NAr)_2Cl_2 \cdot DME$ (40) by Single Crystal X-Ray Diffraction Analysis	54
2.2	Ethylene Dimerization Systems Produced From Reaction of Imido Halide Complexes with the co-Initiators $EtAlCl_2$ and $B(C_6F_5)_3$	56
2.2.1	Activation of $W(NPh)(Cl)_2(PMe_3)_3$ (34) for Ethylene Dimerization	59
2.2.2	Dimerization Systems Based on Tantalum <i>mono</i> (Imido) Complexes	60
2.2.3	Reaction of $Mo(NAr)_2(NH^tBu)_2$ (55) with Me_3Al	60
2.3	Investigating the Reactivity of $EtAlCl_2$ and $Et_3Al_2Cl_3$ with <i>mono</i> - and <i>bis</i> (Imido) Complexes	61
2.3.1	Reaction of $EtAlCl_2$ and $Et_3Al_2Cl_3$ with <i>bis</i> (Imido) Complexes	61
2.3.2	Reaction of $W(NAr)_2Cl_2 \cdot DME$ (40) with $Et_3Al_2Cl_3$ and $EtAlCl_2$	62
2.3.3	Reaction of <i>mono</i> (Imido) Complexes with one Equivalent of $EtAlCl_2$	64
2.3.4	Reaction of <i>mono</i> (Imido) Complexes with Excess $EtAlCl_2$ and $Et_3Al_2Cl_3$	64
2.4	Micro-Scale Investigations Into <i>mono</i> (Imido)-based Alkene Dimerization Systems	66
2.5	Dimerization of C_2D_4 and C_2H_4 Using Systems Based Upon <i>mono</i> (Imido) Pre-catalysts	68
2.6	Assessing the Abilities of Grignard Reagents to Activate <i>mono</i> (Imido) Complexes	

	For Alkene Dimerization	70
2.7	Attempts to Investigate the Mode of Activation of <i>mono</i> (Imido)-Based Dimerization Systems Using C ₂ D ₄	72
2.8	Contrasting the Capacity of EtMgCl and EtAlCl ₂ to Co-Initiate Propylene Dimerization	73
2.8.1	Investigating the impact of Lewis acidity on <i>mono</i> (imido) based dimerization systems	74
2.9	Attempts to Identify any Imido Complexes Formed in the STUK WCl ₆ Dimerization System	76
2.10	Conclusions	78
2.11	References	78

Chapter 3: Reaction of Tungsten and Molybdenum *bis*(Imido) Complexes with Aluminium Methyl Reagents

3.0	Introduction	81
3.0.1	Reactions Group VI Imido Halide Complexes and Group VIII-based co-Initiators	83
3.1	Reaction of W(NAr) ₂ Cl ₂ .DME (40) and Me ₃ Al	84
3.1.1	Characterization of W(N{Ar}AlMe ₂ {μ-Cl})(NAr)Me ₂ (67) Using Single Crystal X-Ray Diffraction Analysis	86
3.2	Synthesis, Characterization and Structure of W(N{Ar}.AlMe ₂ {μ-Cl})(NAr)Me ₂ (67) and Comparison with Related Complexes	89
3.3	Reaction of M(NAr) ₂ Cl ₂ .DME (Mo or W) Complexes with Me ₂ AlCl and MeAlCl ₂	93
3.3.1	Synthesis of Mo(N{Ar}.AlMe ₂ {μ-Cl})(NAr)Me ₂ (76)	93
3.3.2	Reaction of W(NAr) ₂ Cl ₂ .DME (40) with Me ₂ AlCl	94
3.3.3	Reaction of M(NAr) ₂ Cl ₂ .DME (M = Mo or W) with MeAlCl ₂	95
3.3.4	Characterization of W(N{Ar}AlCl ₂ {μ-Cl})(NAr)Me ₂ (78) and Mo(N{Ar}.AlCl ₂ {μ-Cl})(NAr)Me ₂ (79) using Single Crystal X-ray Diffraction	97
3.4	Reaction of the Mixed <i>imido</i> Complex Mo(NAr)(N ⁱ Bu)Cl ₂ .DME (11) with Me ₃ Al and MeAlCl ₂	99
3.4.1	Reaction of Mo(NAr)(N ⁱ Bu)Cl ₂ .DME (11) with Me ₃ Al	99

3.4.2	Synthesis and Characterisation of Mo(N{Ar}.AlCl ₂ {μ-Cl})(N ^t Bu)Me ₂ (81)	100
3.5	Investigating the Reactivity of M(N{Ar}AlMe _(x-1) Cl _(3-x) {μ-Cl})(NAr)Me ₂ (M = W or Mo) Complexes	103
3.5.1	Reaction of W(N{Ar}AlMe ₂ {μ-Cl})(NAr)Me ₂ (67) with MeAlCl ₂	103
3.5.2	Reaction of M(N{Ar}AlMe ₂ {μ-Cl})(NAr)Me ₂ (Mo or W) with Lewis Bases	104
3.6	Reaction of Dialkyl Mo ^{VI} bis(Imido) Complexes with Me _x AlCl _(3-x)	106
3.7	Synthesis, Characterization and Reactivity of W(NAr) ₂ Me ₂ .THF (84)	108
3.7.1	Synthesis and Characterization of W(NAr) ₂ Me ₂ .THF (84)	109
3.7.2	Reaction of W(NAr) ₂ Me ₂ .THF (84) with Group 13 Compounds	113
3.8	Reaction of M(N{Ar}AlMe _x Cl _{2-x} {μ-Cl})(NAr)Me ₂ (Mo or W) with Ethylene	115
3.8.1	Reaction of W(N{Ar}AlMe ₂ {μ-Cl})(NAr)Me ₂ (67) and Mo(N{Ar}AlMe ₂ {μ-Cl})(NAr)Me ₂ (76) with Ethylene	115
3.8.2	Assessing the Capacity of Me ₂ AlCl to Activate W(NAr) ₂ Cl ₂ .DME (40) for Ethylene Dimerization	116
3.9	Reaction of W(NAr) ₂ Me ₂ .THF (84) and Mo(NAr) ₂ R ₂ (R = Me or CH ₂ CMe ₃) with Alkenes	118
3.9.1	Reaction of W(NAr) ₂ Me ₂ .THF (84) with Ethylene	118
3.9.2	Reaction of W(NAr) ₂ Me ₂ .THF (84) with Propylene	121
3.9.3	Reaction of Mo(NAr) ₂ Me ₂ (27) with Ethylene	122
3.9.4	Rationalizing the Different Reactivity of W(NAr) ₂ Me ₂ .THF (84) and Mo(NAr) ₂ Me ₂ (27) with Ethylene	122
3.9.5	Addition of Ethylene to Mo(NAr) ₂ (CH ₂ CMe ₃) ₂ (82)	123
3.10	Reaction of W(NAr) ₂ Me ₂ .THF (84) with a 1:1 Mixture of C ₂ D ₄ and C ₂ H ₄	124
3.11	Attempts to Synthesise Tungsten and Molybdenum Hydrides From Reaction of Discrete Imido Complexes	126
3.11.1	Treatment of Discrete Imido Complexes with HSiMe ₂ ^t Bu	126

3.11.2	Reaction of Discrete Imido Complexes with NaBH ₄	127
3.12	Summary and Conclusions	127
3.13	References	130

Chapter 4: Reaction of Tungsten *mono*(Imido) Chloride Complexes with Methyl Aluminium Reagents

4.0	Introduction	133
4.1	Reaction of W(NR)Cl ₄ .THF (R = Ph or Ar) with Me ₃ Al in C ₆ D ₆	135
4.2	Synthesis and Characterization of W(NR)(Cl)Me ₃ (96)	137
4.3	Reaction of W(NPh)(Cl)Me ₃ (96) with LiMe	139
4.3.1	Reaction of W(NPh)(Cl)Me ₃ (96) with Me ₃ SiOSO ₂ CF ₃	140
4.3.2	Reaction of W(NPh)Me ₃ (OSO ₂ (CF ₃)) (100) with Ethylene	141
4.4	Reaction of W(NR)(Cl)Me ₃ (R = Ph, Ar) with [Li(OEt ₂) ₂][B(C ₆ F ₅) ₄] and [Na][B(3,5-(CF ₃) ₂ C ₆ H ₃)]	142
4.5	Investigation of the Reactivity of W(NR)(Cl)Me ₃ (R = Ph and Ar) with the Lewis Acid MeAlCl ₂	145
4.6	Investigating the Interaction Between MeAlCl ₂ and W(NPh)(Cl)Me ₃ (96) in Solution	151
4.6.1	Investigating the Interaction of W(NPh)(Cl)Me ₃ (96) with MeAlCl ₂ at Low Concentrations	153
4.7	Activation of <i>mono</i> (Imido) Tetrahalide pre-Catalysts Using Me _x AlCl _{3-x} co-Initiators	155
4.8	Activation of <i>mono</i> (Imido) Tetrahalide pre-Catalysts with Me ₃ Al	155
4.8.1	Examining the Route of Methane Formation in the W(NR)Cl ₄ .THF/Me ₃ Al Dimerization Systems	157
4.8.2	Contrasting the Abilities of the Lewis Acids MeAlCl ₂ , Me ₂ AlCl, Me ₃ Al to co-Initiate Ethylene Dimerization	158
4.8.3	Evaluating the Role of Adduct Formation in Me _x AlCl _{3-x} co-Initiated Dimerization Systems	159
4.9	Summary and Conclusions	161
4.10	References	162

Chapter 5: Experimental

5.0	Introduction	164
5.1	General Procedure for the Preparation of Ethylene Dimerization Systems Based on the Reaction of Imido Complexes	165
5.2	Synthesis of $W(NAr)_2Cl_2 \cdot DME$ (40)	165
5.3	Synthesis of $Mo(NAr)_2(NH^tBu)_2$ (55)	166
5.4	Reaction of $Mo(NAr)_2(NH^tBu)_2$ (55) with Me_3Al	166
5.5	Reaction of $W(NPh)(Cl)_2(PMe_3)_3$ (34) with Me_3Al	166
5.6	Reaction of $Mo(N^tBu)_2Cl_2 \cdot DME$ (26) with One Equivalent of $EtAlCl_2$	167
5.7	Synthesis of $Mo(N^tBu)_2Cl_2 \cdot PPh_3$ (60)	167
5.8	Reaction of $Mo(N^tBu)_2Cl_2 \cdot DME$ (26) with PPh_3	168
5.9	Reaction of $Mo(N^tBu)_2Cl_2$ (26) and Excess $EtAlCl_2$	168
5.10	Reaction of $W(NAr)_2Cl_2 \cdot DME$ (40) with $EtAlCl_2$	168
5.11	Reaction of $W(NAr)_2Cl_2 \cdot DME$ (40) with $Et_3Al_2Cl_3$	169
5.12	Synthesis of $EtAlCl_2 \cdot (THF)_2$	169
5.13	Reaction of $W(NPh)Cl_4 \cdot THF$ (32) with One Equivalent of $EtAlCl_2$	169
5.14	Reaction of $W(NPh)Cl_4 \cdot THF$ (32) with $Et_3Al_2Cl_3$	170
5.15	Reaction of $W(NPh)Cl_4 \cdot THF$ (32) with $EtAlCl_2$	170
5.15.1	Reaction of $Ta(NAr)Cl_3(TMEDA)$ (59) with $EtAlCl_2$	170
5.16	Activation of $W(NAr)Cl_4$ (62) using $Et_3Al_2Cl_3$ and Subsequent Propylene Dimerization	170
5.17	Activation of $W(NAr)Cl_4 \cdot THF$ (38) using $Et_3Al_2Cl_3$ and $EtAlCl_2$ and Subsequent Ethylene Dimerization/Oligomerization	170
5.18	Dimerization of C_2D_4 and C_2H_4 (1:1) using $W(NAr)Cl_4 \cdot THF$ (38)	171
5.19	Activation of $W(NAr)Cl_4$ (62) using $EtMgCl$ and Subsequent Ethylene Dimerization	171
5.20	Attempts to Activate $W(NAr)Cl_4$ (62) for Ethylene Dimerization using $MeMgCl$ and Mg	171
5.21	Activation of $W(NAr)Cl_4 \cdot THF$ (38) with $Et_3Al_2Cl_3$ and Subsequent C_2D_4 Dimerization	172

5.22	Activation of W(NAr)Cl ₄ .THF (38) for Propylene Dimerization	172
5.23	Addition of Ethylene and Propylene to EtAlCl ₂	172
5.24	Reaction of WCl ₆ with Et ₃ N and H ₂ NR (R = Ph or Ar)	173
5.25	Reaction of W(NPh)Cl ₄ .THF (32) with H ₂ NAr	173
5.26	Reaction of W(NAr)Cl ₄ .THF (38) with Et ₃ N and H ₂ NAr	173
5.27	Reaction of W(NAr) ₂ Cl ₂ .DME with Me ₃ Al in C ₆ D ₆ : Generation of W(N{Ar}AlMe ₂ {μ-Cl})(NAr)Me ₂ (67) <i>in situ</i>	174
5.28	Addition of Ethylene to W(N{Ar}AlMe ₂ {μ-Cl})(NAr)Me ₂ (67)	175
5.29	Synthesis of Mo(N{Ar}AlMe ₂ {μ-Cl})(NAr)Me ₂ (76)	175
5.30	Attempted Reaction of Mo(N{Ar}AlMe ₂ {μ-Cl})(NAr)Me ₂ (76) with Ethylene	176
5.31	Reaction of W(NAr) ₂ Cl ₂ .DME (40) with Me ₂ AlCl in C ₆ D ₆ : Generation of W(N{Ar}AlMeCl{μ-Cl})(NAr)Me ₂ (77) and Additional Products <i>in situ</i>	176
5.32	Activation of W(NAr) ₂ Cl ₂ .DME (40) by MeAlCl ₂ for Ethylene Dimerization	177
5.33	Reaction of W(NAr) ₂ Cl ₂ .DME (40) with MeAlCl ₂ in C ₆ D ₆ : Generation of W(N{Ar}AlCl ₂ {μ-Cl})(NAr)Me ₂ (78) <i>in situ</i>	177
5.34	Synthesis of Mo(N{Ar}AlCl ₂ {μ-Cl})(NAr)Me ₂ (79) from Reaction of MeAlCl ₂ and Mo(NAr) ₂ Cl ₂ .DME	178
5.35	Reaction of Mo(NAr)(N ^t Bu)Cl ₂ .DME (11) with Me ₃ Al: Generation of MoN{Ar}AlMe ₂ {μ-Cl})(N ^t Bu)Me ₂ (80) <i>in situ</i>	179
5.36	Synthesis of MoN{Ar}AlCl ₂ {μ-Cl})(N ^t Bu)Me ₂ (81)	180
5.37	Reaction of WN{Ar}AlMe ₂ {μ-Cl})(N ^t Bu)Me ₂ (67) with MeAlCl ₂ : generation of WN{Ar}AlMeCl{μ-Cl})(N ^t Bu)Me ₂ (77) <i>in situ</i>	181
5.38	Reaction of Mo(NAr) ₂ (CH ₂ C(CH ₃) ₃) ₂ (82) with MeAlCl ₂	181
5.39	Addition of Me ₃ Al to Mo(NAr) ₂ (CH ₂ C(CH ₃) ₃) ₂ (82)	181
5.40	Attempted Reaction of Mo(NAr) ₂ Me ₂ (27) with Me ₃ Al	182
5.41	Reaction of Mo(NAr) ₂ Me ₂ (27) with MeAlCl ₂ : Formation of Mo(N{Ar}AlMeCl{μ-Cl})(NAr)Me ₂ (83) <i>in situ</i>	182
5.42	Reaction of Mo(N{Ar}AlMe ₂ {μ-Cl})(NAr)Me ₂ (76) with PMe ₃ , NEt ₃ , and NEt ₃ Cl	183
5.43	Reaction of W(N{Ar}AlMe ₂ {μ-Cl})(NAr)Me ₂ (67) with NEt ₃	184
5.44	Reaction of W(NAr) ₂ Cl ₂ .DME (40) with MeMgBr	184

5.45	Synthesis of $W(NAr)_2Me_2 \cdot THF$ (84)	185
5.46	Synthesis of $W(NAr)_2Me_2 \cdot PMe_3$ from reaction of $W(NAr)_2Me_2 \cdot THF$ (84) and PMe_3	186
5.47	Addition of $B(C_6F_5)_3$ to $W(NAr)_2Me_2 \cdot THF$ (84)	186
5.48	Reaction of $[Ph_3C][B(C_6F_5)_4]$ with $W(NAr)_2Me_2 \cdot THF$ (84)	187
5.49	Addition of $[PhNMe_2H][B(C_6F_5)_4]$ to $W(NAr)_2Me_2 \cdot THF$ (84)	187
5.50	Reaction of $W(NAr)_2Cl_2 \cdot DME$ (40) with MAO	187
5.51	Reaction of $W(NAr)_2Me_2 \cdot THF$ (84) with Ethylene and Propylene	187
5.52	Reaction of $Mo(NAr)_2Me_2$ (27) and $Mo(NAr)_2(CH_2C(CH_3)_3)_2$ (82) with Ethylene	188
5.53	Reaction of $W(NAr)_2Me_2 \cdot THF$ (84) with C_2D_4 and C_2H_4	188
5.54	Addition of $HSiMe_2^tBu$ to Discrete Imido Complexes	188
5.55	Reaction of $W(NAr)_2Cl_2 \cdot DME$ (40) with $NaBH_4$	189
5.56	Addition of $NaBH_4$ to $W(NAr)Cl_4 \cdot THF$ (38) and $W(NPh)(Cl)_2(PMe_3)_3$ (34)	189
5.57	Reaction of $W(NPh)Cl_4 \cdot THF$ (38) with Me_3Al	189
5.58	Reaction of $W(NAr)Cl_4$ (62) and $W(NAr)Cl_4 \cdot THF$ (38) with Me_3Al in C_6D_6	190
5.59	Synthesis of $W(NPh)(Cl)Me_3$ (96) <i>via</i> Reaction of Me_3Al	190
5.60	Synthesis of $W(NAr)(Cl)Me_3$ (97) <i>via</i> Reaction of Me_3Al with $W(NAr)Cl_4$ (62)	191
5.61	Synthesis of complex (97) <i>via</i> Reaction of $W(NAr)Cl_4 \cdot THF$ (38) and Me_3Al	191
5.62	Reaction of $Ta(NAr)Cl_3(TMEDA)$ (59) with Me_3Al	191
5.63	Reaction of $W(NPh)(Cl)Me_3$ (96) with $LiMe$	192
5.64	Reaction of $W(NPh)(Cl)Me_3$ (96) with $Me_3SiOS(O)_2CF_3$: Generation of $W(NPh)Me_3(OSO_2(CF_3))$ (100)	192
5.65	Reaction of $W(NPh)(Cl)Me_3$ (96) with $[Na][B(3,5-(CF_3)_2-C_6H_3)_4]$ in $MeCN$	192
5.66	Reaction of $W(NAr)(Cl)Me_3$ (97) with $[Li(OEt)_2][B(C_6F_5)_4]$	193
5.67	Reaction of $W(NAr)(Cl)Me_3$ (97) with $[Na][B(3,5-(CF_3)_2-C_6H_3)_4]$	193
5.68	Reaction of $W(NPh)(Cl)Me_3$ (96) with $[Na][B(3,5-(CF_3)_2-C_6H_3)_4]$	194
5.69	Synthesis and Characterization of $[W(NPh)(Cl)Me_3 \cdot AlCl_3]$ (104)	194

5.70	Synthesis and Characterization of $[W(NAr)(Cl)Me_3 \cdot AlCl_3]$ (105)	195
5.71	Characterization of $[AlCl_4][P(N^iPr_2)_2]$ (107) using ^{27}Al NMR Spectroscopy	195
5.72	Reaction of $W(NPh)(Cl)Me_3$ (96) with $MeAlCl_2$ in C_6D_6	195
5.72.1	Reaction of $W(NPh)(Cl)Me_3$ (96) with $MeAlCl_2$ in C_6D_6 at Low Dilutions	196
5.72.2	Dilution of a $W(NPh)(Cl)Me_3/MeAlCl_2$ Reaction Solution	196
5.73	Catalytic Ethylene Dimerization Testing using $W(NR)Cl_4 \cdot THF$ ($R = Ph, Ar$) and Me_3Al	197
5.73.1	Addition of Ethylene to Me_3Al	197
5.73.2	Addition of Ethylene to $W(NPh)(Cl)Me_3$ (96)	197
5.73.3	Analysis of Me_3Al in CD_2Cl_2	197
5.74	Reaction of $W(NAr)Cl_4 \cdot THF$ (38), Me_3Al and C_2D_4	198
5.75	Activation of $W(NPh)(Cl)Me_3$ (96) for Ethylene Dimerization using Me_3Al	198
5.76	Activation of $W(NPh)(Cl)Me_3$ (96) for ethylene dimerization using Me_2AlCl or $MeAlCl_2$	198
5.77	Using $MeAlCl_2$ to activate $W(NPh)Cl_4 \cdot THF$ (32) for Ethylene Dimerization	199
5.78	References	199

Chapter 6: Further Work

6.1	Hex-1-ene Dimerization	201
6.2	Further Ethylene Dimerization Studies	201
6.3	Potential DFT Calculations	202
6.3.1	Examining the Reaction of $M(NAr)_2Me_2$ ($M = Mo$ or W) Complexes With Ethylene	202
6.3.2	Examining the $W(NAr)_2Me_2 \cdot THF$ (84) C_2D_4/C_2H_4 Reaction	202
6.3.3	Examining the Solution Structure of $[W(NR)(Cl)Me_3 \cdot AlCl_3]$ ($R = Ph$ or Ar) Adducts	203
6.4	References	203

Appendixes

204-212

Abbreviations used in the text

Ar = 2,6-Diisopropylphenyl

Bu^t = *tert*-Butyl

Bz = Benzyl

COSY = Correlated Spectroscopy

CP MAS NMR = Cross-Polarised Magic Angle Spinning NMR

Cp = C₅H₅

Cp* = C₅Me₅

CSD = Cambridge Structural Database

Cy = Cyclohexyl

DCM = Dichloromethane

DEPT = Distortionless Enhancement by Polarisation Transfer

DME = 1,2-Dimethoxyethane

DPPE = Diphenyl Phosphino Ethane

EI = Electron Ionisation

ES = Electrospray

Et = Ethyl

FMES = 2,4,6 tris(trifluoromethyl) phenyl

GC = Gas Chromatography

GCMS = Gas Chromatography Mass Spectrum

h = hour

hh = head-to-head olefin dimerization product

HOMO = Highest occupied Molecular Orbital

ht = head-to-tail olefin dimerization product

LUMO = Lowest Unoccupied Molecular Orbital

M = Generic transition metal, unless otherwise stated.

MAO = Methylaluminoxane

MAS = Magic Angle Spinning

Me = Methyl

MMAO = Modified Methylaluminoxane

MMA = Methyl Methacrylate

MO = Molecular Orbital

MS = Mass Spectrometry

m/z = Mass/charge ratio

NMR = Nuclear Magnetic Resonance

NOESY = Nuclear Overhauser Effect Spectroscopy

OTf = Triflate

Ph = Phenyl

ppm = parts per million

ⁱPr = isopropyl

Py = Pyridine

R = Generic alkyl, aryl group

SHOP = Shell Higher Olefin Process

STUK = Sasol Technology UK Ltd

THF = Tetrahydrofuran

th = tail-to-head olefin dimerization product

TMEDA = *N,N,N',N'*-Tetramethylethylenediamine

TOF = Turnover Frequency

TON = Turnover Number

Tos = Tosylate

tt = tail-to-tail olefin dimerization product

VT NMR = Variable Temperature Nuclear Magnetic Resonance Spectroscopy

wt = weight %

XPS = X-ray photoelectron Spectroscopy

NMR Abbreviations

δ = chemical shift (in ppm)

b = broad signal

(s) = singlet

(d) = doublet

(t) = triplet

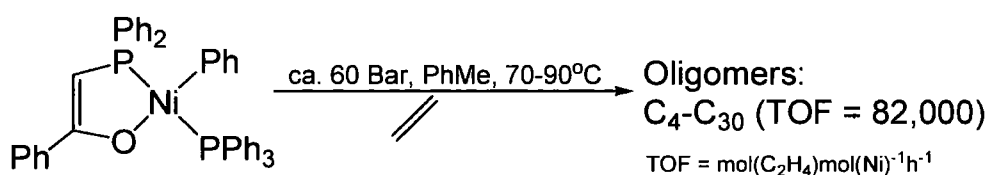
(m) = complex multiplet

Chapter 1 Introduction

1.0 The Significance of α -Olefin Manufacture and Dimerization

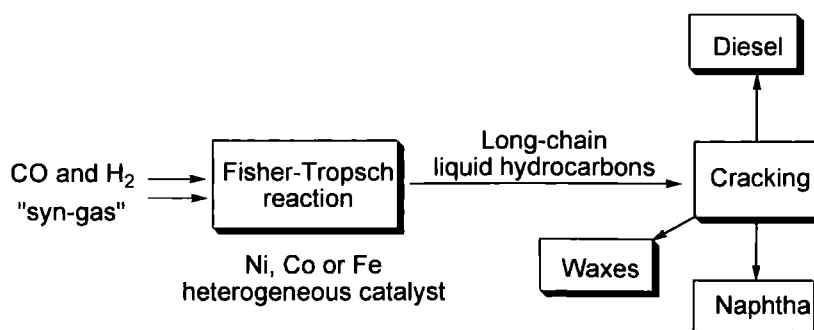
The production of α -olefins is of great industrial significance providing the raw materials for a range of applications, including, the manufacture of synthetic lubricants and surfactants. Furthermore, α -olefins have found application as monomers (particularly as co-monomers in polyethylene), with 10^8 tons of polyolefins being consumed world wide per year.¹ α -Olefins are produced in a number of ways: the cracking and dehydrogenation of paraffins; from CO and H₂ via the Fischer-Tropsch process; dehydration of alcohols; electrolysis of straight chain C₃-C₃₀ carboxylic acids; dimerization and metathesis of olefins; and oligomerization of ethylene, the latter being the main method used for the production of C₉-C₃₀ olefins.² One important industrial processes by which linear α -olefins are produced via ethylene oligomerization is the Shell Higher Olefin Process (SHOP), in which nickel-based homogeneous catalysts are employed (**Scheme 1.1**).³

Scheme 1.1 Ethylene oligomerization via SHOP-type nickel-based pre-initiators



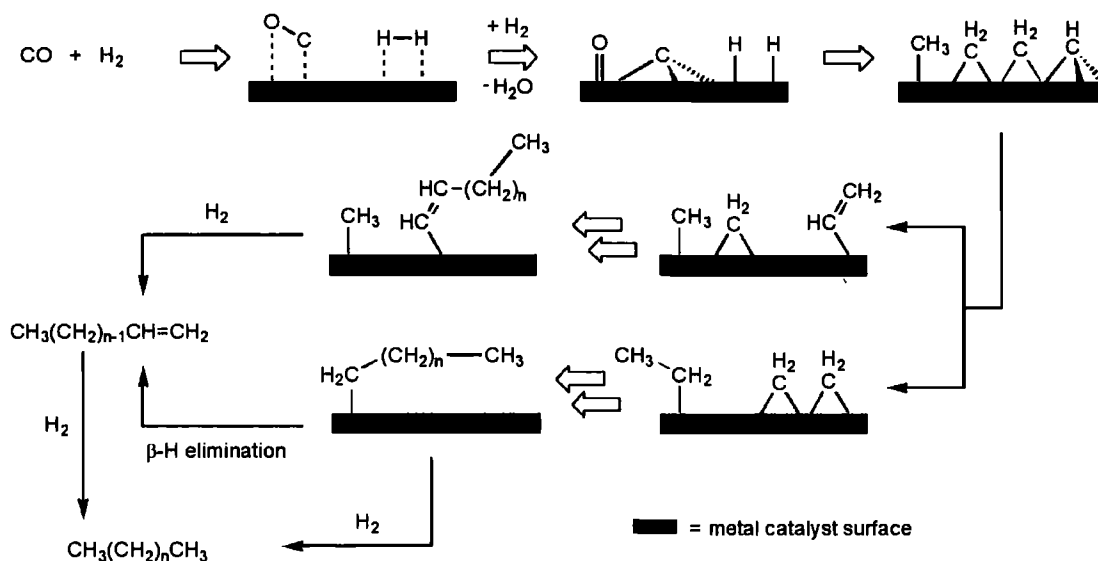
Of significance is that ethylene oligomerization, via the SHOP and related processes, exclusively produces olefins containing even numbers of carbon atoms. This is in contrast to the Fischer-Tropsch process (**Scheme 1.2**) in which olefins are obtained from a C₁ unit ("syn-gas"), resulting in the formation of both odd- and even-numbered olefin products.^{4,5}

Scheme 1.2 The Fisher-Tropsch process



The conversion of CO and H₂ into hydrocarbons *via* the Fischer-Tropsch reaction requires that the C-O bond of carbon monoxide is first broken, which occurs upon the surface of a heterogeneous catalyst. This is followed by C-H and C-C bond formation steps. Next, hydrogenolysis occurs, followed by hydrogenation forming a hydrocarbon which then dissociates from the metal surface (**Scheme 1.3**).⁶

Scheme 1.3 Simplified mechanism of hydrocarbon formation in the Fischer-Tropsch process



Fischer-Tropsch synthesis is of great commercial importance, with South Africa alone using the process to manufacture approximately four million tonnes of hydrocarbon products a year.⁷ Depending on the reaction conditions, up to 25% of the material produced by Fischer-Tropsch synthesis can be comprised of C₂-C₄ olefins. Often the uses of these light products is restricted, for instance there is a limit to the amount of short chain hydrocarbons that can be accommodated in motor gasoline (which consists mainly of C₅-C₁₀ molecules). As such olefin dimerization or oligomerization provides a means to convert C₂-C₄ olefins into heavier products that can be included in liquid fuels.⁸

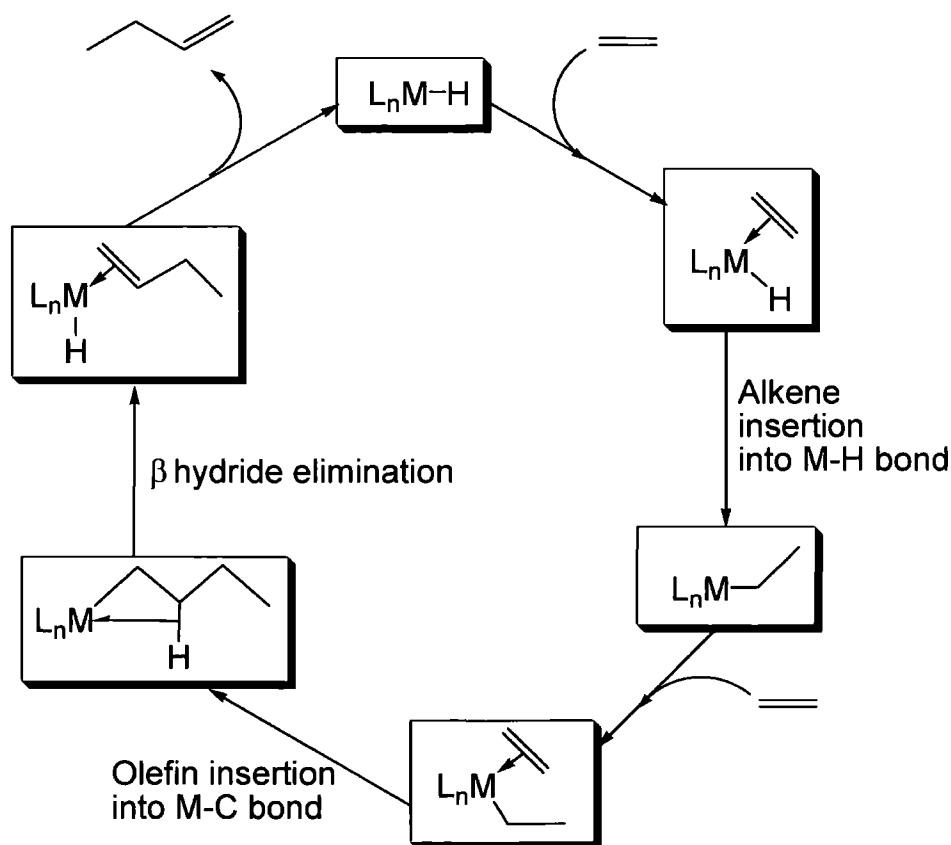
Significantly, industrial processes, optimised to convert even-numbered olefins, into commercial products cannot readily utilize the odd-numbered olefins produced *via* Fischer-Tropsch synthesis. This is because odd-numbered olefins tend to have lower boiling points than those found for related even-number olefins.⁹ Hence, for a given process switching from an even-numbered to an odd-numbered olefin feedstock could potentially require significant plant re-engineering (e.g. the redesigning of distillation columns). Thus, dimerization of odd-numbered olefins has

the potential to produce heavier even-numbered olefins, compatible with optimised industrial processes that are based on the more common even-numbered olefins derived from ethylene.

1.1 Alternate Mechanisms of Transition Metal-initiated Olefin Dimerization

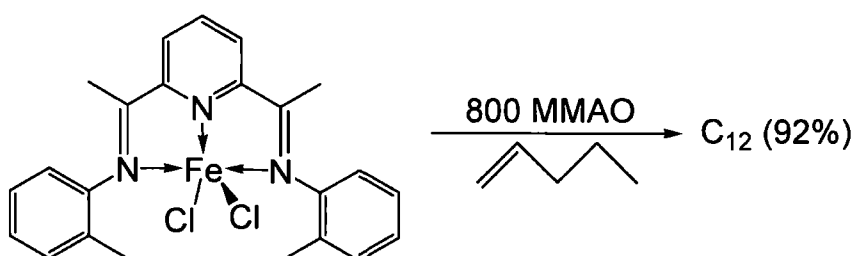
Dimerization of olefins by transition metal catalysts can proceed via one of three general mechanisms: degenerate polymerization, concerted coupling, or reductive dimerization.¹⁰ Degenerate polymerization, also referred to as the hydride cycle, (**Scheme 1.4**) is initiated by coordination of an olefin to a metal hydride, followed by formation of a metal-alkyl species via migratory insertion. Propagation and termination are achieved by sequential coordination and insertion (into the newly formed metal-carbon bond) of a second olefin, followed by reformation of the metal-hydride species by β -hydride elimination. Dissociation of the newly formed olefin then regenerates the metal initiator complex. A catalyst selective for olefin dimerization, not oligomerization, is obtained when the rate of termination exceeds the rate of propagation.

Scheme 1.4 General mechanism for ethylene dimerization via a hydride cycle



An example of an initiator known to dimerize α -olefins *via* a hydride cycle has been published by Small *et al.*¹¹ In Small's dimerization system pyridine *bis*(imine) ligands are coordinated to FeCl_2 , giving a family of complexes, which when treated with excess MMAO (800 equivalents)ⁱ can initiate but-1-ene or hex-1-ene dimerization, in high activity and selectivity for linear head-to-head products (**Scheme 1.5**).

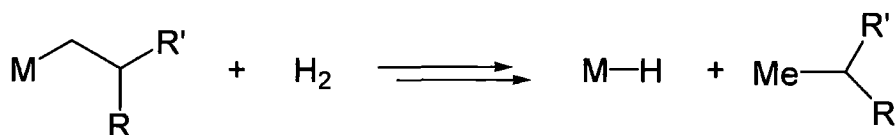
Scheme 1.5 Pyridine *bis*(imine) Fe^{II} -based hex-1-ene dimerization systems



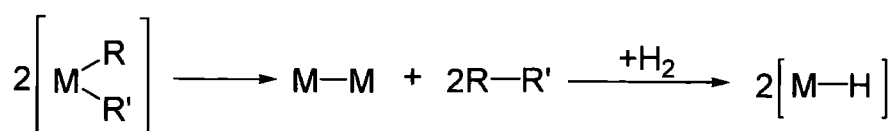
An alternative means of achieving olefin dimerization is through reductive dimerization (**Scheme 1.6**). This process is observed when a metal alkyl complex is exposed to a pressure of H_2 gas or a reducing agent.¹² It is reasoned that reductive dimerization occurs *via* one of two potential pathways, with the reducing agent acting as either a chain transfer agent (**Scheme 1.6, Pathway A**) or as a hydride source (**Scheme 1.6, Pathway B**).

Scheme 1.6 Proposed mechanisms of reductive dimerization (R or R' = alkene moieties)

Pathway A



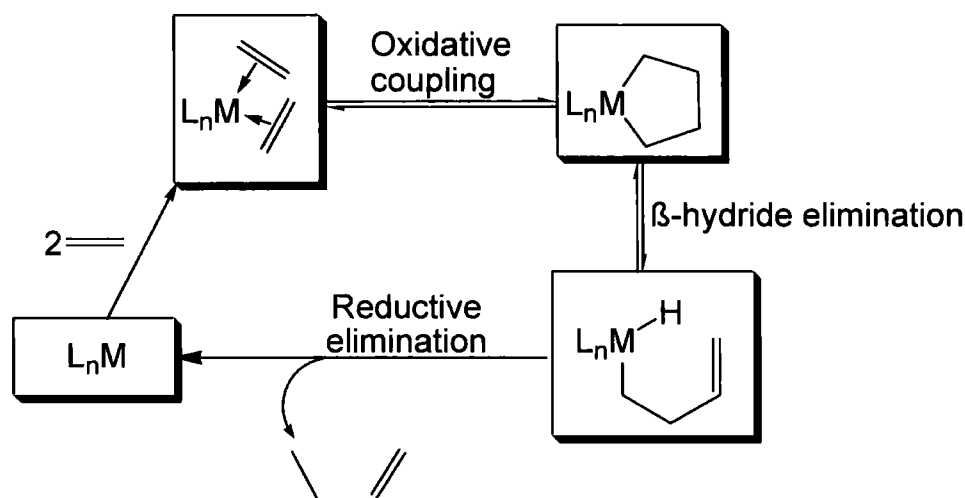
Pathway B



ⁱ MMAO = Modified methylalumoxane (25% of methyl groups replaced by isobutyl)

The third olefin dimerization methodology commonly used is concerted coupling. Here, dimerization is initiated by coordination of two olefins to a electronically and coordinatively unsaturated metal centre and is followed by the generation of a metallacycle *via* oxidative coupling. Termination results from β -hydride elimination, followed by reductive elimination of the olefin (**Scheme 1.7**).

Scheme 1.7 General mechanism of concerted coupling – *via* metallacycle formation

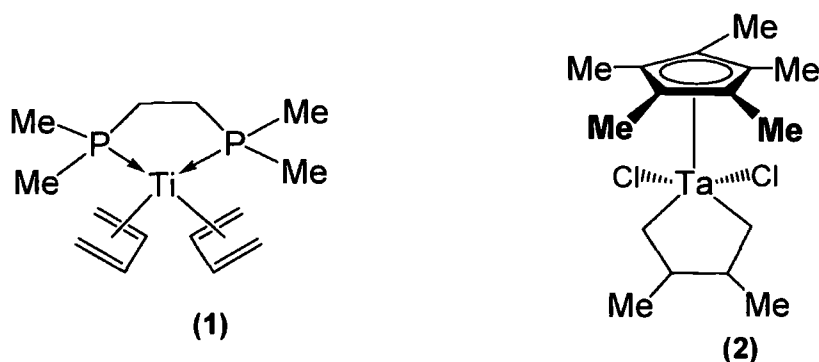


One potential advantage associated with olefin dimerization *via* a concerted coupling mechanism, when contrasted with many degenerate polymerization initiators, would be no observable isomerization, which would enable both high selectivity and activity. Also, for processes that operate *via* a concerted coupling mechanism, high selectivity for the dimerization product is often obtained (although trimerization of ethylene proceeds *via* a related mechanism,¹³ the formation of metallacyclo-heptane intermediates is disfavoured in many systems).¹⁴

In order for the concerted coupling mechanism to be effective, for dimerization there must be a sufficiently low energy barrier for a five-membered metallacycle to undergo β -hydride elimination. This is often believed to be disfavoured since five-membered rings are considered to be stabilized due to the chelate effect. Furthermore, the conformation of a five membered ring tends to orientate the β -hydrogen away from the metal, disfavoring β -hydride elimination. However, recent B3LYP density functional calculations on 16-electron ruthenium metallacycle complexes indicate that β -hydride eliminations from a five membered ring can in fact occur relatively readily.¹⁵ Indeed, many examples of early transition metal systems that are believed to catalyze the dimerization of olefins *via* a

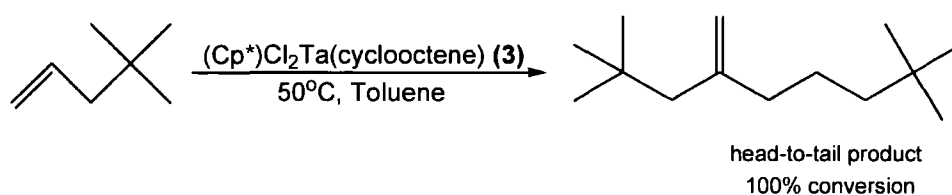
concerted coupling mechanism are known, including those based on titanium butadiene **(1)**¹⁶ and tantalocyclopentate **(2)**¹⁷ complexes (**Figure 1.1**).

Figure 1.1 Early transition metal dimerization initiators operating via a concerted coupling pathway

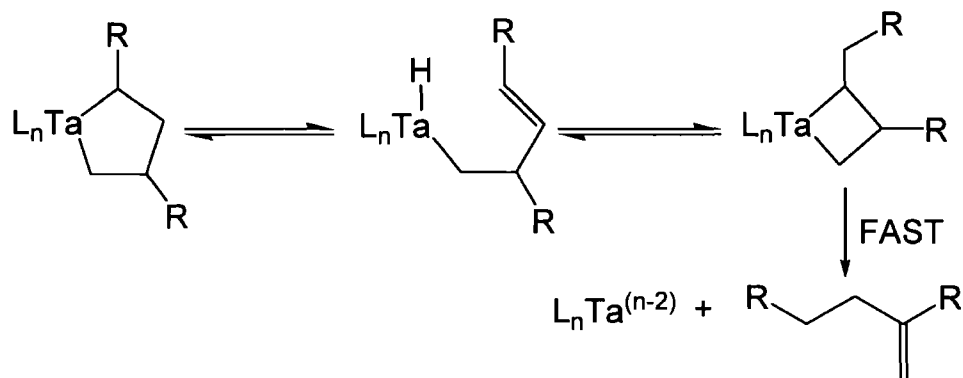


Variations of complex **2** have been reported such as $(Cp^*)Cl_2Ta(\text{cyclooctene})$ **(3)** ($Cp^* = \eta^5-C_5Me_5$), which also readily dimerizes olefins. Of significance is that when complex **3** initiates dimerization of 4,4-dimethyl-1-pentene, complete selectivity for the head-to-tail (ht) dimerization product 2,2,7,7-tetramethyl-3-methyleneoctane is obtained (**Scheme 1.8**).¹⁸

Scheme 1.8 Dimerization of 4,4-dimethyl-1-pentene



The mechanism by which the tantalum based pre-catalysts **2** and **3** initiate olefin dimerization has been examined through the use of deuterium labelling study on model systems. This determined that olefin dimerization is initiated by the formation of a tantalacyclopentane ring, which then contracts via a hydride intermediate to give a metallocyclobutane. Fast degradation of the metallocyclobutane then liberates the product olefin (**Scheme 1.9**).

Scheme 1.9 Concerted coupling via a Ta metallocyclobutane

The formation of head-to-tail products in dimerization systems based upon complexes **2** and **3** is attributed to catalysis proceeding *via* formation of α,β -disubstituted metallacycles in preference to the α,α -analogues, which would result in tail-to-tail products. Thus, selectivity for the head-to-tail dimerization product can be attributed to carbon-carbon bond formation *via* a metallacycle intermediate, characteristic of a concerted coupling mechanism.

1.2 Recently Developed Ethylene Dimerization Systems

A number of ethylene dimerization systems in which nickel complexes are employed as pre-catalysts have recently been reported. Le Floch *et al.* has synthesised a new family of N-P ligands containing a phosphino group and an iminophosphorane moiety.¹⁹ These ligands readily react with $\text{NiBr}_2\cdot\text{DME}$ to give a family of complexes (**4-5**) which when treated with MAO give highly active ethylene dimerization initiators (**Figure 1.2** and **Table 1.1**)

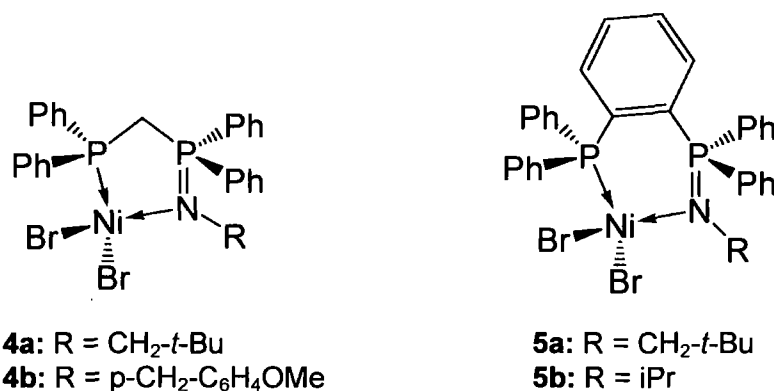
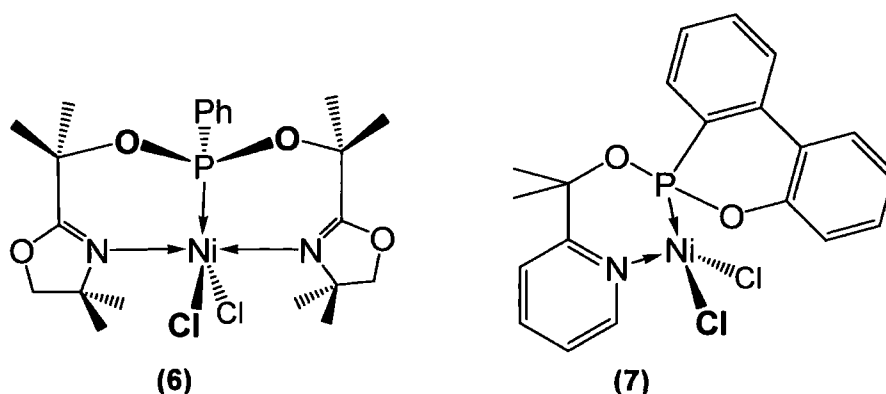
Figure 1.2 P-N Nickel(II) ethylene dimerization pre-catalysts

Table 1.1 Ethylene Oligomerization by complexes **4-5**^a

Pre-Catalyst	TOF × 10 ⁻³ ^(b)	C ₄ (%) [1-C ₄ (%)]	C ₆ (%) [1-C ₆ (%)]
4a	45.3	93.9 [83.4]	6.1 [32.7]
4b	65.8	92.8 [77.0]	7.2 [29.4]
5a	96.7	96.3 [67.5]	3.7 [39.8]
5b	106.5	97.7 [61.4]	2.3 [73.9]

a) Conditions: $T = 45^{\circ}\text{C}$, 30 bar ethylene, 1 h reaction time, 0.02 mmol Ni complex, 6 mmol MAO, solvent: toluene (30 mL). b) TOF = mol ethylene consumed per mol of Ni per hour ($\text{mol}^{-1}\text{mol}^1\text{h}^{-1}$).

Of note is that for all four systems outlined in **Table 1.1**, high selectivity for C₄ dimerization products were obtained. Also of significance are the high activities of the initiator solutions, particularly those of **5a** and **5b**. Indeed, Le Floch states that **5b** gives one of the most active dimerization systems that have currently been reported. In a related study, Braunstein *et al.* have also mixed donor P-N ligands to synthesise nickel complexes with oxazoline (**6**) or pyridine-phosphonite (**7**) donors (**Figure 1.3**).²⁰

Figure 1.3 Nickel-based ethylene dimerization pre-catalysts

The ability of the pre-catalysts **6** and **7** to dimerize ethylene after treatment with EtAlCl₂ or MAO was assessed. It was determined that increasing the moles of co-initiator (EtAlCl₂ or MAO) in the systems based on **6** and **7** simultaneously resulted in a marked increase in initiator activity, but a significant decrease in initiator selectivity (**Table 1.2**). A higher selectivity for C₄ products was obtained when MAO was

employed as a co-initiator. In contrast, the highest TOFs were obtained when EtAlCl_2 was used.

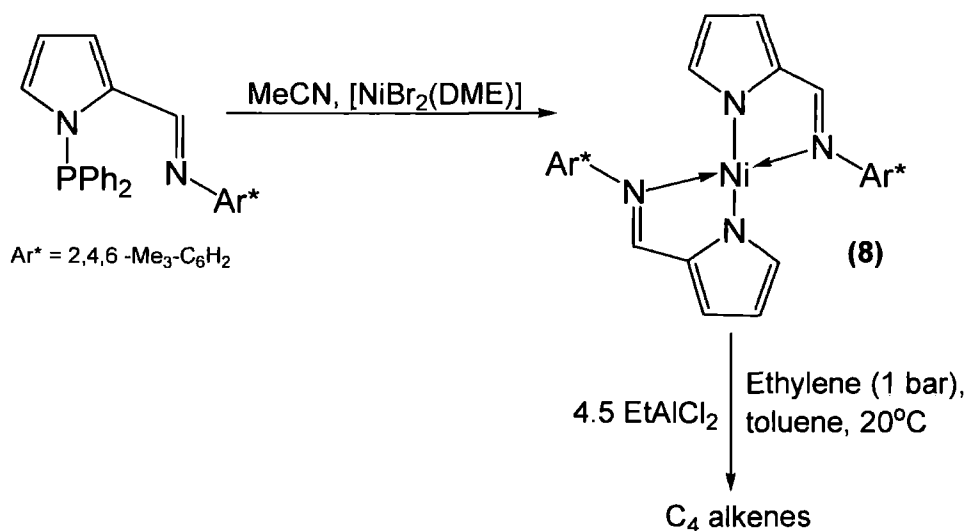
Table 1.2 Ethylene dimerization using the pre-catalysts **6** and **7**

Pre-Catalyst	Activator [eq]	Selectivity C_4 (%)	TOF ($\text{mol C}_2\text{H}_4/\text{mol Ni/ h}$)
6	EtAlCl_2 [2] ^a	76	12,700
6	EtAlCl_2 [6] ^a	70	31,400
7	EtAlCl_2 [2] ^a	82	21,100
7	EtAlCl_2 [6] ^a	75	27,400
7	MAO [400] ^b	94	7,400
7	MAO [800] ^b	90	13,200

a) General conditions: $T = 30^\circ\text{C}$, 10 Bar C_2H_4 , 35 min, 4.0×10^{-2} mmol Ni complex, solvent 15 mL toluene
 b) General conditions: $T = 30^\circ\text{C}$, 10 Bar C_2H_4 , 35 min, 4.0×10^{-2} mmol Ni complex, solvent 20 mL toluene

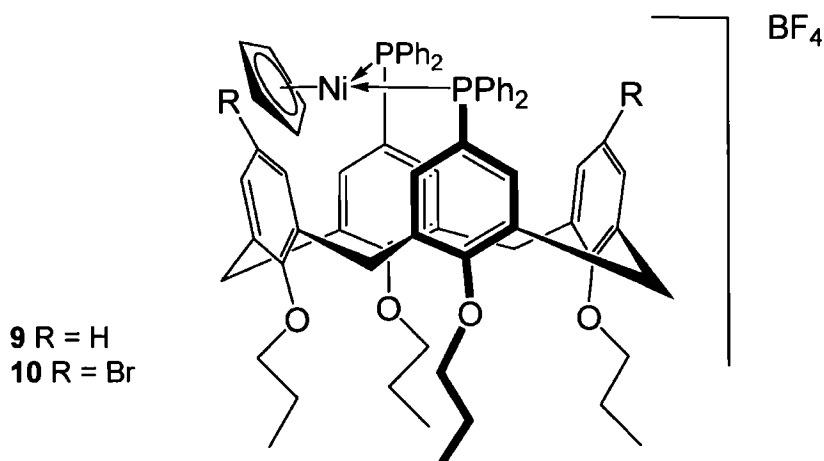
The P-N nickel complexes employed by both Le Floch (**Table 1.1**) and Braunstein (**Table 1.2**) give both high selectivity and activity for ethylene dimerization. However, related nickel systems have been reported for which the selectivity for ethylene dimerization is even higher. Dyer *et al.* have reported the *bis*(pyrrolatoimine) complex $[\text{Ni}\{2\text{-}(\text{mes-N-CH})\text{C}_4\text{H}_3\text{N}\}_2]$ (**8**) which when activated by EtAlCl_2 generates an initiator complex that gives exclusively ethylene dimerization (**Scheme 1.10**).²¹ Though the dimerization system based on complex **8** is highly selective for butenes, the activity obtained was low (1g ethylene/mmol Ni/ h/ bar).

Scheme 1.10 Synthesis and reactivity of complex **8**



One novel nickel-based dimerization initiator, which combines both high activities with excellent selectivity stems from the use of diphosphinated calix[4]arenes by Matt *et al.* (Figure 1.4).²²

Figure 1.4 Nickel-base diphosphinated calix[4]arenes pre-catalysts



Both complexes **9** and **10** (Figure 1.4) can be activated for ethylene dimerization by EtAlCl_2 . Although the initiator systems based around **9** and **10** were examined under a range of conditions it was stated that the selectivity for butenes always exceeded 95%. Furthermore, the selectivity for but-1-ene specifically could be enhanced by modification of the reaction conditions, with low pre-catalyst concentrations resulting in outstanding selectivity for but-1-ene (91% for entry 1, Table 1.3) as well as favouring higher TOF (Table 1.3).

Table 1.3 Ethylene dimerization with nickel calix[4]arene pre-catalysts^a

Entry	Precursor	n(Ni) [μmol]	Pressure	T C°	ΔT^b C°	MAO [equiv/Ni]	TOF ^c
1	9	0.09	20	25	3	400	83.53
2	9	4.5	20	25	57	400	11.74
3	10	0.09	20	25	3	400	120.54

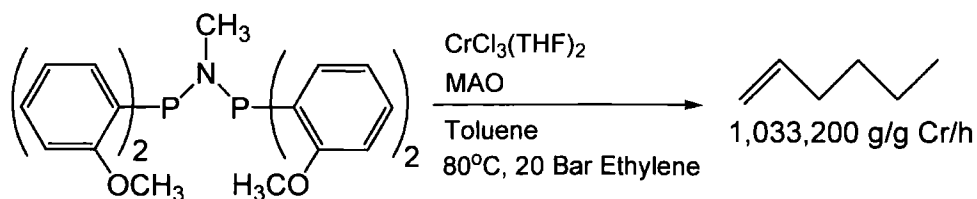
a) The solvent toluene (22 mL) was employed in all runs. b) Maximum temperature increase during the catalytic run. c) TOF reported in mol of C_2H_4 converted per mol of Ni per hour (mol C_2H_4 / mol Ni / h).

For runs in which relatively high pre-catalyst concentrations of **9** and **10** were employed (**Table 1.3** entry **2**) rapid rises in the temperature of the initiator solutions occurred, as ethylene dimerization is an exothermic process. In contrast, when lower concentrations of both **9** and **10** were used better temperature control was obtained. This data suggests that it is tighter temperature control which leads to higher TOF and greater selectivity for but-1-ene (**Table 1.3**, entries **2** and **3**). Also of note, is that the highest TOF was attained from the pre-initiator **10** (**Figure 1.4 R = Br**). It is suggested that the bulky bromine atoms present in the ligand backbone of **10**, will be able to interact with intermediately formed Ni-butyl moieties, a steric interaction which will favour fast reductive elimination of butenes. Significantly, the TOF obtained with either complexes **9** or **10** are reported as exceeding the activities of any currently known nickel diphosphine catalysts.²³ As such, the use of a diphosphinated calix[4]arene ligand backbone provides an alternative, yet attractive, approach to developing new ethylene dimerization systems.

1.3 Ethylene Trimerization Initiated by Homogeneous Chromium-based Initiators

Although this thesis concerns the use of molybdenum and tungsten dimerization systems, it should be noted that chromium based pre-catalysts are arguably more widely used to initiate alkene dimerization and oligomerization reactions. Indeed, the use of chromium complexes to initiate ethylene trimerization is especially prominent.²⁴ The importance of ethylene trimerization stems from the Schulz-Flory (or Poisson) distribution of linear α -olefins obtained from ethylene oligomerization systems.² Often this Schulz-Flory product distribution does not match the market demand for linear α -olefins in the valued co-monomer range (1-C₆ and 1-C₈).²⁵ As such an immense emphasis has been placed on developing ethylene trimerization systems which offer an atom efficient route to hex-1-ene, which is widely utilized as a co-monomer in polyethylene manufacture. An important development in the field of ethylene trimerization concerns the use of diphosphazane (or "PNP") ligands (**Scheme 1.11**).²⁶

Scheme 1.11 Ethylene trimerization using orthomethoxy-substituted diphosphazanes

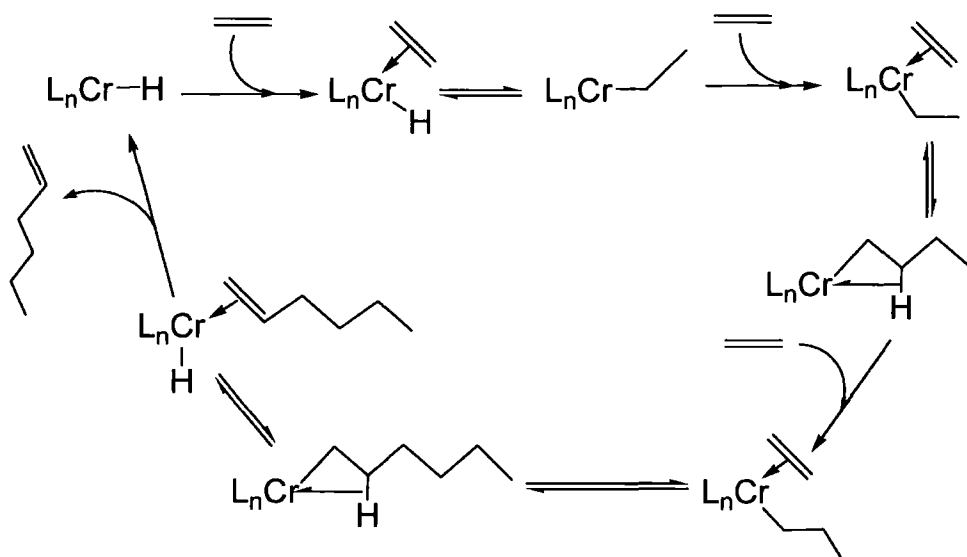


The most active trimerization systems were obtained when the diphosphazane backbone contained *ortho*-methoxy moieties as in **Scheme 1.11**. Indeed the ethylene trimerization system illustrated in **Scheme 1.11** gives an activity that is two orders of magnitude higher than those previously reported.²⁴ Furthermore, this initiator system was highly selective, producing 90% C₆ products of which 99.9% was hex-1-ene (giving an overall selectivity of 89.9% for the 1-C₆ product). This high selectivity for hex-1-ene makes this initiator system particularly attractive for commercial application.

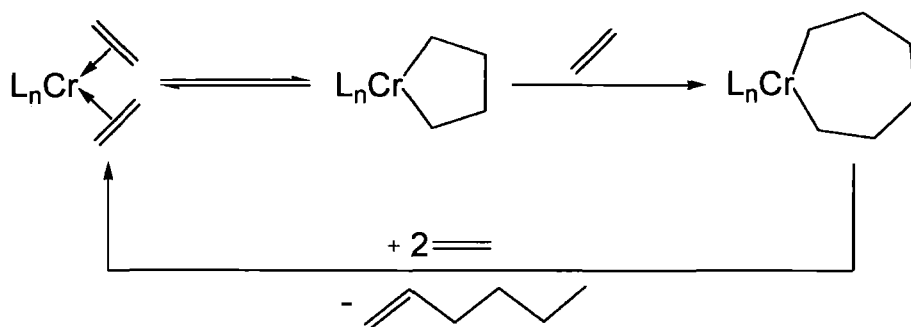
1.4 Determining the Mechanism of a Chromium-based Ethylene Trimerization by Reaction of C₂D₄ and C₂H₄

In **Section 1.2** the range of mechanisms by which olefin dimerization can be achieved was discussed. Particularly prominent are catalytic cycles that proceed *via* hydride or metallacycle intermediates. Similarly, trimerization of ethylene by a chromium-based initiator could also feasibly occur *via* a hydride (degenerate polymerization) (**Scheme 1.12**) or a metallacycle (oxidative coupling) (**Scheme 1.13**) mechanism.

Scheme 1.12 Chromium-initiated ethylene trimerization via a hydride cycle

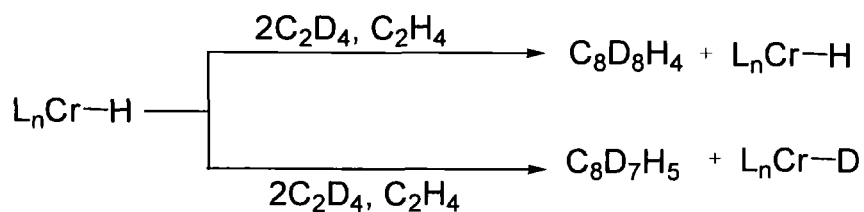


Scheme 1.13 Chromium-initiated ethylene trimerization via metallacycle intermediates

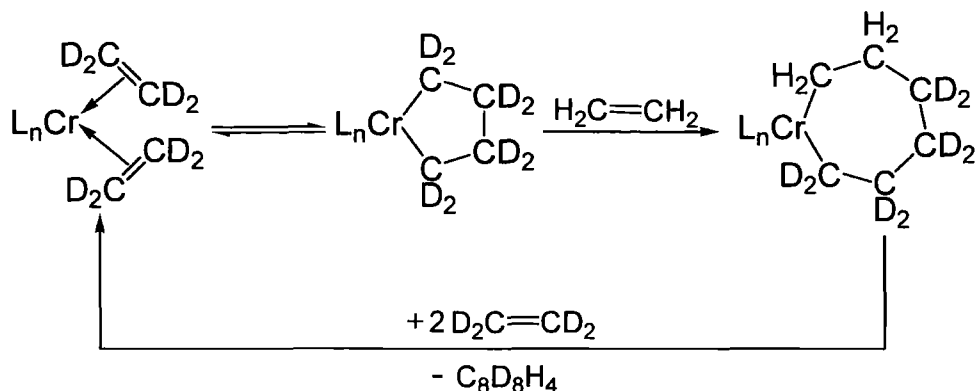


With regard to gaining understanding of the trimerization mechanism, of particular significance is the potential for the hydride or metallacycle mechanisms to give different product distributions when reacted with a 1:1 mixture of C_2D_4 and C_2H_4 . If a hydride regime was in operation, a C_2D_4/C_2H_4 mixture would undoubtedly give olefins containing both odd and even numbers of deuterium atoms (**Scheme 1.14**).

Scheme 1.14 Products obtainable from trimerization of a C_2D_4/C_2H_4 mixture via a hydride initiator



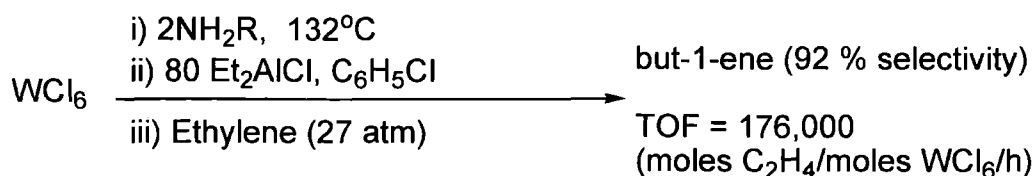
In contrast to a hydride cycle, trimerization *via* metallacycles can result in the exclusive production of olefins containing even numbers of deuterium and hydrogen atoms. For instance trimerization of two molecules of C_2H_4 with one of C_2D_4 *via* first a five, and then a seven membered ring, can only result in the formation of the “even” product $C_6H_8D_4$ (**Scheme 1.15**).

Scheme 1.15 Production of $C_6H_8D_4$ via an oxidative coupling mechanism

Bercaw *et al.* have employed a 1:1 C_2D_4/C_2H_4 feedstock to investigate their trimerization system which is based upon complexation of the PNP ligand (*o*-MeO- C_6H_4)₂PN(Me)P(*o*-MeO- C_6H_4)₂ to the Cr^{III} precursor $CrCl_3 \cdot THF_2$, followed by addition of the co-initiator MAO.²⁷ Using these conditions Bercaw and co-workers observed the formation of C_6 products containing exclusively even numbers of D and H atoms. This was cited as being proof of a metallacycle mechanism, as only this type of mechanism could give such a product distribution. Hence, reaction of a C_2D_4/C_2H_4 mixture has been successful in identifying the mechanism of Bercaw's trimerization system. As such, similar investigations could also feasibly provide mechanistic information regarding related dimerization initiators.

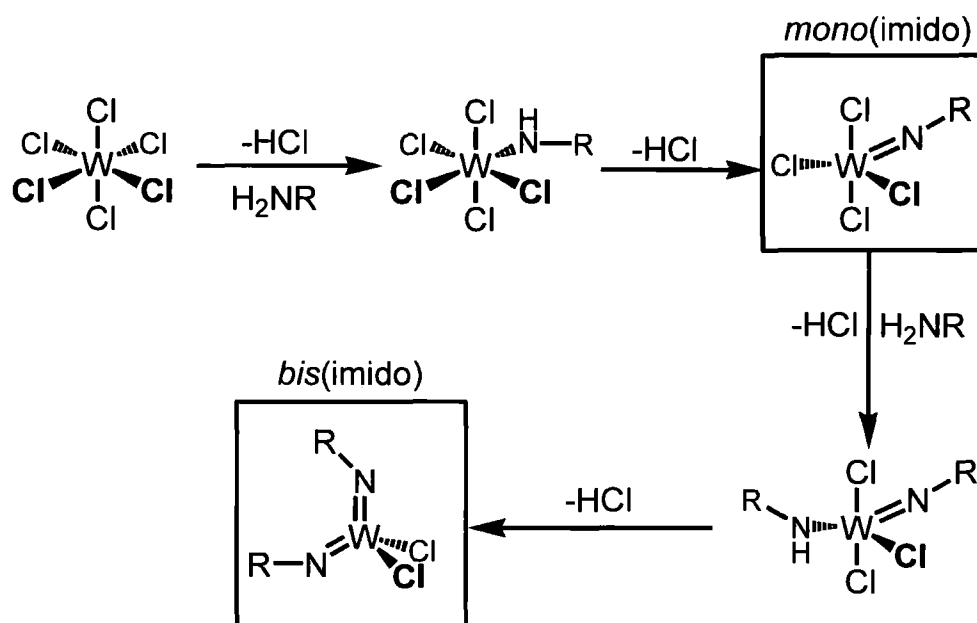
1.5 Olefin Dimerization Systems Based on WCl_6

Processes describing the dimerization of olefins using solutions of WCl_6 were first outlined by Goodyear in the 1970's.²⁸ In the Goodyear system, an unknown initiator complex is formed *in situ* from reaction of WCl_6 with two equivalents of an aniline in chlorobenzene, followed by addition of an excess of an aluminium alkyl halide, typically $EtAlCl_2$, Et_2AlCl or $Et_3Al_2Cl_3$. Through this procedure a highly active alkene dimerization initiator is obtained (Scheme 1.16).²⁹

Scheme 1.16 Ethylene dimerization based on WCl_6 

Of significance, is that HCl has been found to evolve during initiator preparation. Furthermore, a patent was awarded to Exxon, specifying that it was advantageous to remove HCl from the $WCl_6/2NH_2R$ reaction solution through the use of an N_2 gas stream.³⁰ Purging the initiator solution of HCl enabled the use of lower co-catalyst loadings in the Exxon system, with $W:Al$ molar ratios of between 3:1 to 5:1 stated as being preferable. Hence, although the identity of the actual active compound is not firmly established, the evolution of HCl in both the Exxon and Goodyear systems is suggestive of the formation of nitrogen–metal bonds (e.g. $W-NR(H)$ or $W=NR$) *in situ* (Scheme 1.17).

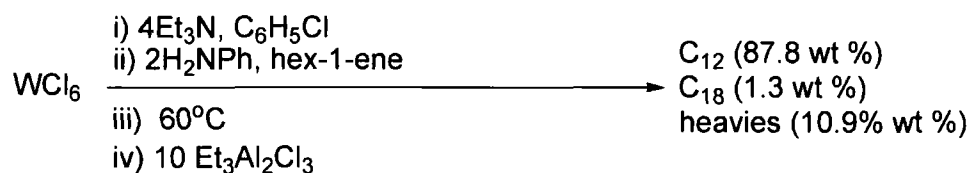
Scheme 1.17 Generation of metal imido bond through elimination of HCl



In both the Goodyear and Exxon systems, the aniline is generally used in an excess relative to WCl_6 (two equivalents) and as such, there is the possibility that either *mono* or *bis(imido)* tungsten complexes could evolve *in situ*. Furthermore, there is also the potential that amido complexes are present in the initiator solution. In order to evaluate the plausibility of imido formation *in situ*, catalysis has been carried out by Olivier *et al.* using discrete pre-formed imido complexes (of the general formula $W(NR)Cl_4 \cdot THF$) and results directly compared to those obtained using the Goodyear catalyst system ($WCl_6/ArNH_2/EADC$, 1:2:11).³¹ Although the activities given by the discrete imido complexes tended to be slightly lower than that obtained using the Goodyear system, the TON and initiator selectivity were comparable, strongly suggesting that the active initiator species is a tungsten imido complex.

Although Exxon employed a flow of nitrogen to remove HCl from the initiator solution and hence enhance initiator performance, in a recent patent filed by Sasol Technology UK (STUK) a separate base (such as Et₃N) was used as a HCl scavenger.³² The STUK patent also outlines procedures for the dimerization of heavier olefins such as hex-1-ene (**Scheme 1.18**).

Scheme 1.18 Dimerization of Hex-1-ene using the STUK WCl₆ based process^a



a) heavies are defined as being hydrocarbon products containing 24 or more carbon atoms

The activity obtained for the hex-1-ene dimerization system outlined in **Scheme 1.18** was 107.2 (mol hex-1-ene/mol WCl₆/h) and the TON was 428.7 (mol hex-1-ene/mol WCl₆). Analysis of the skeletal selectivity (through the use of a hydrogenating GC) of the C₁₂ product fraction indicated a high preference for the branched dimerization products, with no linear products observed (**Table 1.4**).

Table 1.4 Analysis of C₁₂ skeletal selectivity obtained from hex-1-ene dimerization using the STUK WCl₆ system

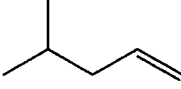
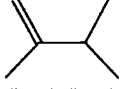
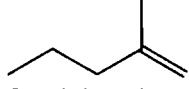
Hydrocarbon backbone	Skeletal selectivity (wt %)
Linear product	0
5-methyldecenes	65
5,6 dimethyldecenes	35

Clearly the STUK WCl₆ hex-1-ene dimerization system exhibits good activity and the selectivity for C₁₂ dimerization products are high. As such, the WCl₆ STUK dimerization system provides a means to dimerize heavier α-olefins. Furthermore, initiator preparation using procedures outlined in the STUK patent from WCl₆ is relatively simple and does not require the timely synthesis of bi-dentate ligands. This is in contrast to many of the nickel based dimerization systems previously outlined in **Section 1.3**.

1.6 Examining the Selectivity of the WCl_6 Goodyear Dimerization System

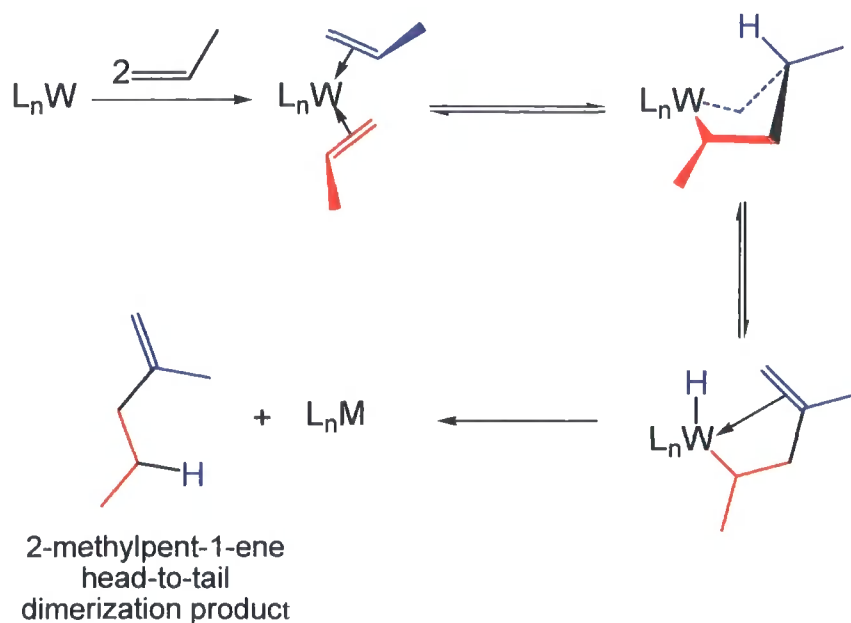
Insights into the mechanism by which systems based on WCl_6 initiate alkene dimerization can be obtained from examination of the olefin dimerization products. From the examples provided by Goodyear (**Table 1.5**), it is clear that alkene dimerization results in a significant amount of both the tail-to-tail (tt) as well as the head-to-tail (ht) and tail-to-head (th) products. Conversely, linear head-to-head (hh) products are produced in trace amounts (less than 2%).

Table 1.5 Product distributions obtained from a Goodyear WCl_6 -based propylene dimerization system

Aniline used in initiator preparation.	C_6 (%)	 4-methylpent-1-ene (molar % of product) (th)	 2,3-dimethylbut-1-ene (molar % of product) (tt)	 2-methylpent-1-ene (molar % of product) (ht)
2,6-dichloro-4-fluoroaniline	55	11	49	38
2,4-difluoroaniline	74	10	50	34
2,4,6-trichloroaniline	53	8.3	76	10

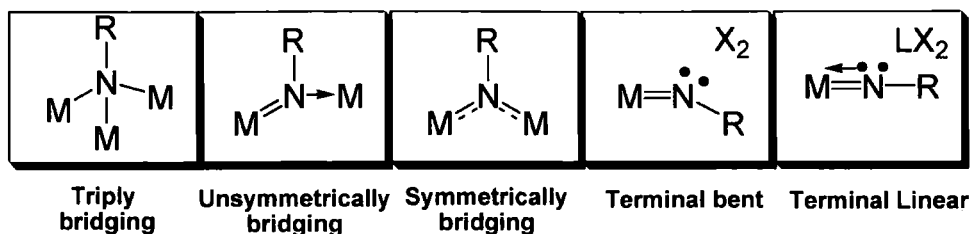
The evolution of both ht and th product, from the WCl_6 Goodyear (and STUK) dimerization systems can be explained by the formation of α - β -substituted metallacycles (**Scheme 1.18**). Indeed, dimerization of olefins to give both ht and tt products is characteristic of a concerted coupling mechanism.³³ This is suggestive that for systems generated *in situ* from WCl_6 dimerization occurs *via* a tungsten metallacycle complex, formed from an imido/amido pro-initiator.

Scheme 1.18 Formation of *ht* dimerization products via a concerted coupling mechanism

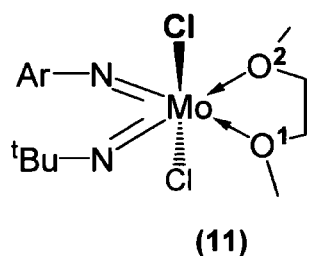


1.7 Applications and Bonding Modes of Transition Metal Imido Complexes

Evolution of HCl during the formation of the STUK, Exxon and Goodyear WCl_6 based dimerization systems strongly suggests the *in situ* formation of an imido initiator complex. As discussed above this conclusion was confirmed by the use of *mono(imido)* pre-catalysts ($W(NR)Cl_4 \cdot THF$) by Olivier *et al.*³¹ The chemistry of imido systems has been extensively investigated, as such, a wide range of imido transition metal complexes are known and have been the subject of a number of reviews.³⁴ Indeed, transition metal complexes containing imido ligands (NR^{2-}) alongside use as alkene dimerization precatalysts have many other possible applications. For instance, imido complexes are viewed as potential aziridination and amination reagents.³⁵ Imido complexes have also been considered to be prospective metal nitride film growth precursors,³⁶ as well as being employed as ligands in ring opening metathesis polymerization,³⁷ Ziegler-Natta olefin³⁸ and MMA-polymerization initiators.³⁹ The imido ligand is known to adopt one of five different bonding modes as illustrated in **Figure 1.5**, utilizing the formal 2- charge and lone pair of the nitrogen atom.

Figure 1.5 Known imido bonding modes

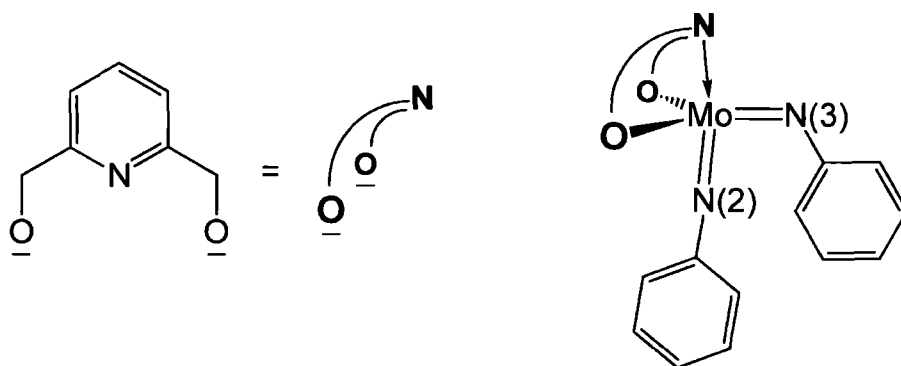
In the terminal linear imido bonding mode, the interaction between the metal and the nitrogen can be considered to consist of one σ - and two π -bonds, with the nitrogen being formally sp -hybridized. Thus, for linear imido ligands the ideal M-N-C bond angle is 180° and consequently the imido ligand is assigned as being a 4-electron donor (neutral ligand formalism). In practice, the M-N-C bond angle of a linear imido ligand is highly variable, with bond angles in the range of 150 - 180° .⁴⁰ This is because the M-N-C bond angle associated with a given imido moiety can be heavily influenced by factors such as crystal packing forces. As such, in many systems it is the relative M-N bond lengths that are more descriptive of a given imido ligands bonding mode. The inaccuracy of assigning imido bonding modes based on the M-N-C angle is illustrated by the mixed *bis*(imido) complex $\text{Mo}(\text{NAr})(\text{N}^t\text{Bu})\text{Cl}_2\cdot\text{DME}$ (**11**) (Figure 1.6).⁴¹ With a M-N-C bond angle of $174.3(2)^\circ$ the NAr ligand of $\text{Mo}(\text{NAr})(\text{N}^t\text{Bu})\text{Cl}_2\cdot\text{DME}$ (**11**) is seemingly adopting the linear bonding mode. However, it is the N^tBu ligand which has a shorter Mo-N contact ($1.728(2)$ vs $1.753(2)$ Å) and it is the N^tBu imido that is observed to exert a greater *trans* influence on the corresponding *trans* Mo-O contact (Table 1.6). Thus, contrary to the apparent linear geometry of the NAr ligand, for $\text{Mo}(\text{NAr})(\text{N}^t\text{Bu})\text{Cl}_2\cdot\text{DME}$ (**11**) it is the N^tBu ligand that has a Mo-N contact with the greatest triple bond character.

Figure 1.6 and **Table 1.6** Assessing the relative *trans* influences of the NAr and N^tBu ligands of complex **11**

	Bond distance (Å)
Mo-O ₁	2.330(2)
Mo-O ₂	2.392(1)

Although it is often difficult to assign a bonding mode (linear vs bent) to a given imido ligand, *bona fide* examples of truly bent terminal imido ligands (i.e. 2-electron donors, neutral formalism) with a sp^2 hybridized N atom have been identified. For example, the complex $[\text{Mo}(\text{NAr})_2(\text{L})]$ (L is a tridentate pyridinediolato ligand) (**12**) is observed to have two inequivalent imido ligands one adopting a linear geometry ($\text{Mo-N}(2)\text{-C}_{\text{ipso}} 164.7(4)^\circ$; $\text{Mo-N}2, 1.760(4)\text{\AA}$) and the other a bent ($\text{Mo-N}(3)\text{-C}_{\text{ipso}}, 144.8(5)^\circ$; $\text{Mo-N}3, 1.771(4)$).⁴² This situation arises in this “ π -loaded” *bis(imido)* complex, to avoid the unfavourable valence electron count of twenty that would result from both imido ligands adopting the linear bonding mode and donating 4 electrons to the molybdenum atom. Instead, one imido ligand adopts the bent bonding mode and as an X_2 donor, donates 2 electrons to the Mo atom, enabling the more favourable electron count of eighteen (**Figure 1.7**). A second commonly cited example of a bent imido ligand can be found in the complex $\text{Mo}(\text{NC}_6\text{H}_5)_2(\text{S}_2\text{CN}(\text{C}_2\text{H}_5)_2)_2$ (**13**).⁴³ The molecular structure of complex **13** contains a distinctly bent imido ligand with a Mo-N-C bond angle of 139.4° and a Mo-N bond length of 1.789 \AA as well as a linear imido ligand ($\text{Mo-N-C} = 169.4^\circ$ and $\text{Mo-N} = 1.754\text{ \AA}$).

Figure 1.7 Simplified structure of the “ π -loaded” *bis(imido)* complex **12** (only key atoms are included for clarity)



Imido π -bonding can be considered to result from overlap of a filled nitrogen p-orbital with an empty metal d-orbitals (**Figure 1.8**). As empty metal d-orbitals of the correct symmetry and similar energy are required for formation of metal-nitrogen multiple bonds, linear imido complexes are favoured for high oxidation state and early transition metals.³⁴ However, many mid-series transition metal imido complexes have been reported, for example, those of osmium.⁴⁴ The homoleptic osmium imido complex $\text{Os}(\text{NAr})_3$ (**14**) is of particular interest, as with three seemingly

linear imido ligands (verified using X-ray crystallography) **14** is outwardly a 20 electron complex (**Figure 1.9**).⁴⁴

Figure 1.8 Imido π -bonding

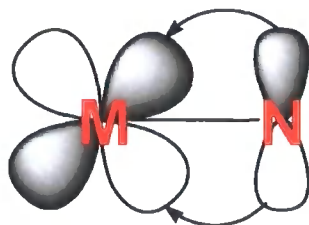
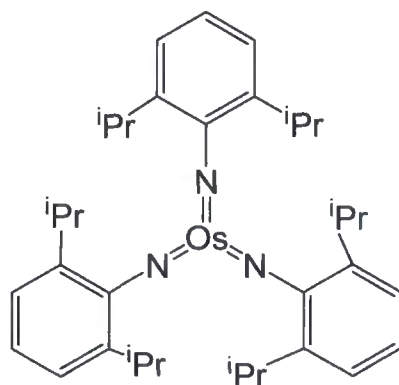


Figure 1.9 The tris(imido) complex $\text{Os}(\text{NAr})_3$ (**14**)



It is reasoned that although all three imido ligands of complex **14** adopt a linear geometry, at least one imido ligand does not donate the maximum of four electrons to the metal. Instead, one imido N-lone pair is located in a non-bonding orbital centred on a nitrogen atom. Thus, **14** can be considered as being an 18 electron complex. Hence, characterization of the osmium complex $\text{Os}(\text{NAr})_3$ (**14**) further demonstrates that a linear imido ligand does not necessarily have to act as a formal four electron donor. This again emphasises that a given imido ligands geometry is a poor indication of π -donor capacity.

Although osmium imido complexes have been reported, few structures of late transition metal complexes (beyond group 8) with terminal imido ligands are currently deposited in the Cambridge Structural data base. However, late transition metal complexes with bridging imido ligands are known,⁴⁵ though this bonding mode does not require the acceptance of a nitrogen lone pair to a single metal centre. Metal nitrogen multiple bonds are not exclusive to transition metals, both lanthanide and

actinide⁴⁶ imido complexes have been identified, with those of uranium-imido being particularly prevalent.⁴⁷

1.8 Attempts to Spectroscopically Distinguish between Imido Bonding Modes

As mentioned in **Section 1.8**, determination of an imido fragment's bonding mode (X_2 vs LX_2) on the basis of M-N-C bond angle, is often inaccurate and requires material suitable for single crystal X-ray diffraction. Consequently, assessment of imido coordination modes has been attempted using a range of alternative techniques. For example, complexes containing imido ligands have been examined using X-ray photoelectron spectroscopy (XPS), measuring the 1s binding energy of the imido nitrogen atom.⁴⁸ However, it was determined that the resulting XPS spectrum cannot be used to conclusively assign a given nitrogen atom's hybridization (sp vs sp^2). This indicates that XPS is unsuitable for determining a given imido ligands bonding mode.

In an alternative approach Bradley *et al.* conducted a comprehensive study of complexes containing both linear and bent imido ligands using both ^{14}N and ^{15}N NMR spectroscopy.⁴⁹ Again, this analysis was unsuccessful in differentiating between bent and linear bonding modes, with nitrogen chemical shifts (both ^{14}N and ^{15}N) being insensitive to the deshielding observed on imido bending.

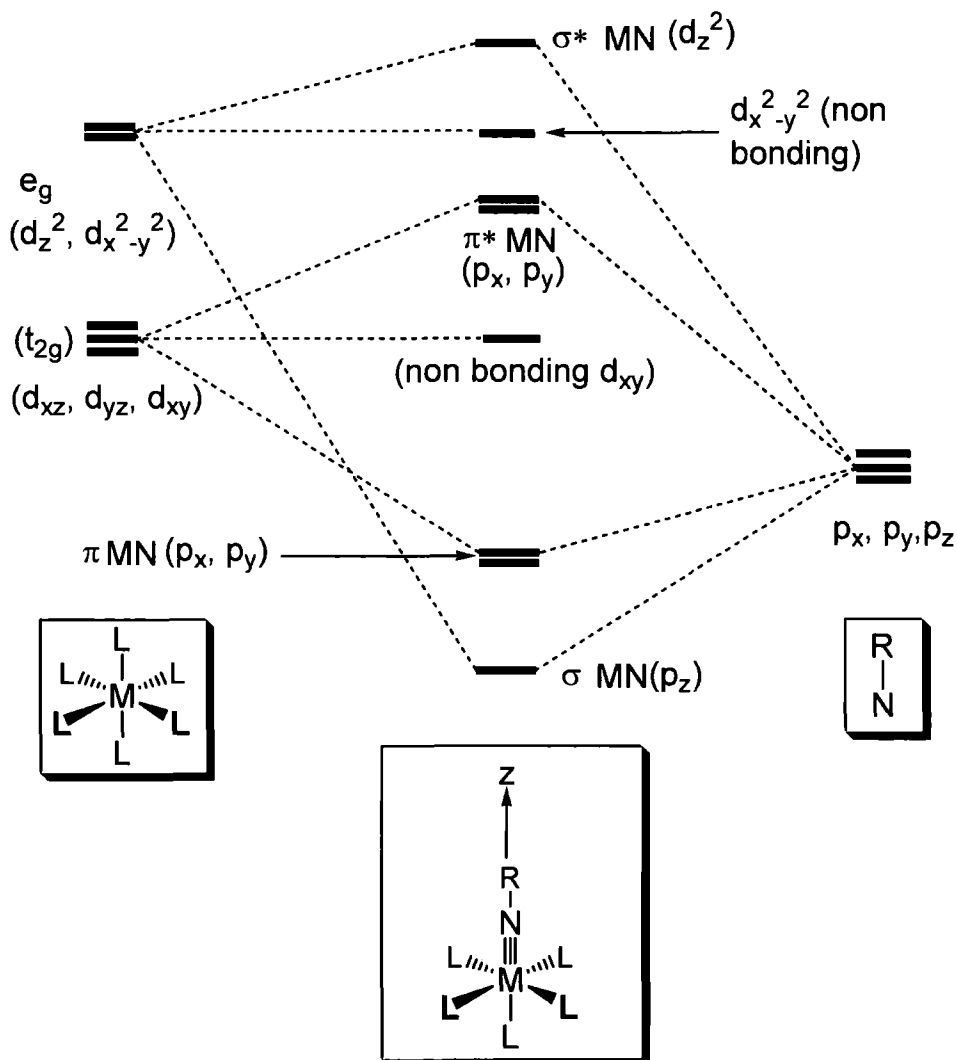
In contrast, ^{13}C NMR spectroscopy can be used to gain insight into the electronic environment of an imido nitrogen atom. Hogarth *et al.* have used ^{13}C MAS-NMR to characterize a series of *bis*(imido) complexes with the general formula $\text{Mo}(\text{NR})_2(\text{S}_2\text{CNET}_2)_2$ and observed two distinct *ipso* carbon resonances corresponding to two different imido environments existing in the solid state.⁵⁰ Strong correlation between $\Delta\delta$ (the difference between C_{ipso} chemical shifts in ppm), and Δ° (the difference in M-N-C bond angles) was observed, enabling quick assignment of the relative bending of the *bis*(imido) ligands. Notably, Hogarth and co-workers did not offer any explanation regarding the origin of the correlation that exists between $\Delta\delta$ and Δ° .

1.9 Molecular Orbital Description of Imido Complexes and Resulting Isolobal Relationships

1.9.1 Molecular Orbital Description of *mono(imido)* Complexes

A molecular orbital description of metal-imido bonding for an *mono(imido)* octahedral complex can be readily defined (**Figure 1.10**). If the z-axis is set as being along the M-N bond, then the d_{xz} (metal) combines with the p_x (nitrogen) and the d_{yz} (metal) with the p_y (nitrogen). The final orbital of the t_{2g} set, d_{xy} (metal), is non-bonding. As the nitrogen atom lies along the z-axis the degeneracy of the $d_{x^2-y^2}$ and d_z^2 orbitals is lost, with the d_z^2 orbital and the p_z (nitrogen) orbitals combining.

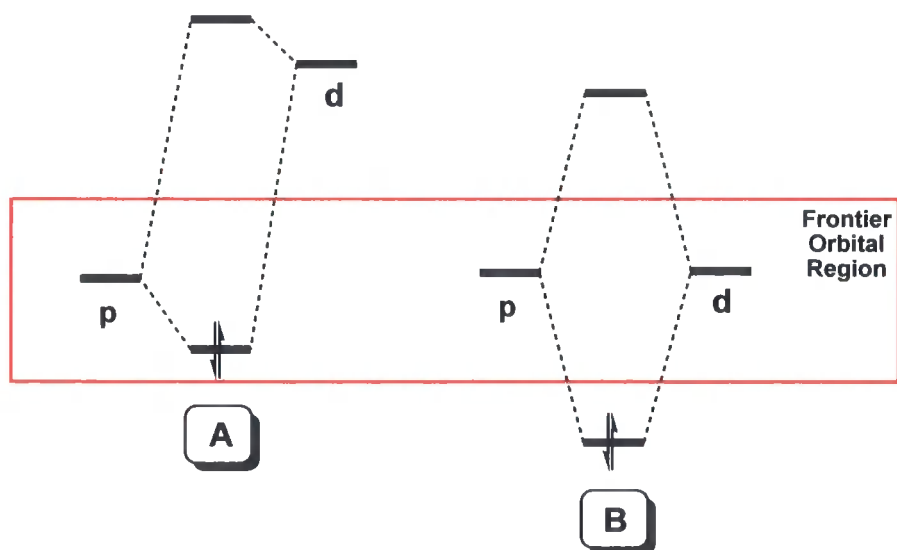
Figure 1.10 Orbital energy diagram for a linear imido ligand of an octahedral metal complex⁴⁹



Thus, for a *mono*(imido) system in an octahedral geometry, combination of the nitrogen p-orbitals with the metal d-orbitals allows for a maximum of three bonding interactions (1σ and 2π). The relative energies of the combining metal and nitrogen orbitals have been shown by Nugent *et al.* to influence the nucleophilicity of a given N^tBu ligand within a homologous series of d^0 complexes (**Figure 1.11**).⁵¹

When an N^tBu ligand is coordinating to an early transition metal (such as tantalum), then bonding occurs between a nitrogen p-orbital and a high energy d-orbital (**Figure 1.11, A**). This gives a HOMO with a relatively high energy and predominantly nitrogen character, resulting in an imido ligand that preferentially reacts as a nucleophile. A bonding regime such as that outlined in **Figure 1.11, B** is argued by Nugent to apply to an imido ligand bound to a more electronegative metal such as chromium which has d-orbitals that are less diffuse and lower in energy.⁵¹ Thus, the relatively low energy of a chromium d-orbital (compared to a tantalum) in turn gives a HOMO of reduced energy, significantly decreasing the nucleophilicity of the corresponding chromium imido ligand.⁵¹

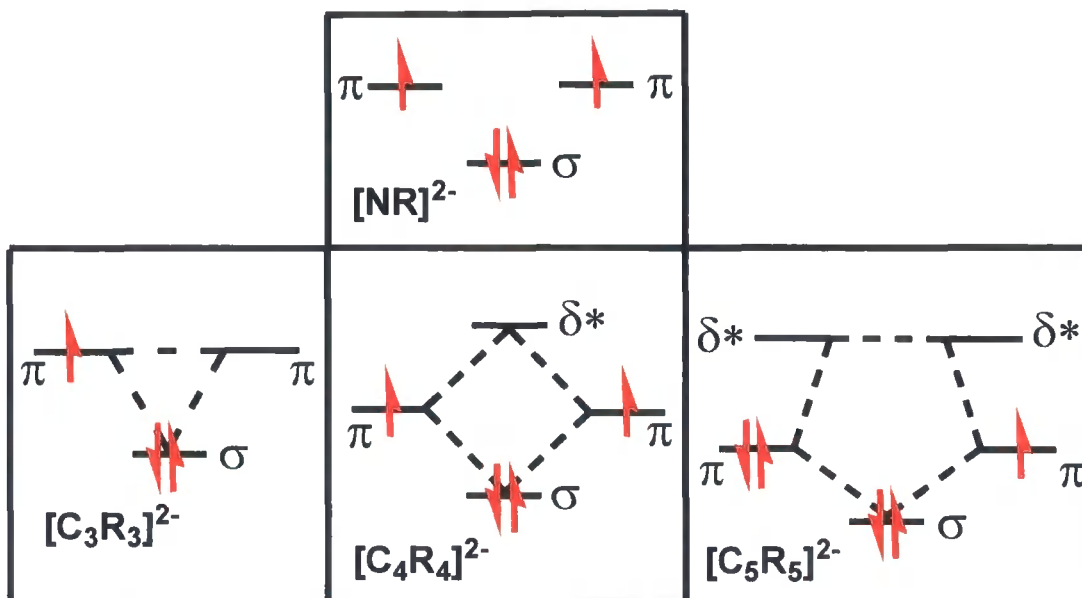
Figure 1.11 Changes to nitrogen/metal π -interactions resulting from variation of the atomic orbital relative energies.



1.9.2. Isolobal Relationships Between $[M(NR)_2]^{2-}$ ($M = Mo$ or W) and $[M(Cp)_2]^{2-}$ ($M = Zr$ or Hf) Complexes

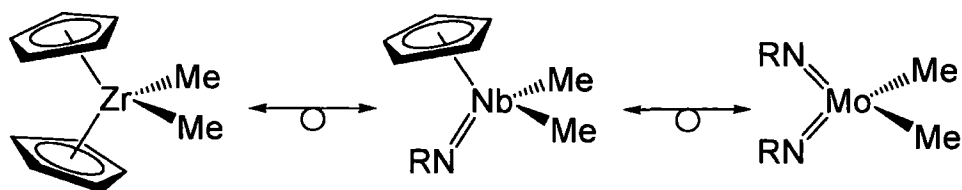
Similarities can be drawn between imido, cyclopentadienyl, cyclobutadiene and cyclopropenyl fragments, as all four ligands have two π -symmetry frontier orbitals available to interact with a given metal (**Figure 1.12**).

Figure 1.12 Simplified energy level diagram denoting the frontier orbitals of NR^{2-} and C_nH_n fragments



It is clear from the energy level diagram outlined in **Figure 1.12** that the imido and cyclobutadiene ligand are isonumeral with both fragments capable of donating a maximum of four electrons to a given metal.⁵² Strictly the imido and C_4H_4 fragment cannot be considered as formally isolobal, as in contrast to an imido ligand the C_4H_4 fragment binds to a metal *via* four atoms and has a δ symmetry orbital available for metal back donation. However, it is clear that C_nH_n and imido moieties have similar frontier orbitals. Using this observation, and the knowledge that imido and Cp ligands have a respective formal charge of 2- and 1-, group VI *bis*(imido) complexes can be related to group IV metallocenes.^{52,53} This gives an isolobal series comprising of complexes with an identical valence metal count of sixteen (**Figure 1.13**).

Figure 1.13 Isolobal relationships between Zr, Nb and Mo cyclopentadienyl and complexes



The isolobal relationship between $(\text{Cp})_2\text{M}$ ($\text{M} = \text{Ti}, \text{Zr}$ or Hf) and $(\text{RN})_2\text{M}$ ($\text{M} = \text{Cr}, \text{Mo}$ or W) fragments has also been investigated by Schrock *et al.*, using SCF- $X\alpha$ SW calculations to examine the bonding of the hypothetical tetrahedral complex $\text{W}(\text{NH})_2(\text{PH}_3)_2$.⁵⁴ It was determined that the $[\text{W}(\text{NR})_2]$ core has three vacant frontier orbitals, two of a_1 and one of b_2 symmetry, which is the same configuration to that found for a $(\text{Cp})_2\text{M}$ ($\text{M} = \text{Ti}, \text{Zr}$ or Hf) fragment.⁵⁵ Hence, Schrock's analysis clearly shows that parallels can be drawn between the frontier orbital configuration and structure of the isolobal fragments $\text{W}(\text{NAr})_2\text{Cl}_2$ and Cp_2HfCl_2 . This isolobal relationship hints that potentially W^{VI} bis(imido) complexes may display similar reactivity to that of established Cp_2MCl_2 ($\text{M} = \text{Ti}, \text{Zr}, \text{Hf}$) ethylene polymerization pre-catalysts.⁵²

1.10 Methods of Imido ligand Synthesis

There are a wide range of synthetic methods available to introduce an imido ligand into a metal complex. The most important being highlighted in **Table 1.6**.

Table 1.6 Synthesis of imido complexes

Synthetic method	Example
N-H bond cleavage- amines/amides ⁵⁶	$\text{W}(\text{NAr})(\text{NEt}_2)\text{Cl}_3(\text{THF}) \xrightarrow[\text{THF}]{\text{LiNHAr}} \text{W}(\text{NAr})_2\text{Cl}_2(\text{THF})_2 + \text{HNEt}_2$
N-Si bond cleavage ⁵⁷	$\text{CrO}_2\text{Cl}_2 \xrightarrow{4\text{Me}_3\text{SiNH}^t\text{Bu}} \text{Cr}(\text{N}^t\text{Bu})_2(\text{OSiMe}_3)_2 + \text{Me}_3\text{Si-SiMe}_3 + 2^t\text{BuNH}_3\text{Cl}$
Imido metathesis [2+2] cycloaddition ⁵⁸	$\text{Re}(\text{OSiPh}_3)_3 \xrightarrow{\text{ArN}=\text{C}=\text{O}} \text{Re}(\text{NAr})_3(\text{OSiPh}_3) + 3\text{CO}_2$
Organic azides (elimination of N_2) ⁵⁹	$\text{MoCl}_4(\text{THF})_2 \xrightarrow{\text{N}_3^t\text{ol}} \text{Mo}(\text{N}^t\text{ol})\text{Cl}_4(\text{THF}) + \text{N}_2$
Azo compounds ⁶⁰	$2\text{Ti}(\eta^2\text{-PhN}=\text{NPh})(\text{OAr})_2(\text{py}')_2 \longrightarrow 2\text{Ti}(\text{NPh})(\text{OAr})_2(\text{py}')_2 + \text{PhN}=\text{NPh}$
Oxidizing agents ⁶¹	$\text{MoO}(\text{S}_2\text{CNEt}_2)_2 \xrightarrow{2\text{C}_5\text{H}_5\text{NNTs}} 2\text{Mo}(\text{NTs})(\text{O})(\text{S}_2\text{CNEt}_2)_2 + \text{C}_5\text{H}_5\text{NNC}_5\text{H}_5$

Many of the synthetic routes outlined in **Table 1.6** result in the evolution of an entropically favoured leaving group such as CO₂, N₂ or the formation of an enthalpically stable product such as lithium chloride or a silyl ether. The formation of such by-products provides a thermodynamic driving force for imido formation, allowing the energy cost associated with the synthesis of a multiple bond to be offset.

1.11 Synthesis and Reactivity of Group 6 Imido Complexes

Particular emphasis has been placed on the development of both low valent tungsten and molybdenum d⁰ (imido) complexes, as their derivatives can be used as precursors to Schrock-type olefin metathesis initiators of the general formula M(NAr)(CHR)(OR')₂ (M=Mo or W) which have been used widely as RCM and ROMP pre-catalysts.⁶² One advantage of using imido ligands to stabilize a M^{VI} centre, in preference to isoelectronic alternatives such as the oxo ligand, is the potential to alter the R group of the imido moiety. This allows for greater variation and control of the steric environment about a given metal. Typically in Schrock type metathesis initiators, bulky R groups such as 2,6-diisopropyl phenyl (Ar) are employed. The steric influence exerted by such bulky fragments, simultaneously stops the imido ligand adopting a bridging bonding mode and 'protects' the reactive alkylidene ligand, which could potentially dimerize with a second metal alkylidene moiety. Although a substantial number of investigations have been undertaken with the aim of developing and improving Schrock-type metathesis initiators, in this thesis such complexes have not been utilized and so will not be discussed in detail. Instead, a brief survey examining Group 6 imido complexes will be undertaken.

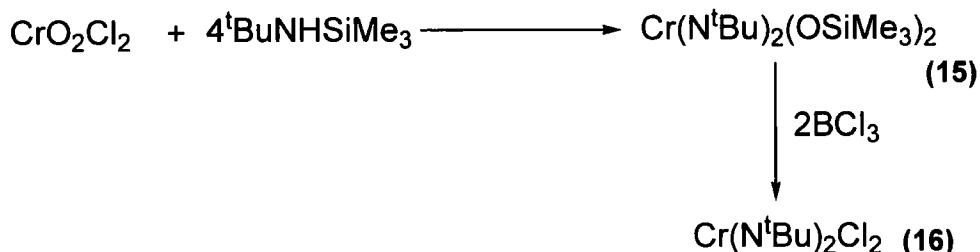
1.11.1 Synthesis of Chromium Imido Complexes

Interest in the synthesis of chromium imido complexes first stemmed from the isolobal relationship that exists between the metal fragments [Cp₂Ti] and [Cr(NR)₂] (**Section 1.10.2**). This isolobal link is significant as complexes such as Cp₂TiCl₂ when reacted with a suitable co-initiator (such as MAO) readily polymerize ethylene *via* a Ziegler-type mechanism.⁶³ Although the isolobal analogy is strictly structural,⁶⁴ and hence cannot be used to map complexes' reactivity, chromium *bis*(imido) complexes can indeed be used as ethylene polymerization pre-catalysts.⁶⁵ Consequently a wide range of chromium *bis*(imido) complexes and their derivatives have been synthesised with the aim of developing discrete and active olefin polymerization initiators.

Reaction of the di-oxo complex CrO₂Cl₂, with ^tBuNHSiMe₃ provides an entry into chromium imido chemistry, with imido formation *via* Si-N bond cleavage giving

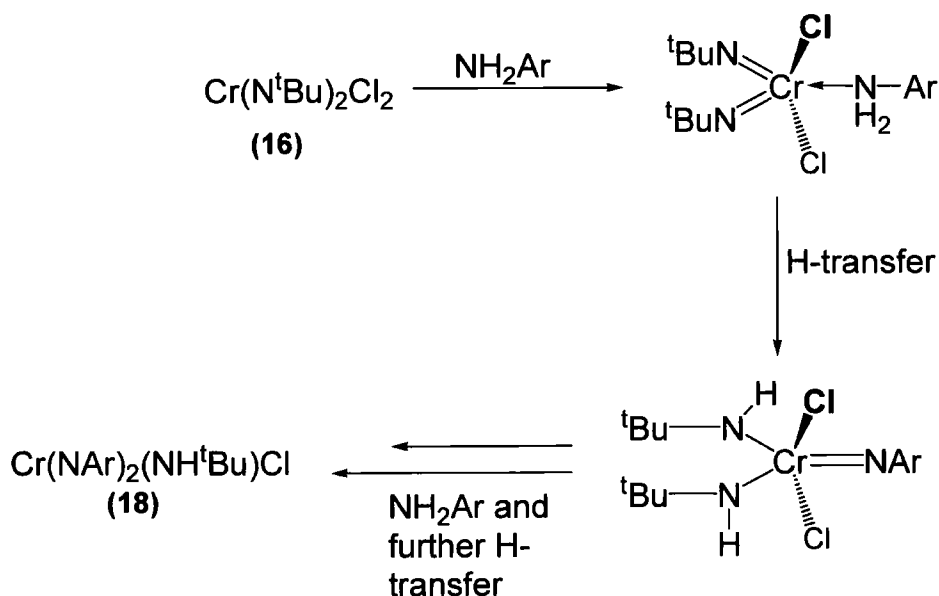
$\text{Cr}(\text{N}^t\text{Bu})_2(\text{OSiMe}_3)_2$ (**15**).⁵⁷ The dichloride *bis*(imido) complex $\text{Cr}(\text{N}^t\text{Bu})_2\text{Cl}_2$ (**16**) can then be obtained by addition of BCl_3 (**Scheme 1.19**).

Scheme 1.19 Synthesis of $\text{Cr}(\text{N}^t\text{Bu})_2(\text{OSiMe}_3)_2$ (**15**) and $\text{Cr}(\text{N}^t\text{Bu})_2\text{Cl}_2$ (**16**)



The d^0 *bis*(imido) complex $\text{Cr}(\text{N}^t\text{Bu})_2\text{Cl}_2$ (**16**) can readily be converted into a range of derivatives including the d^1 *mono*(imido) complex $\text{Cr}(\text{N}^t\text{Bu})\text{Cl}_3$ (**17**) by reaction with Cl_2 .⁶⁶ Addition of amines to **16** results in an imido exchange. Thus, reaction of $\text{Cr}(\text{N}^t\text{Bu})_2\text{Cl}_2$ (**16**) with NH_2Ar gives the *bis*(imido) amido complex $\text{Cr}(\text{NAr})_2(\text{NH}^t\text{Bu})\text{Cl}$ (**18**), which can readily be transformed into $\text{Cr}(\text{NAr})_2\text{Cl}_2$ by addition of BCl_3 .⁶⁷ It is proposed that $\text{Cr}(\text{NAr})_2(\text{NH}^t\text{Bu})\text{Cl}$ (**18**) is generated from complex **16** via a hydrogen transfer mechanism (**Scheme 1.20**).

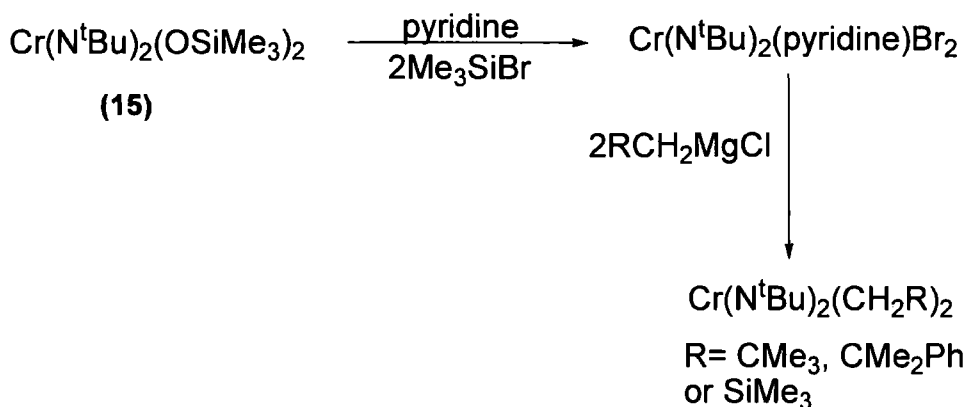
Scheme 1.20 Proposed hydrogen transfer mechanism of imido ligand exchange



Chromium *bis*(imido) systems can readily be alkylated, with addition of $\text{PhCH}_2\text{-MgBr}$ to $\text{Cr}(\text{N}^t\text{Bu})_2\text{Cl}_2$ (**16**) affording the complex $\text{Cr}(\text{N}^t\text{Bu})_2(\text{CH}_2\text{Ph})_2$ (**19**) in high yields.⁶⁸

Alternatively, $\text{Cr}(\text{N}^t\text{Bu})_2(\text{OSiMe}_3)_2$ (**15**) can be used as a precursor for a range of dialkyl complexes, invariably isolated as red oils (**Scheme 1.21**).¹⁴

Scheme 1.21 Synthesis of bis(imido) dialkyl derivatives of $\text{Cr}(\text{N}^t\text{Bu})_2(\text{OSiMe}_3)_2$

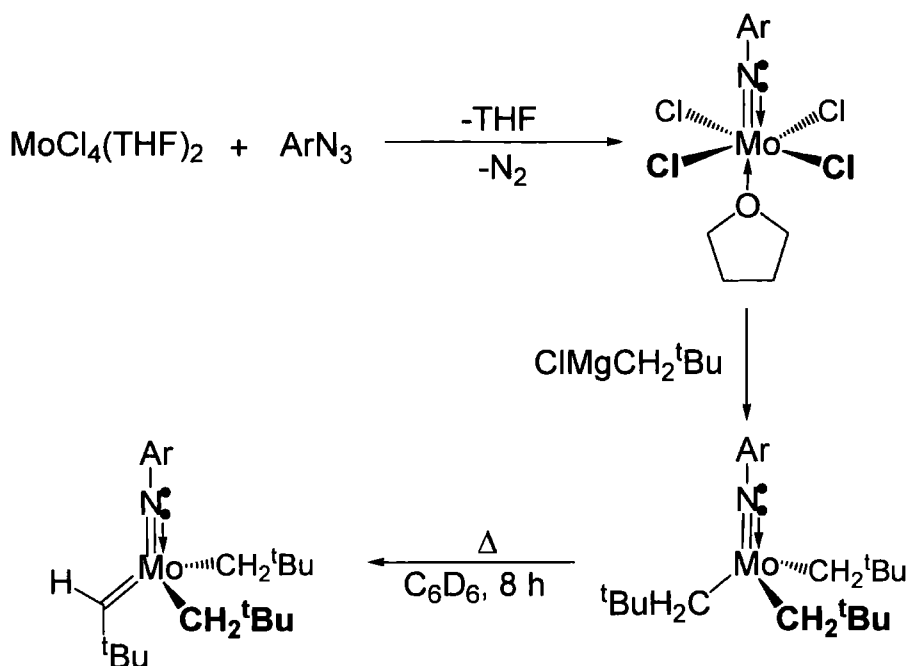


Exploiting the reactivity of $\text{Cr}(\text{N}^t\text{Bu})_2(\text{CH}_2\text{Ph})_2$ (**19**) has led to the development of a new class of well defined single component ethylene polymerization initiator by Gibson *et al.*⁶⁹ Addition of $[\text{Ph}_3\text{C}][\text{B}(\text{C}_6\text{F}_5)]$ to complex **19** generates the ionic complex $[\text{Cr}(\text{N}^t\text{Bu})_2(\eta^2\text{-CH}_2\text{Ph})][\text{B}(\text{C}_6\text{F}_5)]$ (**20**), which Gibson has reported to be able to initiate ethylene polymerization, on an NMR scale, without requiring a separate co-initiator. Thus, the further development of chromium *bis*(imido) systems ultimately may lead to well defined single-component alkene polymerization initiators.

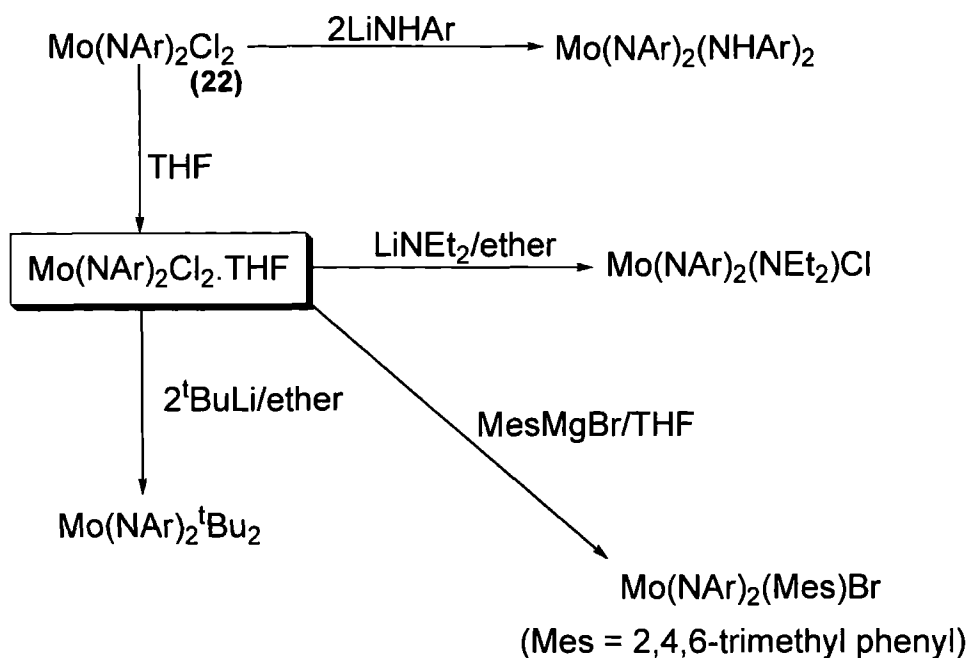
1.11.2 Synthesis and Reactivity of Molybdenum Imido Complexes

In contrast to chromium, a wider range of precursors are known from which the corresponding molybdenum imido complexes can be generated. For example, molybdenum *mono*(imido) complexes have been prepared by Schrock *et al.* and have been used subsequently as precursors to alkyl alkylidene complexes (**Scheme 1.22**).⁷⁰

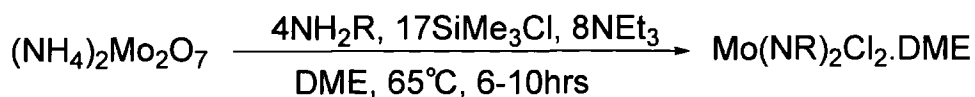
Scheme 1.22 Deriving molybdenum alkylidene complexes from mono(imido) precursors



With the aim of developing precursors to novel molybdenum-alkylidene complexes a range of molybdenum *bis*(imido) complexes have been synthesised, *via* reaction of MoO_2Cl_2 with isocyanates. For example, reaction of MoO_2Cl_2 with ${}^t\text{BuNCO}$ generates $\text{Mo}(\text{N}{}^t\text{Bu})_2\text{Cl}_2$ (**21**) in high yields (~95%).⁷¹ Using a similar procedure, $\text{Mo}(\text{NAr})_2\text{Cl}_2 \cdot \text{THF}$ (**22**) can be prepared *via* reaction of MoO_2Cl_2 with ArNCO .⁷¹ Furthermore, complex **22** provides ready access to a range of *bis*(aryl imido) complexes. For example, reaction with both lithium alkyls and lithiated amines has been utilized to afford access to a range of *bis*(imido) derivatives (**Scheme 1.23**).⁷²

Scheme 1.23 Reactions of $\text{Mo}(\text{NAr})_2\text{Cl}_2 \cdot \text{THF}$ and $\text{Mo}(\text{NAr})_2\text{Cl}_2$ 

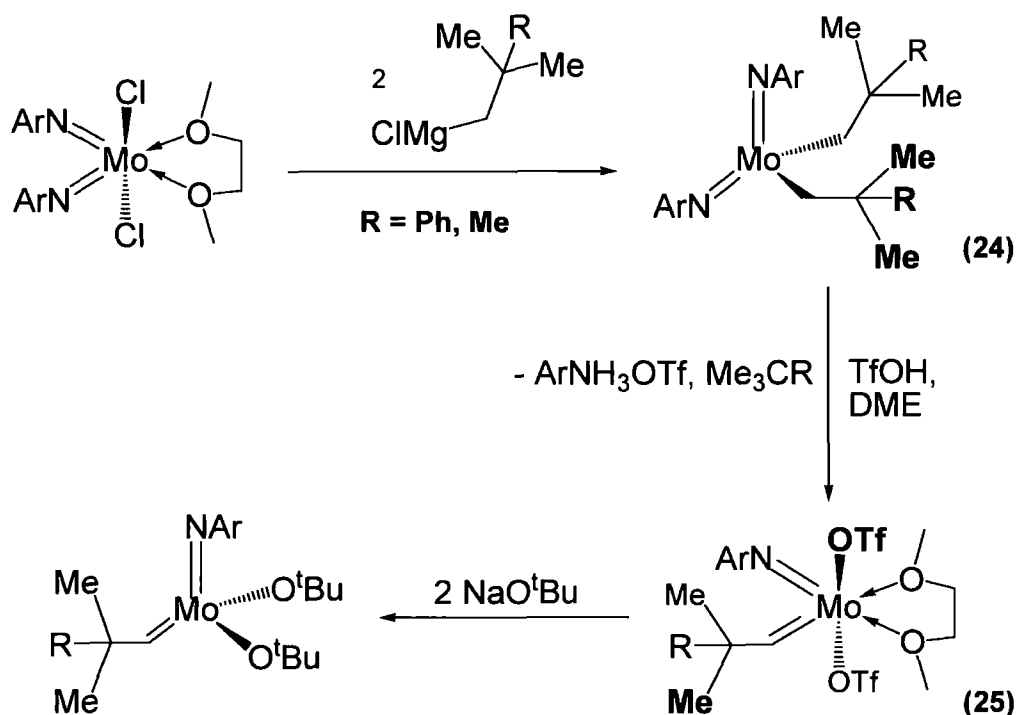
While the reactions between MoO_2Cl_2 and isocyanates are generally high-yielding, synthetic routes employing cheaper, air stable molybdenum starting materials such as $(\text{NH}_4)_2\text{Mo}_2\text{O}_7$ have been reported by Schrock *et al.*⁷³ For example, a straight forward “one-pot” reaction of $(\text{NH}_4)_2\text{Mo}_2\text{O}_7$ suspended in dimethoxyethane (DME), with two equivalents of a substituted aniline, in the presence of excess ClSiMe_3 and Et_3N results in the formation of the *bis*(imido) complexes $\text{Mo}(\text{NR})_2\text{Cl}_2 \cdot \text{DME}$ (**Scheme 1.24**) in near quantitative yields. Imido synthesis occurs *via* Si-N bond cleavage, with the (trimethylsilyl)amine believed to be generated *in situ*.

Scheme 1.24 Synthesis of $\text{Mo}(\text{NR})_2\text{Cl}_2 \cdot \text{DME}$ from $(\text{NH}_4)_2\text{Mo}_2\text{O}_7$ **R=**

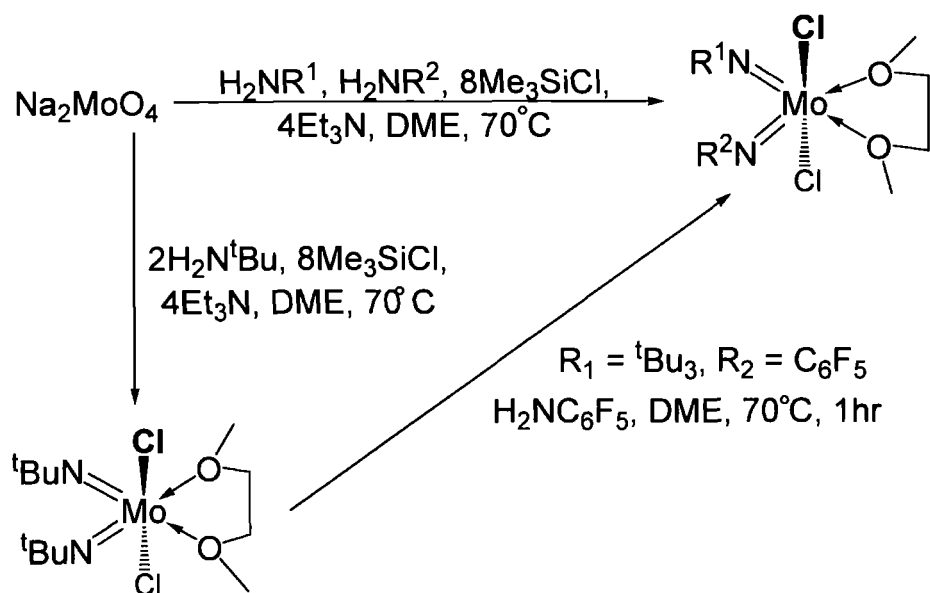
- 2,6-diisopropyl-phenyl
- 2,6-dimethyl-phenyl
- 2-tert-butyl-phenyl
- pentafluorophenyl

As complexes such as $\text{Mo}(\text{NAr})_2\text{Cl}_2\cdot\text{DME}$ (**23**) can be prepared from $(\text{NH}_4)_2\text{Mo}_2\text{O}_7$ in large quantities (in excess of 20 g), the *bis(imido)* complex $\text{Mo}(\text{NAr})_2\text{Cl}_2\cdot\text{DME}$ (**23**) is an ideal precursor to imido alkylidene olefin metathesis initiators (**Scheme 1.25**). This is achieved by initial alkylation of $\text{Mo}(\text{NAr})_2\text{Cl}_2\cdot\text{DME}$ (**23**) with neopentyl or neophyl Grignard reagents. Treatment of the resulting dialkyl complex (**Scheme 1.25**, **24**) with triflic acid, simultaneously results in imido cleavage and formation of the molybdenum-carbon bond, giving an eighteen electron *bis(triflate)* complex **25** (**Scheme 1.25**). Finally, addition of alkoxide or arloxide salts (Li, Na or K) gives the desired alkylidene complex *via* nucleophilic substitution.⁷⁴

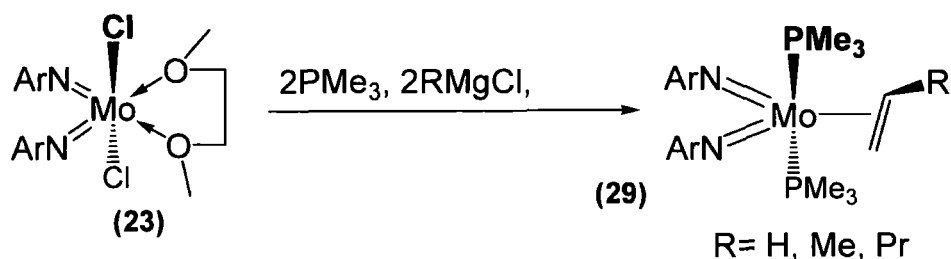
Scheme 1.25 Preparation of $\text{Mo}(\text{NAr})(\text{CHC}(\text{CMe})_2\text{R})(\text{O}^t\text{Bu})_2$



Using a similar procedure to that employed in Schrock's synthesis of $\text{Mo}(\text{NAr})_2\text{Cl}_2\cdot\text{DME}$ (**23**) from $(\text{NH}_4)_2\text{Mo}_2\text{O}_7$. Gibson *et al.*, have synthesised molybdenum *bis(imido)* complexes using the precursor Na_2MoO_4 .⁷⁵ Addition of two separate amines to a DME suspension of Na_2MoO_4 was found to be a viable route to mixed *bis(imido)* complexes, which have also been used as intermediates in the synthesis of metathesis initiators. Alternatively mixed *bis(imido)* complexes can be obtained by treatment of $\text{Mo}(\text{N}^t\text{Bu})_2\text{Cl}_2\cdot\text{DME}$ (**26**) with a substituted aniline (such as $\text{H}_2\text{NC}_6\text{F}_5$) (**Scheme 1.26**).

Scheme 1.26 Synthetic routes to mixed bis(imido) complexes

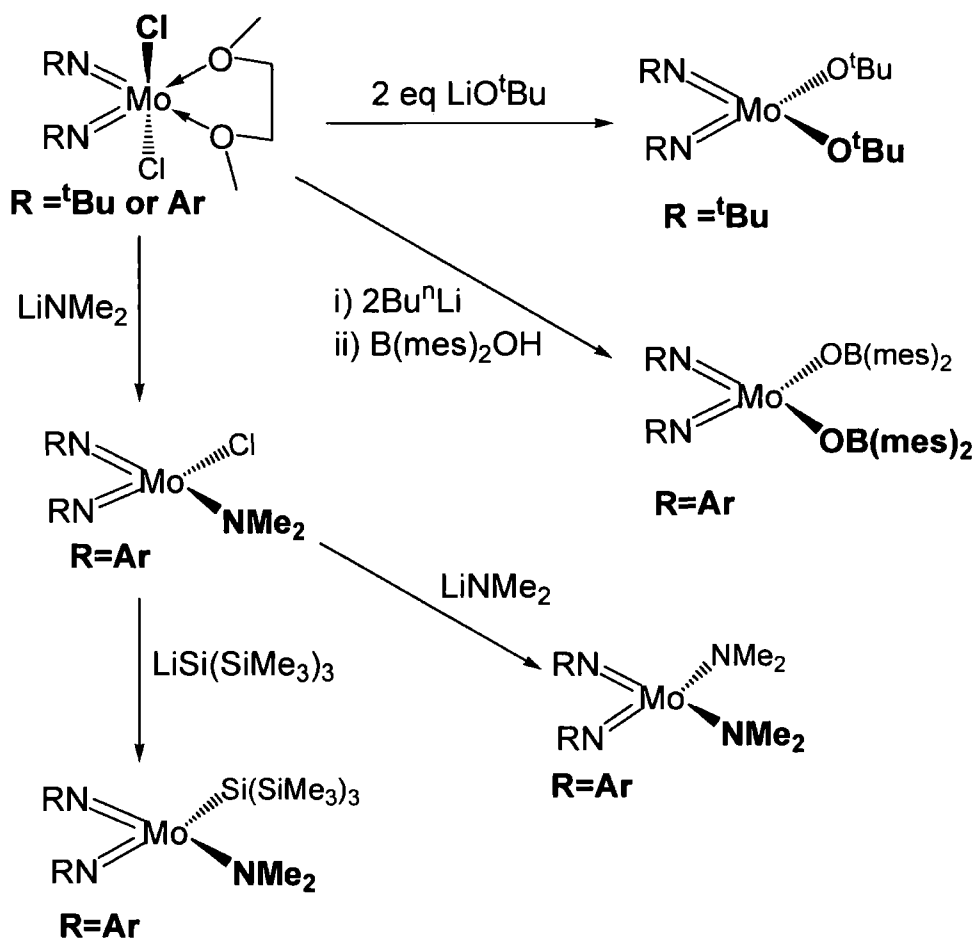
The ready availability of $\text{Mo}(\text{NR})_2\text{Cl}_2\cdot\text{DME}$ complexes on large scales has allowed a broad number of derivatives to be synthesised containing the molybdenum *bis*(imido) moiety. For example, reaction with simple Grignard reagents such as MeMgBr ⁷⁶ or $\text{Li}(\text{fmes})$ ⁷⁷ (*fmes* = 2,4,6 tris(trifluoromethyl) phenyl) have shown that DME can be displaced, allowing access to the *pseudo*-four-coordinate dialkyl products $\text{Mo}(\text{NAr})_2\text{Me}_2$ (**27**) and $\text{Mo}(\text{NAr})_2(\text{fmes})_2$ (**28**) respectively. Alternatively, similar reactions using Grignard reagents containing β -hydrogen atoms results in reduction of the molybdenum centre. Thus, addition of $\text{CH}_3\text{CH}_2\text{MgCl}$ or $\text{CH}_3\text{CH}_2\text{CH}_2\text{MgCl}$ to $\text{Mo}(\text{NAr})_2\text{Cl}_2\cdot\text{DME}$ (**23**) in the presence of PMe_3 has been shown, to generate *bis*(imido) Mo^{IV} -olefin complexes such as $\text{Mo}(\text{NAr})_2(\text{PMe}_3)_2(\eta^2\text{CH}_2\text{CH}_2\text{CH}_3)$ (**29**) (**Scheme 1.27**).⁷⁸

Scheme 1.27 Alkene complexes stabilized by PMe_3 with a $\text{Mo}(\text{NAr})_2$ moiety

In contrast, the related ^tBu imido analogue to complex **29**, Mo(N^tBu)₂(PMe₃)(η²-CH₂CHCH₃) (**30**), is only four coordinate. It is reasoned that in the aforementioned NAr *bis*(imido) system there is greater scope for the aryl imidos to alter their orientation, allowing coordinating of a second PMe₃ ligand, giving a five coordinate molybdenum centre.⁷⁹

As well as Grignard reagents, the chloride ligands of Mo(NR)₂Cl₂.DME complexes can be readily replaced by nitrogen and silyl,⁸⁰ oxygen,⁸¹ and oxygen-boron nucleophiles,⁸² to give tetrahedral Mo(NR)₂X₂ complexes and a salt, typically LiCl (**Scheme 1.28**). The *bis*(imido) molybdenum core has also been chelated by both *bis*(sulphur) donors⁸³ and 1,4,7-triazacyclononane macrocycles.⁸⁴

Scheme 1.28 Reaction of lithium-based reagents with Mo(NR)₂Cl₂.DME (R = ^tBu or Ar)



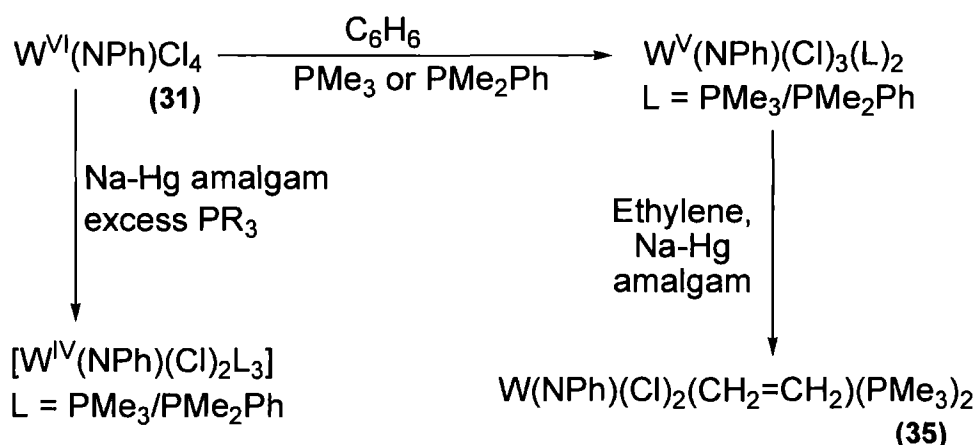
Thus, there is evidently a large range of synthetic procedures that can be used to modify molybdenum *bis*(imido) complexes, generating a plethora of derivatives. Similarly a wide range of tungsten *mono* and *bis*(imido) complexes have been reported, some of which will be discussed in the following subsection.

1.11.3 Synthesis and Reactivity of Tungsten Imido Complexes

A notable recent application of tungsten imido complexes comes from the potential of thin tungsten carbonitride films as barrier layers in electronic devices. One method of preparing WC_xN_y films is *via* low pressure chemical vapour deposition of tungsten imido complexes onto suitable surfaces.⁸⁵ As for chromium and molybdenum, tungsten imido complexes can be prepared from readily available tungsten oxo compounds. For example, polymeric $WOCl_4$ can be reacted with an isocyanate ($PhNCO$) to give $W(NPh)Cl_4$ (**31**), which may upon subsequent addition of THF, be converted to the adduct $W(NPh)Cl_4 \cdot THF$ (**32**).⁸⁶

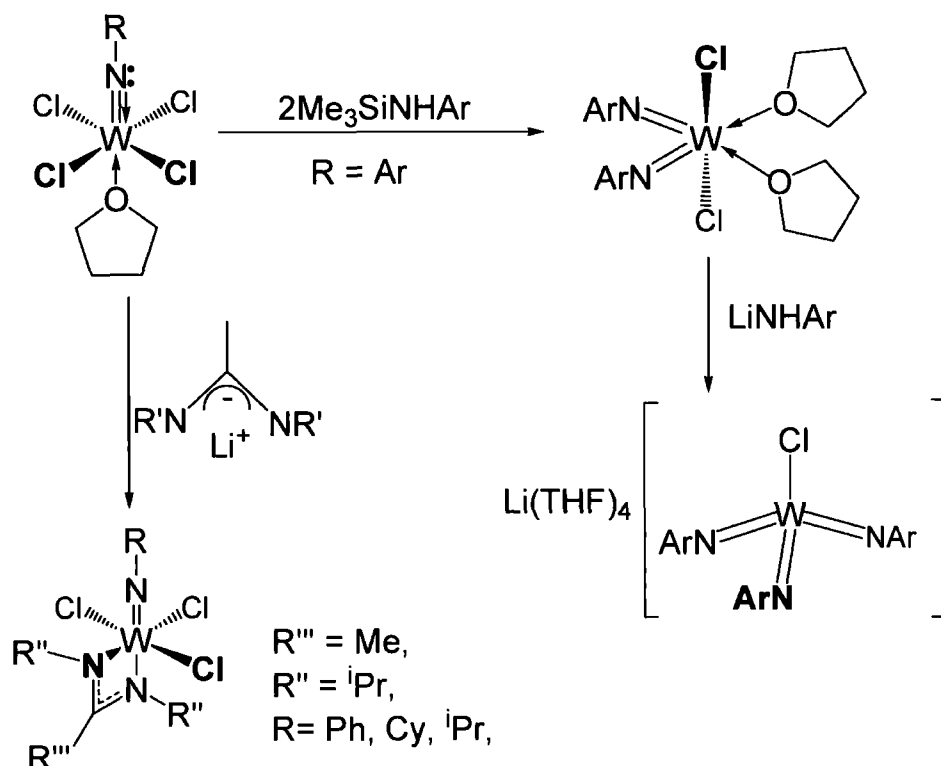
The *mono(imido)* complex $W(NPh)Cl_4$ (**31**) can be used as a precursor to make a range of derivatives (**Scheme 1.29**).⁸⁷ Heating a solution of $W(NPh)Cl_4$ (**31**) dissolved in benzene in the presence of a phosphine, results in reduction of the tungsten atom, giving the W^V *mono(imido)* complexes $W(NPh)(Cl)_3L_2$ ($L = PMe_3$ or PMe_2Ph). The W^V complex $W(NPh)(Cl)_3(PMe_3)_2$ (**33**) can itself be further reduced by Na/Hg amalgam, again presence of a phosphine, to give the W^{IV} complex $W(NPh)(Cl)_2(PMe_3)_3$ (**34**). Ethylene can then be used to displace a phosphine ligand from **34** to give the complex $[WCl_2(NPh)(CH_2=CH_2)(PMe_3)_2]$ (**35**). Using closely related procedures $W(NAr)(Cl)_2(PMe_3)_3$ (**36**) can be prepared and reacted with ethylene to give $[W(NAr)(CH_2=CH_2)(PMe_3)_2]$ (**37**).⁸⁸

Scheme 1.29 Synthesis of tungsten *mono(imido)* complexes via reduction of $W(NPh)Cl_4$



As well as being readily reduced, *mono(imido)* complexes such as $W(NAr)Cl_4 \cdot THF$ (**38**) can be reacted with nitrogen-based reagents such as silyl amines to give both *bis-* and *tris(imido)* complexes.⁸⁹ Alternatively, reaction of lithiated amines results in *mono(imido)* amidinate and guanidinate complexes (**Scheme 1.30**).⁹⁰

Scheme 1.30 Derivatives obtained from addition of nitrogen-based reagents to *mono(imido) complexes*

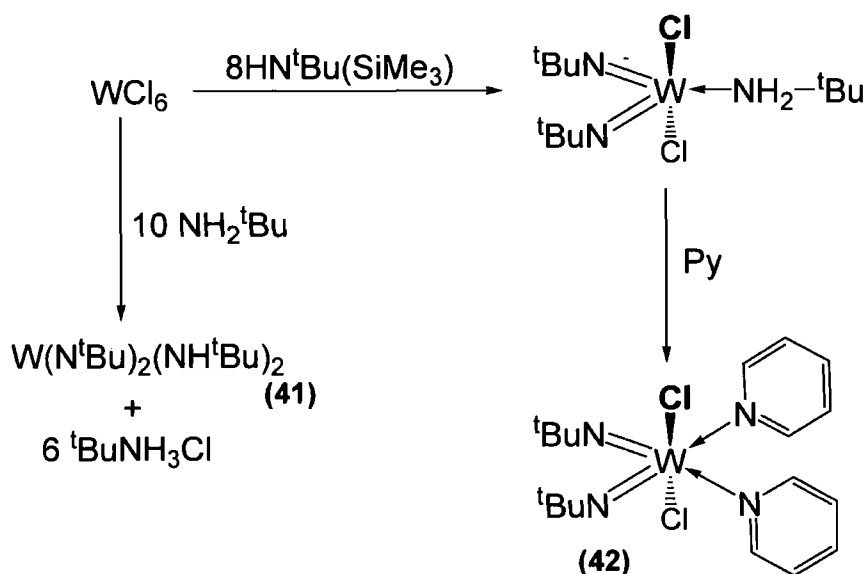


Reaction of the *mono(imido) complexes* $W(NR)Cl_4 \cdot THF$ with silyl amines has become an established route to the synthesis of related *bis(imido) complexes*. For example, Nielson *et al.* have synthesised the mixed *bis(imido) complex* $W(NPh)(N(C_6H_4-p-Me)Cl_2(bipy))$ (**39**) *via* reaction of $W(NPh)Cl_4 \cdot THF$ (**32**) and $p-MeC_6H_4N(SiMe_3)_2$.⁹¹ Alternatively, *bis(imido) complexes* can be prepared directly, in “one-pot” procedures, without the requirement of isolating a *mono(imido) intermediate*. Schrock *et al.* has reported the synthesis of $W(NAr)_2Cl_2 \cdot DME$ (**40**) directly from the precursor WO_2Cl_2 *via* reaction of isocyanates, amines or silyl amines.⁹² It has also been reported that the cheap, readily available tungsten complex $W(CO)_6$ can be used to synthesise tosyl *bis(imido) complexes* such as $W(NTs)_2Cl_2$.⁹³

Of relevance to WCl_6 -based dimerization systems (see **Section 1.6**) is that *bis(imido) complexes* can be prepared directly from reaction of WCl_6 with excess NH_2^tBu giving the *bis(imido) bis(amido) complex* $W(N^tBu)_2(NH^tBu)_2$ (**41**).⁹⁴ Similarly the *bis(imido) complex* $W(N^tBu)_2Cl_2 \cdot (py)_2$ (**42**) can be made from reaction of WCl_6 and $NH(SiMe_3)^tBu$ (**Scheme 1.31**).⁹⁵ Thus, the synthesis of **41** and **42** directly from WCl_6 , further indicates that imido moieties can be formed *in situ* in the Goodyear or STUK

dimerization processes (**Section 1.6, Scheme 1.7**), in which an unknown initiator complex is formed *via* reaction of WCl_6 with two equivalents of an aniline.

Scheme 1.31 Direct synthesis of tungsten bis(imido) complexes from WCl_6

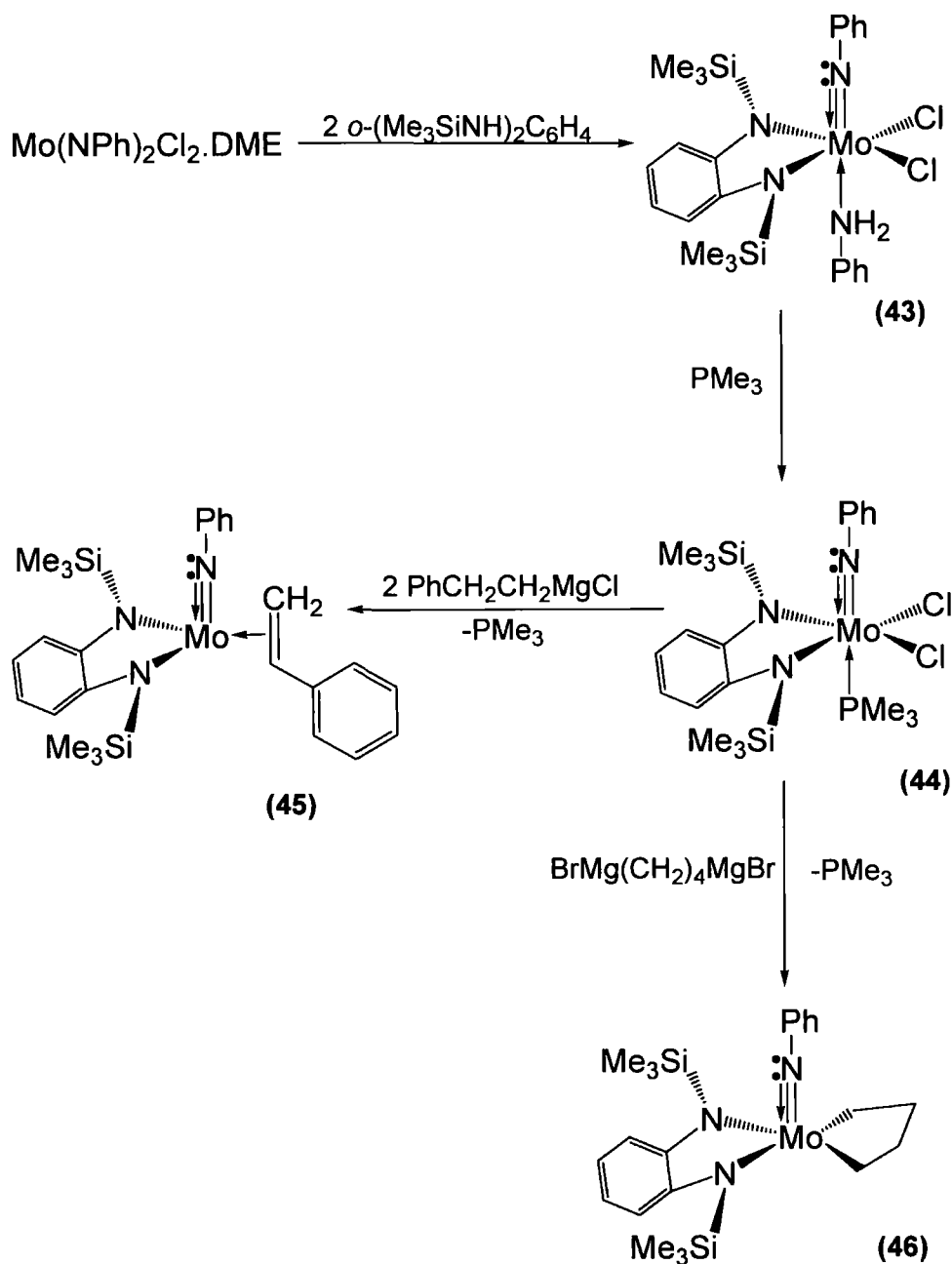


1.12 Synthesis and Reactivity of Tungsten and Molybdenum Diamine-chelated Complexes

Both tungsten and molybdenum *mono*(imido) complexes can be stabilized by a diamine to give a family of M^{VI} complexes with the general formula $M(NPh)Cl_2(L)(o-(Me_3SiN)_2C_6H_4)$ ($M = W$ or Mo , $L = NH_2R$ or PR_3). This class of complex displays interesting reactivity with Grignard reagents and olefins, which suggest that tungsten or molybdenum imido complexes can act as dimerization initiators *via* a metallacycle pathway.^{96,97} Thus, the general reactivity of $M(NPh)Cl_2(L)(o-(Me_3SiN)_2C_6H_4)$ ($M = W$ or Mo) complexes supports the notion that in the WCl_6 -based olefin dimerization systems outlined in **Section 1.6** an imido initiator complex is forming *in situ*.

Boncella *et al.*, synthesised the *mono*(imido) molybdenum complex $Mo(NPh)Cl_2(NH_2Ph)(o-(Me_3SiN)_2C_6H_4)$ (**43**) from reaction of $Mo(NPh)_2Cl_2 \cdot DME$ with $(Me_3SiNH_2)_2$.⁹⁶ The bound NH_2Ph ligand of **43** can readily be displaced by PMe_3 to give the complex $Mo(NPh)Cl_2(PMe_3)(o-(Me_3SiN)_2C_6H_4)$ (**44**), which readily undergoes reaction with a range of Grignard reagents forming, for example, the complexes $Mo(NPh)(CH_2CHPh)(o-(Me_3SiN)_2C_6H_4)$ (**45**) and $Mo(NPh)(CH_2)_4(o-(Me_3SiN)_2C_6H_4)$ (**46**) (**Scheme 1.32**).⁹⁷

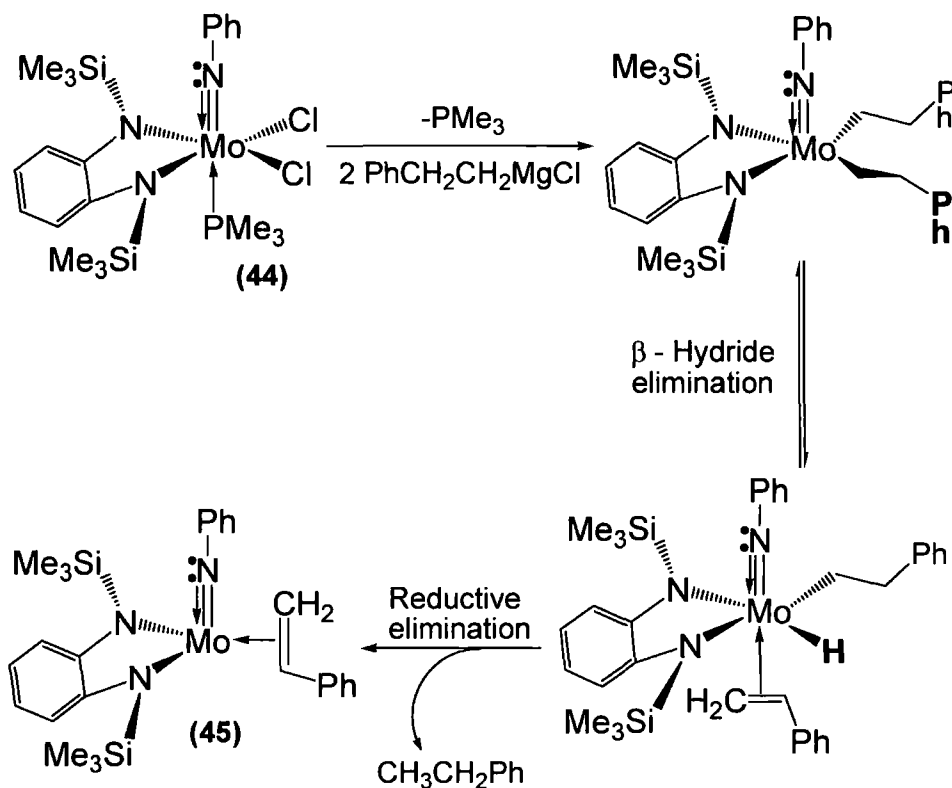
Scheme 1.32 Synthesis and reactivity of chelate-stabilized mono (molybdenum) d^2 complexes from $\text{Mo}(\text{NPh})_2\text{Cl}_2\cdot\text{DME}$



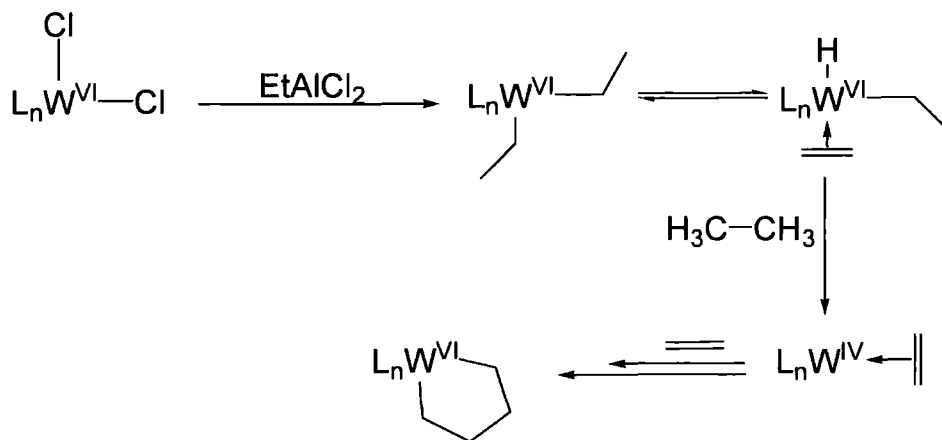
The formation of complex **45** undoubtedly occurs *via* alkylation of **44**, giving a di-alkyl intermediate, which then undergoes β -hydride elimination, followed by reductive elimination (**Scheme 1.33**). Thus, the isolation of **45** demonstrates that a Mo^{VI} complex can be reduced to a Mo^{IV} species by reaction with an appropriate alkylating agent. It is possible to envisage a similar reaction pathway occurring in WCl_6 -based dimerization systems (**Section 1.6**). The isolation of complex **45**, suggests that alkylation of a tungsten core (by a $\text{Et}_x\text{AlCl}_{3-x}$ co-initiator) could then result in reduction,

yielding a W^{IV} intermediate capable of initiating dimerization via metallacycle formation (**Scheme 1.34**).

Scheme 1.33 Formation of complex **45** via β -hydride elimination



Scheme 1.34 Potential formation of W^{VI} complexes in WCl_6 -based dimerization systems



Boncella has characterized $Mo(NPh)(CH_2CHPh)(o-(Me_3SiN)_2C_6H_4)$ (**45**) using 2D COSY NMR experiments, which indicate that **45** adopts one of two conformations in

solution, resulting from differing positions of the molybdenum η^2 bound styrene moiety of complex **45** relative to the "fixed" imido. It is proposed that with a large degree of back bonding from the d^2 -metal, there is a considerable barrier to olefin rotation (CH_2CHPh), forcing the olefin moiety of complex **45** to adopt one of two orientations.

Synthesis of the metallacyclic complex $\text{Mo}(\text{NPh})(\text{CH}_2)_4(o\text{-(Me}_3\text{SiN)}_2\text{C}_6\text{H}_4)$ (**46**) (Scheme 1.32) is of great significance as it demonstrates that group VI metallacyclopentanes are stable; suggesting that alkene coupling *via* a metallacycle (or oxidative coupling) mechanism in the STUK WCl_6 dimerization system is viable (Section 1.6). Indeed, complex **46** is sufficiently stable to allow investigations into its reactivity to be made. Thus, Boncella has reacted the metallacyclic complex **46** with isocyanides (resulting in displacement of the metallacycle by isocyanide ligands)⁹⁸ and AlMe_3 (Scheme 1.35).⁹⁹

Scheme 1.35 Reactivity of a chelate-stabilized mono(imido) complex with AlMe_3

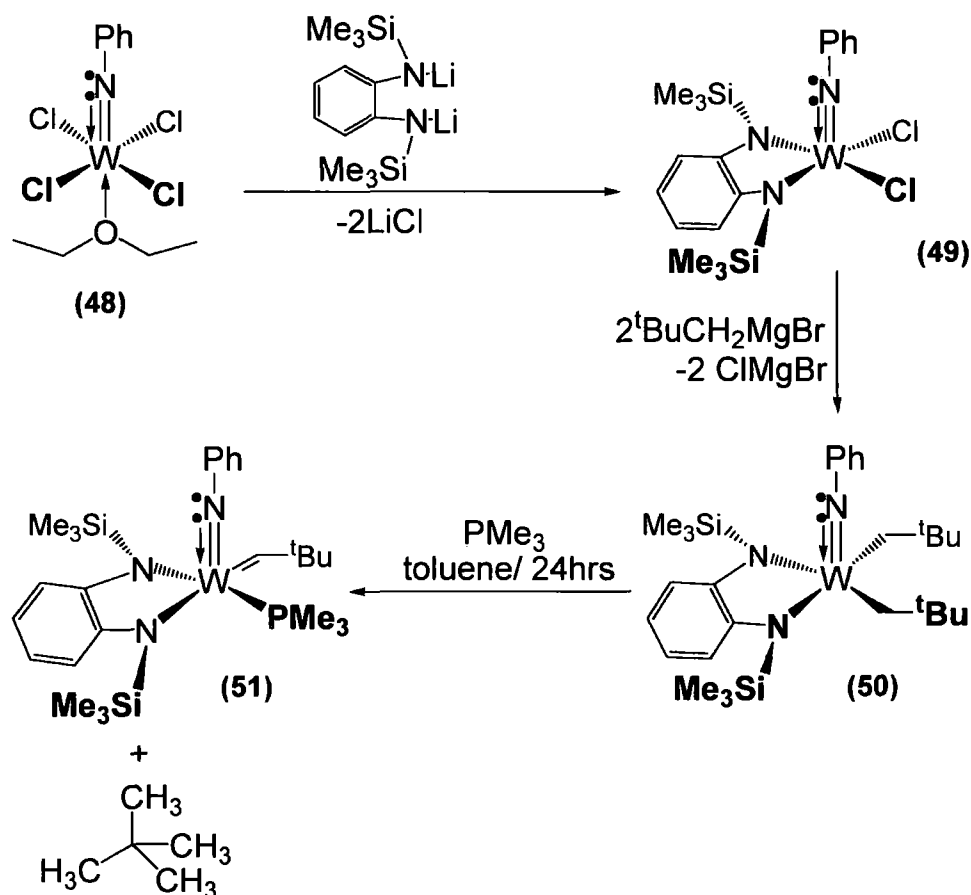


Addition of Me_3Al to $\text{Mo}(\text{NPh})(\text{CH}_2)_4(o\text{-(Me}_3\text{SiN)}_2\text{C}_6\text{H}_4)$ (**46**) (Scheme 1.35) does not simply result in alkylation of the molybdenum centre. Instead, Me_3Al also reacts as a Lewis acid forming an aluminium-centred anion, which stabilizes the new d^0 -molybdenum centre giving complex $\text{Mo}(\text{NPh})\text{CH}_3(\text{CH}_2)_4(\eta^4\text{-C}_6\text{H}_4\text{-}o\text{-(Me}_3\text{SiN)}_2\text{AlMe}_2)$ (**47**) (Scheme 1.35). The formation of **47** *via* reaction of Me_3Al as a Lewis acid indicates that for the STUK WCl_6 dimerization system, the EtAlCl_2 co-initiator is unlikely to react only as a simple alkylating agent. Indeed, the synthesis of **47** demonstrates that aluminium based Lewis acids such as EtAlCl_2 or Me_3Al , have the capacity to interact with electron-rich nitrogen donors, such as imido ligands.

Tungsten *mono*(imido) diamine complexes can also be readily prepared, directly from *mono*(imido) precursors. Thus, $\text{W}(\text{NPh})\text{Cl}_4(\text{OEt})$ (**48**) can easily be converted into $\text{W}(\text{NPh})\text{Cl}_2(o\text{-(Me}_3\text{SiN)}_2\text{C}_6\text{H}_4)$ (**49**) (Scheme 1.36), which readily reacts with Grignard reagents to give relatively stable di-alkyl complexes (Scheme 1.36, complex **50**).¹⁰⁰ Although the dialkyl complex **50** is stable and does not readily

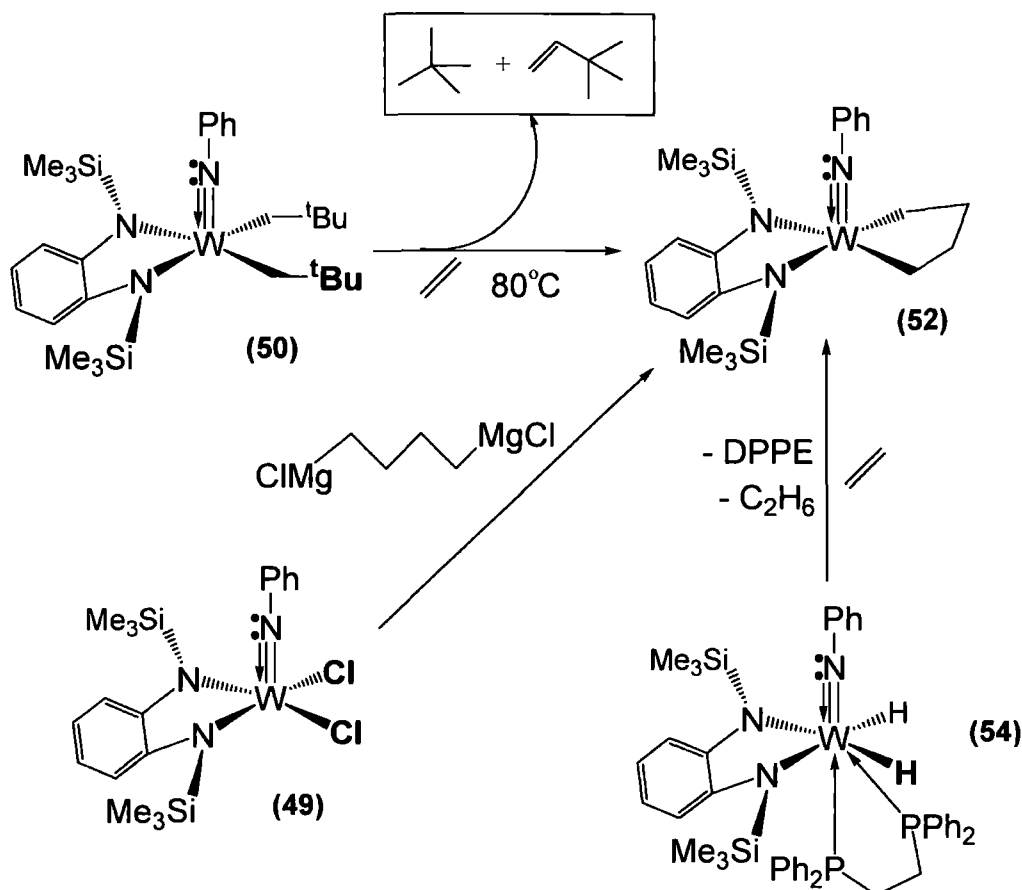
undergo reductive elimination, complex **50** can be induced to undergo α -elimination in the presence of PMe_3 to give an alkylidene product (**Scheme 1.36**, complex **51**).

Scheme 1.36 Synthesis of tungsten chelate-stabilized *mono(imido)* complexes

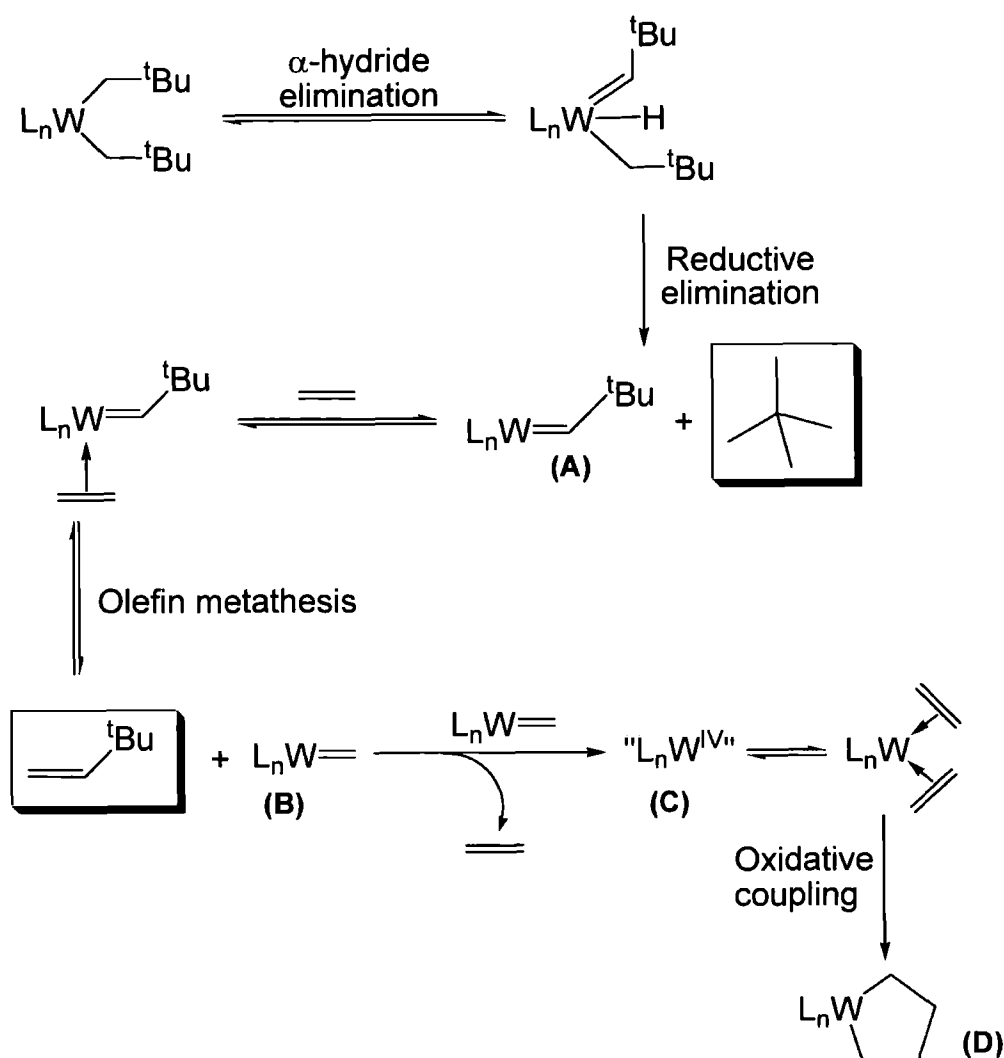


The stabilized *mono(imido)* tungsten metallacyclic complex $\text{W}(\text{NPh})(\text{CH}_2)_4(o\text{-(Me}_3\text{SiN)}_2\text{C}_6\text{H}_4)$ (**52**) can be formed *via* reaction of the di-Grignard $\text{Mg}(\text{CH}_2)_4$ with complex **49** (**Scheme 1.37**). Alternatively a metallacycle moiety can be synthesised by reaction of ethylene with an alkyl¹⁰¹ (**53**) or hydride¹⁰² (**54**) complexes (**Scheme 1.37**).

Scheme 1.37 – Formation of W^VI metallacycles from both alkyl and hydride precursors



A mechanism rationalizing the conversion of **50** to **52** can be proposed, following identification of the reaction by-products, neohexene and $\text{CH}_2\text{CH}^t\text{Bu}$ (**Scheme 1.38**).¹⁰¹ Production of neohexene demonstrates that **50** initially undergoes α -hydride elimination reaction, followed by a reductive elimination to give an alkylidene functionality (**Scheme 1.38**, intermediate **A**). Metathesis with ethylene then generates the second reaction by-product $\text{CH}_2\text{CH}^t\text{Bu}$ and a tungsten methylidene complex (**Scheme 1.38**, intermediate **B**). Reaction of two tungsten methylidene complexes then gives a W^VI core (**Scheme 1.38**, intermediate **C**), which can readily undergo oxidative coupling with ethylene to give a metallacycle (**Scheme 1.38**, intermediate **D**).

Scheme 1.38 Mechanism of metallacycle formation from tungsten dialkyl species

Examination of the mechanism by which $\text{W}(\text{NPh})(\text{CH}^t\text{Bu})_2(o\text{-(Me}_3\text{SiN)}_2\text{C}_6\text{H}_4)$ (**53**) reacts with ethylene to give $\text{W}(\text{NPh})(\text{CH}_2)_4(o\text{-(Me}_3\text{SiN)}_2\text{C}_6\text{H}_4)$ (**52**), reveals that oxidative coupling of two ethylene molecules to a W^{VI} atom is indeed a favourable reaction pathway. This is of relevance to the STUK WCl_6 olefin dimerization system (WCl_6 , $2\text{NH}_2\text{R}$, $4\text{Et}_3\text{N}$, 10EtAlCl_2), in which alkene dimerization is believed to proceed *via* metallacycle formation, in an oxidative coupling mechanism. Thus, the synthesis of complex **52** further suggests that metallacycle intermediates are generated in alkene dimerization systems based on WCl_6 .

1.13 Aims of this Thesis

The broad aim of this thesis is to increase understanding of the STUK WCl_6 -based olefin dimerization system (WCl_6 , $2H_2NR$, $4Et_3N$, $10 EtAlCl_2$), with the view of identifying both the mechanism of alkene coupling and the nature of the active initiator complex. Evolution of HCl in the STUK system, strongly suggests that either *mono* or *bis*(imido) complexes are formed *in situ* from reaction of WCl_6 and H_2NR . This has been corroborated by Olivier *et al.* who have shown that discrete *mono*(imido) complexes can initiate ethylene dimerization, when co-initiated by $EtAlCl_2$.³¹ Significantly, reactions of $EtAlCl_2$ and *mono*(imido) complexes, e.g. $W(NR)Cl_4 \cdot THF$, have not been studied in the absence of olefin. Thus, a key aim of this work is to investigate the reaction of $EtAlCl_2$ and $W(NR)Cl_4 \cdot THF$ complexes, with the aim of assessing the mode by which $EtAlCl_2$ acts as a co-initiator. It is clear that aluminium alkyl halides such as $EtAlCl_2$ have the capacity to interact with either the chloride or imido ligands of a $W(NR)Cl_4$ fragment as both types of ligands have lone pairs available to donate to a R_xAlCl_{3-x} Lewis acid. Hence, an endeavour of this work is to assess, through the use of model reactions, the ability of a range of R_xAlCl_{3-x} reagents to bind to tungsten *mono*(imido) chloride complexes. The consequence of R_xAlCl_{3-x} coordination, to the reactivity of tungsten systems with ethylene is also of general interest. It is hoped that understanding the influence of R_xAlCl_{3-x} coordination, to a given complexes reactivity with alkenes, could provide key insights into the mode by which imido chloride pre-catalysts are activated by aluminium-based co-initiators.

It is clear from the reaction stoichiometry of the STUK system, in which WCl_6 is reacted with two equivalents of H_2NR that a *bis*(imido) complex could readily be formed *in situ*. As for *mono*(imido) systems it is known that both $M(NR)_2Cl_2 \cdot DME$ ($M = W$ or Mo) complexes, when treated with $EtAlCl_2$ can initiate ethylene dimerization,¹⁰³ although further clarification as to the relative activities of *bis* and *mono*(imido) systems is required. Again it is unclear as to how $EtAlCl_2$ activates $W(NR)_2Cl_2 \cdot DME$ complexes for ethylene dimerization. Indeed, no previous experimental investigations assessing the reactivity of R_xAlCl_{3-x} reagents with relevant *bis*(imido) complexes have been made. One aspiration of this work is to clarify the reactivity of tungsten and molybdenum *bis*(imido) systems with a range of R_xAlCl_{3-x} reagents. It is hoped that such investigations will increase insight into how $EtAlCl_2$ activates *bis*(imido) pre-catalysts for alkene dimerization.

1.14 References

- ¹ F. Speiser, P. Braunstein and L. Saussine, *Acc. Chem. Res.*, **2005**, *38*, 784.
- ² J. Skupinska, *Chem. Rev.*, **1991**, *91*, 613.
- ³ i) P.Kuhn, D. Sémeril, D. Matt, M.J. Chetcuti and P. Lutz, *Dalton Trans.*, **2007**, 515; ii) P.M. Morse, *Chem. Eng. News*, **1999**, *77*, 19; iii) R.F. Mason, Shell Oil Co., *US Pat.*, 3,676,523, **1972**; iv) R.F. Mason, Shell Oil Co., *US Pat.*, 3,686,351, **1972**.
- ⁴ A.A. Adesina, *Applied Catalysis A, General.*, **1996**, *138*, 345.
- ⁵ i) C. Elschenbroich and A. Salzer, "Organometallics, a Concise Introduction," VCH, 1992; ii) *Oilfield Review.*, **2003**, Vol 15, No 3, 32.
- ⁶ J. Gaube and H.F. Klein, *J. Mol. Catal. A*, **2008**, *283*, 60.
- ⁷ M.E. Dry, *Catal. Today.*, **1990**, *6*, 183.
- ⁸ A. de Klerk, *Green Chem.*, **2008**, *10*, 1249.
- ⁹ P.J. Hansen and P.C. Jurs, *Anal. Chem.*, **1987**, *59*, 2322.
- ¹⁰ S. Muthukumar Pillai, M. Ravindranathan and S. Sivaram, *Chem. Rev.*, **1988**, *86*, 353.
- ¹¹ B.L. Small and A.J. Marcucci, *Organometallics*, **2001**, *20*, 5738.
- ¹² R. Barone, M. Chanon and M.L.H Green, *J. Organomet. Chem.*, **1980**, *185*, 85.
- ¹³ R. Emrich, O. Heinemann, P.W. Jolly, C. Krüger and G.P.J. Verhovnik, *Organometallics*, **1997**, *16*, 1511.
- ¹⁴ N. Meijboom, C.J. Schaverien and G.A. Orpen, *Organometallics*, **1990**, *9*, 774.
- ¹⁵ X. Huang, J. Zhu and Z. Lin, *Organometallics*, **2004**, *23*, 4154.
- ¹⁶ S. Datta, M.B. Fischer and S.S. Wreford, *J. Organomet. Chem.*, **1980**, *188*, 353.
- ¹⁷ S.J. McLain and R.R. Schrock, *J. Am. Chem. Soc.*, **1978**, *15*, 1315.
- ¹⁸ S.J. McLain, J. Sancho and R.R. Schrock, *J. Am. Chem. Soc.*, **1980**, *102*, 5610.
- ¹⁹ A. Buchard, A. Auffrant, C. Klemps, L. Vu-Do, L. Boubekour, X.F. Le. Goff and P. Le Floch, *Chem. Commun.*, **2007**, 1503.
- ²⁰ F. Speiser, P. Braunstein and L. Saussine, *Dalton Trans.*, **2004**, 1539.
- ²¹ C.E. Anderson, A.S. Batsanov, P.W. Dyer, J. Fawcett and J.A.K. Howard, *Dalton Trans.*, **2006**, 5378.
- ²² M. Lejeune, D. Sémeril, C. Jeunesse, D. Matt, F. Peruch, P. J. Lutz and L. Ricard, *Chem. Eur. J.*, **2004**, *10*, 5354.
- ²³ i) A.Carter, N.A. Cooley, P.G. Pringle, J. Scutt and D.F. Wass, *Polym. Mater. Sci. Eng.*, **2002**, *86*, 314; ii) V.C. Gibson and S.K. Spitzmesser, *Chem. Rev.*, **2003**, *103*, 283.

- 24 J.T. Dixon, M.J. Green, F.M. Hess and D.H. Morgan, *J. Organomet. Chem.*, **2004**, *689*, 3641.
- 25 US Patent 6,184,428 (2001) to Saudi Basic Industries Corporation, M.Zahoor, F. Al-Sherehy, O. Alabisi, M.M. Abdillahi and M.R. Saeed.
- 26 i) WO 2002/04119, to BP Chemicals Ltd, D.F. Wass; ii) A.Carter, S.A. Cohen, N.A. Cooley, A. Murphy, J. Scutt and D.F. Wass, *Chem. Commun.*, **2002**, 858.
- 27 T. Agapie, J.A. Labinger and J.E. Bercaw, *J. Am. Chem. Soc.*, **2007**, *129*, 14295.
- 28 US Patents, 3,784,631, 3,784,630, 3,784,629, 3,903,193 and 3,897,512 to The Goodyear Tire and Rubber Company (1974-75), H.R. Menapace, G.S. Benner and N.A. Maly.
- 29 US Patent 3,813,453 The Goodyear Tire and Rubber Company (1974)., L.G. Wideman.
- 30 US Patent 5,059,739 (1989) to Exxon Chemical Inv., D.E. Hendriksen.
- 31 H. Olivier and P.L. Gerot, *J. Mol. Cat A*, **1999**, *148*, 43.
- 32 World patent 2005/089940 to Sasol Technology (UK) Ltd (2005), M.J. Hanton and R.P. Tooze.
- 33 Y.You and G.S. Girolami, *Organometallics*, **2008**, *27*, 3172.
- 34 i) R.A. Eikey and M.M. Abu-Omar, *Coord. Chem. Rev.*, **2003**, *243*, 83; ii) D.E. Wigley, *Prog. Inorg. Chem.*, **1994**, *42*, 239.
- 35 i) P.J. Walsh, A.M. Baranger and R.G. Bergman, *J. Am. Chem. Soc.*, **1992**, *114*, 1708; ii) D. Mansuy, J.P. Mahy, A. Dureault, G. Bedi and P. Battioni, *J. Chem. Soc, Chem. Commun.*, **1984**, 1161.
- 36 O.M. El-Kadri, M.J. Heeg and C.H. Winter, *Dalton Trans.*, **2006**, 1943.
- 37 i) R.R. Schrock, in *Topics in Organometallic Chemistry Alkene Metathesis in Organic Synthesis*, Vol. 1 (Ed.: A. Fürstner), Springer, Berlin, **1998**, pp 1-36; ii) R.R. Schrock in *Metathesis Polymerization of Olefins and Polymerization of Alkynes* (Ed.: Y. Imamoglu), Kluwer, Dordrecht, **1998**, pp 375-380.
- 38 P.D. Bolton and P. Mountford, *Adv. Synth. Catal.*, **2005**, *347*, 355.
- 39 J.Jin and E.Y.X. Chen, *Organometallics*, **2002**, *21*, 13.
- 40 W.A. Nugent and J.M. Mayer, "Metal-Ligand Multiple Bonds", Wiley-Interscience, New York, 1988.
- 41 R.C.B. Copley, P.W. Dyer, V.C. Gibson, J.A.K. Howard, E.L. Marshall, W. Wang and B. Whittle, *Polyhedron*, **1996**, *15*, 3001.
- 42 V.C. Gibson, E.L. Marshall, C. Redshaw, W. Clegg and M.R.J. Elsegood, *Dalton Trans.*, **1996**, 4197.

- 43 B.L. Haymore, E.A. Maatta and R.A.D. Wentworth, *J. Am. Chem. Soc.*, **1979**, *101*, 2063.
- 44 i) J.T. Anhaus, T.P. Kee, M.H. Schofield and R.R. Schrock, *J. Am. Chem. Soc.*, **1990**, *112*, 1642; ii) A. Danopoulos, G. Wilkinson, B. Hussain-Bates and M.B. Hursthouse, *Dalton Trans.*, **1991**, 269.
- 45 P.R. Sharp, *Dalton Trans.*, **2000**, 2647.
- 46 G. Giesbrecht and J.C. Gordon, *Dalton Trans.*, **2004**, 2392.
- 47 D.S.J. Arney and C.J. Burns, *J. Am. Chem. Soc.*, **1995**, *117*, 9448.
- 48 J.B. Wu, Y.F. Lin, J. Wang, P.J. Chang, C.P. Tasi, C.C. Lu, H.T. Chiu and Y.W. Yang, *Inorg. Chem.*, **2003**, *42*, 4516.
- 49 D.C. Bradley, S.R. Hodge, J.D. Runnacles, M. Hughes, J. Mason and R.L. Richards, *Dalton Trans.*, **1992**, 1663.
- 50 P. Barrie, T.A. Coffey, G.D. Forster and G. Hogarth, *Dalton Trans.*, **1999**, 4519.
- 51 W.A. Nugent, R.J. McKinney, R.V. Kasowski and F.A. Van-Catledge, *Inorg. Chim. Acta*, **1982**, *65*, L91.
- 52 V.C. Gibson, *J. Chem. Soc. Dalton Trans.*, **1994**, 1607.
- 53 D.S. Williams, M.H. Schofield, J.T. Anhaus and R.R. Schrock, *J. Am. Chem. Soc.*, **1990**, *112*, 6728.
- 54 D.S. Williams, M.H. Schofield and R.R. Schrock, *Organometallics*, **1993**, *12*, 4560.
- 55 J.W. Lauher and R. Hoffmann, *J. Am. Chem. Soc.*, **1976**, *98*, 1729.
- 56 J. Chatt, J.R. Dilworth and R.L. Richards, *Chem. Rev.*, **1978**, *78*, 589.
- 57 W. A. Nugent and R.L. Harlow, *Inorg. Chem.*, **1980**, *19*, 777.
- 58 S. Cenini and G. La Monica, *Inorg. Chim. Acta*, **1976**, *18*, 279.
- 59 A.A. Danopoulos, G. Wilkinson, T. Sweet and M.B. Hursthouse, *J. Chem. Soc. Chem. Commun.*, **1993**, 495.
- 60 G. Parkin, A. van Asselt, D.J. Leahy, L. Whinnery, N.G. Hua, R.W. Quan, L.M. Henling, W.P. Schaefer, B.D. Santarsiero and J.E. Bercaw, *Inorg. Chem.*, **1992**, *31*, 82.
- 61 P.J. Walsh, F.J. Hollander and R.G. Bergman, *J. Am. Chem. Soc.*, **1988**, *110*, 8729.
- 62 R.R. Schrock and A.H. Hoveyda, *Angew. Chem. Int. Ed.*, **2003**, *42*, 4592.
- 63 M. Bochmann, *J. Chem. Soc., Dalton Trans.*, **1996**, 255.
- 64 R. Hoffmann, Nobel Lecture, **1981**.
- 65 M.P. Coles and V.C. Gibson, *Polymer Bull.*, **1994**, *33*, 529.

- ⁶⁶ W.H. Leung, A.A. Danopoulos, G. Wilkinson, B. Hussain-Bates and M.B. Hursthouse, *Dalton Trans.*, **1991**, 2051.
- ⁶⁷ M.P. Coles, C.I. Dalby, V.C. Gibson, W. Clegg and M.R.J. Elsegood, *Polyhedron*, **1995**, *14*, 2455.
- ⁶⁸ M.P. Coles, C.I. Dalby, V.C. Gibson, W. Clegg and M.R.J. Elsegood, *J. Chem. Soc. Chem. Commun.*, **1995**, 1709.
- ⁶⁹ M.P. Coles, C.I. Dalby, V.C. Gibson, I.R. Little, E.L. Marshall, M.H. Ribeiro da Costa S. Mastroianni, *J. Organomet. Chem.*, **1999**, *591*, 78.
- ⁷⁰ T.S. Pilyugina, R.R. Schrock, A.S. Hock and P. Muller, *Organometallics*, **2005**, *24*, 1929.
- ⁷¹ G. Schoettel, J. Kress and J.A. Osborn, *Chem. Commun.*, **1989**, 1062.
- ⁷² N. Bryson, T.M. Yuinou and J.A. Osborn, *Organometallics*, **1991**, *10*, 3389.
- ⁷³ H.H. Fox, K.B. Yap, J. Robbins, S. Cai and R.R. Schrock, *Inorg. Chem.*, **1992**, *31*, 2287.
- ⁷⁴ R.R. Schrock, J.S. Murdzek, G.C. Bazan, J. Robbins, M. DiMare and M. O'Regan, *J. Am. Chem. Soc.*, **1990**, *112*, 3875.
- ⁷⁵ A. Bell, W. Clegg, P.W. Dyer, M.R.J. Elsegood, V.C. Gibson and E.L. Marshall, *Chem. Commun.*, **1994**, 2247.
- ⁷⁶ V.C. Gibson, C. Redshaw, G.L.P. Walker, J.H. Howard, V.J. Hoy, J.M. Cole, L.G. Kuzmina and D.S. de-Silva, *Dalton Trans.*, **1998**, 161.
- ⁷⁷ K.B. Dillon, V.C. Gibson, J.A.K. Howard, C. Redshaw, L. Sequera and J.W. Yao, *J. Organomet. Chem.*, **1997**, *528*, 179.
- ⁷⁸ P.W. Dyer, V.C. Gibson and W. Clegg, *J. Chem. Soc. Dalton Trans.*, **1995**, 3313.
- ⁷⁹ U. Radius, J. Sundermeyer and H. Pritzkow, *Chem. Ber.*, **1994**, *127*, 1827.
- ⁸⁰ T. Chen, K.R. Soraseanee, Z. Wu, J.B. Diminnie and Z. Xue, *Inorg. Chim. Acta*, **2005**, *345*, 113.
- ⁸¹ M. Jolly, J.P. Mitchell and V.C. Gibson, *Dalton Trans.*, **1992**, 1329.
- ⁸² S.C. Cole, M.P. Coles and P.B. Hitchcock, *Dalton Trans.*, **2002**, 4168.
- ⁸³ B.L. Haymore, E.A. Maatta and R.A.D. Wentworth, *J. Am. Chem. Soc.*, **1979**, *101*, 2063.
- ⁸⁴ M.C.W. Chan, F.W. Lee, K.K. Cheung and C.M. Che, *Dalton Trans.*, **1999**, 3197.
- ⁸⁵ S.E. Potts, C.J. Carmalt, C.S. Blackman, T. Leese and H.O. Davies, *Dalton Trans.*, **2008**, 5730.

- i) D.C. Bradley, M.B. Hursthouse, K.M.A. Malik, A.J. Nielson and R.L. Short, *Dalton Trans.*, **1983**, 2651; ii) D.C. Bradley, R.J. Errington, M.B. Hursthouse, R.L. Short, B.R. Ashcroft, G.R. Clark, A.J. Nielson and C.E.F. Rickard, *Dalton Trans.*, **1987**, 2067.
- ⁸⁷ G.R. Clark, A.J. Nielson, C.E.F. Rickard and D.C. Ware, *Dalton Trans.*, **1990**, 1173.
- ⁸⁸ G.R. Clark, A.J. Nielson and C.E.F. Rickard, *Dalton Trans.*, **1995**, 1907.
- ⁸⁹ D.L. Morrison, P.M. Rodgers, Y.W. Chao, M.A. Bruck, C. Grittini, T.L. Tajima, S.J. Alexander, A.L. Rheingold and D.E. Wigley, *Organometallics*, **1995**, *14*, 2435.
- ⁹⁰ C. B. Wilder, L.L. Reitford, K.A. Abboud and L. McElwee-White, *Inorg. Chem.*, **2006**, *45*, 263.
- ⁹¹ G.R. Clark, A.J. Nielson and C.E.F. Rickard, *Polyhedron*, **1998**, *7*, 117.
- ⁹² R.R. Schrock, R.T. DePue, J. Feldman, K.B. Yap, D.C. Yang, W.M. Davis, L. Park, M. Di Mare, M. Schofield, J. Anhaus, E. Walborsky, E. Evitt, C. Kruger and P. Betz, *Organometallics*, **1990**, *9*, 2262.
- ⁹³ W.H. Leung, M.C. Wu, J.L.C. Chim and W.T. Wong, *Polyhedron*, **1998**, *17*, 457.
- ⁹⁴ W.A. Nugent, *Inorg. Chem.*, **1983**, *22*, 965.
- ⁹⁵ D. Rische, A. Baunemann, M. Winter and R.A. Fischer, *Inorg. Chem.*, **2006**, *45*, 269.
- ⁹⁶ C.G. Ortiz, K.A. Abboud and J.M. Boncella, *Organometallics*, **1999**, *18*, 4253.
- ⁹⁷ T.M. Cameron, C.G. Ortiz, I. Ghiviriga, K.A. Abboud and J.M. Boncella, *Organometallics*, **2001**, *20*, 2032.
- ⁹⁸ E.A. Ison, C.O. Ortiz, K. Abboud and J.M. Boncella, *Organometallics*, **2005**, *24*, 6310.
- ⁹⁹ E.A. Ison, K.A. Abboud, I. Ghiviriga and J.M. Boncella, *Organometallics*, **2004**, *23*, 929.
- ¹⁰⁰ D.D. Vander Lende, K.A. Abboud and J.M. Boncella, *Organometallics*, **1994**, *13*, 3378.
- ¹⁰¹ S.Y.S. Wang, D.D. Vander Lende, K.A. Abboud and J.M. Boncella, *Organometallics*, **1998**, *17*, 2628.
- ¹⁰² J.M. Boncella, S.Y.S. Wang and D.D. Vander Lende, *J. Electroanalytical Chem.*, **1999**, *591*, 8.
- ¹⁰³ M.A. Hanton, unpublished work.

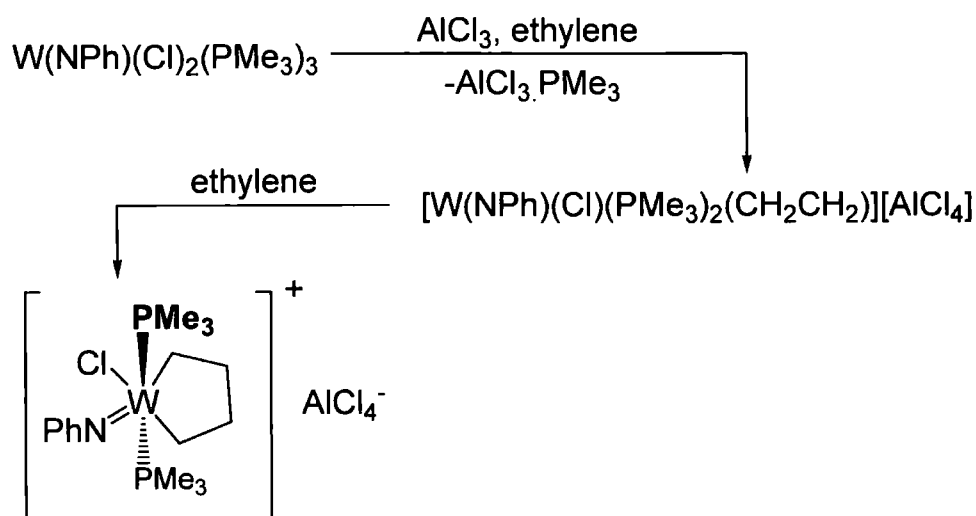
Chapter 2: Evaluating the Ethylene Dimerization Capacity of Discrete Imido Complexes

2.0 Introduction

The possibility that imido complexes are formed *in situ* during the preparation of alkene dimerization systems generated through reaction of WCl_6 with an aniline (**Chapter 1, Section 1.5, Scheme 1.17**) has led to investigation into the capacity of both discrete *bis*(imido) and *mono*(imido) tungsten complexes to initiate alkene dimerisation.¹ For example, work conducted at Sasol Technology UK Ltd (STUK) concluded that tungsten and molybdenum *bis*(imido) dichloride complexes, e.g. $W(NPh)_2Cl_2 \cdot TMEDA$ and $Mo(NAr)_2Cl_2 \cdot DME$ (**23**) can both readily initiate ethylene dimerization when co-initiated with $EtAlCl_2$.² Similarly, in a related study Olivier *et al.* have investigated the initiator ability of a range of discrete *mono*(imido) pre-catalysts. Olivier and co-workers established that complexes such as $W(NAr)Cl_4 \cdot THF$ (**38**), when activated by $EtAlCl_2$ generate initiator systems capable of inducing both ethylene and propylene dimerization.³

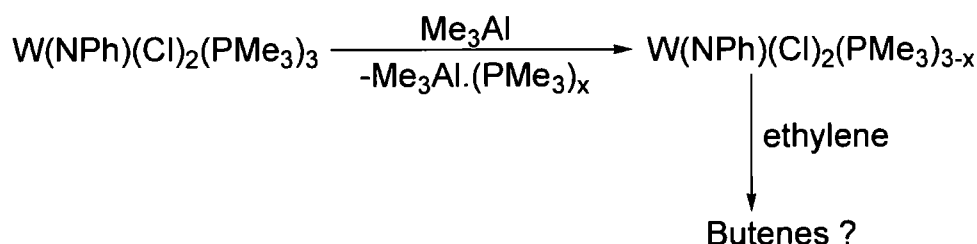
A second conclusion of Olivier's investigation concerned the reaction of the W^{IV} complex $W(NPh)(Cl)_2(PMe_3)_3$ (**34**) with $AlCl_3$ (in chlorobenzene or chloroaluminate ionic liquids), which was found to produce an active ethylene dimerization initiator.³ As $AlCl_3$ has the capacity to react as a Lewis acid, Olivier proposed that the active initiator in the $W(NPh)(Cl)_2(PMe_3)_3/AlCl_3$ system is formed *via* halide abstraction giving an $AlCl_4^-$ anion. Thus, displacement of a chloride ligand by $AlCl_3$ is postulated to generate a coordinatively unsaturated tungsten centre, which can then react with ethylene to form a metallacycle (**Scheme 2.1**), enabling dimerization of ethylene *via* an oxidative coupling cycle. However, it should be stressed that this proposed activation pathway has not been proven experimentally as none of the intermediates suggested by Olivier have been isolated or observed spectroscopically.

Scheme 2.1 Formation of a charged active initiator complex (ethylene dimerization) as proposed by Olivier et al.³



With a view to examining the plausibility of an ionic complex forming in Olivier's $\text{W(NPh)(Cl)}_2(\text{PMe}_3)_3/\text{AlCl}_3$ dimerization system (**Scheme 2.1**), in this chapter the relative capacity of the Lewis acids EtAlCl_2 , $\text{B(C}_6\text{F}_5)_3$, and Me_3Al to activate $\text{W(NPh)(Cl)}_2(\text{PMe}_3)_3$ (**34**) towards ethylene dimerization has been examined. Particular emphasis has been placed on assessing if abstraction of a chloride moiety from **34** is a pre-requisite for initiator formation, as activation of the W^{IV} complex **34** may be achievable by simply displacing a PMe_3 ligand using a weak Lewis acid (**Scheme 2.2**).

Scheme 2.2 Potential activation of $\text{W(NPh)(Cl)}_2(\text{PMe}_3)_3$ (**34**) by Me_3Al



The investigations made by Olivier and co-workers³ and STUK² have established that tungsten imido chloride complexes can be used as alkene dimerization pre-catalysts. However, neither study examined the relative activities given by each type of imido complex. Thus, in this Chapter the relative abilities of both *mono*- and *bis*(imido) pre-catalysts to initiate ethylene dimerization have been

assessed using directly comparable reaction conditions for the first time. In particular, attention here has focussed on any differences displayed by *mono* and *bis*(imido) pre-catalysts, in order to establish if similar active initiator complexes are operating in each system. Notably, the studies conducted by Olivier³ and STUK² concerned exclusively the use of *mono* and *bis*(imido) chloride complexes. Hence, no previous investigations have been made into the activation of imido complexes with groups other than chloride ligands (such as amido groups). This is relevant since it is quite feasible that mixed amido/imido complexes may be formed in the STUK dimerization system during preparation of initiator solutions, which requires reaction of WCl_6 with an amine.⁴ Indeed, it has previously been reported that reaction of WCl_6 with $10H_2N^tBu$ gives the *bis*(imido) *bis*(amido) complex $W(N^tBu)_2(NH^tBu)_2$ (**41**).⁵ Thus, assessing the ability of $EtAlCl_2$ to activate discrete amido complexes for ethylene dimerization is of interest and has also been examined in this Chapter.

2.1 Synthesis and Characterization of the *bis*(Imido) Pre-catalysts $W(NAr)_2Cl_2 \cdot DME$ (40**) and $Mo(NAr)_2(NH^tBu)_2$ (**55**)**

To provide starting pre-catalysts for an ethylene dimerization study, both $W(NAr)_2Cl_2 \cdot DME$ (**40**) and the new complex $Mo(NAr)_2(NH^tBu)_2$ (**55**) have been synthesised using simple “one-pot” procedures. Both **40** and **55** have been characterized by single crystal X-ray diffraction studies; the resulting molecular structures will be discussed in this section.

2.1.1 Synthesis and Characterization of the Mixed *bis*(Imido) *bis*(Amido) Complex $Mo(NAr)_2(NH^tBu)_2$ (55**)**

Wilkinson *et al.* have previously reported the synthesis of the mixed *bis*(alkyl imido) *bis*(amido) complex $Mo(N^tBu)_2(NH^tBu)_2$ (**56**).⁶ However, complex **56** contains electron donating ^tBu imido ligands; this is undesirable as it has been found that pre-catalysts with ^tBu *bis*(imido) moieties tend to generate inactive alkene dimerization systems.² Consequently, attention turned to synthesising a more appropriate mixed *bis*(aryl imido) *bis*(amido) complex containing electron withdrawing imido ligands.

Addition of two equivalents of $LiNH^tBu$ to $Mo(NAr)_2Cl_2 \cdot DME$ (**23**) (Ar = 2,6-diisopropylphenyl) was found to give the *bis*(aryl imido) *bis*(amido) complex $Mo(NAr)_2(NH^tBu)_2$ (**55**) (Scheme 2.3). Characterization of **55** using ¹H NMR spectroscopy gives a single ^tBu resonance as well as a single set of ⁱPr resonances (doublet and septet). This is consistent with both imido ligands of **55** being equivalent. Recrystallization of complex **55** from hexane gave large, bright red

crystals of sufficient quality for single crystal X-ray diffraction analysis (**Figure 2.1** and **Table 2.1**).

Scheme 2.3 Synthesis of $\text{Mo}(\text{NAr})_2(\text{NH}^t\text{Bu})_2$ (**55**)

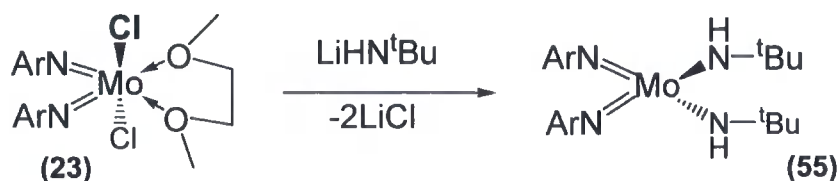


Figure 2.1 Solid state structure of $\text{Mo}(\text{NAr})_2(\text{NH}^t\text{Bu})_2$ (**55**) with the thermal ellipsoids set at the 50% level. Two orientations of **55** have been included for clarity

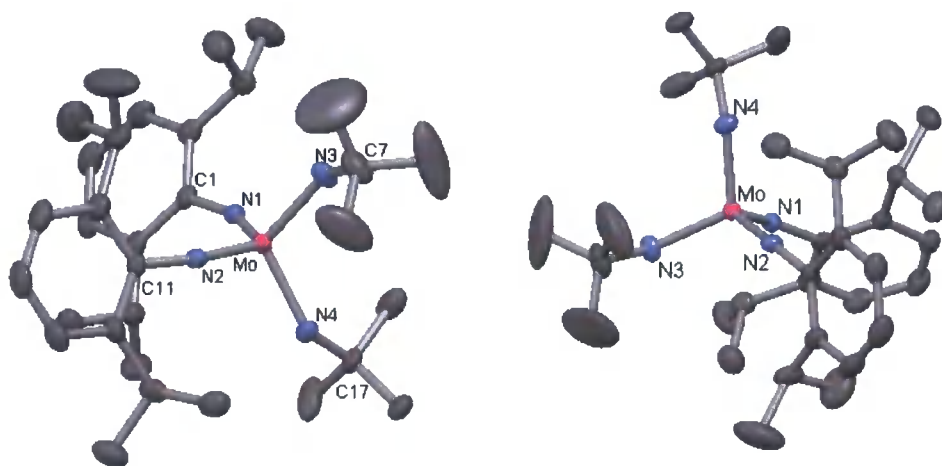


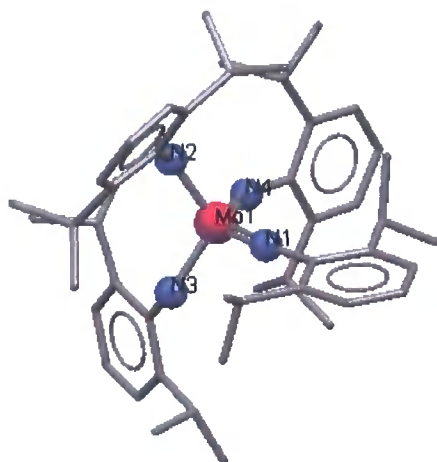
Table 2.1 Selected bond distances (Å) and bond angles (°) for $\text{Mo}(\text{NAr})_2(\text{NH}^t\text{Bu})_2$ (**55**)

Mo-N2	1.7543(15)	N3-C7	1.476(2)
Mo-N1	1.7609(14)	N4-C17	1.476(2)
Mo-N4	1.9495(16)	N2-Mo-N1	112.32(7)
Mo-N3	1.9537(16)	N3-Mo-N4	111.88(7)
N1-C1	1.401(2)	Mo-N1-C1	155.32(13)
N2-C11	1.392(2)	Mo-N2-C11	170.28(13)

As discussed in **Chapter 1, Section 1.7** for a given *bis*(imido) system it is the relative lengths of the M-N contacts that gives the most accurate indication as to the bonding mode adopted by each imido ligand. For complex (**55**) the Mo-N1 and Mo-N2 contacts at 1.7543(15) Å and 1.7609(14) Å respectively are similar. This indicates that both imido ligands of **55** adopt a bonding mode between that of a 2 and 4 electron donor (neutral formalism), an arrangement which is commonly associated

with terminal *bis*(imido) complexes.⁷ It is clear from the N2-Mo-N1 112.32(7)° and N3-Mo-N4 111.88(7)° bond angles that complex **55** is *pseudo* tetrahedral, a similar geometry being adopted by the closely related complex Mo(NAr)₂(NHAr)₂ (**57**).⁸ One notable difference between the structures adopted by the complexes **55** and **57** concerns the orientation of the 2,6-diisopropyl phenyl fragments. In the molecular structure of **55**, the 2,6-diisopropyl phenyl groups lie approximately parallel to each other (**Figure 2.1**). In contrast, in the molecular structure adopted by Mo(NAr)₂(NHAr)₂ (**57**) the two diisopropylphenyl moieties adopt a perpendicular orientation, which presumably minimizes steric interactions between the *bis*(imido) and bulky *bis*(amido) NHAr ligands (**Figure 2.2**).

Figure 2.2 Solid state structure of Mo(NAr)₂(NHAr)₂⁸ (**57**) obtained from the Cambridge structural data base



2.1.2 Synthesis and Characterization of W(NAr)₂Cl₂.DME (**40**) by Single Crystal X-Ray Diffraction Analysis

The complex W(NAr)₂Cl₂.DME (**40**) was prepared using a variation of the procedure described by Schrock *et al.*⁹ A suspension of WO₂Cl₂ in DME was treated with H₂NAr in the presence of excess 2,6-lutidine and ClSiMe₃. Following work-up, complex **40** was isolated in approximately 30% yield. As reported by Schrock, W(NAr)₂Cl₂.DME (**40**) was found to present a single set of ¹Pr resonances in its ¹H NMR spectrum when analysed in either C₆D₆ or CDCl₃. Recrystallization of W(NAr)₂Cl₂.DME (**40**) from a concentrated DME solution at room temperature gave single crystals of complex **40** of sufficient quality for X-ray diffraction analysis (**Figure 2.3** and **Table 2.2**).ⁱ

ⁱ Surprisingly the molecular structure of W(NAr)₂Cl₂.DME (**40**) is not currently deposited in the Cambridge Structural Database.

Figure 2.3 Solid state structure of $W(NAr)_2Cl_2 \cdot DME$ (**40**) with the thermal ellipsoids set at the 50% level. Two orientations of **40** have been included for clarity

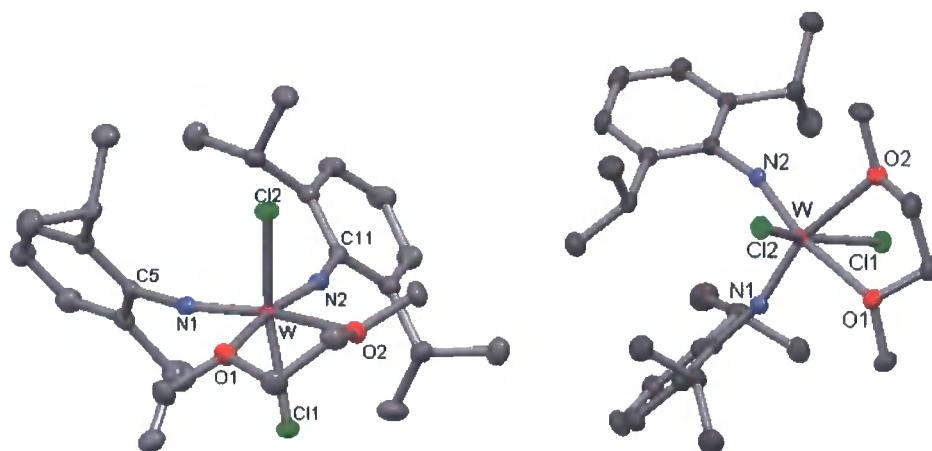


Table 2.2 Selected bond distances (\AA) and bond angles ($^\circ$) for $W(NAr)_2Cl_2 \cdot DME$ (**40**)

W-N1	1.7598(17)	O2-W-O1	70.06(6)
W-N2	1.7599(17)	N1-W-N2	103.89(8)
N2-C11	1.395(3)	N2-W-O2	96.69(7)
W-Cl1	2.3841(7)	W-N2-C11	161.47(15)
W-O1	2.3494(15)	Cl1-W-Cl2	154.28(2)

The complex $W(NAr)_2Cl_2 \cdot DME$ (**40**) adopts a distorted octahedral structure, with the chloride ligands lying *trans* to one another. Distortion from an ideal octahedral polyhedron is clear from the obtuse Cl-W-Cl bond angle of $154.28(2)^\circ$. A similar distortion is observed in the molecular structure of the closely related complex $Mo(N(C_6H_4-o-CN)_2)_2Cl_2 \cdot DME$ (**58**),¹⁰ which has a Cl-Mo-Cl bond angle of $159.71(5)^\circ$. Schrock has carried out SCRF- $X\alpha$ -SW calculations on a $W(NH)_2(PH_3)_2$ core, concluding that minimizing of the P-W-P bond angle maximizes the stabilizing interaction between the phosphine ligand frontier orbitals and the vacant tungsten 5a1 orbital.¹¹ Although the $W(NH)_2(PH_3)_2$ fragment considered by Schrock was tetrahedral and the complexes **40** and **58** are both distorted octahedral, it is reasonable to speculate that a similar effect may be occurring for the complexes **40** and **58**, with a bending of the Cl-M-Cl bond angle potentially occurring to increase interaction between the chloride and tungsten/molybdenum frontier orbitals.

2.2 Ethylene Dimerization Systems Produced From Reaction of Imido Halide Complexes with the co-Initiators EtAlCl₂ and B(C₆F₅)₃

As stated in Section 2.1 complexes **40** and **55** were synthesised for use as catalyst precursors in an ethylene dimerization study. To extend the range of complexes available for this study, additional *mono* and *bis*(imido) complexes have been prepared using established literature procedures. Subsequently, the capacity of each of the discrete imido complexes to initiate ethylene dimerization after reaction with a given co-initiator (typically EtAlCl₂) was assessed (Table 2.3). It should be stressed that the high pressure ethylene dimerization study reported herein, was conducted in collaboration with Dr. M.J. Hanton (Sasol Technology UK Ltd). In this study the pre-catalyst solutions were charged to an autoclave, which was then pressurized with ethylene. Through the use of a mass flow controller the pressure of the reaction vessel was kept constant throughout the catalyst test run. As ethylene uptake could be monitored, the reactions were terminated as soon as it became apparent that reaction of ethylene had ceased. This approach allows for a more accurate measure of a given initiator's activity.

Table 2.3 Ethylene dimerization using pre-formed mono and bis(imido) pre-catalysts^a

run	Pre-Catalyst	Co-initiator	Time (mins)	TON ^b	Activity ^{c,d}	C ₄ (%)	1-C ₄ in C ₄ (%)
1	W(NAr) ₂ Cl ₂ .DME (40)	EtAlCl ₂	20	58,043	174,128	84.1	57.2
2	Mo(NAr) ₂ Cl ₂ .DME (23)	EtAlCl ₂	55	58,503	63,821	88.9	63.7
3	Mo(NAr) ₂ (NH ^t Bu) ₂ (56)	EtAlCl ₂	54	56,938	62,876	87.7	62.9
4	Mo(NAr)(N ^t Bu)Cl ₂ .DME (11)	EtAlCl ₂	80	59,508	44,874	89.3	61.5
5	Mo(N ^t Bu) ₂ Cl ₂ .(DME) (26)	EtAlCl ₂	74	14,028	11,361	88.9	63.7
6	W(NPh)Cl ₄ .THF (32)	EtAlCl ₂	61	21,385	20,807	90	74.5
7	W(NAr)Cl ₄ .THF (38)	EtAlCl ₂	80.0	46,321	34,857	88.2	64.2
8	W(NPh)(Cl) ₂ (PMe ₃) ₃ (34)	EtAlCl ₂	68	62,632	55,195	90.5	63.1
9	W(NPh)(Cl) ₂ (PMe ₃) ₃ (34)	B(C ₆ F ₅) ₃	18.3	0	0	0	0
10	Ta(NAr)Cl ₃ (TMEDA) (59)	EtAlCl ₂	75	26,447	21,158	86.3	72.4

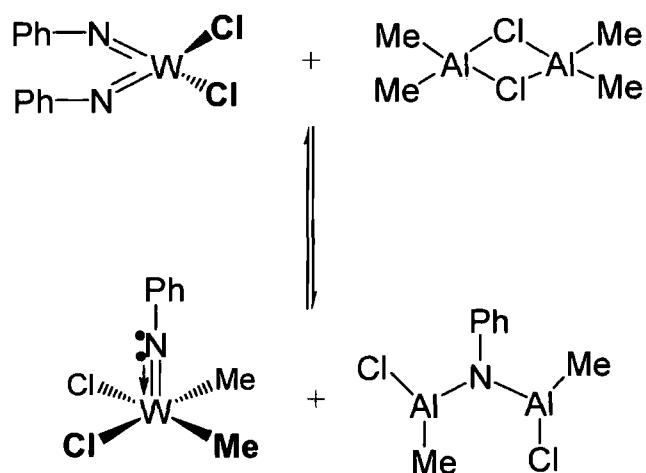
a) General conditions: 0.2 mmol precatalyst for all runs; 3.0 mmol EtAlCl₂ (runs 1-9 inclusive); 0.8 mmol B(C₆F₅)₃ (run 10); PhCl (solvent) 74.2 ml; 60°C; ethylene pressure (40 bar); stirrer speed 1000 rpm; nonane standard (0.5 mL). **b)** TON is reported in mol/mol. **c)** Activity is reported in mol/mol/h. **d)** In all runs C₆ alkenes were produced (8-15%) as well as trace C₈ (2-3%).

For the range of pre-initiators screened (**Table 2.3**) the highest activity and TON was obtained from the system based on $W(NAr)_2Cl_2 \cdot DME$ (**40**) (174,128 mol/mol/h; run 1). Notably similarly high TONs were obtained from molybdenum *bis*(imido) pre-catalysts (runs 2-4). This demonstrates that molybdenum *bis*(imido) complexes can readily be activated by $EtAlCl_2$ to give productive ethylene dimerization initiators. Moreover, for runs 2-4 the selectivity of these molybdenum-based ethylene dimerization systems for butenes was high ranging between 84-89%.

It is interesting to note the similarity in TONs and activities obtained in the catalyst runs 2 and 3 in which the pre-catalysts $Mo(NAr)_2(NH^iBu)_2$ (**55**) and $Mo(NAr)_2Cl_2 \cdot DME$ (**23**) are employed. This suggests that $EtAlCl_2$ can effectively activate both molybdenum amido and chloride species generating a very similar active molybdenum initiator complex in each case.

The higher TON and activity displayed by the tungsten *bis*(imido) system (run 1) relative to the runs in which tungsten *mono*(imido) pre-catalysts were employed (runs 6 and 7) contradicts a recent DFT investigation made by Tobisch.¹² In this theoretical study it is proposed that *mono*(imido) ethylene dimerization initiators are inherently more active than related *bis*(imido) complexes. Tobisch also states that the activity observed in systems based on a *bis*(imido) pre-catalyst must result from the evolution of *mono*(imido) active initiator complexes *in situ*. This transformation is proposed to occur *via* displacement of an imido ligand of a *bis*(imido) fragment by an aluminium alkyl dimer (**Scheme 2.3**).

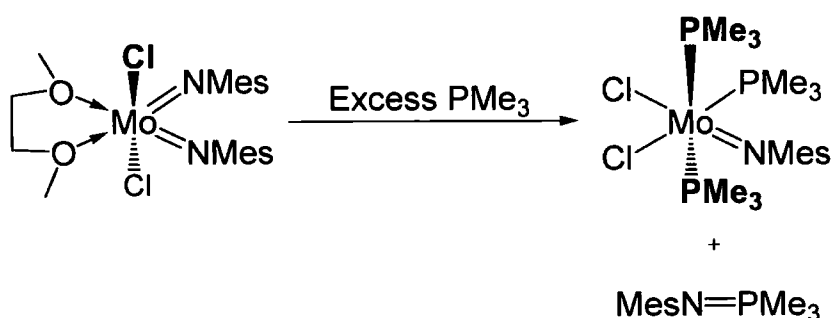
Scheme 2.3 Tobisch's proposed route to a *mono*(imido) initiator from a *bis*(imido) pre-catalysts.



If indeed *bis*(imido) pre-catalysts were converting to give *mono*(imido) initiators, then one would expect the *bis*(imido) systems never to exceed the activity and TON observed in the *mono*(imido) runs. From the data outlined in **Table 2.3** this is clearly

not the case. Also of significance is the extremely limited precedent in the literature for the type of reaction outlined in **Scheme 2.3**. Although it has been found that displacement of an imido ligand of a *bis*(imido) moiety is achievable *via* reaction of a phosphine (**Scheme 2.4**)¹³ or HCl,¹⁴ to date there are no procedures that have been outlined in which an imido ligand is displaced from a metal centre *via* reaction with an aluminium alkyl halide or a similar group 13 Lewis Acid.

Scheme 2.4 Displacement of an imido ligand by PMe_3



A further argument against the formation of a *mono*(imido) active initiator complex from a *bis*(imido) pre-catalyst *via* the pathway outlined in **Scheme 2.3** can be made by comparison of the activities obtained in runs **2**, **4**, and **5**, which employ $\text{Mo}(\text{NAr})_2\text{Cl}_2\cdot\text{DME}$ (**23**), $\text{Mo}(\text{NAr})(\text{N}^t\text{Bu})\text{Cl}_2\cdot\text{DME}$ (**11**), and $\text{Mo}(\text{N}^t\text{Bu})_2\text{Cl}_2\cdot\text{DME}$ (**26**), respectively (**Table 2.3**). Although similar catalyst TONs are obtained in runs **2** and **4**, a marked decrease in activity results from substitution of the pre-catalysts $\text{Mo}(\text{NAr})_2\text{Cl}_2\cdot\text{DME}$ (**23**) (run **2**, 63,821 mol/mol/h) for the mixed imido complex $\text{Mo}(\text{NAr})(\text{N}^t\text{Bu})\text{Cl}_2\cdot\text{DME}$ (**11**) (run **4**, 44,874 mol/mol/h). This can be attributed to the influence of the electron donating ^tBu ligand, which clearly inhibits catalysis. This effect is further highlighted by reaction of the pre-catalysts $\text{Mo}(\text{N}^t\text{Bu})_2\text{Cl}_2\cdot\text{DME}$ (**26**), which results in the lowest TON and activity of all the *bis*(imido) systems (run **5**; 14,028 mol/mol and 11,361 mol/mol/h). If the pre-catalysts **23**, **11**, and **26** were converted to *mono*(imido) initiators, then one would predict that the mixed complex $\text{Mo}(\text{NAr})(\text{N}^t\text{Bu})\text{Cl}_2\cdot\text{DME}$ (**11**) would give the same activity as either $\text{Mo}(\text{NAr})_2\text{Cl}_2\cdot\text{DME}$ (**23**) or $\text{Mo}(\text{N}^t\text{Bu})_2\text{Cl}_2\cdot\text{DME}$ (**26**). Clearly this is not the case, further suggesting that formation of a *mono*(imido) initiator complex from *bis*(imido) pre-catalysts *via* the pathway outlined in **Scheme 2.3** is not viable.

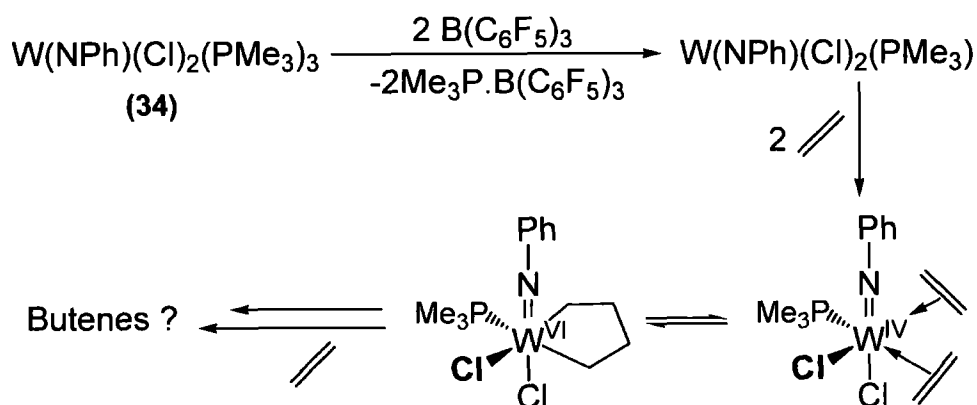
Notably, systems based on the *mono*(imido) complexes $\text{W}(\text{NAr})\text{Cl}_4\cdot\text{THF}$ (**38**) and $\text{W}(\text{NPh})\text{Cl}_4\cdot\text{THF}$ (**32**) (runs **6** and **7**, **Table 2.3**) were less active than related *bis*(imido) systems. However, both **38** and **32** gave good selectivity for C₄ products.

Furthermore, the highest selectivity for but-1-ene in all runs was obtained using complex **32** (run 6). As such, discrete *mono*(imido) complexes could find application as highly selective alkene dimerization initiators.

2.2.1 Activation of $W(NPh)(Cl)_2(PMe_3)_3$ (**34**) for Ethylene Dimerization

Olivier *et al.* have shown that $W(NPh)(Cl)_2(PMe_3)_3$ (**34**) can be activated by $AlCl_3$ to give an ethylene dimerization system.³ To assess if it is possible to activate **34** through the use of reagents other than $AlCl_3$, $W(NPh)(Cl)_2(PMe_3)_3$ (**34**) was treated with $EtAlCl_2$ or $B(C_6F_5)_3$ (Table 2.3, runs 8 and 9). The boron-based Lewis acid $B(C_6F_5)_3$ was selected because $B(C_6F_5)_3$ is known to be an effective phosphine scavenger. For example, $B(C_6F_5)_3$ can be used activate ruthenium carbene Grubbs alkene metathesis initiators by typically displacing a PCy_3 ligand, which simultaneously generates a vacant coordination site at Ru and a $Cy_3P.B(C_6F_5)_3$ Lewis base/Lewis acid adduct.¹⁵ Thus, reaction of $B(C_6F_5)_3$ and $W(NPh)(Cl)_2(PMe_3)_3$ (**34**) is anticipated to result in dissociation of PMe_3 ligands giving a W^V complex potentially capable of accommodating ethylene coordination. This in turn could result in ethylene dimerization *via* a metallacycle (oxidative coupling) mechanism (Scheme 2.5).

Scheme 2.5 Potential activation of $W(NPh)(Cl)_2(PMe_3)_3$ (**34**) with $B(C_6F_5)_3$



It was found that treatment of **34** with $B(C_6F_5)_3$ failed to produce an active initiator complex, with no ethylene dimerization being observed (run 9, Table 2.3). Evidently activation of **34** by displacement of a PMe_3 ligand by $B(C_6F_5)_3$ is not viable. Consequently, the reactivity of $W(NPh)(Cl)_2(PMe_3)_3$ (**34**) with the Lewis acid Me_3Al was examined. Following treatment of $W(NPh)(Cl)_2(PMe_3)_3$ (**34**) with Me_3Al in C_6D_6 , the ^{31}P NMR spectrum of the reaction mixture presented a new broad resonance at

-21.2 ppm. This is consistent with the *in situ* formation of $(\text{Me}_3\text{P})_x(\text{AlMe}_3)_y$ adducts,³ suggesting that the PMe_3 moieties of **34** are indeed being displaced by Me_3Al . Subsequent addition of ethylene to the Me_3Al reaction mixture did not result in ethylene dimerization. This again indicates that **34** cannot be activated for ethylene dimerization by displacement of PMe_3 ligands alone, with further modification of the $\text{W}(\text{NPh})\text{Cl}_2$ framework being necessary.

In contrast to run **9** reaction of $\text{W}(\text{NPh})(\text{Cl})_2(\text{PMe}_3)_3$ (**34**) and EtAlCl_2 (Table 2.3, run **8**) generated a dimerization system with both high TON and activity (62,632 mol/mol and 55,195 mol/mol/h). Notably, run **8** has the highest TON and activity of all the dimerization systems based on *mono(imido)* complexes described in Table 2.3. It can be concluded that activation of **34** by EtAlCl_2 undoubtedly occurs *via* phosphine displacement and then modification of the $\text{W}(\text{NPh})\text{Cl}_2$ moiety.

2.2.2 Dimerization Systems Based on Tantalum *mono(imido)* Complexes

In Section 2.2 it was shown that a range of tungsten *mono(imido)* chloride complexes can be used as pre-catalysts for ethylene dimerization. Of general interest is assessing if other related *mono(imido)* complexes can be similarly activated for ethylene dimerization. As such, attention turned to investigating the activities of systems based on *mono(imido)* tantalum complexes, which can easily be prepared from TaCl_5 .¹⁶ While tantalum imido complexes have been shown by Wigley *et al.* to react with alkynes to form metallacycles,¹⁷ no previous investigations into the potential application of $\text{Ta}(\text{NR})\text{Cl}_3$ complexes as alkene dimerization pre-catalysts have been made. Hence, the complex $\text{Ta}(\text{NAr})\text{Cl}_3(\text{TMEDA})$ (**59**) was included in the ethylene dimerization study outlined in Table 2.3. It was found that moderate activity was obtained for the dimerization system based on complex **59** (run **10**, 21,158 mol/mol/h). Indeed, the activity obtained from **59** is comparable to that found for $\text{W}(\text{NPh})\text{Cl}_4\cdot\text{THF}$ (**32**) (run **6**, 20,807 mol/mol/h). Evidently, the production of C_4 olefins in run **10** shows that a group 6 metal is not an essential prerequisite for *mono(imido)* alkene dimerization pre-catalyst.

2.2.3 Reaction of $\text{Mo}(\text{NAr})_2(\text{NH}^t\text{Bu})_2$ (55**) with Me_3Al**

In Section 2.2 it was established that $\text{Mo}(\text{NAr})_2(\text{NH}^t\text{Bu})_2$ (**55**) can be activated for ethylene dimerization using EtAlCl_2 (run **3**, 62,876 mol/mol/h). To further assess the reactivity of $\text{Mo}(\text{NAr})_2(\text{NH}^t\text{Bu})_2$ (**55**) with $\text{R}_x\text{AlCl}_{3-x}$ reagents, complex **55** was treated with Me_3Al in C_6D_6 . It was found that reaction of Me_3Al resulted in the formation of the known complex $\text{Mo}(\text{NAr})_2\text{Me}_2$ (**27**).¹⁸ This demonstrates that molybdenum amido moieties can be alkylated by $\text{R}_x\text{AlCl}_{3-x}$ reagents, indicating that reaction of EtAlCl_2 and

55 in run 3 generates a molybdenum ethyl intermediate, from which the active initiator complex is then derived.

2.3 Investigating the Reactivity of EtAlCl₂ and Et₃Al₂Cl₃ with *mono*- and *bis*(Imido) Complexes

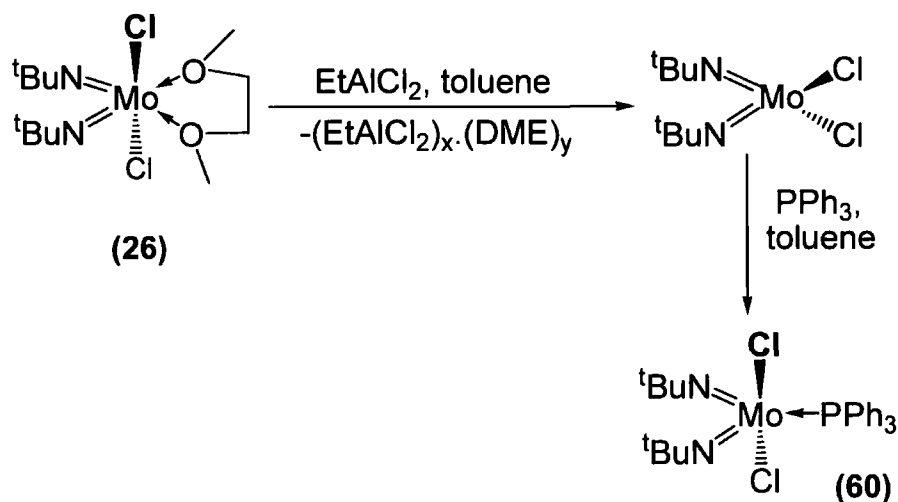
It has been established in Section 1.2 that both *mono* and *bis*(imido) complexes of molybdenum and tungsten can initiate ethylene dimerization in the presence of an ethyl aluminium species. With the aim of trying to understand the mode by which EtAlCl₂ co-initiates reaction of ethylene, attention turned to investigating the stoichiometric reactions of both types of imido complexes with EtAlCl₂ or Et₃Al₂Cl₃.

2.3.1 Reaction of EtAlCl₂ and Et₃Al₂Cl₃ with *bis*(Imido) Complexes

Addition of one equivalent of EtAlCl₂ to a hexane solution of Mo(N^tBu)₂Cl₂.DME (**26**) results in the formation of an unknown (EtAlCl₃)_x.(DME)_y Lewis base/Lewis acid adduct and the known complex Mo(N^tBu)₂Cl₂ (**21**).¹⁹ To further clarify the reactivity of complex **26** with one equivalent of EtAlCl₂, the reaction of **26** in the presence of a phosphine (PPh₃) has been examined. Thus, in a “one-pot” procedure, Mo(N^tBu)₂Cl₂.DME (**26**) was treated with one equivalent of EtAlCl₂ and then PPh₃, this generated the new complex Mo(N^tBu)₂Cl₂.PPh₃ (**60**) (Scheme 2.6).ⁱⁱ

The formation of Mo(N^tBu)₂Cl₂ (**21**) and complex **60** from reaction of Mo(N^tBu)₂Cl₂.DME (**26**) and EtAlCl₂ indicates that the first action of the aluminium alkyl halide is to displace the coordinating DME moiety. Of greater interest is determining the reaction products obtained from treatment of **26** with excess EtAlCl₂, as it is through reaction of excess EtAlCl₂ that *bis*(imido) pre-catalysts are activated. Hence, a toluene solution of Mo(N^tBu)₂Cl₂.DME (**26**) was treated with three equivalents of EtAlCl₂. However, this procedure generated numerous reaction products, unidentifiable by NMR spectroscopic analysis.

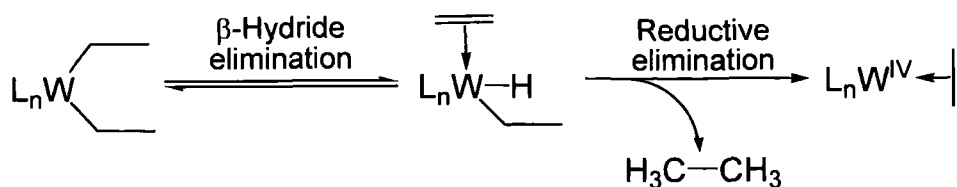
ⁱⁱ Although Mo(N^tBu)₂Cl₂.DME (**26**) does react with excess PPh₃ to give Mo(N^tBu)₂Cl₂.PPh₃ (**60**) in the absence of EtAlCl₂ the reaction is slow (2 h) and only 60% conversion of **26** is obtained.

Scheme 2.6 Synthesis of $\text{Mo}(\text{N}^t\text{Bu})_2\text{Cl}_2\cdot\text{PPh}_3$ (**60**)

2.3.2 Reaction of $\text{W}(\text{NAr})_2\text{Cl}_2\cdot\text{DME}$ (**40**) with $\text{Et}_3\text{Al}_2\text{Cl}_3$ and EtAlCl_2

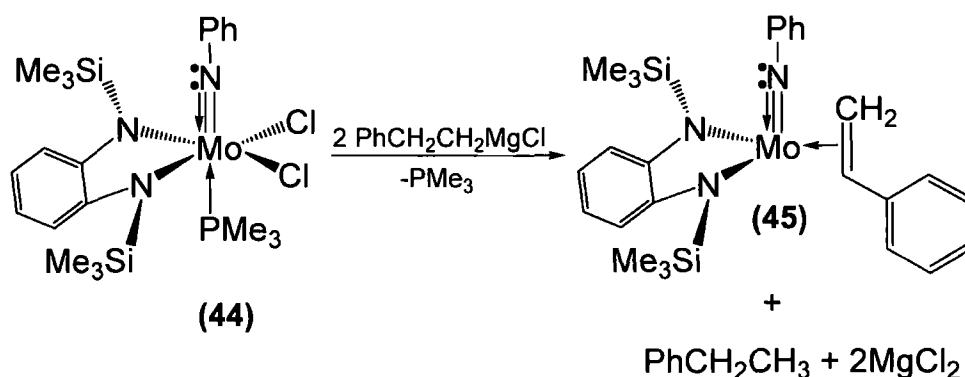
The dimerization system based on the pre-catalyst $\text{W}(\text{NAr})_2\text{Cl}_2\cdot\text{DME}$ (**40**) has been shown to be the most active system identified in the comparative ethylene dimerization study outlined in **Section 2.2, Table 2.3**. Consequently, attention turned to studying the reactivity of $\text{W}(\text{NAr})_2\text{Cl}_2\cdot\text{DME}$ (**40**) with excess $\text{Et}_x\text{AlCl}_{3-x}$ reagents, with a view to identifying the mode by which **40** is activated. Thus, $\text{W}(\text{NAr})_2\text{Cl}_2\cdot\text{DME}$ (**40**) has been reacted with both $\text{Et}_3\text{Al}_2\text{Cl}_3$ and EtAlCl_2 in C_6D_6 in sealed NMR tubes and the reactions probed using ^1H and ^{13}C NMR spectroscopy. For both aluminium reagents, numerous reaction products were observed to form. Although it was clear that complex **40** had been completely consumed in each reaction, it was not possible to identify the structure of the resulting products from reaction of $\text{W}(\text{NAr})_2\text{Cl}_2\cdot\text{DME}$ (**40**) with either $\text{Et}_3\text{Al}_2\text{Cl}_3$ or EtAlCl_2 . However, ^1H NMR spectroscopic analysis of each reaction mixture indicated the formation of ethane in both cases. It is proposed that this ethane originates from a tungsten diethyl precursor (formed from W-Cl/Al-Et exchange), which first undergoes β -hydride elimination and then reductive elimination, generating a W^{V} intermediate (**Scheme 2.7**).

Scheme 2.7 Possible mechanism for the formation of ethane upon reaction of $W(NAr)_2Cl_2 \cdot DME$ (**40**) with $EtAlCl_2$ or $Et_3Al_2Cl_3$.



The operation of the type of reaction pathway outlined in **Scheme 2.7** would be further supported by the identification of a tungsten-bound ethylene ligand or the evolution of a molecule of free ethylene. Although no ethylene moieties were observed using 1H NMR spectroscopy there is, however, strong precedent in the literature for the activation of a W^{VI} complex *via* the pathway summarized in **Scheme 2.7**. For instance, as mentioned in **Chapter 1, Section 1.13**, reaction of $Mo(NPh)Cl_2(PMe_3)(o-(Me_3SiN)_2C_6H_4)$ (**44**) with $PhCH_2CH_2MgCl$ has been shown by Boncella *et al.* to give the olefin complex $Mo(NPh)(CH_2CHPh)(o-(Me_3SiN)_2C_6H_4)$ (**45**) *via* elimination of $Ph_2CH_2CH_3$ (**Scheme 2.8**).²⁰

Scheme 2.8 Synthesis of $Mo(NPh)(CH_2CHPh)(o-(Me_3SiN)_2C_6H_4)$ (**45**)



The reaction pathway proposed in **Scheme 2.7** is also supported by recent work conducted by Girolami *et al.* who have synthesised the d^8 $W(-II)$ salt $[Li(TMEDA)]_3[WH(C_2H_4)_4]$ (**61**) *via* reaction of $EtLi$ with $WCl_3(OMe)_3$ in the presence of TMEDA.²¹ The ethylene and hydride ligands of **61** must form *via* β -hydride elimination from an intermediate tungsten ethyl group as in **Scheme 2.7**. Furthermore, the synthesis of **61** demonstrates that W^{VI} complexes can be reduced by organometallic ethylating agents.

To further investigate the nature of dimerization systems based on $W(NAr)_2Cl_2 \cdot DME$ (**40**), ethylene was added to the Et_xAlCl_{3-x}/C_6D_6 reaction mixtures. It

was found that addition of ethylene (~1 bar) to the $W(NAr)_2Cl_2 \cdot DME / EtAlCl_2$ and $W(NAr)_2Cl_2 \cdot DME / Et_3Al_2Cl_3$ reactions did not result in higher olefin formation. This is surprising since the product from the reaction of $W(NAr)_2Cl_2 \cdot DME$ (**40**) with $EtAlCl_2$ (Section 1.2, Table 2.3, run 1) readily initiates ethylene dimerization under more forcing conditions. This is suggestive that for *bis*(imido) systems to produce butenes, high ethylene pressures are essential. Evidently, the activities of dimerization systems based on *bis*(imido) pre-catalyst $W(NAr)_2Cl_2 \cdot DME$ (**40**) are highly dependent on the reaction conditions.

2.3.3 Reaction of *mono*(Imido) Complexes with one Equivalent of $EtAlCl_2$

The comparative ethylene dimerization study highlighted in Section 2.2 clearly indicates that *mono*(imido) complexes can be activated by $EtAlCl_2$ for ethylene dimerization. As such, treatment of $W(NR)Cl_4 \cdot THF$ complexes with Et_xAlCl_{3-x} reagents in the absence of alkenes could yield information regarding the mode of initiator formation. Thus, the reaction of one equivalent of $EtAlCl_2$ with $W(NPh)Cl_4 \cdot THF$ (**32**), in toluene was undertaken. This gave a light brown precipitate, which was collected *via* filtration and analysed using NMR spectroscopy. A marked shift in the position of both the THF 1H NMR resonances was observed in the 1H NMR spectrum (compared to the related THF resonances of complex **32**), consistent with the formation of the adduct $EtAlCl_2 \cdot (THF)_2$.ⁱⁱⁱ This was established by analysis of an authentic sample of $EtAlCl_2 \cdot (THF)_2$ which gave identical 1H NMR resonances to that obtained in the $EtAlCl_2 / W(NPh)Cl_4 \cdot THF$ reaction. Hence, as for $Mo(N^tBu)_2Cl_2 \cdot DME$ (**26**) (Section 2.3.1), addition of one equivalent of $EtAlCl_2$ to $W(NPh)Cl_4 \cdot THF$ (**32**) has been shown to result in displacement of the coordinating solvent moiety (THF), presumably generating a $W(NPh)Cl_4$ framework. It has not been possible to verify the formation of $W(NPh)Cl_4$ (**31**) in this system, as reaction of $EtAlCl_2$ generated tungsten containing products that were insoluble in polar solvents, preventing their characterization using 1H NMR spectroscopy.

2.3.4 Reaction of *mono*(Imido) Complexes with Excess $EtAlCl_2$ and $Et_3Al_2Cl_3$

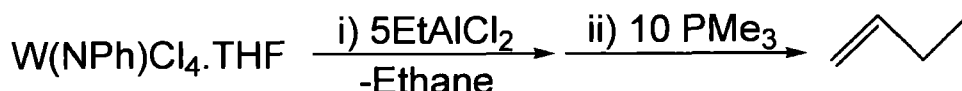
In Section 2.3.3 it was established that reaction of $W(NPh)Cl_4 \cdot THF$ (**32**) with one equivalent of $EtAlCl_2$ results in displacement of the coordinated THF moiety. Of greater interest the reactivity of *mono*(imido) complexes with an excess of $EtAlCl_2$ or

ⁱⁱⁱ The adduct $EtAlCl_2 \cdot (THF)_2$ has been characterized by both NMR spectroscopy and mass spectrometry, $m/z = 242.8$ ($Al(THF)_2Cl_2^+$). Integration of the 1H NMR spectrum is also consistent with two THF moieties binding to an $EtAlCl_2$ core.

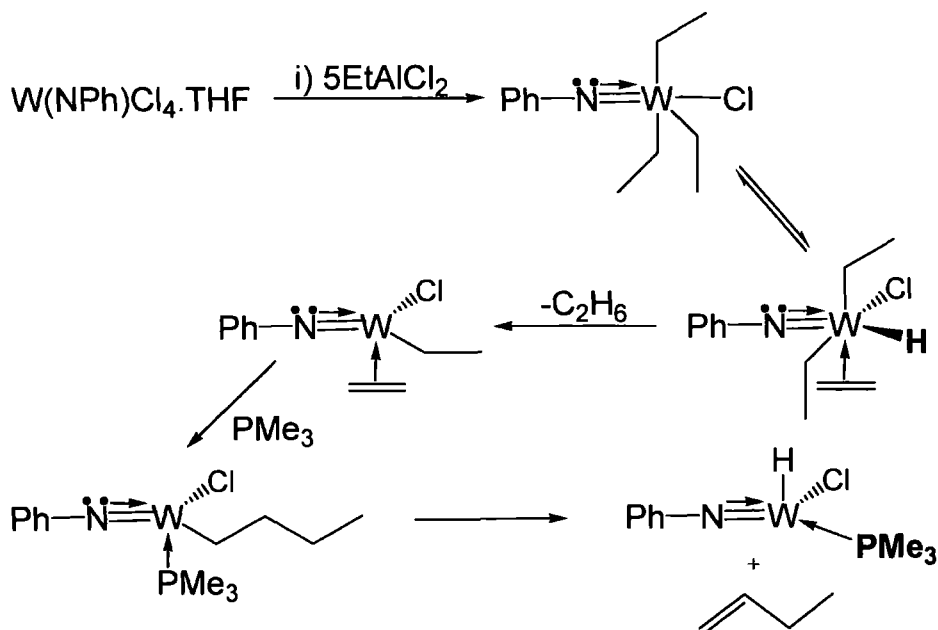
$\text{Et}_3\text{Al}_2\text{Cl}_3$, as it is through the reaction of excess EtAlCl_2 that *mono(imido)* pre-catalysts are activated (**Section 2.2, Table 2.3**). Thus, in two separate experiments $\text{W}(\text{NPh})\text{Cl}_4 \cdot \text{THF}$ (**32**) was dissolved in C_6D_6 and reacted with excess EtAlCl_2 or $\text{Et}_3\text{Al}_2\text{Cl}_3$. In both reactions ethane was observed to form. This indicates that as for the related *bis(imido)* systems (**Section 2.3.2**), addition of $\text{Et}_x\text{AlCl}_{3-x}$ reagents to complex **32** results in the formation of a tungsten diethyl intermediate, which undergoes β -hydride and then reductive elimination (see **Section 2.3.2 Scheme 2.7**).

Notably, addition of PMe_3 to the $\text{W}(\text{NPh})\text{Cl}_4 \cdot \text{THF} / \text{EtAlCl}_2$ reaction solution resulted in the formation of but-1-ene, which was only observable using ^1H NMR spectroscopy after PMe_3 addition (**Scheme 2.9**). The formation of but-1-ene upon treatment of $\text{W}(\text{NPh})\text{Cl}_4 \cdot \text{THF}$ (**32**) with EtAlCl_2 and then PMe_3 (**Scheme 2.9**) can be explained by PMe_3 destabilizing $\text{L}_n\text{W}^{\text{VI}}\text{-Et}$ intermediates (**Scheme 2.10**). However, it is unclear as to the exact pathway by which but-1-ene is formed, as at no stage have any reaction intermediates been positively identified using NMR spectroscopy.

Scheme 2.9 But-1-ene formation via reaction of $\text{W}(\text{NPh})\text{Cl}_4 \cdot \text{THF}$ (**32**)



Scheme 2.10 Proposed route of but-1-ene formation via reaction of $\text{W}(\text{NPh})\text{Cl}_4 \cdot \text{THF}$ (**32**) with EtAlCl_2 and PMe_3



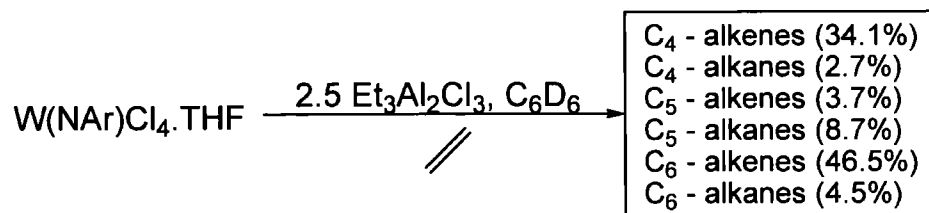
Upon addition of EtAlCl_2 (five equivalents) to $\text{W}(\text{NPh})\text{Cl}_4 \cdot \text{THF}$ (**32**), broad ^1H NMR resonances were observed. Such spectral features could be due to the reduction of the W^{VI} centre *via* the pathway outlined in **Scheme 2.10** to give paramagnetic species. Indeed, reduction of **32** by EtAlCl_2 could feasibly generate paramagnetic W^{IV} or W^{II} complexes *via* reductive elimination of ethane. Similarly, broad ^1H NMR signals were found after reaction of $\text{Ta}(\text{NAr})\text{Cl}_3 \cdot \text{TMEDA}$ (**59**) with EtAlCl_2 (five equivalents) in C_6D_6 , with ethane also being observed, which is suggestive of the formation of Ta^{III} complexes *in situ*.

2.4 Micro-scale Investigations into *mono*(imido)-based Alkene Dimerization Systems

In **Section 2.2** both *mono*- and *bis*(imido) complexes have been used as ethylene dimerization pre-catalysts. At high ethylene partial pressures (40 bar) (**Table 2.3, Section 2.2**) it has been shown that both these *mono*- and *bis*(imido) systems can initiate ethylene dimerization. However, at lower ethylene partial pressures (~1 bar) a $\text{W}(\text{NAr})_2\text{Cl}_2 \cdot \text{DME} / \text{EtAlCl}_2$ reaction solution failed to initiate ethylene dimerization (**Section 2.3.2**). To investigate if the same difference occurs for systems based on $\text{W}(\text{NR})\text{Cl}_4 \cdot \text{THF}$ complexes, attention turned to evaluating the reactions of *mono*(imido) systems when lower partial pressures (~1 bar) of alkenes are employed.

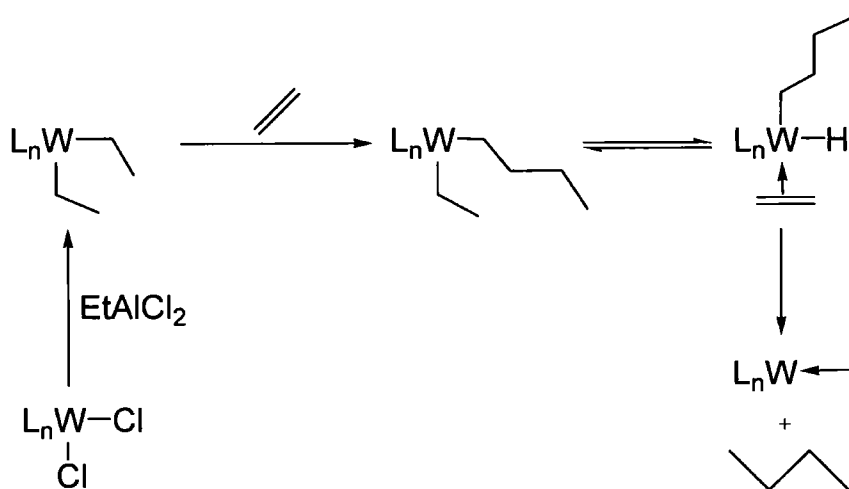
An initiator solution was formed by reaction of $\text{W}(\text{NAr})\text{Cl}_4 \cdot \text{THF}$ (**32**) with eight equivalents of EtAlCl_2 in C_6D_6 . Addition of ethylene to this mixture, resulted in an exothermic reaction with produced C_4 (73.3%), C_6 (22.5%) and C_8 (2.1%) alkenes (established using GC). Similarly, addition of ethylene to a $\text{W}(\text{NAr})\text{Cl}_4 \cdot \text{THF} / \text{Et}_3\text{Al}_2\text{Cl}_3$ C_6D_6 solution results in the production of a range of higher olefins, the relative ratios of which were determined using GC and GC-MS (**Scheme 2.11**). Using related procedures it was found that addition of propylene, to a mixture of $\text{W}(\text{NAr})\text{Cl}_4$ (**62**) and $\text{Et}_3\text{Al}_2\text{Cl}_3$ in C_6D_6 generated exclusively 2,3-dimethylbut-1-ene.

Scheme 2.11 Using the pre-catalysts $W(NAr)Cl_4 \cdot THF$ (**38**) to initiate ethylene dimerization on a micro-scale.

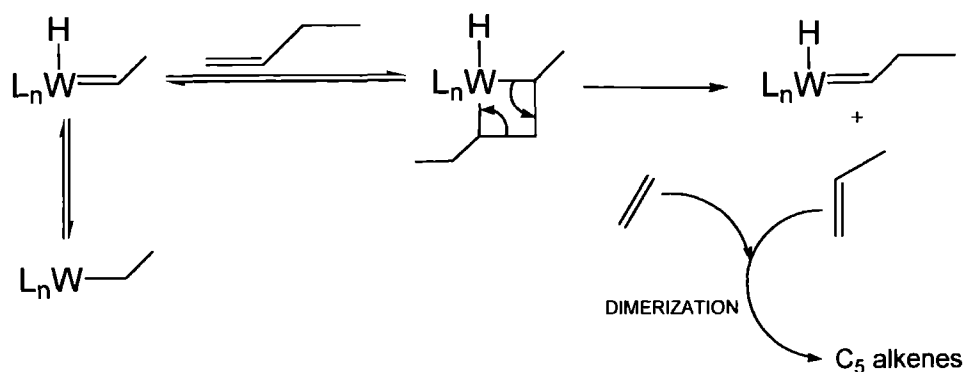


Notably, significant traces of alkanes were produced using the $W(NAr)Cl_4 \cdot THF/Et_3Al_2Cl_3$ system and were detected using GC-MS (**Scheme 2.11**). One plausible route by which these alkanes could form is *via* reductive elimination from a hydride complex as illustrated in **Scheme 2.12**.

Scheme 2.12 Mechanism of butane formation



It is clear that the selectivity of the $W(NAr)Cl_4 \cdot THF/Et_3Al_2Cl_3$ initiator system for ethylene dimerization is low (~35%), with a high degree of ethylene trimerization occurring (~47%). In addition to ethylene dimerization or trimerization, alkene metathesis is also being initiated in this reaction, generating "odd" C₅ hydrocarbons, presumably from reaction of "even" alkenes derived *in situ* from ethylene (**Scheme 2.13**).

Scheme 2.13 Production of C₅ products via but-1-ene metathesis

Menapace *et al.* have shown that the selectivity of their WCl_6 dimerization system (generated from WCl_6 , $2NH_2R$ and $Et_3Al_2Cl_3$) for propylene dimerization vs. olefin metathesis was highly dependent on the relative concentration of $Et_3Al_2Cl_3$ co-initiator.²² Thus, at relatively low $Et_3Al_2Cl_3$ loadings propylene metathesis occurs (W:Al molar ratio of 1:1.5). In contrast, a large excess of $Et_3Al_2Cl_3$ (1:10) was found to “switch” the selectivity of the initiator system to give exclusively propylene dimerization. Hence, parallels can be drawn between the selectivity of Menapace’s WCl_6 system at low $Et_3Al_2Cl_2$ loadings and the $W(NAr)Cl_4 \cdot THF/Et_3Al_2Cl_3$ system highlighted in **Scheme 2.11**. In both systems alkene metathesis is initiated, suggesting that similar active species are formed *in situ* in both cases.

2.5 Dimerization of C₂D₄ and C₂H₄ using Systems Based upon *mono*(Imido) Pre-catalysts

The discovery that systems based on *mono*(imido) complexes can induce ethylene dimerization on a micro-scale using small quantities of alkene feedstock, made it of interest to investigate the mechanism of ethylene dimerization *via* reaction of a mixture of C_2H_4 and C_2D_4 . As discussed in detail in **Chapter 1, Section 1.5** Bercaw *et al.* have examined the mechanism of their Cr^{III} ethylene trimerization initiator through the reaction of a 1:1 mixture of C_2D_4 and C_2H_4 .²³ They observed that reaction of C_2D_4/C_2H_4 was found to give C₆ alkenes containing exclusively even numbers of deuterium and hydrogen atoms. This was cited as proof of trimerization proceeding *via* a metallacycle mechanism, as the alternative degenerate polymerization (or hydride) cycle would inevitably give olefin products with odd

numbers of deuterium atoms.^{iv} As alkene trimerization and dimerization are often closely related, it is feasible that using a procedure similar to that employed in Bercaw's study could yield information as to the reaction mechanism operative for a *mono(imido)*-based dimerization system.

To this end, a 1:1 mixture of C_2D_4 and C_2H_4 was added to a $W(NAr)Cl_4 \cdot THF / Et_3Al_2Cl_3 \cdot C_6D_6$ initiator solution. This resulted in an immediate and exothermic reaction. Following reaction analysis of the volatile components of the mixture by both GC and GC-MS confirmed that a similar distribution of C_4 and C_6 products was obtained to that given by the $W(NPh)Cl_4 \cdot THF / Et_3Al_2Cl_3 / C_2H_4$ system discussed in the previous section (**Scheme 2.4**). GC-MS analysis was hampered by the fact that under the conditions used, it was found that all the C_4 isotopomers co-elute. However, using ion separation the abundance of each isotopomer of but-1-ene has been determined (**Table 2.4**).

Table 2.4 Relative abundances of but-1-ene isotopomers obtained from dimerization of a 1:1 C_2D_4/C_2H_4 mixture initiated by $W(NPh)Cl_4 \cdot THF / Et_3Al_2Cl_3$

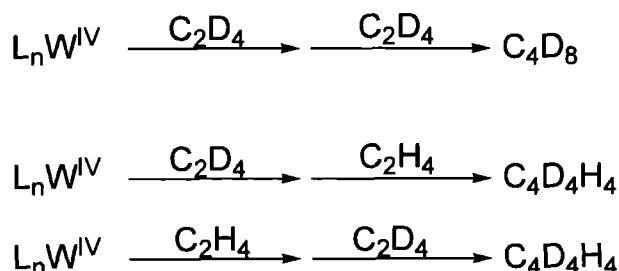
Isotopomers	Relative abundance predicted for a hydride cycle	Relative abundance predicted for a oxidative coupling mechanism	Observed relative abundance
C_4H_8	1	1	1.08
C_4H_7D	1	0	1.71
$C_4H_6D_2$	0	0	2.70
$C_4H_5D_3$	1	0	3.80
$C_4H_4D_4$	2	2	4.29
$C_4H_3D_5$	1	0	3.68
$C_4H_2D_6$	0	0	1.13
C_4HD_7	1	0	1.00
C_4D_8	1	1	>0.2

The relative abundance of a given isotopomer predicted to be produced *via* a hydride or metallacycle mechanism has been determined from the number of pathways by which each isotopmer can be produced. For example, C_4H_8 can only be produced by reaction of two molecules of C_2H_4 and thus has a predicted relative frequency of one for both mechanisms. In contrast, $C_4H_4D_4$, could result from reaction of C_2H_4 and

^{iv} For example, trimerization of 3 molecules of C_2D_4 by a $L_nCr^{III}-H$ or $L_nCr^{II}-H$ initiator, can generate the products C_6D_{12} or $C_6D_{11}H$.

then C_2D_4 or *vice versa*, giving two reaction pathways. Hence, $C_4H_4D_4$ is assigned a predicted relative frequency of two (**Scheme 2.14**).

Scheme 2.14 Predicting the relative abundances of $C_4H_4D_4$ and C_2D_4 assuming an oxidative coupling mechanism



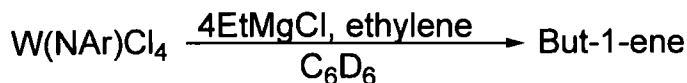
It is clear that the isotopmer distribution obtained upon reaction of C_2H_4 and C_2D_4 with the $W(NPh)Cl_4 \cdot THF/Et_3Al_2Cl_3$ initiator system (**Table 2.4**) does not fit uniquely that for either a hydride or metallocycle cycle process. Furthermore, the formation of olefins containing both odd and even numbers of deuterium atoms could feasibly result from the operation of either mechanism. Consequently, no detailed conclusions as to the mechanism by which the $W(NAr)Cl_4 \cdot THF/Et_3Al_2Cl_3$ system dimerizes ethylene can be made.

2.6 Assessing the Abilities of Grignard Reagents to Activate *mono(imido)* Complexes for Alkene Dimerization

In **Section 2.3.4** it was established that addition of $EtAlCl_2$ or $Et_3Al_2Cl_3$ to *mono(imido)* complexes resulted in ethane evolution, indicating that catalyst activation was occurring *via* a diethyl intermediate undergoing first β -hydride and then reductive elimination. To evaluate the implication of β -hydride elimination on catalyst activation, the introduction of an ethyl group to the coordination sphere of a tungsten centre using $EtMgCl$ was explored. Particular emphasis was placed on assessing the capacity of $EtMgCl$ to activate the *mono(imido)* pre-catalysts $W(NAr)Cl_4$ (**62**).

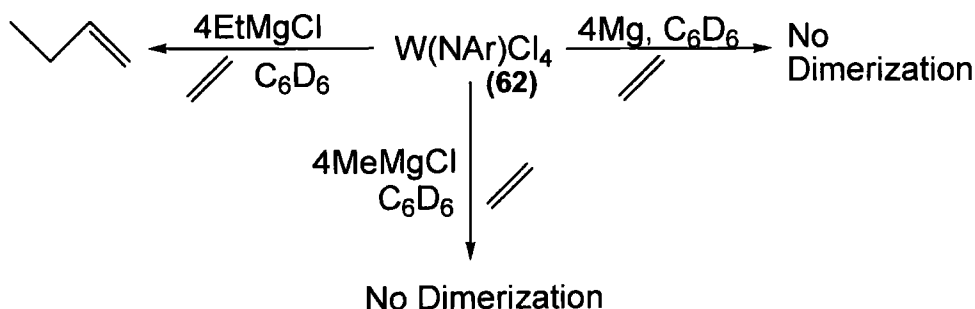
Notably, reaction between $EtMgCl$ and $W(NAr)Cl_4$ (**62**) in C_6D_6 results in ethane evolution. Subsequent addition of ethylene to the resulting reaction mixture was found to result in the slow formation of but-1-ene (verified by 1H NMR analysis) over a 2 h reaction period (**Scheme 2.15**).

Scheme 2.15 Activation of $W(\text{NAr})\text{Cl}_4$ (**62**) by EtMgCl and subsequent reaction with ethylene



To further assess the role of EtMgCl as a co-initiator, the abilities of the reagents MeMgCl and Mg to activate $W(\text{NAr})\text{Cl}_4$ (**62**) have also been studied. It was found that in contrast to EtMgCl , neither MeMgCl nor Mg was able to co-initiate ethylene dimerisation, although ^1H NMR spectroscopy confirms that reaction of **62** occurred in each case (**Scheme 2.16**). As Mg turnings were unable to activate complex **62** it can be concluded that the ethylene dimerization observed in the EtMgCl system is not attributable to traces of magnesium likely to be present as an impurity in the commercially purchased EtMgCl solution. It is also evident that reduction of the W^{VI} atom of complex **62** by Mg does not induce dimerization. Of note is that ethane was not observed upon addition of MeMgCl to $W(\text{NAr})\text{Cl}_4$ (**62**), suggesting that MeMgCl was unable to reduce **62**. Evidently alkylation of **62** to give tungsten methyl groups, which are unable to undergo β -hydride elimination, disbars initiator formation. This highlights the importance of β -hydride elimination in the formation of the active initiator complex in the $W(\text{NAr})\text{Cl}_4/\text{EtMgCl}$ ethylene dimerization system. Indeed, in the EtMgCl system the active initiator complex is likely to be formed *via* a tungsten diethyl species undergoing first β -hydride elimination, and then reductive elimination, generating a W^{IV} -ethylene complex and ethane *in situ* (see **Section 2.3.2, Scheme 2.7**).

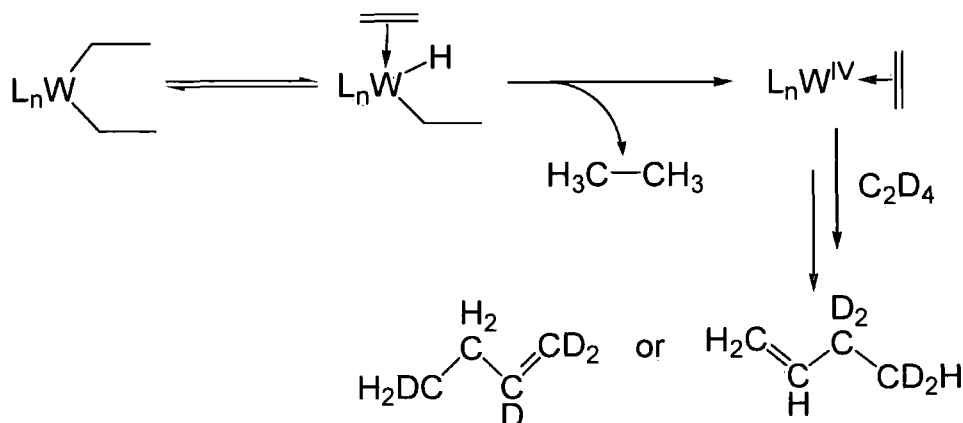
Scheme 2.16 Assessing the relative capacities of EtMgCl , MeMgCl and Mg to activate $W(\text{NAr})\text{Cl}_4$ (**62**)



2.7 Attempts to Investigate the Mode of Activation of *mono(imido)*-based Dimerization Systems Using C₂D₄

In Section 2.3.4 it was proposed that reduction of *mono(imido)* complexes by Et₃Al₂Cl₃ or EtAlCl₂ generates L_nW^{IV}(CH₂CH₂) intermediates, from which the active initiator complex is believed to be derived. Further evidence to support this mode of initiator activation could be provided by the detection of alkenes containing both deuterium and hydrogen atoms, resulting from the reaction of a L_nW^{IV}(CH₂CH₂) intermediate with C₂D₄ (**Scheme 2.17**). Hence, using procedures outlined in this Section a C₂D₄ feedstock was reacted with a range of *mono(imido)* based initiator systems.

Scheme 2.17 Potential route to olefins containing both deuterium and hydrogen atoms via reaction of a L_nW^{IV}(CH₂CH₂) intermediate

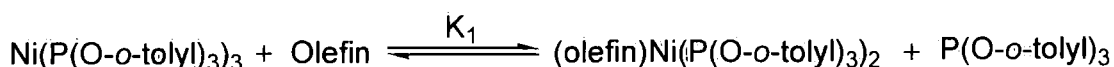


Activation of complex W(NAr)Cl₄.THF (**38**) by Et₃Al₂Cl₃ followed by later addition of C₂D₄ resulted in C₄ (~23%), C₅ (~6%), and C₆ (~67%) products, but no alkenes containing H-atoms were detected by either GC-MS or ¹H NMR spectroscopy. Similarly, addition of EtMgCl and then C₂D₄ to a solution of W(NAr)Cl₄.THF (**38**) resulted in the formation of both C₄ (~90%) and C₆ (~10%) products. Notably, no olefins with both deuterium and hydrogen atoms were found using GC-MS and no alkene ¹H NMR resonances were detected. Unfortunately, the failure to detect mixed olefins such as CH₂CHCD₂CD₂H upon reaction of C₂D₄ in either the EtMgCl or Et₃Al₂Cl₃ co-initiated *mono(imido)* systems neither supports nor contradicts the activation of complex **38** via the pathway outlined in **Scheme 2.17**. This is because activation of **38** by Et₃Al₂Cl₃ or EtMgCl followed by reaction of C₂D₄ could feasibly produce alkenes such as C₄H₄D₄ in concentrations that are too low to be detected by either ¹H NMR spectroscopy or GC-MS.

2.8 Contrasting the Capacity of EtMgCl and EtAlCl₂ to Co-Initiate Propylene Dimerization

As discussed in **Section 2.7**, both EtMgCl and EtAlCl₂ have been shown to activate *mono(imido)* complexes generating species capable of initiating ethylene dimerization. Of note is that ethylene is a relatively reactive alkene, with coordination of a C₂H₄ ligand to a given metal centre being comparatively unaffected by steric constraints. In contrast, the reactivity of propylene as a neutral ligand towards organometallic reagents tends in general to be lower. For instance, Tolman has reported that the capacity of propylene to bind to Ni(P(*O-o-tolyl*)₃)₃ is significantly lower than that of ethylene (**Scheme 2.18**).²⁴ Thus, although the W(NAr)Cl₄.THF/EtMgCl and W(NAr)Cl₄.THF/EtAlCl₂ systems are both active for ethylene dimerization, the two systems may display different reactivity with less reactive propylene. Hence, assessing the abilities of EtMgCl and EtAlCl₂ to co-initiate propylene dimerization is likely to give a more descriptive, general indication as to the effectiveness of the two reagents as alkene dimerization co-initiators.

Scheme 2.18 *Contrasting the coordination of ethylene and propylene to Ni(P(O-*o-tolyl*)₃)₃*



Olefin	K ₁
Ethylene	2.5×10 ²
Propylene	5.3×10 ⁻¹

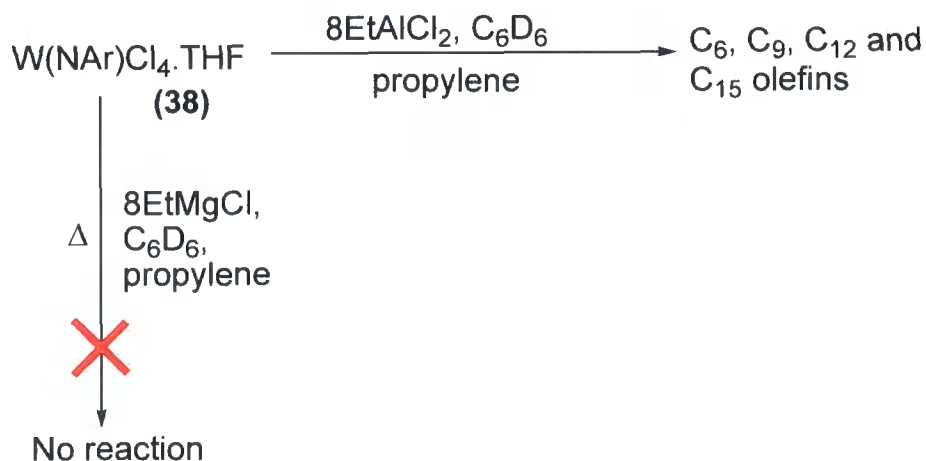
With this in mind, the *mono(imido)* complex W(NAr)Cl₄.THF (**38**) was reacted with EtAlCl₂ (eight equivalents) in C₆D₆ and to this reaction solution propylene was then added. Subsequent analysis of the volatile components resulting from this reaction using GC demonstrated that propylene dimerization, trimerization, and oligomerization had indeed been initiated, with C₆, C₉ and even trace C₁₂ products being observed.[†] This demonstrates that W(NAr)Cl₄.THF/EtAlCl₂ will readily initiate the coupling of propylene. Notably, propylene metathesis was also co-initiated by the W(NAr)Cl₄.THF/EtAlCl₂ system resulting in both C₂ and C₄ products (as detected by GC). Significantly, reaction of propylene was initiated immediately and at room

[†] This is consistent with the related ethylene reaction, which also resulted in higher olefins C₄ (73.3%) C₆ (22.5%) and C₈ (2.1%) (see **Section 2.4**).

temperature. This shows that the EtAlCl_2 co-initiated system is highly reactive towards propylene.

Addition of MgEtCl and then propylene to a C_6D_6 solution of $\text{W}(\text{NAr})\text{Cl}_4 \cdot \text{THF}$ (**38**) using the same conditions to that employed in the EtAlCl_2 study, repeatedly failed to result in any reaction of the propylene. The formation of higher olefins was not detected using ^1H NMR spectroscopy, even after heating of the reaction solution (60°C , 2 h). Thus, there is a clear difference between the capacity of the reagents EtMgCl and EtAlCl_2 to activate $\text{W}(\text{NAr})\text{Cl}_4 \cdot \text{THF}$ (**38**) for propylene dimerization/oligomerization (**Scheme 2.19**). This indicates that an aluminium-based moiety may be an intimate component of the active initiator species in the EtAlCl_2 co-initiated system.

Scheme 2.19 *Contrasting the capacity of EtMgCl and EtAlCl_2 to activate complex **38***

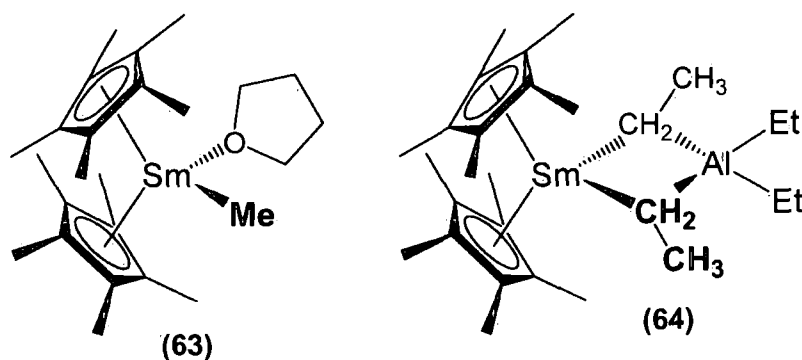


2.8.1 Investigating the Impact of Lewis acidity on *mono(imido)* Based Dimerization Systems

The difference between the capacity of EtMgCl and EtAlCl_2 co-initiators activate $\text{W}(\text{NAr})\text{Cl}_4 \cdot \text{THF}$ (**38**) for propylene dimerization could be attributed to a number of factors. Both EtMgCl and EtAlCl_2 are likely to have different reactivity with a tungsten chloride bond due to different Mg-C and Al-C bond strengths. Furthermore, any differences between the solution structures of EtMgCl and EtAlCl_2 (i.e. dimers) could also influence their relative reactivity with a W-Cl moiety. One crucial difference between the two species is their different Lewis acidity. Indeed, aluminium-based reagents such as EtAlCl_2 or AlCl_3 are known to be strong Lewis acids. In contrast, Grignard reagents such as EtMgCl or magnesium salts such as MgCl_2 are accepted as being much weaker Lewis acids.²⁵ For instance, the weak Lewis acidity of

Grignard reagents has been used to rationalise the low activity observed for ethylene polymerization systems based upon reaction of $[\text{SmCl}_2(\text{Cp}^*)_2][\text{Li}(\text{OEt}_2)_2]$ ($\text{Cp}^* = \text{C}_6\text{Me}_6$) with ${}^n\text{BuMgEt}$.^{25;26} Furthermore, the complex $[\text{Sm}(\text{Cp}^*)_2\text{Me}(\text{THF})]$ (**63**) (Figure 2.4), which has no associating Lewis acid fragment, is used as a model for the Mg/Sm ethylene polymerization system.²⁷ Although no molecular structures of bimetallic complexes of samarium and magnesium alkyls currently exist, aluminium-based reagents are known to readily bind to $(\text{Cp}^*)_2\text{Sm}$ fragments as coordinating Lewis acids. Thus, the synthesis of $[\text{Sm}(\text{Cp}^*)_2\text{AlEt}_4]$ ²⁸ (**64**) (Figure 2.4) is entirely consistent with the greater Lewis acid acidity of aluminium alkyls compared with their magnesium-based counterparts.

Figure 2.4 Molecular structures of $[\text{Sm}(\text{Cp}^*)_2\text{Me}(\text{THF})]$ and $[\text{Sm}(\text{Cp}^*)_2\text{AlEt}_4]$

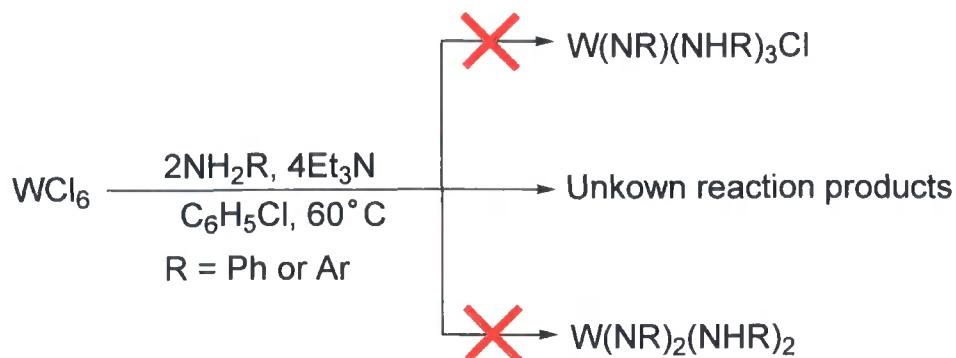


Another relevant difference between RMgCl and $\text{R}_x\text{AlCl}_{3-x}$ reagents concerns the reactivity of the two classes of compounds with ethylene. In contrast to RMgX reagents, it is known that simple aluminium alkyl halides can function as ethylene polymerization initiators.²⁹ To investigate if alkene dimerization is occurring at an aluminium centre in the $\text{W}(\text{NAr})\text{Cl}_4\cdot\text{THF}/\text{EtAlCl}_2$ system rather than at the tungsten, control reactions were undertaken. Hence, a C_6D_6 solution containing both EtAlCl_2 and propylene was heated; no higher olefins were detected by ${}^1\text{H}$ NMR spectroscopy. This indicates that the propylene dimerization and oligomerization initiated by the $\text{W}(\text{NAr})\text{Cl}_4\cdot\text{THF}/\text{EtAlCl}_2$ system do not result from reaction of EtAlCl_2 as a chain transfer agent. Instead, the propylene dimerization initiated by the $\text{EtAlCl}_2/\text{W}(\text{NAr})\text{Cl}_4\cdot\text{THF}$ system, can be attributed to the formation of an active tungsten initiator complex *via* reaction of EtAlCl_2 as a Lewis acid. However, the definitive structure of the active tungsten initiator complex derived from $\text{W}(\text{NAr})\text{Cl}_4\cdot\text{THF}$ (**38**) remains unclear.

2.9 Attempts to Identify any Imido Complexes Formed in the STUK WCl_6 Dimerization System

In Section 2.2 a range of *bis*- and *mono*(imido) complexes were employed as ethylene dimerization pre-catalysts, with a series of initiator test runs conducted at high pressure and temperatures (40 bars, 60 °C). It was consistently found that both molybdenum and tungsten *bis*(imido) complexes gave higher TON and activities than related *mono*(imido) tungsten pre-catalysts. Initially, this observation would suggest that it is a *bis*(imido) complex that is the active initiator in the STUK WCl_6 dimerization system. However, some results contradict this proposition, notably the fact that the reaction of $W(NAr)_2Cl_2 \cdot DME$ (**40**) on a micro scale with $Et_3Al_2Cl_3$ in C_6D_6 gave a reaction solution that failed to initiate ethylene dimerization (Section 2.3.2). In contrast, on a micro scale, in which significantly lower ethylene partial pressures were employed (<1 bar) systems based on *mono*(imido) complexes are capable of initiating ethylene dimerization or oligomerization at room temperature. For example, reaction of $W(NAr)Cl_4 \cdot THF$ (**38**) with $Et_3Al_2Cl_3$ in C_6D_6 generates C_4 and C_6 dimerization and trimerization products as well as C_5 alkenes, produced *via* metathesis reactions. Evidently, the relative activities of *bis*- and *mono*(imido) systems for ethylene dimerization are highly dependent on reaction conditions, with systems based on *mono*(imido) complexes being more active when lower ethylene concentrations are used. Hence, the observed activities of both discrete *mono*- and *bis*(imido) complexes makes it unclear as to which type of imido complex is forming in the WCl_6 based STUK dimerization system.

To assess if it is a *bis*- or *mono*(imido) complex that is formed *in situ* in the STUK dimerization system (WCl_6 , $2NH_2R$, $4Et_3N$, $10EtAlCl_2$), WCl_6 was reacted with NH_2Ph and Et_3N in chlorobenzene and the resulting material analysed using multinuclear NMR spectroscopy. Neither the resulting 1H nor the ^{13}C NMR spectrum could be used to ascertain information as to the structure of the new tungsten-containing reaction products, as broad non-assignable resonances were observed. Similar results were obtained upon reaction of the amine NH_2Ar (Scheme 2.20). This indicates that more than one tungsten complex may be produced upon reaction of WCl_6 using the STUK conditions.

Scheme 2.20 Reaction of WCl_6 using the STUK conditions

It is reasonable to assume that any *bis*(imido) complexes formed *in situ* in the WCl_6 dimerization system must result from reaction of an intermediate *mono*(imido) complex with an amine. Hence, to ascertain the plausibility of *bis*(imido) complexes evolving in the STUK system, $W(NPh)Cl_4 \cdot THF$ (**32**) was reacted with H_2NAr in C_6D_6 (Scheme 2.21).

Scheme 2.21 Reaction of $W(NPh)Cl_4 \cdot THF$ (**32**) with H_2NAr ($Ar = 2,6$ Diisopropylphenyl)

Disappointingly, NMR spectroscopy could not be used to categorically determine the structure of the reaction products obtained from addition of HN_2Ar to $W(NPh)Cl_4 \cdot THF$ (**32**), as analysis of the reaction solution presented multiple 1H and ^{13}C alkyl resonances. Of note, however, is that a broad NH_2 resonance was identified at approximately 9.5 ppm, which indicates that coordination of the amine or an amide moiety to the tungsten atom does occur. In a separate reaction $W(NAr)Cl_4 \cdot THF$ (**38**) was dissolved in C_6D_6 and then mixed with Et_3N and H_2NAr . Here, no reaction of the aniline was observed to occur, with no new *bis*(imido) species being identified using NMR spectroscopy. Hence, it has not been possible to determine if a *bis*(imido) complex could form *in situ* from a *mono*(imido) intermediate in the STUK process.

Although it is still unclear as to whether *mono* or *bis*(imido) complexes are forming in the STUK WCl_6 system, it is apparent that both types of imido complex react with Et_xAlCl_{3-x} co-initiators to give systems active for ethylene dimerization

(Table 2.3, Section 2.2). As such it is reasonable to speculate that both *mono*- and *bis*(imido) complexes could be formed *in situ* upon reaction of WCl_6 with Et_3N and NH_2R . Thus, the reactivity of both *mono* and *bis* imido pre-catalysts with R_xAlCl_{3-x} reagents is worthy of further investigation.

2.10 Conclusions

In this Chapter the reaction of $EtAlCl_2$ and $Et_3Al_2Cl_3$ with $W(NAr)_2Cl_2 \cdot DME$ (**40**), $W(NAr)Cl_4 \cdot THF$ (**38**) or $W(NPh)Cl_4 \cdot THF$ (**32**) in C_6D_6 resulted, in all cases, in the simultaneous production of multiple unidentifiable tungsten complexes and ethane. Ethane evolution upon addition of Et_xAlCl_{3-x} reagents to W^{VI} chloride complexes strongly indicates that ethylation of tungsten chloride moieties results in reduction of the W^{VI} atom giving $L_nW^{IV}(CH_2CH_2)$ intermediates. Although significant to initiator formation, undoubtedly it is the instability of the tungsten ethyl moiety to β -hydride elimination that results in the formation of the observed multitude of tungsten-containing products. This, in turn, has prevented detailed examination as to how Et_xAlCl_{3-x} activates both *mono* and *bis*(imido) pre-catalysts for ethylene dimerization. However, comparison of the relative abilities of $EtMgCl$ and $EtAlCl_2$ to activate *mono*(imido) pre-catalysts for propylene dimerization indicates that the greater capacity of $EtAlCl_2$ to react as a Lewis acid is crucial to the activation of *mono*(imido) systems (Section 2.8).

To gain a clearer insight into how R_xAlCl_{3-x} Lewis acids interact with imido complexes, attention turned to studying the reactivity of discrete imido complexes with methyl aluminium reagents, such as $MeAlCl_2$, Me_2AlCl or Me_3Al . Hence, in the following Chapters, the reaction of imido complexes with Me_xAlCl_{3-x} reagents will be examined. Here, the stability of tungsten methyl groups, for which β -hydride elimination reactions are impossible, is anticipated to facilitate the formation of stable discrete complexes. This will enable any potential interactions between Me_xAlCl_{3-x} Lewis acid and chloride or imido tungsten ligands to be clearly identified.

2.11 References

- ¹ US Patent 5,059,739 (1989) to Exxon Chemical Inv., D.E. Hendriksen.
- ² M.J. Hanton, Unpublished results.
- ³ H. Olivier and P. Laurent-Gérot, *J. Mol. Cat. A.*, **1999**, *148*, 43.
- ⁴ World patent 2005/089940 to Sasol Technology (UK) Ltd (2005), M.J. Hanton and R.P. Tooze.
- ⁵ W.A. Nugent, *Inorg. Chem.*, **1983**, *22*, 965.

- ⁶ A.A. Danopoulos, G. Wilkinson, B. Hussain-Bates and M.B. Hursthouse, *Dalton Trans.*, **1990**, 2753.
- ⁷ D.S. Williams, M.H. Schofield, J.T. Anhaus and R.R. Schrock, *J. Am. Chem. Soc.*, **1990**, *112*, 6728.
- ⁸ T. Chen, K.R. Sorasance, Z. Wu, J.B. Diminnie and Z. Xue., *Inorg. Chim. Acta*, **2003**, *345*, 113.
- ⁹ R.R. Schrock, R.T. DePue, J. Feldman, K.B. Yap, D.C. Yang, W.M. Davis, L. Park, M. Di Mare, M. Schofield, J.T. Anhaus, E. Walborsky, E. Evitt, C. Kruger and P. Betz, *Organometallics*, **1990**, *9*, 2262.
- ¹⁰ V.C. Gibson, C. Redshaw, W. Clegg and M.R.J. Elsegood, *Dalton, Trans.*, **1997**, 3207.
- ¹¹ D.S. Williams, M.H. Schofield and R.R. Schrock, *Organometallics*, **1993**, *12*, 4560.
- ¹² S. Tobisch, *Dalton Trans.*, **2008**, 2120.
- ¹³ F. Montilla, A. Galindo, E. Carmona, E. Gutiérrez-Puebla and A. Monge, *J. Chem. Soc., Dalton Trans.*, **1998**, 1299.
- ¹⁴ E. A. Maatta and R.A.D. Wentworth, *Inorg. Chem.*, **1979**, *18*, 2409.
- ¹⁵ J.C. Waslike, G. Wu, X. Bu, G. Kehr and G. Erker, *Organometallics*, **2005**, *24*, 4289.
- ¹⁶ K.S. Heinselman, V.M. Miskowski, S.J. Geib, L.C. Wang, M.D. Hopkins, *Inorg. Chem.*, **1997**, *36*, 5530.
- ¹⁷ Y.W. Chao, P.A. Wexler and D.E. Wigley, *Inorg. Chem.*, **1989**, *28*, 3860.
- ¹⁸ V.C. Gibson, C. Redshaw, G.L.P. Walker, J.A.K. Howard, V.J. Hoy, J.M. Cole, L.G. Kuzmina and D.S. De Silva, *J. Chem. Soc., Dalton Trans.*, **1998**, 161.
- ¹⁹ G. Schoettel, J. Kress and J.A. Osborn, *Chem. Commun.*, **1989**, 1062.
- ²⁰ T.M. Cameron, C.G. Ortiz, I. Ghiviriga, K.A. Abbound and J.M. Boncella, *Organometallics*, **2001**, *20*, 2032.
- ²¹ P. M. Morse, Q.D. Shelby, D.Y. Kim, G.S. Girolami, *Organometallics*, **2008**, *27*, 984.
- ²² H.R. Menapace, N.A. Maly, J.L. Wang and L.G. Wideman, *J. Org. Chem.*, **1975**, *40*, 2983.
- ²³ T. Agapie, J.A. Laybinger and J.E. Bercaw, *J. Am. Chem. Soc.*, **2007**, *129*, 14295.
- ²⁴ C.A. Tolman, *J. Am. Chem. Soc.*, **1974**, *96*, 1974.
- ²⁵ R. Kempe, *Chem. Eur. J.*, **2007**, *13*, 2764.
- ²⁶ T.D. Tilley and R.A. Andersen, *Inorg. Chem.*, **1981**, *20*, 3267.

-
- ²⁷ W.J. Evans, L.R. Chamberlain, T.A. Ulibarri and J.W. Ziller, *J. Am. Chem. Soc.*, **1988**, *110*, 6423.
- ²⁸ W.J. Evans, L.R. Chamberlain and J.W. Ziller, *J. Am. Chem. Soc.*, **1987**, *109*, 7209.
- ²⁹ M.P. Shaver, L.E.N. Allan and V.C. Gibson, *Organometallics*, **2007**, *26*, 2252.

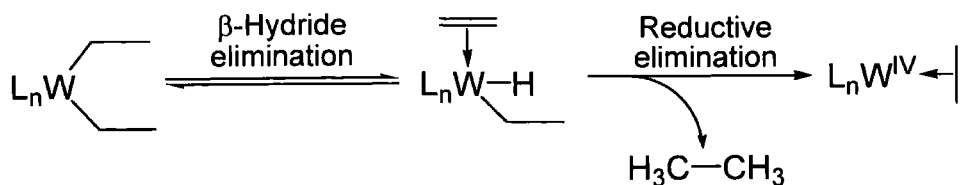
Chapter 3: Reaction of Tungsten and Molybdenum *bis*(Imido) Dihalide Complexes with Aluminium Methyl Reagents

3.0 Introduction

Patents outlining alkene dimerization systems based on WCl_6 invariably specify that high loadings of Et_xAlCl_{3-x} co-initiators are optimal.¹ For example, in the WCl_6 dimerization system patented by Sasol Technology (UK) Ltd (STUK), the most favourable W:Al molar ratios are stated as being between 1:5 to 1:12 (W:Al).² This is directly related to the patented innovation of the STUK system, which is addition of a separate base, Et_3N , to the initiator solution after treatment of WCl_6 with H_2NR . Efficient removal of HCl, before the addition of the Et_xAlCl_{3-x} co-initiator, is believed to prevent reaction between Et_xAlCl_{3-x} reagents and HCl. As a result, in the STUK WCl_6 -based dimerization system aluminium-based co-initiators ($Et_3Al_2Cl_3$ or $EtAlCl_2$) are present in higher effective concentrations than related processes in which HCl is not removed,¹ leading to higher initiator activity and selectivity. However, to date, the reasons why high Et_xAlCl_{3-x} co-initiator loadings are beneficial for WCl_6 -based dimerization systems remain unclear.

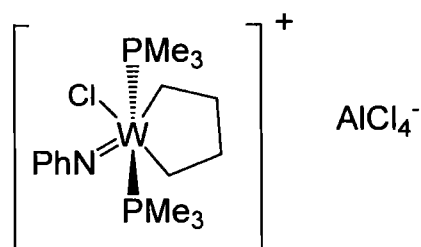
As *bis*(imido) complexes are postulated to be intermediates in WCl_6 -based dimerization systems, the performance of alkene dimerization systems based on discrete *bis*(imido) pre-catalysts have previously been investigated.³ Expanding on this preliminary investigation a comparative ethylene dimerization study was undertaken, in **Chapter 2, Section 2.2**. This new study clearly showed that both molybdenum and tungsten *bis*(imido) halide complexes can be activated for ethylene dimerization by $EtAlCl_2$ (**Table 2.3**). Furthermore, when high ethylene partial pressures were employed (40 bar) the activities of *bis*(imido) systems were found to be greater than those based upon related *mono*(imido) complexes. With a view to identifying the mode by which complexes such as $W(NAr)_2Cl_2 \cdot DME$ (**40**) are activated, in **Chapter 2, Section 2.3**, complex **40** was treated with $EtAlCl_2$ in C_6D_6 . Analysis of the resulting reaction mixtures using NMR spectroscopy revealed the formation of multiple tungsten complexes, which presented overlapping sets of CH and CH_3 1Pr NMR resonances. However, a notable by-product from the reaction of $W(NAr)_2Cl_2 \cdot DME$ (**40**) with $EtAlCl_2$ was found to be ethane, which is believed to result from β -hydride elimination from a tungsten ethyl ligand (**Scheme 3.1**). Although such reactions may be crucial to the activation of *bis*(imido) pre-catalysts, the formation of numerous products from the $W(NAr)_2Cl_2 \cdot DME/EtAlCl_2$ reactions meant that a detailed understanding of the mode by which $W(NAr)_2Cl_2 \cdot DME$ (**40**) is activated was prevented.

Scheme 3.1 Proposed route of ethane formation in the $W(\text{NAr})_2\text{Cl}_2\cdot\text{DME}/\text{EtAlCl}_2$ reaction



In order to try and circumvent the inherent instability of metal ethyl complexes, attention was shifted to the study of the reactions of $M(\text{NAr})_2\text{Cl}_2\cdot\text{DME}$ ($M = \text{Mo}$ or W) with methyl aluminium reagents such as Me_3Al , Me_2AlCl or MeAlCl_2 . It was anticipated that addition of $\text{Me}_x\text{AlCl}_{3-x}$ reagents to *bis*(imido) complexes would give more stable tungsten (or molybdenum) methyl complexes. This in turn, would allow a clearer insight into the possible role of $\text{R}_x\text{AlCl}_{3-x}$ fragments in the activation of *bis*(imido) dihalide pre-catalysts, which may involve abstraction of a halide ligand by a $\text{R}_x\text{AlCl}_{3-x}$ fragment. Indeed, interaction of an $\text{R}_x\text{AlCl}_{3-x}$ group with a chloride ligand could be significant to initiator formation, something highlighted by the development of the $W(\text{NPh})(\text{Cl})_2(\text{PMe}_3)_3/\text{AlCl}_3$ ethylene dimerization system by Olivier *et al.*⁴ Here, Olivier has proposed that abstraction of a tungsten chloride ligand by AlCl_3 , leads to an active ionic initiator species (**Figure 3.1**). It is plausible that a related ionic complex could be obtained upon addition of $\text{Me}_x\text{AlCl}_{3-x}$ reagents to *bis*(imido) complexes such as $W(\text{NAr})_2\text{Cl}_2\cdot\text{DME}$ (**40**).

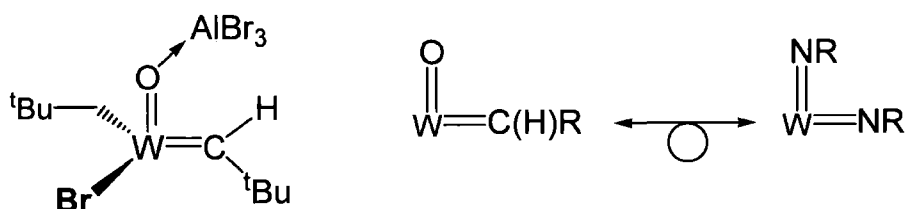
Figure 3.1 Charged initiator proposed by Olivier



3.0.1 Reactions Group 6 Imido Halide Complexes and Group 13-based co-Initiators

In this Chapter reactions between $\text{Me}_x\text{AlCl}_{3-x}$ reagents and $\text{M}(\text{NR})\text{Cl}_2\cdot\text{DME}$ ($\text{M} = \text{Mo}$ or W) complexes are examined. To date no related investigations have been reported, which is surprising as isolobal tungsten oxo complexes, when bound to species such as AlBr_3 , are known alkene metathesis initiators (**Figure 3.2**).⁵ This hints that $\text{Me}_x\text{AlCl}_{3-x}$ fragments may also be able to interact with imido ligands giving a complex capable of accommodating alkene coordination. In addition, reaction of $\text{W}(\text{NAr})_2\text{Cl}_2\cdot\text{DME}$ (**40**) with $\text{Me}_x\text{AlCl}_{(3-x)}$ reagents is also arguably relevant to the activation of the previously reported $\text{Cr}(\text{NR})_2\text{Cl}_2$ ethylene polymerization pre-catalysts by EtAlCl_2 or MAO.⁶ Since, in both instances, group VI *bis*(imido) chloride complexes are reacted with aluminium-based reagents.

Figure 3.2 AlBr_3 -bound metathesis initiators and the isolobal relationship between the fragments $\text{W}(\text{NAr})_2$ and $\text{WO}(\text{CHR})$

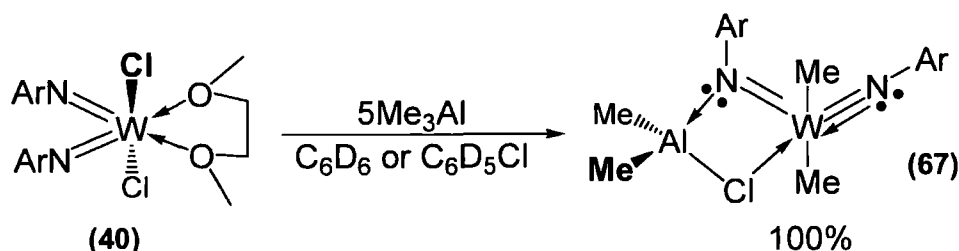


In work conducted for this thesis, particular emphasis has been placed upon investigating the reactivity of $\text{Me}_x\text{AlCl}_{(3-x)}$ species with *bis*(imido) halide complexes containing relatively bulky 2,6-diisopropylphenyl imido ligands (NAr). The large steric bulk of the NAr ligand is generally regarded as being sufficient to prevent bridging of imido groups between two W or Mo atoms, disbaring the formation of complexes such as $[\text{W}(\text{N}^t\text{Bu})\text{Me}_2]_2(\mu\text{-N}^t\text{Bu})_2$ (**65**),⁷ $[\text{Mo}(\text{N}^t\text{Bu})(\mu\text{-N}^t\text{Bu})\text{Me}_2]_2$ (**66**),⁸ or even potentially a mixture of complexes. Hence, complexes with bulky imido moieties such as $\text{Mo}(\text{NAr})_2\text{Cl}_2\cdot\text{DME}$ (**23**) or $\text{W}(\text{NAr})_2\text{Cl}_2\cdot\text{DME}$ (**40**) are predicted as being more likely to yield discrete complexes when treated with $\text{Me}_x\text{AlCl}_{3-x}$ reagents.

3.1 Reaction of $W(NAr)_2Cl_2 \cdot DME$ (**40**) and Me_3Al

To explore the reactivity of $W(NAr)_2Cl_2 \cdot DME$ (**40**) with Me_xAlCl_{3-x} reagents, attention turned to investigating the reactivity of Me_3Al with **40**. A C_6D_6 solution of $W(NAr)_2Cl_2 \cdot DME$ (**40**) was treated with five equivalents of Me_3Al (Scheme 3.2).ⁱ The resulting mixture was analysed using 1H NMR spectroscopy. Following addition of Me_3Al , the 1H NMR spectrum of the reaction solution was found to contain signals consistent with both $W-Me$ and $Al-Me$ species, present in a 1:1 ratio by integration (Figure 3.3). The resonance observed at -0.15 ppm can readily be assigned to an $Al-Me$ functionality since $Al-Me$ groups typically appear at low frequency. Indeed, the broad low frequency signal at -0.42 ppm is attributable to the $Al-Me$ moiety of free Me_3Al .ⁱⁱ Conversely the singlet at $\delta 1.56$ ppm can be assigned to a $W-Me$ resonance, as this chemical shift is typical for a W -alkyl moiety.⁹ The 1H NMR spectrum of this reaction mixture also exhibits three inequivalent doublets (in approximately a 1:1:2 ratio by integration) corresponding to CH_3 iPr resonances, and two distinct septets corresponding to two CH iPr resonances (in a 1:1 ratio). This inequivalence of the aryl imido substituents has been attributed to the coordination a Me_2AlCl fragment to a NAr imido ligand on the basis of the single crystal X-ray diffraction analysis (Section 3.1.1).

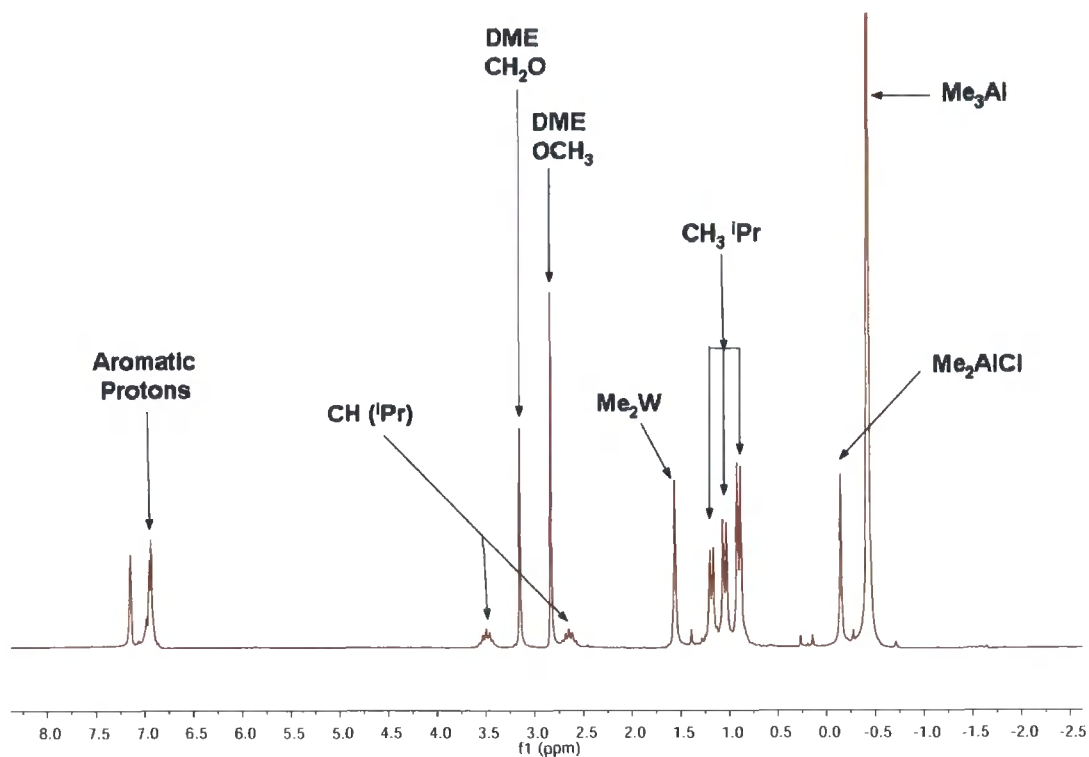
Scheme 3.2 Synthesis of $W(N\{Ar\}AlMe_2\{\mu-Cl\})(NAr)Me_2$ (**67**)



ⁱ To further investigate the reactivity of $W(NAr)_2Cl_2 \cdot DME$ (**40**) with Me_3Al , in a separate experiment complex **40** was reacted with a large excess (fourteen equivalents) of Me_3Al in C_6D_6 . Identical results were obtained as to when five equivalents were employed.

ⁱⁱ Analysis of authentic samples of $MeAlCl_2$ and Me_3Al in C_6D_6 reveals a single 1H resonance at -0.42 ppm in both cases.

Figure 3.3 ^1H NMR (C_6D_6 , 200 MHz) spectrum of mixture obtained following reaction of $\text{W}(\text{NAr})_2\text{Cl}_2\cdot\text{DME}$ (**40**) with 5 Me_3Al



Parallels can be drawn between this Me_3Al reaction, and the reactions of *bis*(imido) complexes with EtAlCl_2 outlined in **Chapter 2**. As discussed in detail in **Chapter 2**, **Section 2.3.1**, the complex $\text{Mo}(\text{N}^i\text{Bu})_2\text{Cl}_2$ (**21**) was synthesised *via* addition of one equivalent of EtAlCl_2 to $\text{Mo}(\text{N}^i\text{Bu})_2\text{Cl}_2\cdot\text{DME}$ (**26**). This shows that the first action of the Lewis acid EtAlCl_2 , upon addition to **26**, is to displace the coordinating DME moiety. Thus, the new DME resonances observed by ^1H NMR spectroscopy following reaction of complex **40** with Me_3Al are attributed to the formation of an $\text{AlMe}_3\cdot\text{DME}$ adduct. Again, this conclusion is supported by a single crystal X-ray diffraction study (**Section 3.1.1**), which confirms the displacement of the DME moiety from the tungsten core. Notably, adducts of $\text{Me}_x\text{AlCl}_{(3-x)}$ species and DME have been reported previously by Atwood, although spectroscopic or structural details are unknown.¹⁰

The reaction of $\text{W}(\text{NAr})_2\text{Cl}_2\cdot\text{DME}$ (**40**) with five equivalents of Me_3Al has been repeated using $\text{C}_6\text{D}_5\text{Cl}$ as the reaction solvent. This was undertaken as it has been established that chlorobenzene is the preferred solvent for both the Goodyear and STUK WCl_6 -based dimerization systems, as well as being the solvent of choice when activating $\text{M}(\text{NAr})_2\text{Cl}_2\cdot\text{DME}$ ($\text{M} = \text{Mo}$ or W) complexes with EtAlCl_2 (**Chapter 2**

Section 2.2). Analysis of the resulting C_6D_5Cl reaction mixture presented a 1H NMR spectrum that was identical to that obtained when C_6D_6 was used as the reaction solvent (**Figure 3.3**). Evidently, reaction selectivity of the $W(NAr)_2Cl_2.DME/Me_3Al$ system is not altered by the use of C_6D_5Cl instead of C_6D_6 , confirming the relevance of this study to “real” initiator systems.

3.1.1 Characterization of $W(N\{Ar\}AlMe_2\{\mu-Cl\})(NAr)Me_2$ (67) Using Single Crystal X-Ray Diffraction Analysis

In order to clarify the precise structure of the products obtained from the reaction of $W(NAr)_2Cl_2.DME$ (**40**) with excess Me_3Al , a sample of the product was prepared by addition of five equivalents of Me_3Al to $W(NAr)_2Cl_2.DME$ (**40**) in C_6D_6 . This solution was then dried *in vacuo* giving a light brown solid, which when recrystallized in hexane, afforded light brown needles of sufficient quality for single crystal X-ray diffraction analysis (**Figure 3.4** and **Table 3.1**). This revealed the structure of the product to be $W(N\{Ar\}AlMe_2\{\mu-Cl\})(NAr)Me_2$ (**67**) in which a single $AlMe_2Cl$ fragment bridges one of the N-imido atoms and the W-centre, forming a four-membered ring. The geometry around the tungsten atom of complex **67** is distorted trigonal bipyramidal. Notably, the aluminium and tungsten atoms of complex **67** remain in their original respective formal oxidation states of (+III) and (+VI). Thus, Me_3Al reacts with complex **40** as an alkylating agent generating both a $W(Me)_2$ moiety and Me_2AlCl . A single Me_2AlCl molecule then coordinates to an imido ligand *via* donation of the N-atom's lone pair to the Me_2AlCl Lewis acid. This structure of $W(N\{Ar\}AlMe_2\{\mu-Cl\})(NAr)Me_2$ (**67**) is consistent with the 1H NMR spectrum obtained following treatment of $W(NAr)_2Cl_2.DME$ (**40**) with Me_3Al (**Figure 3.4**). The inequivalent 1Pr resonances observed presumably result from impeded free rotation around the N- C_{ipso} bond of the 2,6-diisopropylphenyl imido ligand bound to $AlMe_2Cl$. Hence, the 1H NMR spectrum of the crude reaction mixture (displayed in **Figure 3.4**) is consistent with complete conversion of $W(NAr)_2Cl_2.DME$ (**40**) to $W(N\{Ar\}AlMe_2\{\mu-Cl\})(NAr)Me_2$ (**67**). Furthermore, it is clear that complex **67** adopts the same structure in both the solution and the solid states.

Figure 3.4 Solid state structure of $W(N\{Ar\}AlMe_2\{\mu\text{-Cl}\})(NAr)Me_2$ (**67**) with the thermal ellipsoids set at the 50% level

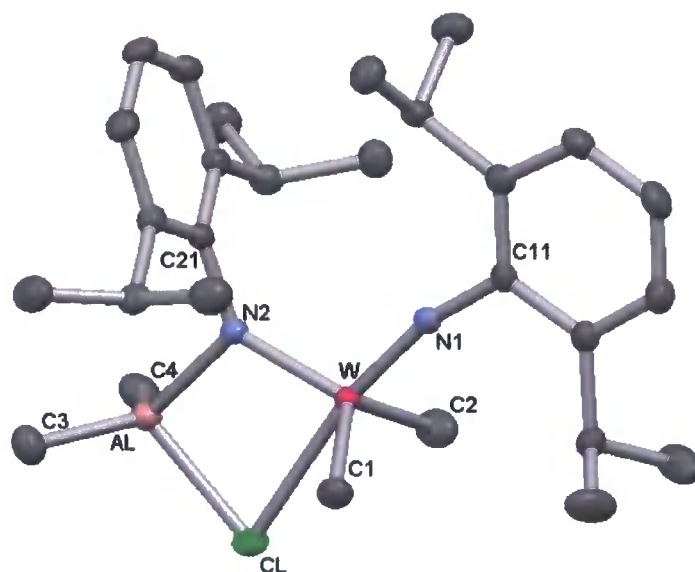


Table 3.1 Selected bond distances (Å) and bond angles ($^{\circ}$) for $W(N\{Ar\}AlMe_2\{\mu\text{-Cl}\})(NAr)Me_2$ (**67**).

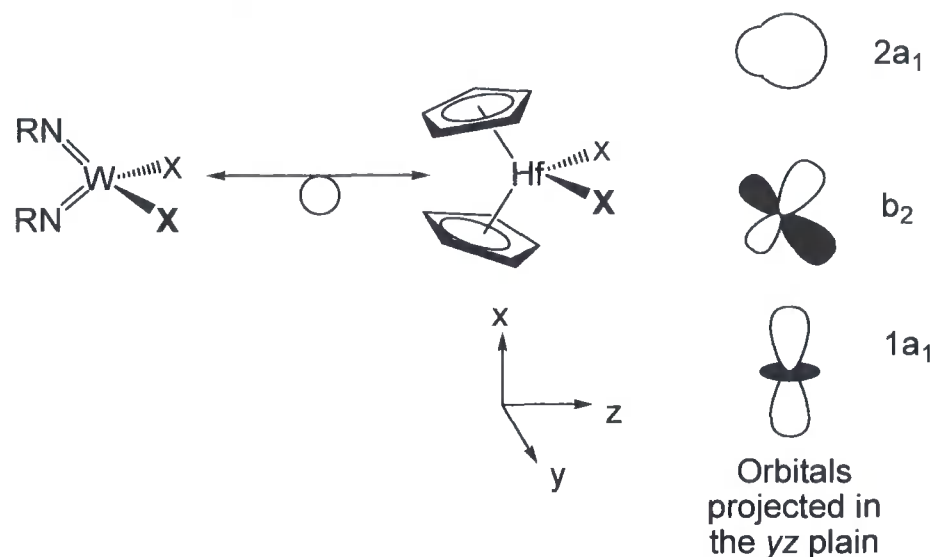
W-N1	1.7402(15)	N2-Al	1.9578(16)
W-N2	1.8613(15)	W-N1-C11	165.90(13)
N1-C21	1.439(2)	W-N2-C21	133.24(12)
N2-C11	1.399(2)	W-N2-Al	109.10(8)
W-C1	2.129(2)	C21-N2-Al	117.64(11)
W-C2	2.139(2)	Al-Cl-W	78.07(2)
W-Cl	2.6440(6)	C1-W-C2	123.63(10)
Al-Cl	2.2757(8)	N1-W-N2	108.27(7)

Examination of the W-N bond distances of **67** (Table 3.1) confirms that coordination of the Me_2AlCl fragment to the imido ligand results in a significant lengthening of the tungsten imido W-N2 bond (1.8613(15) Å), relative to the W-N contacts of the precursor complex $W(NAr)_2Cl_2 \cdot DME$ (**40**) (1.7598(17) Å) (See Chapter 2, Section 2.1). In contrast, the W-N1 bond associated with the free imido ligand of **67** at 1.7402(15) Å is shorter than the W-N contacts of the precursor complex **40**. The sum of the bond angles around N2 is close to 360° and the W-N2-C21 bond angle is $133.24(12)^{\circ}$, indicating a 2-electron donor imido ligand (neutral formalism), with a trigonal planar geometry around the N atom. In contrast, the W-N1-C11 bond angle

of the free imido ligand is $165.90(13)^\circ$, which is within the range of that generally accepted for a 4-electron donor ligand (neutral formalism).¹¹

Interaction between the W^{VI} and Cl atoms of complex $W(N\{Ar\}AlMe_2\{\mu\text{-Cl}\})(NAr)Me_2$ (**67**) is dative in nature, with donation of a chloride lone pair to the highly electropositive W^{VI} centre. The chloride moiety of **67** originates from the starting material $W(NAr)_2Cl_2 \cdot DME$ (**40**), with ligand metathesis of the W-Cl and Al-Me bonds giving the W-Me and Al-Cl moieties. The $[W(NAr)_2]^{2+}$ core of complex **67** can be viewed as being isolobal to a $[Hf(Cp)_2]^{2+}$ fragment and, as such, has three frontier orbitals available for interaction with a given ligand (two of a_1 and one of b_2 symmetry) (**Figure 3.5**).¹² Thus, coordination of the chloride ligand to the W centre generates a coordinatively-saturated W complex, with full occupancy of all available coordination sites. Due to the dative nature of the W-Cl interaction, the chloride ligand can be counted as being a 2 electron donor, making **67** formally a 16-electron species.

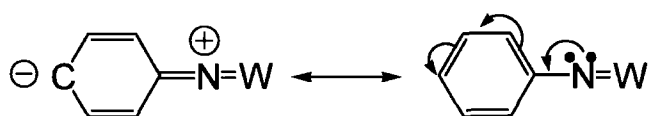
Figure 3.5 Isolobal relationship and frontier orbitals of the metal fragments $[W(NAr)_2]^{2+}$ and $[Hf(Cp)_2]^{2+}$



The W-Cl bond of **67** at $2.6440(6)$ Å is relatively long, compared to the analogous contacts of the precursor complex $W(NAr)_2Cl_2 \cdot DME$ (**40**) at $2.3841(7)$ Å (**Chapter 2, Section 2.1.2**). Indeed, the W-Cl contact of **67** is long, but does not exceed the longest W-Cl bond distance currently deposited in the Cambridge Structural data base.¹³ This is recorded for the complex $[WOCl_3(OAr)]_2$ ($2.876(2)$ Å).¹⁴ Also of note for complex **67**, is that coordination of the chloride ligand to the tungsten atom gives an acute Al-Cl-W bond angle of $78.07(2)^\circ$. Another prominent structural feature of **67**

is the greater length of the N-C_{ipso} bond of the Me₂AlCl bound imido ligand 1.439(2) Å (N1-C21) compared with that of the free imido ligand 1.399(2) Å (N2-C11). The N-C_{ipso} bond can be viewed as having some double bond character (**Figure 3.6**) when the C_{ipso} is formally sp² hybridized.¹⁵ Hence, the greater length of the N1-C21 contact can be attributed to coordination of the Me₂AlCl fragment to the nitrogen atom of the imido ligand. This makes the nitrogen lone pair less available for delocalization into the π-system of the 2,6-diisopropyl-phenyl group, and reduces the double bond character of the N-C_{ipso} contact.

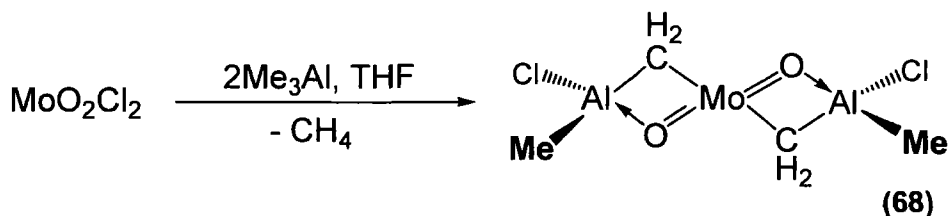
Figure 3.6 Partial double bond character of N-C_{ipso} bond for a W phenyl imido moiety



3.2 Synthesis, Characterization and Structure of W(N{Ar}.AlMe₂{μ-Cl})(NAr)Me₂ (67) and Comparison with Related Complexes

Interaction of an R_xAlCl_{3-x} fragment and an imido ligand in bonding modes analogous to that observed in complex **67** are uncommon, with only a very few related complexes having been disclosed in the literature. Notably, reaction of the related *bis(oxo)* complex MoO₂Cl₂, which is isolobal to a W(NAr)₂Cl₂ fragment also results in the formation of a 4-membered chelate (**Scheme 3.3**). However, in this system methane is evolved, *via* α-hydride elimination and then a reductive elimination, generating the bridging Al-CH₂ moiety. Hence, in contrast to complex **67** in this oxo-containing example it is a CH₂ fragment and not a Cl ligand that bridges between the Mo and Al atoms.¹⁶

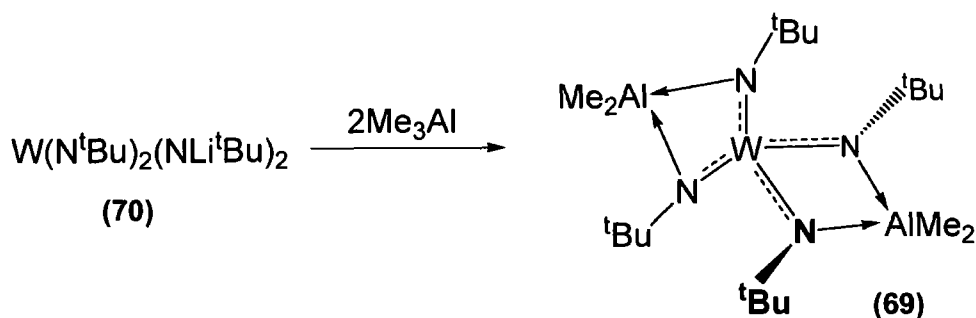
Scheme 3.3 Reaction of MoO₂Cl₂ with Me₃Al



Although α-hydride elimination readily occurs following reaction of MoO₂Cl₂ with Me₃Al, a similar elimination reaction is clearly disfavoured for W(N{Ar}AlMe₂{μ-Cl})(NAr)Me₂ (**67**), which retains the WMe₂ fragment, preventing the formation of a

bridging CH₂ group. It has also previously been shown that aluminium-based Lewis acid fragments can coordinate to *bis*(imido) systems by Wilkinson *et al.* who prepared $W[(\mu\text{-N}^t\text{Bu})_2\text{AlX}_2]_2$ (**69**) from reaction the lithiated *bis*(imido) *bis*(amido) complex $W(\text{N}^t\text{Bu})_2(\text{NLi}^t\text{Bu})_2$ (**70**) with Me_3Al (Scheme 3.4).¹⁷

Scheme 3.4 Synthesis of $W[(\mu\text{-N}^t\text{Bu})_2\text{AlMe}_2]_2$

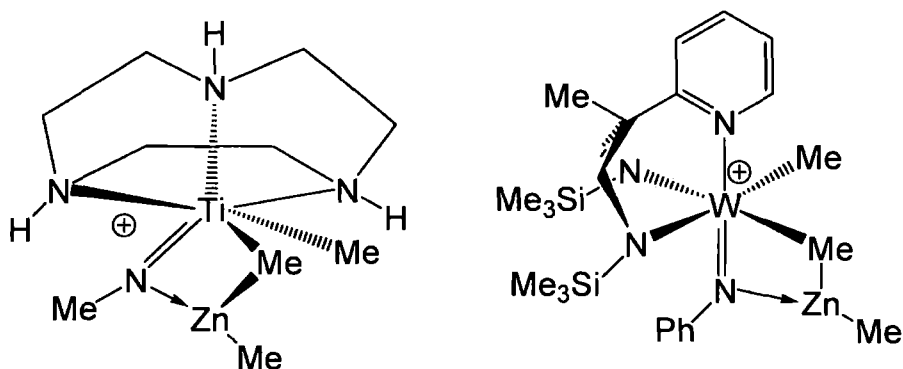


Notably, the structure of $W[(\mu\text{-N}^t\text{Bu})_2\text{AlMe}_2]_2$ (**69**) has parallels with that of $W(\text{N}\{\text{Ar}\})\text{AlMe}_2\{\mu\text{-Cl}\}(\text{NAr})\text{Me}_2$ (**67**). In both **67** and **69** an imido ligand bridges between aluminium and tungsten atoms forming a four-membered chelate. Indeed, the similar N-Al contacts at 1.992(7) Å and 1.990(9) Å for $W[(\mu\text{-N}^t\text{Bu})_2\text{AlX}_2]_2$ (**69**) and 1.9578(16) Å for **67** are typical bond distances for an Al-N dative interaction (1.86 Å to 2.04 Å).¹⁸ However, in contrast to the $W(\text{N}^t\text{Bu})_2(\text{NLi}^t\text{Bu})_2/\text{Me}_3\text{Al}$ reaction (Scheme 3.4), conversion of $W(\text{NAr})_2\text{Cl}_2\cdot\text{DME}$ (**40**) to **67** demonstrates that in the $W(\text{NAr})_2\text{Cl}_2\cdot\text{DME}/\text{Me}_3\text{Al}$ system, coordination of both imido ligands to a single aluminium centre is disfavoured. This is because in **67** the lone pair of the unbound imido ligand is strongly π -bonding to the W^{VI} centre. Hence, the delocalization of the N2 lone pair, between the N2 and W^{VI} atoms, significantly reduces the Lewis basicity of the imido ligand, reducing the tendency for the formation of a second Al-N contact in this system. Furthermore, for complex **67** the bulk of the NAr ligands results in little space between the two imido groups, making coordination of both imido moieties to a single $R_x\text{AlCl}_{3-x}$ fragment sterically highly disfavoured.

While there are clear differences between $W[(\mu\text{-N}^t\text{Bu})_2\text{AlX}_2]_2$ (**69**) and **67**, complexes have been disclosed in the literature that are directly analogous to **67**, in which a $R_x\text{AlCl}_{3-x}$ fragment bridges between an imido N-atom and a metal centre. Such an interaction was postulated by Schrock *et al.* as being present in the complex $W(\text{NPh})(\text{CCMe}_3)(\text{PMe}_3)_2\text{Cl}(\text{AlMe}_2\text{Cl})$, although this has not been confirmed by single crystal X-ray diffraction analysis. Similarly, a dative interaction between an N^tBu imido lone pair and an Me_3Al fragment has been considered computationally by

Mountford *et al.*¹⁹ In Mountford's study the capacity of complexes such as $\text{Ti}(\text{N}^i\text{Bu})(\text{Me}_3[9]\text{aneN}_3)\text{R}_3$ (R = a range of alkyl groups including Me or CH_2SiMe_3) to initiate ethylene polymerization when activated by Al^iBu_3 and $[\text{Ph}_3\text{C}][\text{BAR}^{\text{F}}_4]$ was assessed. In an effort to further understand the nature of the active species, a comprehensive DFT investigation was undertaken. It was determined computationally that lone pair donation from an N^iBu imido ligand to an Me_3Al fragment, forming a four-membered chelate with connectivity analogous to **67** was a relatively stable arrangement. However, Me_3Al coordination in this manner was concluded as unfavourable since the resulting complexes were believed to be less able to initiate reaction of ethylene than the analogous Me_3Al -free complexes. In related studies, the cations $[\text{Ti}(\mu\text{-N}^i\text{Bu})(\text{Me}_3[9]\text{aneN}_3)(\mu\text{-Me})_2\text{ZnMe}]^+$ and $[\text{W}(\mu\text{-NPh})(\text{N}_2\text{Npy})\text{Me}(\mu\text{-Me})\text{ZnMe}]^+$ were predicted by Mountford, again through the use of DFT, to contain four-membered chelates, resulting from a dative interaction between the N^iBu ligand and the zinc-based Lewis acid (**Figure 3.7**).^{20,21} Hence, Mountford's investigations show that coordination of Lewis acids to imido ligands, in bonding modes similar to that of **69** is often thermodynamically favourable.

Figure 3.7 Examples computationally studied imido-bridged ZnMe_2 complexes



The Cambridge Structural Database was searched for complexes containing a $\text{Me}_x\text{AlCl}_{3-x}$ fragment bridging between a transition metal and a nitrogen centre in an interaction related to that of **67**. This search revealed that only three such complexes have been deposited. These structures were reported by Binger²² (Complex **72**), Norton²³ (Complex **73**) and Duchateau²⁴ (Complex **74**) (**Figure 3.8**). In addition, Mayer has prepared an osmium imido complex **75** in which an imido ligand coordinates to a Ph_2BCl unit (**Figure 3.9**).²⁵

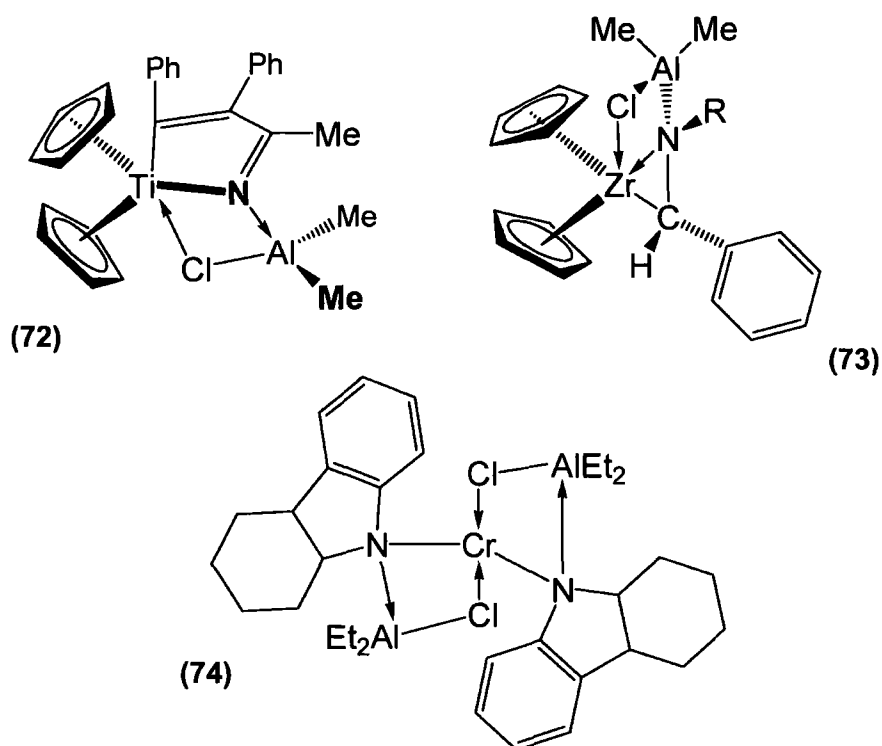
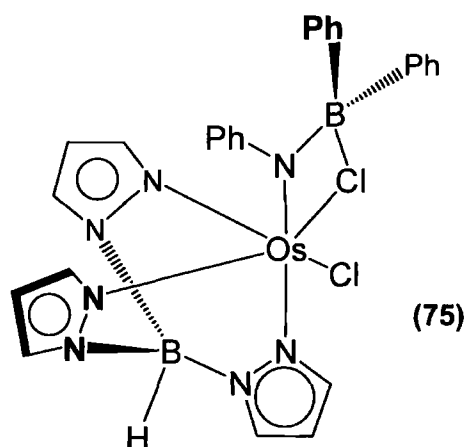
Figure 3.8 Examples of bridging $R_xAlCl_{(3-x)}$ fragments

Figure 3.9 Osmium imido complex (75) containing a bridging B-Cl fragment



In complex **75** the phenyl imido ligand bridges between the Os and B centres. This connectivity is comparable to that determined for **67**, with the imido nitrogen atom of **75** adopting the same *pseudo*-trigonal planar geometry found for complex **67**. The similarities between the structures of **75** and **67** demonstrate that although the connectivity of **67** is unusual, a similar bonding arrangement is found in related complexes.

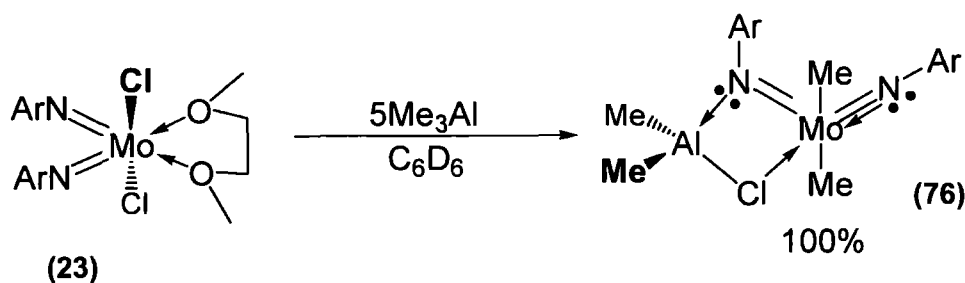
3.3 Reaction of $M(\text{NAr})_2\text{Cl}_2\cdot\text{DME}$ ($M = \text{Mo}$ or W) Complexes with Me_2AlCl and MeAlCl_2

In Section 3.1 it was determined that reaction of $\text{W}(\text{NAr})_2\text{Cl}_2\cdot\text{DME}$ (**40**) with Me_3Al in C_6D_6 affords exclusively $\text{W}(\text{N}\{\text{Ar}\}.\text{AlMe}_2\{\mu\text{-Cl}\})(\text{NAr})\text{Me}_2$ (**67**). In this regard, it is also of interest to investigate the reactivity of **40** with the aluminium-based reagents Me_2AlCl and MeAlCl_2 , as this could result in different reaction products to that obtained in the Me_3Al system. Indeed, the ability of Me_2AlCl and MeAlCl_2 to transfer a methyl group is considerably lower than that of Me_3Al .²⁶ Furthermore, reaction of $\text{Mo}(\text{NAr})_2\text{Cl}_2\cdot\text{DME}$ (**23**) with $\text{Me}_x\text{AlCl}_{3-x}$ reagents is also worthy of study as $\text{Mo}(\text{NR})_2\text{Cl}_2\cdot\text{DME}$ complexes can also be utilized as dimerization pre-catalysts (Chapter 2, Section 2.2, Table 3.3). Thus, reaction of **23** with $\text{Me}_x\text{AlCl}_{3-x}$ reagents could yield information as to the mode by which molybdenum *bis*(imido) pre-catalysts are activated for ethylene dimerization.

3.3.1 Synthesis of $\text{Mo}(\text{N}\{\text{Ar}\}.\text{AlMe}_2\{\mu\text{-Cl}\})(\text{NAr})\text{Me}_2$ (**76**)

With a view to exploring the reactivity of $\text{Mo}(\text{NAr})_2\text{Cl}_2\cdot\text{DME}$ (**23**) with $\text{R}_x\text{AlCl}_{3-x}$ species, attention turned to investigating the reaction of **23** with Me_3Al . On an NMR scale treatment of $\text{Mo}(\text{NAr})_2\text{Cl}_2\cdot\text{DME}$ (**23**) with excess Me_3Al in C_6D_6 resulted in full conversion of **23** to the complex $\text{Mo}(\text{N}\{\text{Ar}\}.\text{AlMe}_2\{\mu\text{-Cl}\})(\text{NAr})\text{Me}_2$ (**76**), which presents a ^1H NMR spectrum comparable to that observed for the analogous tungsten complex **67** (Scheme 3.5). The composition of **76** has been confirmed by reaction of $\text{Mo}(\text{NAr})_2\text{Cl}_2\cdot\text{DME}$ (**23**) with excess Me_3Al on a preparatory scale, which afforded a synthetically pure sample of **76** upon recrystallization from hexane in a 24 % yield. It is clear that the complexes $\text{Mo}(\text{NAr})_2\text{Cl}_2\cdot\text{DME}$ (**23**) and $\text{W}(\text{NAr})_2\text{Cl}_2\cdot\text{DME}$ (**40**) have identical reactivity with Me_3Al .

Scheme 3.5 Synthesis of $\text{Mo}(\text{N}\{\text{Ar}\}.\text{AlMe}_2\{\mu\text{-Cl}\})(\text{NAr})\text{Me}_2$ (**76**)



3.3.2 Reaction of $W(NAr)_2Cl_2 \cdot DME$ (40) with Me_2AlCl

With a view to gauging if treatment of $W(NAr)_2Cl_2 \cdot DME$ (40) with Me_2AlCl generates similar or different products to that of the $W(NAr)_2Cl_2 \cdot DME/Me_3Al$ system, the reactivity of complex 40 with Me_2AlCl was investigated. Addition of Me_2AlCl to $W(NAr)_2Cl_2 \cdot DME$ in C_6D_6 results in the formation of complex $W(N\{Ar\} \cdot AlMeCl\{\mu\text{-}Cl\})(NAr)Me_2$ (77) *in situ*. The complexes 67 and 77 are closely related, varying only in the nature of the bridging Me_xAlCl_{3-x} fragment (Me_2AlCl and $MeAlCl_2$, respectively). However, in contrast to the Me_3Al system where 67 is obtained in 100% conversion, it is clear from 1H NMR spectrum presented by the Me_2AlCl reaction solution (Figure 3.10) that reaction of Me_2AlCl also generates additional as yet unidentified tungsten-containing products (Scheme 3.6).

Scheme 3.6 Contrasting the $W(NAr)_2Cl_2 \cdot DME/Me_3Al$ and $W(NAr)_2Cl_2 \cdot DME/Me_2AlCl$ reaction systems.

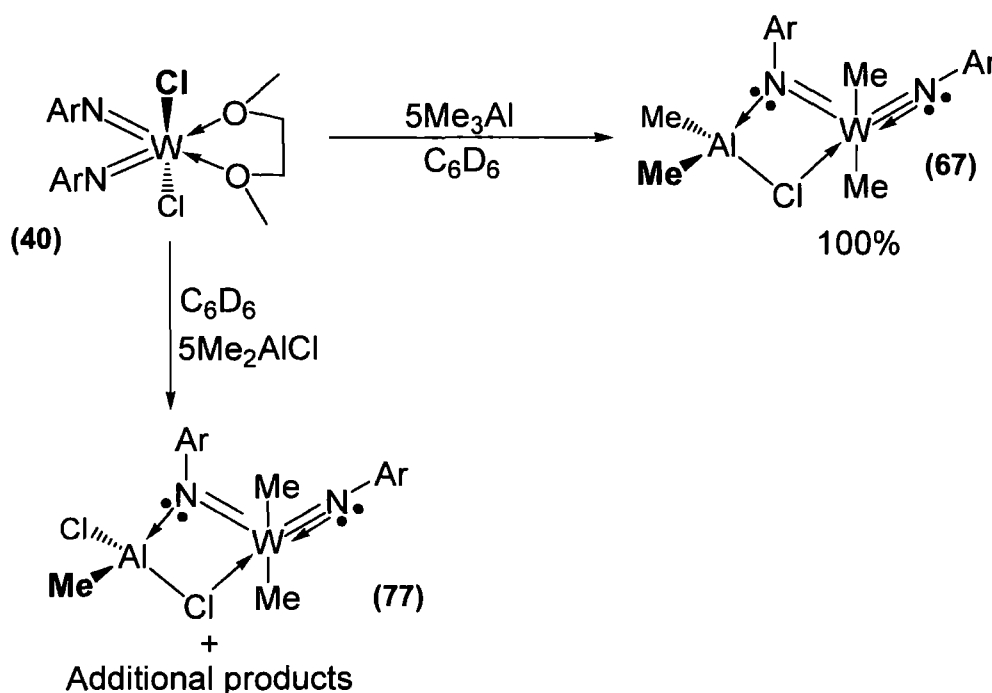
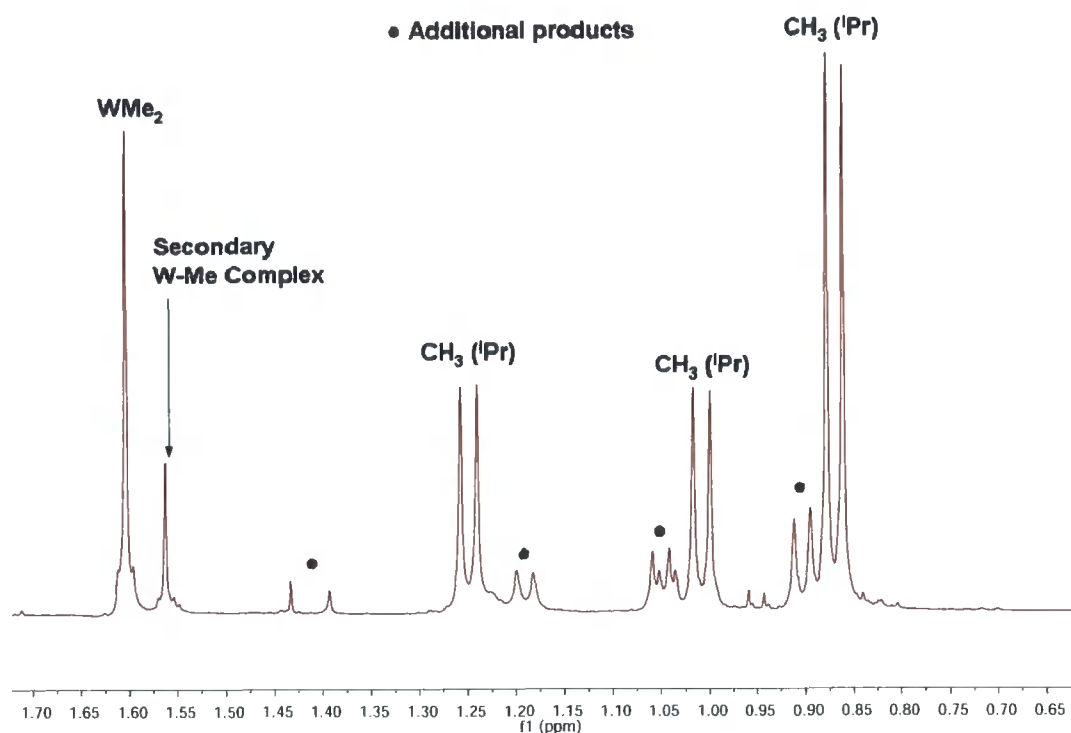


Figure 3.10 ^1H NMR (400 MHz, C_6D_6) spectrum of the mixture obtained following reaction of $\text{W}(\text{NAr})_2\text{Cl}_2\cdot\text{DME}$ (**40**) with Me_2AlCl (aromatic region omitted).



As for complex **67**, coordination of an $\text{Me}_x\text{AlCl}_{3-x}$ fragment, to a NAr imido ligand in complex **77** results in inequivalent CH_3 ^1H NMR resonances. Although it has been possible to assign the structure of **77** using ^1H NMR spectroscopy, the connectivity of the additional reaction products remains unclear. It is evident that reaction of a stronger Lewis acid (Me_2AlCl) does indeed give a different reactivity to that obtained in the Me_3Al system (**Scheme 3.6**).²⁷ This observation is significant since Me_2AlCl and Me_3Al have different capacities to activate $\text{W}(\text{NAr})_2\text{Cl}_2\cdot\text{DME}$ (**40**) towards ethylene dimerization (refer to **Section 3.8.2**).

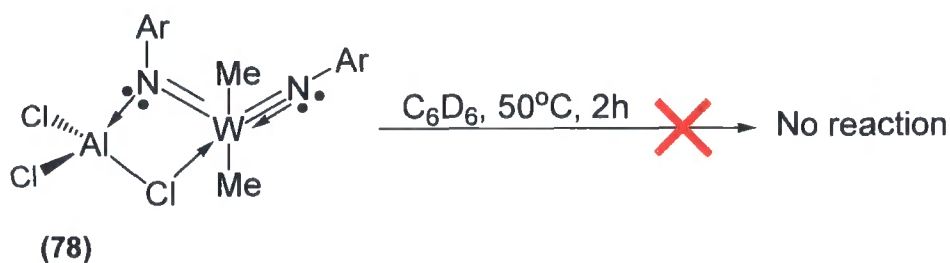
3.3.3 Reaction of $\text{M}(\text{NAr})_2\text{Cl}_2\cdot\text{DME}$ ($\text{M} = \text{Mo}$ or W) with MeAlCl_2

To further investigate the interaction between *bis*(imido) halide complexes and strong aluminium-based Lewis acids, the reactivity of both $\text{Mo}(\text{NAr})_2\text{Cl}_2\cdot\text{DME}$ (**23**) and $\text{W}(\text{NAr})_2\text{Cl}_2\cdot\text{DME}$ (**40**) with MeAlCl_2 was investigated. The complexes $\text{W}(\text{N}\{\text{Ar}\}.\text{AlCl}_2\{\mu\text{-Cl}\})(\text{NAr})\text{Me}_2$ (**78**) and $\text{Mo}(\text{N}\{\text{Ar}\}.\text{AlCl}_2\{\mu\text{-Cl}\})(\text{NAr})\text{Me}_2$ (**79**), were obtained from treatment of the appropriate *bis*(imido) dihalide complex with MeAlCl_2 .

Of general interest is determining whether complexes such as **78** or **79** are thermally stable. To assess the thermal stability of **78**, a sample of the complex was

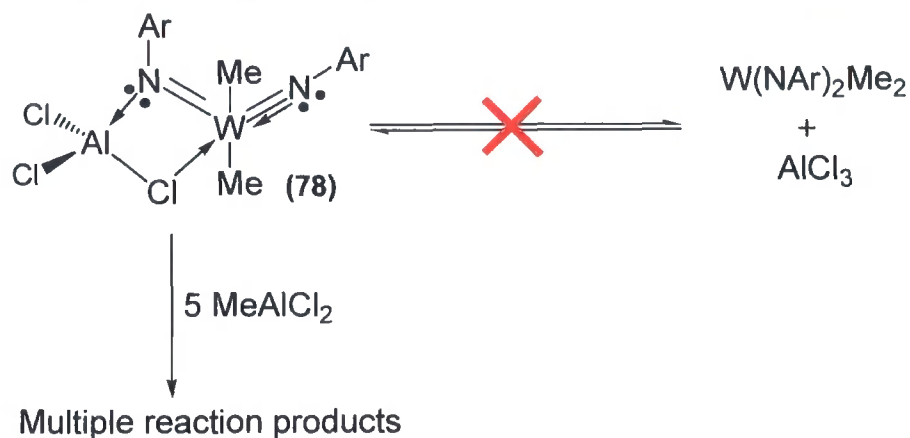
dissolved in C_6D_6 and the resulting solution was heated. No thermal degradation of **78** was observed using 1H NMR spectroscopy (**Scheme 3.7**).

Scheme 3.7 Attempted thermolysis of $W(N\{Ar\}.AlCl_2\{\mu-Cl\})(NAr)Me_2$ (**78**)



It is clear from the NMR spectra of complexes **78** and **79** that neither undergoes facile association/dissociation in solution on an NMR timescale ($\sim 25^\circ C$) (**Scheme 3.8**). However, it was found that addition of excess $MeAlCl_2$ to a sample of either **78** or **79** results in the formation of unknown additional products, the connectivity of which cannot be determined by multinuclear NMR spectroscopic analysis (**Scheme 3.8**).

Scheme 3.8 Reaction of $W(N\{Ar\}.AlCl_2\{\mu-Cl\})(NAr)Me_2$ (**78**) with $MeAlCl_2$



3.3.4 Characterization of $W(N\{Ar\}AlCl_2\{\mu-Cl\})(NAr)Me_2$ (78) and $Mo(N\{Ar\}.AlCl_2\{\mu-Cl\})(NAr)Me_2$ (79) using Single Crystal X-ray Diffraction

To clarify the structures of 78 and 79, both complexes have been characterized by single crystal X-ray diffraction analysis. The molecular structures of 78 (Figure 3.11 and Table 3.2) and 79 (Figure 3.12 and Table 3.3) indicate that they are both isostructural to $W(N\{Ar\}AlMe_2\{\mu-Cl\})(NAr)Me_2$ (67).

Figure 3.11 Solid state structure of $W(N\{Ar\}AlCl_2\{\mu-Cl\})(NAr)Me_2$ (78) with the thermal ellipsoids set at the 50% level

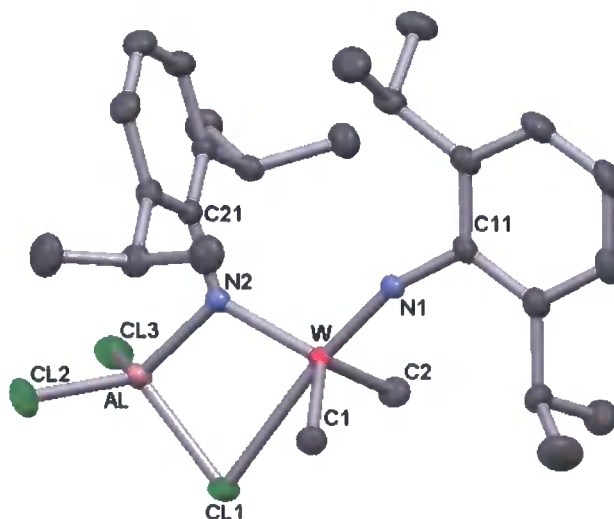


Table 3.2 Selected bond distances (Å) and bond angles (°) for $W(N\{Ar\}.AlCl_2\{\mu-Cl\})(NAr)Me_2$ (78).

W-N1	1.7290(13)	N1-W-N2	108.87(6)
W-N2	1.8750(15)	W-N1-C11	163.78(13)
W-C1	2.1270(18)	W-N2-C21	132.21(11)
W-C2	2.1205(18)	C1-W-C2	122.17(8)
N1-C11	1.409(2)	W-N2-Al	109.76(7)
N2-C21	1.445(2)	C21-N2-Al	117.99(11)
N2-Al	1.8873(14)	Al-N2-W	109.76(7)
Al-Cl1	2.2043(8)	N2-Al-Cl1	93.85(5)
Al-Cl2	2.1061(8)	Al-Cl1-W	76.84(2)
Cl1-W	2.7073(5)	Cl1-Al-Cl2	109.25(3)

As for complex $W(N\{Ar\}AlMe_2\{\mu-Cl\})(NAr)Me_2$ (67), the W-N bond distances and angles of $W(N\{Ar\}.AlCl_2\{\mu-Cl\})(NAr)Me_2$ (78) indicate that the unbound imido ligand of

Direct comparison can be made between the bond lengths and angles of the tungsten complex $W(N\{Ar\}.AlCl_2\{\mu-Cl\})(NAr)Me_2$ (**78**) and those of the molybdenum complex $Mo(N\{Ar\}.AlCl_2\{\mu-Cl\})(NAr)Me_2$ (**79**), as both complexes have an $AlCl_3$ fragment bound to the imido ligand and identical coordination spheres. Of note are the almost identical N-Al bond lengths of 1.8873(14) and 1.884(6) Å respectively. Also the N-Al-Cl bond angles of complexes **78** and **79** are comparable at 93.85(5) and 94.0(2)°. It is apparent that any electronic difference between the Mo^{VI} and W^{VI} centres has little impact on the structural features of the N-Al-Cl chelate.

3.4 Reaction of the Mixed imido Complex $Mo(NAr)(N^iBu)Cl_2.DME$ (11**) with Me_3Al and $MeAlCl_2$**

It has been shown that reaction of $M(NAr)_2Cl_2.DME$ ($M = Mo$ or W) with $Me_xAlCl_{(3-x)}$ generates products of the general formula $M(N\{Ar\}AlMe_{(x-1)}Cl_{(3-x)}\{\mu-Cl\})(NAr)Me_2$ in which an Me_xAlCl_{3-x} fragment coordinates to a single imido ligand of the *bis*(imido) moiety. With this having been established, attention turned to investigating the reactivity of the mixed imido complex $Mo(NAr)(N^iBu)Cl_2.DME$ (**11**). Here, with both NAr and N^iBu imido ligands being present, addition of $Me_xAlCl_{(3-x)}$ reagents to **11** could result in aluminium-based Lewis acid fragments binding to either the NAr or N^iBu ligands, or both. Thus, it was of interest to explore the reactivity of $Mo(NAr)(N^iBu)Cl_2.DME$ (**11**) to establish the preferred binding site of the Lewis acid.

3.4.1 Reaction of $Mo(NAr)(N^iBu)Cl_2.DME$ (11**) with Me_3Al**

To assess which imido ligand of complex **11** a Me_xAlCl_{3-x} fragment would preferentially coordinate, $Mo(NAr)(N^iBu)Cl_2.DME$ (**11**) was reacted with Me_3Al in C_6D_6 . The reaction mixture was then analysed by 1H NMR spectroscopy. The resulting spectrum (**Figure 3.13**) indicates the presence of only one Mo-Me resonance (integrating to 6H) and one N^iBu resonance, demonstrating that only one isomer is formed in solution. Furthermore, a $^1H/^1H$ NOESY correlation experiment revealed that the Me_2AlCl fragment binds preferentially to the NAr ligand. This is further confirmed by the observation of two inequivalent iPr CH_3 resonances in the 1H and ^{13}C NMR spectrum, which has been established as being characteristic of Me_xAlCl_{3-x} fragments coordinating to NAr ligands (**Section 3.1**). Thus, together, these 1H NMR spectral analyses are consistent with full conversion of **11** to $Mo(N\{Ar\}.AlMe_2\{\mu-Cl\})(N^iBu)Me_2$ (**80**) (**Scheme 3.9**).

Scheme 3.9 Formation of $\text{Mo}(\text{N}\{\text{Ar}\}.\text{AlMe}_2\{\mu\text{-Cl}\})(\text{N}^t\text{Bu})\text{Me}_2$ (**80**) in situ.

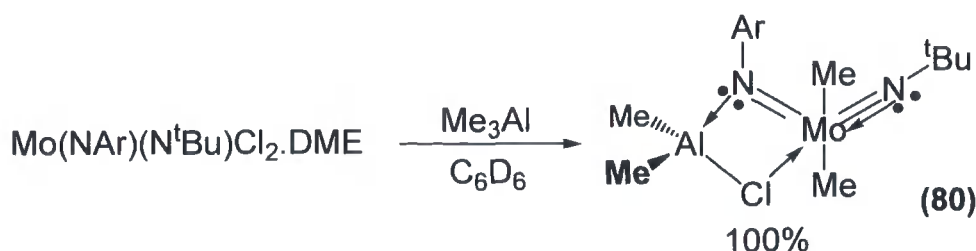
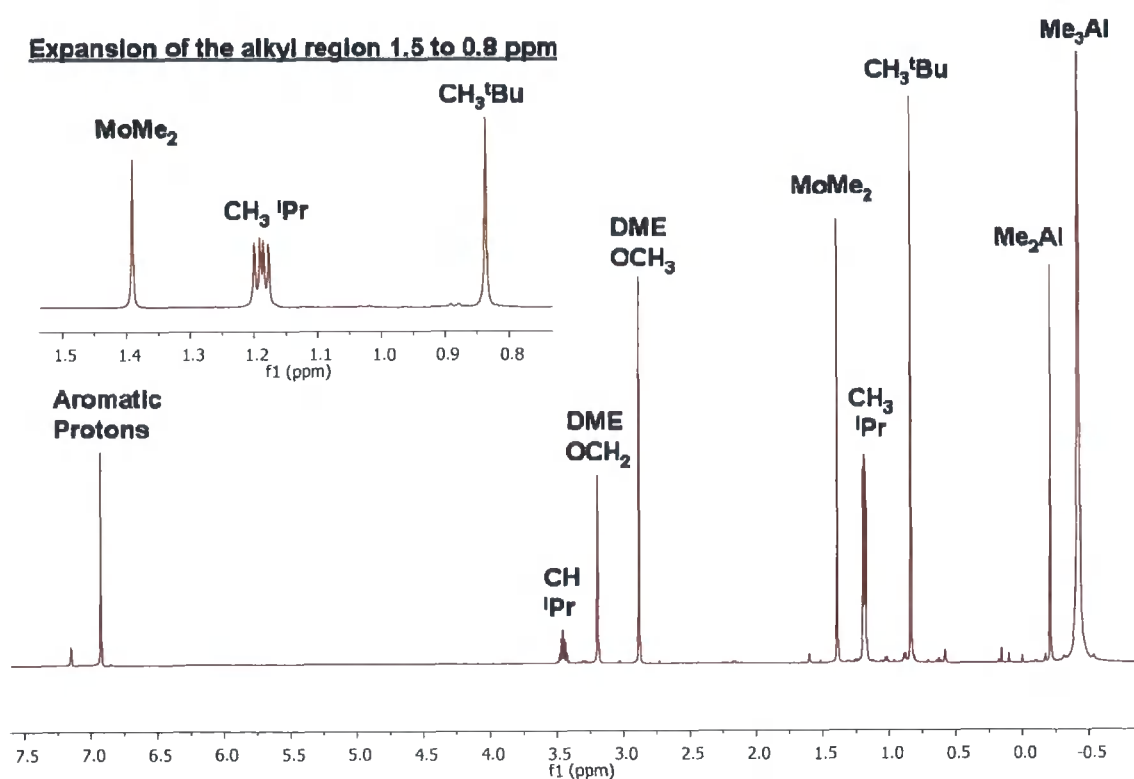


Figure 3.13 ^1H NMR (400 MHz, C_6D_6) spectrum of the reaction of $\text{Mo}(\text{NAr})(\text{N}^t\text{Bu})\text{Cl}_2.\text{DME}$ (**80**) with Me_3Al .



3.4.2 Synthesis and Characterisation of $\text{Mo}(\text{N}\{\text{Ar}\}.\text{AlCl}_2\{\mu\text{-Cl}\})(\text{N}^t\text{Bu})\text{Me}_2$ (**81**)

Having established that reaction of $\text{Mo}(\text{NAr})(\text{N}^t\text{Bu})\text{Cl}_2.\text{DME}$ (**11**) with Me_3Al generates $\text{Mo}(\text{N}\{\text{Ar}\}.\text{AlMe}_2\{\mu\text{-Cl}\})(\text{N}^t\text{Bu})\text{Me}_2$ (**80**) to examine if reaction of alternative $\text{Me}_x\text{AlCl}_{3-x}$ reagents would yield similar complexes, attention turned to investigating the reactivity of **11** with MeAlCl_2 . Addition of MeAlCl_2 to a toluene solution of **11** has enabled, after workup, isolation of the complex $\text{Mo}(\text{N}\{\text{Ar}\}.\text{AlCl}_2\{\mu\text{-Cl}\})(\text{N}^t\text{Bu})\text{Me}_2$ (**81**) in 40% yield. The ^1H NMR spectrum of complex **81** comprised of a single Mo-CH₃ resonance as well as a single ^tBu signal. As for related complexes, inequivalent CH₃ iPr resonances were detected. A sample of **81** of sufficient quality for analysis by single

crystal X-ray diffraction was obtained upon recrystallization of **81** from toluene (Figure 3.14 and Table 3.4).

Figure 3.14 Solid state structure of $\text{Mo}(\text{N}\{\text{Ar}\}\text{AlMe}_2\{\mu\text{-Cl}\})(\text{N}^t\text{Bu})\text{Me}_2$ (**81**) with the thermal ellipsoids set at the 50% level

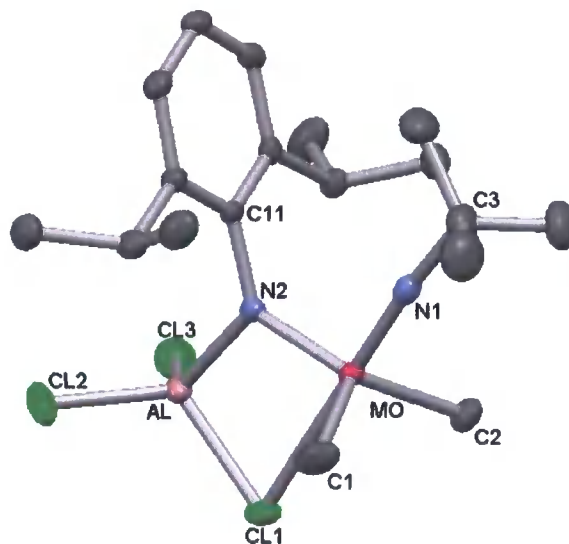


Table 3.4 Key structural parameters, bond lengths (Å) and bond angles ($^\circ$), for $\text{Mo}(\text{N}^t\text{Bu})(\text{N}\{\text{Ar}\}\text{AlCl}_2\{\mu\text{-Cl}\})\text{Me}_2$ (**81**) and $\text{Mo}(\text{N}^t\text{Bu})(\text{NAr})\text{Cl}_2\cdot\text{DME}$ (**11**)

Parameter	$\text{Mo}(\text{N}^t\text{Bu})(\text{N}\{\text{Ar}\}\text{AlCl}_2\{\mu\text{-Cl}\})\text{Me}_2$	$\text{Mo}(\text{N}^t\text{Bu})(\text{NAr})\text{Cl}_2\cdot\text{DME}$
Mo-N1-C3 (N ^t Bu)	174.58(12)	157.9(2)
N1-Mo-N2	103.00(6)	105.91(9)
Mo-N2-C11 (NAr)	127.38(10)	174.3(2)
Mo-N1 (N ^t Bu)	1.7029(15)	1.728(2)
N1-C3	1.465(2)	1.452(3)
Mo-N2 (NAr)	1.8870(13)	1.753(2)
N2-C11	1.4355(19)	1.387(3)

The molecular structure of complex **81** confirms that the aluminium Lewis acid moiety (in this instance AlCl_3) again preferentially coordinates to the NAr ligand. This is in agreement with the NMR spectra of **81**. Examination of the bond angles and distances associated with complex **81** (Table 5.4) reveals that the NAr imido ligand is a 2-electron donor (neutral formalism), with a Mo-N-C_{ipso} bond angle of 127.38(10) $^\circ$ and a relatively long Mo-N2 contact of 1.8870(13) Å. Indeed, coordination of the



AlCl_3 fragment results in a lengthening of the Mo-N contact (1.8870(13) Å) of the NAr ligand relative to the analogous contact for the starting complex $\text{Mo}(\text{NAr})(\text{N}^t\text{Bu})\text{Cl}_2\cdot\text{DME}$ (**11**) (1.753(2) Å). This lengthening can be attributed to the reduction in Mo-N triple bond character resulting from the donation of the N-atom's lone pair to the AlCl_3 fragment. Furthermore, AlCl_3 coordination in **81** also results in a lengthening of the NAr ligand's N- C_{ipso} contact relative to the starting material (1.4355(19) Å for **81** vs 1.387(3) Å for $\text{Mo}(\text{NAr})(\text{N}^t\text{Bu})\text{Cl}_2\cdot\text{DME}$ (**11**)).

Of particular interest is the increased length of the Mo-Cl contact of **81** relative to that for the comparable molybdenum complex **79** (Table 3.5). Both complexes **81** and **79** adopt distorted trigonal bipyramidal geometries, but in **81** the chloride ligand lies *trans* to an N^tBu ligand, while in **79** it occupies a site *trans* to a NAr group (Figure 3.15). As the N^tBu imido ligand is a stronger π -donor, it has a greater *trans* influence than the NAr ligand, resulting in a relative lengthening of the Mo-Cl contact.

Table 3.5 Comparison of Mo-Cl bond lengths for complexes **79** and **81**

Complex	Mo-Cl Bond length (Å)
$\text{Mo}(\text{N}\{\text{Ar}\}\text{AlCl}_2\{\mu\text{-Cl}\})(\text{NAr})\text{Me}_2$ (79)	2.7476(5)
$\text{Mo}(\text{N}\{\text{Ar}\}\text{AlCl}_2\{\mu\text{-Cl}\})(\text{N}^t\text{Bu})\text{Me}_2$ (81)	2.7086(19)

Figure 3.15 Comparison of the complexes $\text{Mo}(\text{N}^t\text{Bu})(\text{N}\{\text{Ar}\}\text{AlCl}_2\{\mu\text{-Cl}\})\text{Me}_2$ (**81**) and $\text{Mo}(\text{NAr})(\text{N}\{\text{Ar}\}\text{AlCl}_2\{\mu\text{-Cl}\})\text{Me}_2$ (**79**)



For both complexes **80** and **81**, the $\text{Me}_x\text{AlCl}_{3-x}$ fragment binds preferentially to the NAr ligand of the mixed *bis*(imido) moiety. Examination of the relative Mo-N bond lengths of the precursor complex $\text{Mo}(\text{NAr})(\text{N}^t\text{Bu})\text{Cl}_2\cdot\text{DME}$ (**11**)²⁸ (Table 3.4) indicates that it is the relative π -donor capacities of the N^tBu and NAr ligands that directs the site of $\text{Me}_x\text{AlCl}_{3-x}$ coordination. Indeed, for complex **11** the Mo-N bond distance corresponding to the N^tBu imido ligand at 1.728(2) Å is relatively short. This reflects the greater triple bond character of this interaction, which results from a high degree

of π -donation from the N^tBu ligand to the Mo^{VI} atom. Conversely, the longer Mo-N interaction of the NAr ligand (1.753(2) Å) shows that this imido ligand is a less effective π -donor. As such the lone pair of the NAr ligand is not as effectively delocalized between the Mo and N atoms and is instead more centred upon the N-atom. This makes the lone pair of the NAr ligand more available for donation to the Lewis acids Me₂AlCl or AlCl₃.

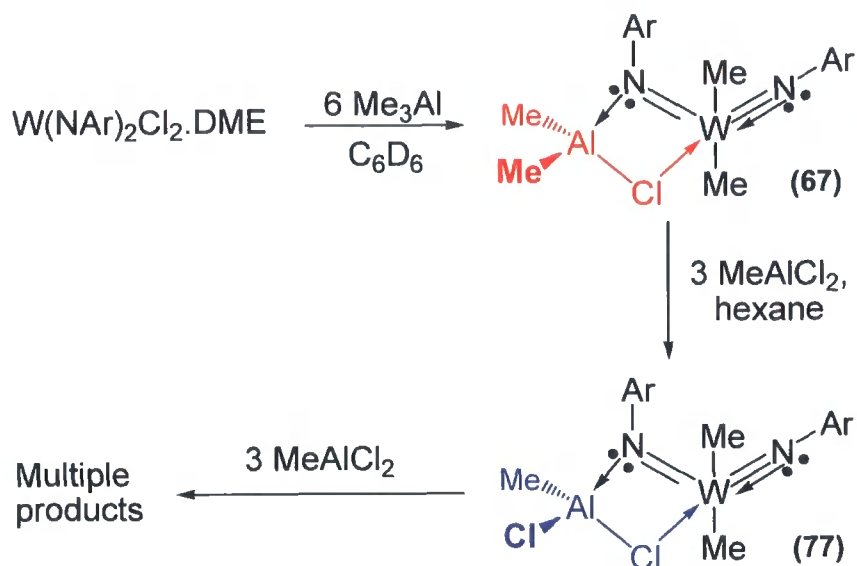
3.5 Investigating the Reactivity of M(N{Ar}AlMe_(x-1)Cl_(3-x){ μ -Cl})(NAr)Me₂ (M = Mo or W) Complexes

Reaction of M(NAr)₂Cl₂.DME (M = W or Mo) complexes with Me_xAlCl_{3-x} reagents gave a new class of compounds with the general formula M(N{Ar}AlMe_(x-1)Cl_(3-x){ μ -Cl})(NAr)Me₂ (M = Mo or W). As discussed previously (Section 3.2), there is little precedent for complexes such as W(N{Ar}AlMe₂{ μ -Cl})(NAr)Me₂ (**67**) in the literature. As a result the fundamental reactivity of this new group of complexes is unknown. Hence, attention turned to investigating the reactions of M(N{Ar}AlMe_(x-1)Cl_(3-x){ μ -Cl})(NAr)Me₂ complexes with both Lewis acids (MeAlCl₂) and Lewis bases (NEt₃ or PMe₃) as outlined in the following sections.

3.5.1 Reaction of W(N{Ar}AlMe₂{ μ -Cl})(NAr)Me₂ (67**) with MeAlCl₂**

To investigate the interaction of M(N{Ar}AlMe_(x-1)Cl_(3-x){ μ -Cl})(NAr)Me₂ complexes with Lewis acids, the reactivity of **67** with MeAlCl₂ was examined. Complex **67** was first formed *in situ* from reaction of W(NAr)₂Cl₂.DME (**40**) and Me₃Al in C₆D₆.ⁱⁱⁱ The reaction mixture was then dried *in vacuo*, removing all volatile species (including any unreacted Me₃Al). The resulting residue was then dissolved in hexane containing MeAlCl₂ (3.5 molar equivalents). After 30 minutes, the hexane and any volatile species (such as MeAlCl₂ or Me₂AlCl) were again removed *in vacuo*. Subsequent analysis using ¹H NMR spectroscopy clearly confirmed the formation of the complex W(N{Ar}AlMeCl{ μ -Cl})(NAr)Me₂ (**77**) (Scheme 3.10). Addition of excess MeAlCl₂ to **77** resulted in the formation of multiple complexes, the identity of which could not be established using ¹H NMR analysis.

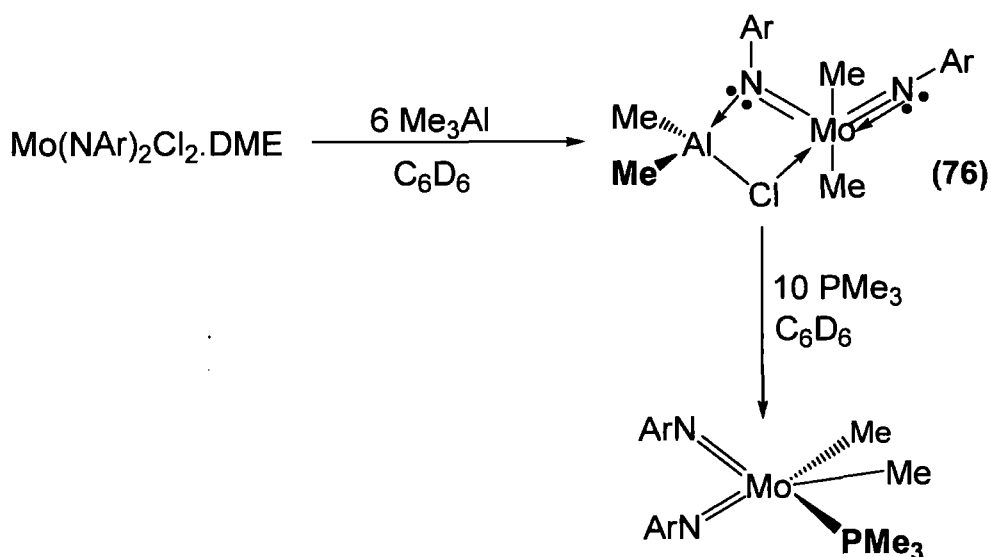
ⁱⁱⁱ Due a tendency of W(N{Ar}AlMe₂{ μ -Cl})(NAr)Me₂ (**67**) to degrade a batch of this starting material was not be made. Instead for each investigation **67** was prepared *in situ*.

Scheme 3.10 Addition of MeAlCl_2 to $\text{W}(\text{N}\{\text{Ar}\}\text{AlMeCl}\{\mu\text{-Cl}\})(\text{NAr})\text{Me}_2$ **67**

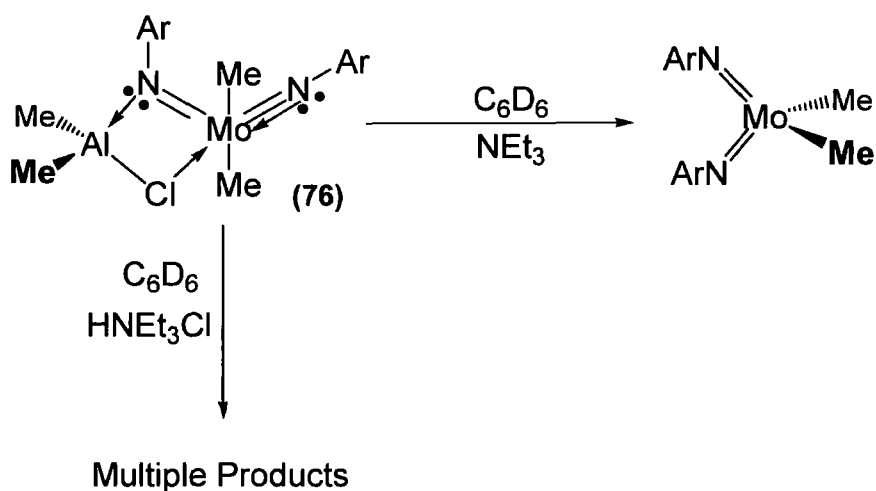
The observation that complex **77** is formed *in situ* from addition of MeAlCl_2 to $\text{W}(\text{N}\{\text{Ar}\}\text{AlMe}_2\{\mu\text{-Cl}\})(\text{NAr})\text{Me}_2$ **67** demonstrates that it is possible to exchange the $\text{Me}_x\text{AlCl}_{3-x}$ fragments of species such as **67**. The formation of **77** is attributable to the greater Lewis acid strength of MeAlCl_2 over Me_2AlCl .²⁷

3.5.2 Reaction of $\text{M}(\text{N}\{\text{Ar}\}\text{AlMe}_2\{\mu\text{-Cl}\})(\text{NAr})\text{Me}_2$ (Mo or W) with Lewis Bases

To further assess the stability of the N-Al-Cl-M chelate present in the complexes $\text{W}(\text{N}\{\text{Ar}\}\text{AlMe}_2\{\mu\text{-Cl}\})(\text{NAr})\text{Me}_2$ (**67**) and $\text{Mo}(\text{N}\{\text{Ar}\}\text{AlMe}_2\{\mu\text{-Cl}\})(\text{NAr})\text{Me}_2$ (**76**), both complexes were reacted with the Lewis bases PMe_3 or NEt_3 . Addition of PMe_3 to a sample of $\text{Mo}(\text{N}\{\text{Ar}\}\text{AlMe}_2\{\mu\text{-Cl}\})(\text{NAr})\text{Me}_2$ (**76**) in C_6D_6 , resulted in the formation of the known complex $\text{Mo}(\text{NAr})_2(\text{PMe}_3)\text{Me}_2$, previously reported by Gibson *et al.*²⁹ (**Scheme 3.11**).

Scheme 3.11 Reaction of PMe_3 with $\text{Mo}(\text{N}\{\text{Ar}\}\text{AlMe}_2\{\mu\text{-Cl}\})(\text{NAr})\text{Me}_2$ (**76**)

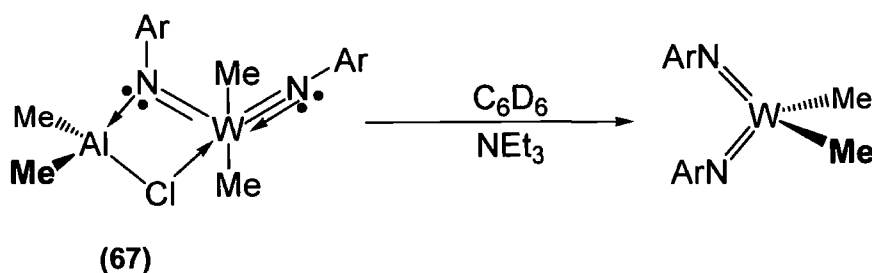
The reactivity of $\text{Mo}(\text{N}\{\text{Ar}\}\text{AlMe}_2\{\mu\text{-Cl}\})(\text{NAr})\text{Me}_2$ (**76**) with both NEt_3 and Et_3NHCl (**Scheme 3.12**) was also investigated. The reagent Et_3NHCl was selected to explore the interaction of **76** with a source of Cl^- . Reaction of **76** with NEt_3 was shown by ^1H NMR spectroscopic analysis to generate the known complex $\text{Mo}(\text{NAr})_2\text{Me}_2$ (**27**) with 100% conversion. In contrast, reaction with HNEt_3Cl resulted in multiple products, the structure of which could not be identified using NMR spectroscopic analysis.

Scheme 3.12 Reaction of NEt_3 and HNEt_3Cl with $\text{Mo}(\text{N}\{\text{Ar}\}\text{AlMe}_2\{\mu\text{-Cl}\})(\text{NAr})\text{Me}_2$ (**76**)

Together, the reactions of complex **76** with PMe_3 and NEt_3 have demonstrated that addition of a nucleophilic species (*i.e.* Lewis bases) to complexes such as

$\text{Mo}(\text{N}\{\text{Ar}\}\text{AlMe}_2\{\mu\text{-Cl}\})(\text{NAr})\text{Me}_2$ (**76**) results in displacement of the bridging Me_2AlCl fragment. The nucleophile then has the potential to coordinate to the electropositive Mo^{VI} centre (as was observed for PMe_3). Having established the reactivity of the molybdenum complex **76** with nucleophiles attention turned towards investigating the reactivity of the analogous tungsten complex $\text{W}(\text{N}\{\text{Ar}\}\text{AlMe}_2\{\mu\text{-Cl}\})(\text{NAr})\text{Me}_2$ (**67**) with NEt_3 , in the hope of attaining a base-free $\text{W}(\text{NAr})_2\text{Me}_2$ fragment. Addition of NEt_3 to a C_6D_6 solution of complex (**67**) was found to result in the formation of a the desired complex $\text{W}(\text{NAr})_2\text{Me}_2$ *in situ* (Scheme 3.13).

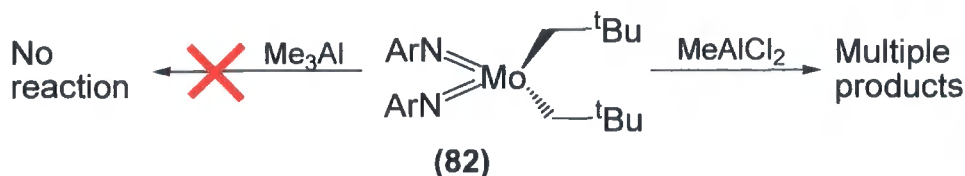
Scheme 3.13 Reaction of $\text{W}(\text{N}\{\text{Ar}\}\text{AlMe}_2\{\mu\text{-Cl}\})(\text{NAr})\text{Me}_2$ (**67**) with Et_3N



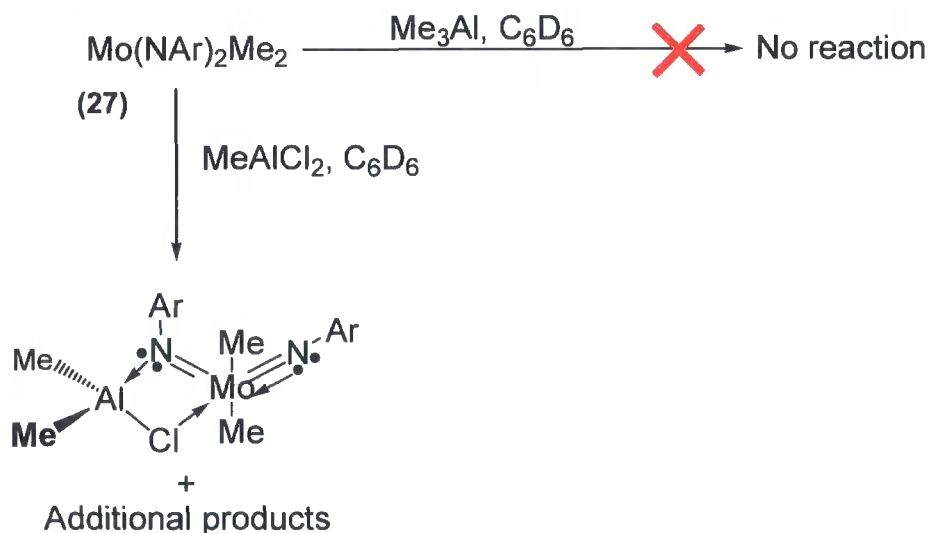
3.6 Reaction of Dialkyl Mo^{VI} *bis*(imido) Complexes with $\text{Me}_x\text{AlCl}_{(3-x)}$

During the synthesis of Lewis acid-bound complexes such as $\text{W}(\text{NAr})(\text{N}\{\text{Ar}\}\text{AlMe}_2\{\mu\text{-Cl}\})\text{Me}_2$ (**67**), it is unclear whether the binding of the Me_2AlCl fragment to the imido ligand occurs in a separate intermolecular reaction, taking place after ligand metathesis, or whether it occurs as part of the metathesis reaction, in an intramolecular fashion. To clarify if metathesis between Al-R and M-Cl moieties is a prerequisite for chelate formation, an investigation was made into the reaction of preformed dialkyl *bis*(imido) Mo^{VI} complexes with $\text{Me}_x\text{AlCl}_{3-x}$ reagents. It can be reasoned that in such systems any $\text{Me}_x\text{AlCl}_{3-x}$ coordination to imido groups must occur *via* intermolecular reactions.

Notably, treatment of $\text{Mo}(\text{NAr})_2(\text{CH}_2\text{C}(\text{Me})_3)_2$ (**82**) with Me_3Al did not result in any reaction taking place (verified using ^1H NMR spectroscopy). In contrast, the reaction of $\text{Mo}(\text{NAr})_2(\text{CH}_2\text{C}(\text{Me})_3)_2$ (**82**) with MeAlCl_2 resulted in the formation of multiple reaction products, none of which could be unambiguously assigned by NMR spectroscopy (Scheme 3.14).

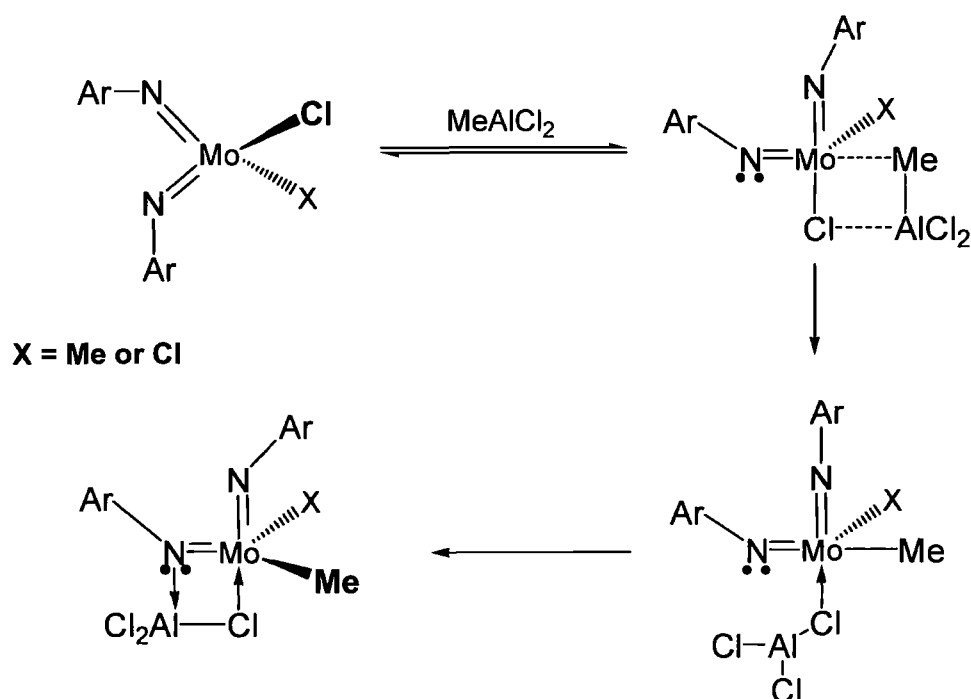
Scheme 3.14 Reaction of $\text{Mo}(\text{NAr})_2(\text{CH}_2\text{C}(\text{Me})_3)_2$ (**82**) with MeAlCl_2 and Me_3Al 

As reaction of $\text{Mo}(\text{NAr})_2(\text{CH}_2\text{C}(\text{Me})_3)_2$ (**82**) failed to give clear insight into the potential interactions of $\text{Me}_x\text{AlCl}_{3-x}$ reagents with *bis*(imido) dialkyl complexes, attention turned to investigating the reactivity of $\text{Mo}(\text{NAr})_2\text{Me}_2$ (**27**) with both MeAlCl_2 and Me_3Al (**Scheme 3.15**). Addition of Me_3Al to **27** failed to result in any reaction taking place, with no new species observable by ^1H NMR spectroscopic analysis. In this system neither Me_3Al nor the complex $\text{Mo}(\text{NAr})_2\text{Me}_2$ (**27**) contains a chloride moiety. As such, the formation of a chelate similar to that found for $\text{Mo}(\text{N}\{\text{Ar}\}\text{AlMe}_2\{\mu\text{-Cl}\})(\text{NAr})\text{Me}_2$ (**76**) in which a chloride ligand bridges between the aluminium and Mo^{VI} atoms is impossible. The failure of Me_3Al to react with $\text{Mo}(\text{NAr})_2\text{Me}_2$ (**27**) is of significance, as this strongly suggests that coordination of a chloride ligand to the Mo^{VI} atom (as in complex **76** or **79**) is essential in order to enable the binding of an $\text{Me}_x\text{AlCl}_{3-x}$ fragment to a *bis*(imido) moiety. Notably, a bridging methyl group did not evolve upon addition of Me_3Al to complex $\text{Mo}(\text{NAr})_2\text{Me}_2$ (**27**). This demonstrates that in this system a methyl moiety does not have the capacity to bridge between the molybdenum and aluminium atoms.

Scheme 3.15 Reaction of $\text{Mo}(\text{NAr})_2\text{Me}_2$ (**27**) with MeAlCl_2 and Me_3Al 

In contrast, reaction between $\text{Mo}(\text{NAr})_2\text{Me}_2$ (**27**) and MeAlCl_2 does indeed occur, with the major product (~70%) as identified by ^1H NMR spectroscopy being $\text{Mo}(\text{N}\{\text{Ar}\}\text{AlMeCl}\{\mu\text{-Cl}\})(\text{NAr})\text{Me}_2$ (**83**) (**Scheme 3.15**). However, the reaction of MeAlCl_2 and $\text{Mo}(\text{NAr})_2\text{Me}_2$ (**27**) also gives additional products, which cannot be separated from **83** by recrystallization and which could not be identified unambiguously by NMR spectroscopy. The formation of **83** upon reaction of **27** with MeAlCl_2 , demonstrates that $\text{Me}_x\text{AlCl}_{3-x}$ reagents can coordinate to *bis*(imido) fragments without metathesis of Mo-Cl and Al-Me ligands. Thus, the $\text{Me}_x\text{AlCl}_{3-x}$ fragments observed to bind in complexes such as **67** or **76** are not restricted to exclusively coordinating to the *bis*(imido) moiety in an intermolecular reaction step occurring after ligand metathesis (**Scheme 3.16**). Instead $\text{Me}_x\text{AlCl}_{3-x}$ is free to coordinate to a *bis*(imido) moiety in a classical Lewis base/Lewis acid intermolecular reaction, with the imido lone pair donated to the vacant LUMO orbital of the MeAlCl_2 .

Scheme 3.16 MeAlCl_2 coordination to a *bis*(imido) fragment via an intramolecular reaction.

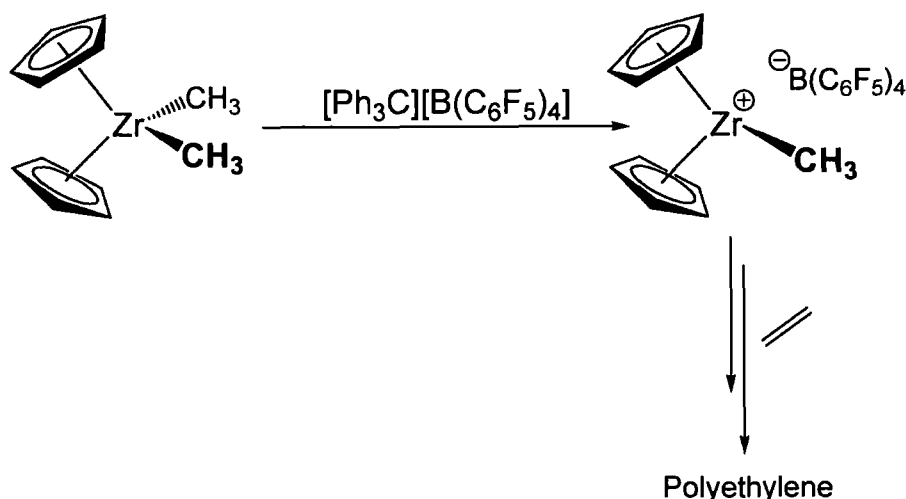


3.7 Synthesis, Characterization, and Reactivity of $\text{W}(\text{NAr})_2\text{Me}_2\cdot\text{THF}$ (84**)**

The synthesis of a tungsten *bis*(imido) dimethyl complex with no coordinating $\text{Me}_x\text{AlCl}_{3-x}$ groups is of interest for numerous reasons. Gibson *et al.* have found that reaction of $\text{Cr}(\text{NAr})_2\text{Me}_2$ with $[\text{PhNMe}_2\text{H}][\text{B}(\text{C}_6\text{F}_5)_4]$ generates an active ethylene polymerization initiator, believed to result from protonation of a Cr-Me moiety by

$[\text{PhNMe}_2\text{H}][\text{B}(\text{C}_6\text{F}_5)_4]$ to give an ionic Cr complex.³⁰ Similarly, it is well established that dimethyl Group 4 metallocenes can be activated by boron-based co-initiators to give highly active ethylene polymerization systems (**Scheme 3.17**).^{31,32,33} As mentioned in **Chapter 1, Section 1.8**, $\text{Hf}(\text{Cp})_2\text{Me}_2$ is isolobal with $\text{W}(\text{NAr})_2\text{Me}_2$. This hints that a $\text{W}(\text{NAr})_2\text{Me}_2$ fragment could be similarly activated by a boron-based co-initiator to give an alkene dimerization or polymerization initiator. Hence, the synthesis of a base-free $\text{W}(\text{NAr})_2\text{Me}_2$ complex is highly desirable.

Scheme 3.17 Activation of $\text{ZrCp}'_2\text{R}_2$ with $[\text{Ph}_3\text{C}][\text{B}(\text{C}_6\text{F}_5)_4]$



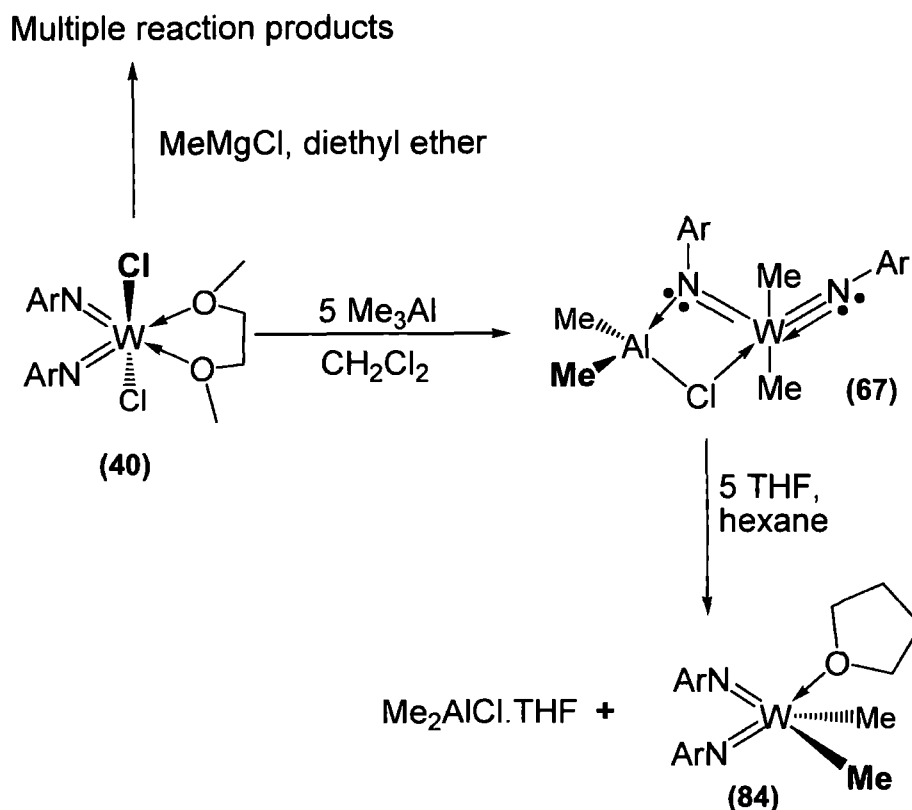
3.7.1 Synthesis and Characterization of $\text{W}(\text{NAr})_2\text{Me}_2 \cdot \text{THF}$ (84)

Reaction of **67** with Et_3N in C_6D_6 (**Schemes 3.13**) indicate that a " $\text{W}(\text{NAr})_2\text{Me}_2$ " complex is sufficiently stable to be isolated on a full preparatory scale. Notably, Gibson *et al.* have previously published the synthesis of both the related Cr and Mo dimethyl complexes $\text{Cr}(\text{NAr})_2\text{Me}_2$, and $\text{Mo}(\text{NAr})_2\text{Me}_2$ (**27**).²⁹ Both are generated from the reaction of the appropriate *bis*(imido) MCl_2 fragment with MeMgBr in diethyl ether, followed by extraction. Because both the chromium and molybdenum complexes can be made in high yields *via* this methodology an analogous procedure was attempted using $\text{W}(\text{NAr})_2\text{Cl}_2 \cdot \text{DME}$ (**40**) and MeMgCl (**Scheme 3.18**). However, this approach repeatedly failed, giving multiple complexes that could not be identified by ^1H NMR spectroscopy.

As reacting $\text{W}(\text{NAr})_2\text{Cl}_2 \cdot \text{DME}$ (**40**) with MeMgCl proved futile, an alternative synthesis was developed using Me_3Al as an alkylating agent. In **Section 3.1**, the reaction between $\text{W}(\text{NAr})_2\text{Cl}_2 \cdot \text{DME}$ (**40**) and Me_3Al was shown to give $\text{W}(\text{N}\{\text{Ar}\}\text{AlMe}_2\{\mu\text{-Cl}\})(\text{NAr})\text{Me}_2$ (**67**) with full conversion. Later, in **Section 3.5.2**, it

was shown that **67** reacts with nucleophiles to give a $W(NAr)_2Me_2$ fragment. With both of these observations in mind, it has been found that the complex $W(NAr)_2Me_2 \cdot THF$ (**84**) can be synthesised on a preparatory scale *via* reaction of complex **67** with THF (**Scheme 3.18**).

Scheme 3.18 Synthesis of $W(NAr)_2Me_2 \cdot THF$ (**84**)



The aluminium by-product $Me_2AlCl \cdot THF$ generated in this reaction can be observed by 1H NMR spectroscopy and is readily removed following recrystallization of the crude reaction material from diethyl ether. The synthetic procedure outlined in **Scheme 3.18** was repeated, but Et_2O instead of THF was used to displace the coordinating Me_2AlCl fragment of complex **67**. This was undertaken with the aim of obtaining a $W(NAr)_2Me_2$ fragment without a bound THF moiety, which would be directly analogues to established $Cr(NR)_2Me_2$ ethylene polymerization pre-catalysts.³⁰ It was found that the Me_2AlCl fragment of **67** was readily displaced by Et_2O to give a $W(NAr)_2Me_2$ complex and an unknown $(Me_2AlCl)_x(Et_2O)_y$ adduct, which could not be removed from the product complex by recrystallization. Attempts were also made to displace the bound THF moiety of **84** by drying a sample of $W(NAr)_2Me_2 \cdot THF$ (**84**) *in vacuo*; this did indeed lead to the removal of the bound THF group, which in turn resulted in degradation of the $W(NAr)_2Me_2$ fragment and the

formation of multiple W-containing complexes, as apparent by ^1H NMR spectroscopy. Recrystallization of a crude sample of **84** gave crystals suitable for single crystal X-ray diffraction analysis (Figure 3.16 and Table 3.6).

Figure 3.16 Solid state structure of $W(\text{NAr})_2\text{Me}_2\cdot\text{THF}$ (**84**) with the thermal ellipsoids set at the 50% level

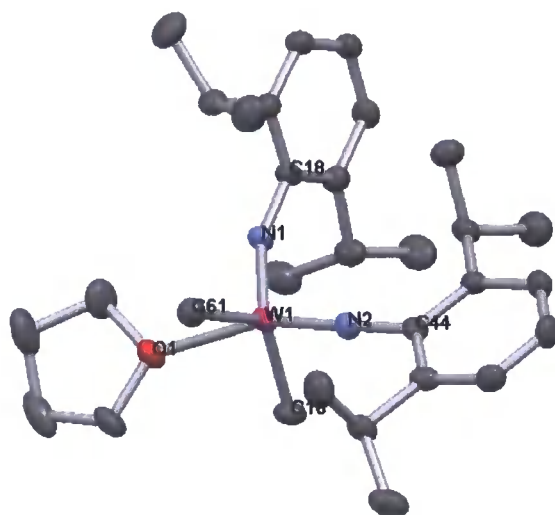


Table 3.6 Selected bond distances (Å) and bond angles ($^\circ$) for $W(\text{NAr})_2\text{Me}_2\cdot\text{THF}$ (**84**).

W1-N1	1.784(4)
W2-N2	1.764(4)
W1-C16	2.157(5)
W1-C61	2.159(5)
W1-O1	2.322(3)
C16-W1-C61	130.2(2)
N1-W1-N2	111.11(18)
W1-N2-C44	176.9(4)
W1-N1-C18	154.7(3)

Examinations of the structural parameters associated with complex **84** indicate that the tungsten core adopts a highly distorted *pseudo* trigonal bipyramidal geometry. This is consistent with the molecular structure of the closely related dimethyl molybdenum complex $\text{Mo}(\text{NAr})_2\text{Me}_2\cdot\text{PMe}_2\text{Ph}$.¹ In both **84** and $\text{Mo}(\text{NAr})_2\text{Me}_2\cdot\text{PMe}_2\text{Ph}$ the two methyl groups occupy axial sites, with the two imido ligands and the Lewis

base moiety lying approximately in the same plane. The W-C bonds of **84** at 2.157(5) and 2.159(5) Å are within the normal range for a W-C contact (2.05 Å to 2.36 Å),³⁴ and are comparable to those of W(N{Ar}AlMe₂{μ-Cl})(NAr)Me₂ (**67**) at 2.129(2) and 2.139(2) Å. The similar W-N bond lengths of 1.764(4) and 1.784(4) Å and W-N-C_{ipso} bond angles of 154.7(3) and 176.9(4)° are suggestive of both imido ligands of **84** adopting a bonding mode intermediate between that of a 4 and 2-electron donor (neutral formalism), an arrangement that is quite common for group 6 bis(imido) fragments.³⁵

The observation that **84** adopts a distorted trigonal bipyramidal geometry can explain the apparent instability of the WMe₂ moiety upon removal of THF *in vacuo*. As both W-Me methyl groups of **84** lie in an approximately axial orientation, the possibility of a reductive elimination reaction is reduced by the relatively large separation of the two Me groups in space. Removal of THF would force the resulting W(NAr)₂Me₂ species to adopt a *pseudo*-tetrahedral geometry in which the two methyl groups have a greater proximity and so an increased possibility of undergoing reductive elimination. The likelihood of **84** undergoing reductive elimination is also undoubtedly heightened in the solid state, by crystal packing forces. In contrast, the analogous Mo complex, Mo(NAr)₂Me₂.THF is stable when dried *in vacuo*, with no loss of the THF moiety occurring, presumably due to a stronger molybdenum-oxygen interaction resulting from a harder molybdenum centre.

Further examination of the ¹H NMR spectrum of W(NAr)₂Me₂.THF (**84**) highlights a discrepancy between the structure of **84** in the solid and solution states. Notably, the ¹H NMR chemical shifts for the two CH₂ moieties of the bound THF in complex **84** at 3.47 and 1.40 ppm are identical to that of an authentic sample of free, unbound THF. This suggests that in solution the THF moiety of **84** dissociates readily from the tungsten centre giving the desired base-free W(NAr)₂Me₂ complex. The weak nature of the THF association in complex **84** has also been demonstrated by the observed ease with which the THF fragment of **84** can be removed *in vacuo*.

In order to study the solution interaction between what is believed to be the base-free "W(NAr)₂Me₂" complex and THF, a solution of **84** in C₆D₅Cl was analysed by ¹H NMR spectroscopy at -40 °C and ambient temperature. No significant deviation in the relative positions and intensity of the spectral features were obtained upon cooling. Consequently, this neither contradicts nor supports the hypothesis that THF is dissociating from **84** in solution. However, the premise that the THF fragment of **84** dissociates is supported by the ¹H NMR spectral data obtained from a study of the reaction of **84** with one equivalent of B(C₆H₅)₃ in C₆D₆. Following addition of B(C₆F₅)₃ to **84** a pronounced shift to lower frequencies is observed for the THF

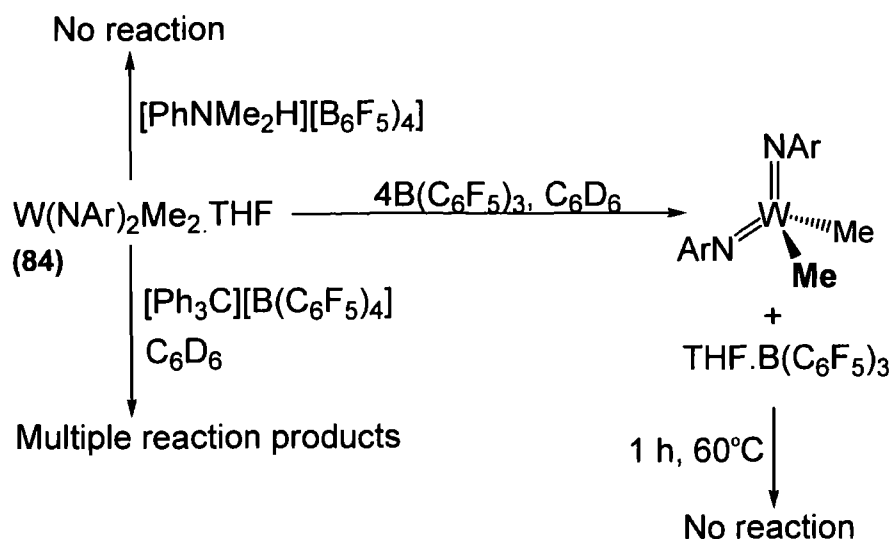
resonances (3.23 and 0.94 ppm), resulting from the formation of a THF. $B(C_6F_5)_3$ Lewis acid/Lewis base adduct.³⁶ In contrast, the 1H NMR resonances associated with the $W(NAr)_2Me_2$ fragment of **84** remain unaffected, consistent with no modification of the $W(NAr)_2Me_2$ moiety having taken place. Thus, the identical 1H NMR chemical shifts of the $W(NAr)_2Me_2$ fragment, both before and after reaction of the THF moiety with $B(C_6F_5)_3$, strongly indicates that in solution **84** undergoes facile dissociation. Although the THF moiety of **84** readily dissociates, it has been found that stronger Lewis bases can more effectively bind to a $W(NAr)_2Me_2$ fragment. Thus, addition of PMe_3 to $W(NAr)_2Me_2 \cdot THF$ (**84**) generates $W(NAr)_2Me_2 \cdot PMe_3$, which in contrast to **84** is stable when dried *in vacuo*.

3.7.2 Reaction of $W(NAr)_2Me_2 \cdot THF$ (84**) with Group 13 Compounds**

As discussed in **Section 3.7**, it is feasible that $W(NAr)_2Me_2 \cdot THF$ (**84**) may be activated by boron-based reagents to give ethylene dimerization or polymerization initiators. As such attention turned to investigating the reactivity of **84** with $[PhNHR_2H][B(C_6F_5)_4]$, $B(C_6F_5)_3$, and $[Ph_3C][B(C_6F_5)_4]$.

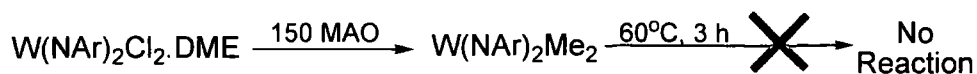
Addition of $[Ph_3C][B(C_6F_5)_4]$ to a C_6D_6 solution of **84** resulted in multiple reaction products, the identify of which could not be ascertained by 1H NMR spectroscopic analysis (**Scheme 3.19**). In contrast, attempts to react complex (**84**) with an excess of $B(C_6F_5)_3$ in C_6D_6 failed, with no modification of the $W(NAr)_2Me_2$ fragment occurring, even after the reaction solution was heated (60 °C, 2 h) (**Scheme 3.19**). This suggests that $B(C_6F_5)_3$ is not a sufficiently strong Lewis acid to abstract a W-Me moiety from of complex **84**. It was also found that the W-Me bond of complex **84** in C_6D_6 is resistant to protonation by $[PhNMe_2H][B(C_6F_5)_4]$ (**Scheme 3.19**).

Scheme 3.19 Attempted reactions of complex $W(NAr)_2Me_2 \cdot THF$ (**84**) with $[Ph_3C][B(C_6F_5)_4]$ and $B(C_6F_5)_3$



As addition of $B(C_6F_5)_3$ to **84** did not result in tungsten methyl abstraction, attention turned to assessing the capacity of MAO to abstract a $W-Me$ moiety of a $W(NAr)_2Me_2$ fragment. This was undertaken as the reagent MAO is used widely as a co-initiator in a broad range of catalytic systems, and is believed to activate transition metal complexes, *via* alkylation and methyl abstraction.³⁷ In this study commercially available MAO was dried *in vacuo* and then reacted, in a large excess, with $W(NAr)_2Cl_2 \cdot DME$ (**40**) in C_6D_5Cl . This resulted in the *in situ* formation of a $W(NAr)_2Me_2$ fragment, with identical $W-CH_3$ and CH_3 (iPr) 1H NMR chemical shifts to that presented by $W(NAr)_2Me_2 \cdot THF$ (**84**) in C_6D_5Cl . The synthesis of a $W(NAr)_2Me_2$ fragment from reaction of $W(NAr)_2Cl_2 \cdot DME$ (**40**) and MAO can undoubtedly attributed to the Me_3Al component of MAO.^{38,39} Of note, is that even after heating ($60^\circ C$, 3 h) of the MAO reaction solution no tungsten methyl abstraction occurred (**Scheme 3.20**). Thus, it can be concluded that the tungsten methyl moieties of a " $W(NAr)_2Me_2$ " fragment cannot be readily abstracted by either MAO or $B(C_6F_5)_3$.

Scheme 3.20 Reaction of $W(NAr)_2Cl_2 \cdot DME$ (**40**) with MAO

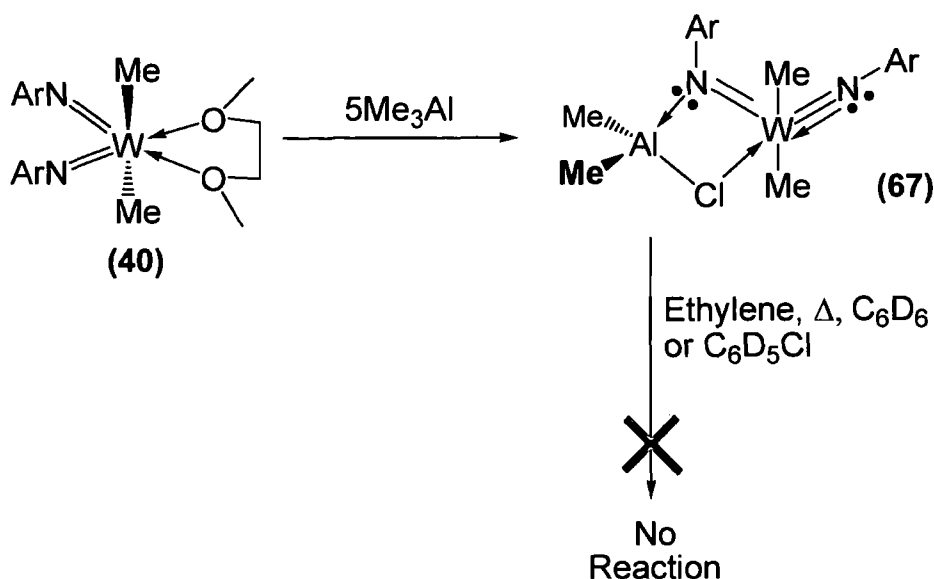


3.8 Reaction of $M(N\{Ar\}AlMe_2Cl_{2-x}\{\mu-Cl\})(NAr)Me_2$ ($M = Mo$ or W) with Ethylene

Tobisch has evaluated the capacity of tungsten *bis*(imido) systems to initiate ethylene dimerization *via* an oxidative coupling mechanism using DFT.⁴⁰ He concluded that the fragments $W^{IV}(NPh)_2$ (**85**), $W^{IV}(N\{Ph\}AlMe_2\{\mu-Cl\})(NPh)$ (**86**), and $W^{IV}(N\{Ph\}AlMe_2\{\mu-Cl\})(N\{Ph\}AlMe_2\{\mu-Cl\})$ (**87**) could all theoretically initiate ethylene dimerization. With the aim of experimentally evaluating Tobisch's DFT investigation, attention turned to assessing the capacity of a range of dimethyl *bis*(imido) complexes to react with ethylene.

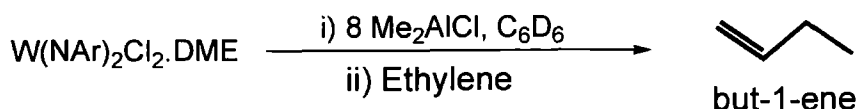
3.8.1 Reaction of $W(N\{Ar\}AlMe_2\{\mu-Cl\})(NAr)Me_2$ (67**) and $Mo(N\{Ar\}AlMe_2\{\mu-Cl\})(NAr)Me_2$ (**76**) with Ethylene**

As it has been postulated that species such as $W(N\{Ph\}AlMe_2\{\mu-Cl\})(NPh)$ (**64**) can initiate ethylene dimerization, it is feasible that the related complexes **67** and **76** could also react with ethylene. To investigate if this is indeed the case, the complexes $W(N\{Ar\}AlMe_2\{\mu-Cl\})(NAr)Me_2$ (**67**) and $Mo(N\{Ar\}AlMe_2\{\mu-Cl\})(NAr)Me_2$ (**76**) were prepared *in situ* from reaction of the appropriate $M(NAr)_2Cl_2 \cdot DME$ ($M = W$ or Mo) precursor with Me_3Al in C_6D_6 . The resulting solutions of both **67** and **76** were then placed under an atmosphere of ethylene. In neither case was any interaction between ethylene and either **67** or **76** observed to occur. Furthermore, even after heating the solutions (50 °C, 1 h), no reaction between complexes **67** and **76** with ethylene could be detected (**Scheme 3.21**). Notably, identical results were obtained when C_6D_5Cl was used as the reaction solvent. It is evident that the connectivity of **67** and **76** are not altered by the addition of the Lewis base ethylene. This indicates that the intramolecularly-coordinating chloride ligands of complexes **67** and **76** are not readily displaced to accommodate ethylene coordination at the metal centres, an essential step prior to any further reaction of the alkene.

Scheme 3.21 Attempted reaction of **67** with ethylene

3.8.2 Assessing the Capacity of Me_2AlCl to Activate $W(NAr)_2Cl_2 \cdot DME$ (**40**) for Ethylene Dimerization

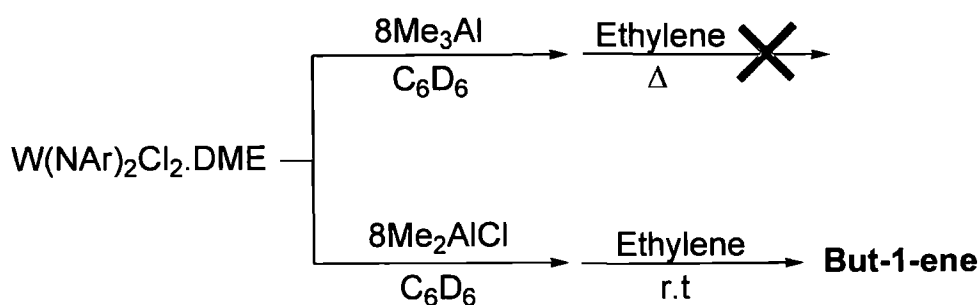
It is clear that Me_3Al cannot activate $W(NAr)_2Cl_2 \cdot DME$ (**40**) for ethylene dimerization as the product of the Me_3Al reaction, $W(N\{Ar\}AlMe_2\{\mu-Cl\})(NAr)Me_2$ (**67**), is inert to reaction with ethylene. Consequently, attention turned to assessing the capacity of the stronger Lewis acid Me_2AlCl to activate complex **40**. Thus, $W(NAr)_2Cl_2 \cdot DME$ (**40**) was reacted with Me_2AlCl (eight equivalents) in C_6D_6 and the resulting solution was treated with ethylene. In contrast to the reaction with Me_3Al , here the immediate formation of but-1-ene was observed, the identity of the organic product being verified by $^1H/^1H$ COSY correlation spectroscopy (Scheme 3.22).

Scheme 3.22 Ethylene dimerization, initiated by $W(NAr)_2Cl_2 \cdot DME$ and Me_2AlCl 

It has been established that treatment of **40** with Me_2AlCl in the absence of alkenes gives $W(N\{Ar\}AlMeCl\{\mu-Cl\})(NAr)Me_2$ (**77**) as the principle reaction product, as well as a number of additional product complexes, the structures of which are unknown (Section 3.3.2, Figure 3.10). It is clear that one of the complexes produced in the

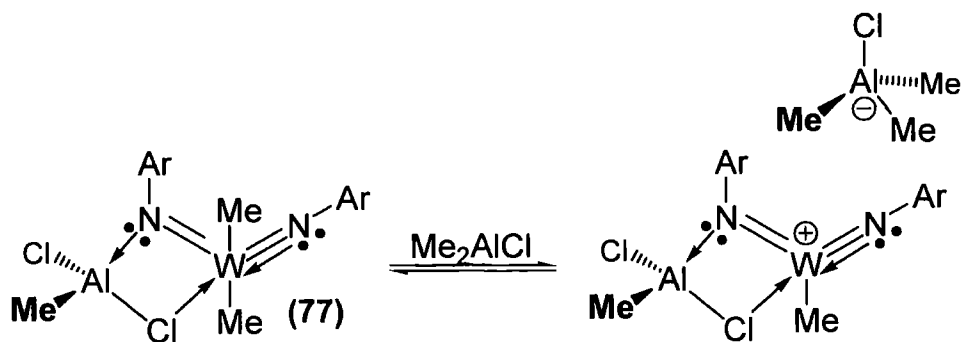
MeAlCl_2 system is capable of initiating ethylene dimerization. As complex **67** has been shown to be inert to reaction with ethylene, it is highly unlikely that $\text{W}(\text{N}\{\text{Ar}\}.\text{AlMeCl}\{\mu\text{-Cl}\})(\text{NAr})\text{Me}_2$ (**77**) is the active initiator complex. Indeed, it is very improbable that “replacing” the Me_2AlCl fragment of **67** with a MeAlCl_2 fragment in $\text{W}(\text{N}\{\text{Ar}\}.\text{AlMeCl}\{\mu\text{-Cl}\})(\text{NAr})\text{Me}_2$ (**77**) would generate an initiator complex. Furthermore comparison with the Me_3Al system (Scheme 3.23) in which **67** is obtained in 100% conversion, suggests that **77** can be viewed as a precursor to the initiator complex.

Scheme 3.23 Performance of Me_3Al vs Me_2AlCl as ethylene dimerization co-initiators



When considering how complex **77** could be activated for ethylene dimerization, it is possible to envisage that Me_2AlCl could react with complex **77**, either as an alkylating agent or as a Lewis acid. Alkylation of the only available chloride moiety of **77** would give the inactive complex $\text{W}(\text{N}\{\text{Ar}\}.\text{AlMe}_2\{\mu\text{-Cl}\})(\text{NAr})\text{Me}_2$ (**67**). One possibility is that the enhanced Lewis acidity of Me_2AlCl compared with that of AlMe_3 enables Me_2AlCl to abstract a methyl moiety of complex **77** generating a charged species with a vacant coordination site (Scheme 3.24). Such an ionic complex could undoubtedly accommodate ethylene coordination, the pre-requisite step for alkene dimerization.

Scheme 3.24 Proposed reaction of **77** with Me_2AlCl



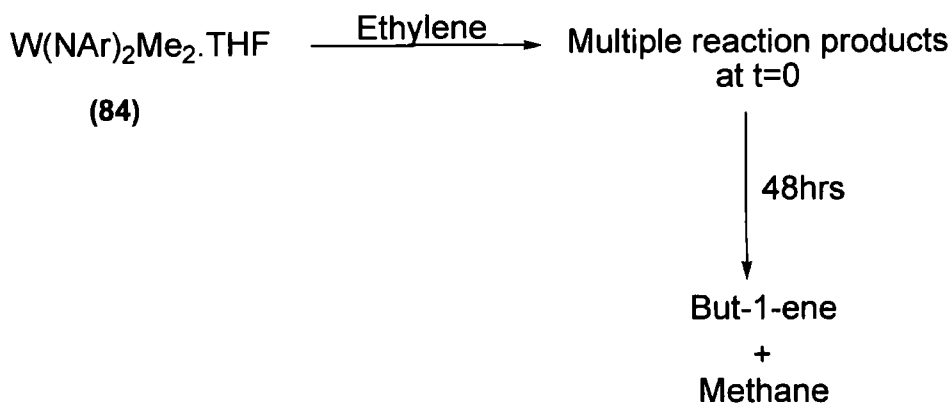
Activation of **77** for ethylene dimerization *via* the formation of a charged complex (**Scheme 3.24**) has some precedent. Discrete cationic *bis*(imido) chromium complexes stabilized by a $B(C_6F_5)_4^-$ counter ion, have been shown to initiate ethylene polymerization without the necessity for any co-initiator. In addition, the charged complex $[Cp^*CoP(OMe)_3(Et)][BAR^F]$ has been shown to initiate α -olefin dimerization, again with no additional co-initiator present.⁴¹ More recently, Schrock *et al.* have synthesised an ionic Mo^{VI} imido alkylidene complex $[Mo(NAr)(CHCMe_2Ph)(py)(THF)_2][BAR^F_4]$ suggesting that a M^{VI} charged imido complex is viable.⁴² Indeed, it has long been established for Ziegler-type polymerization initiators that charged intermediates are significant in initiating the reaction of ethylene.⁴³ As such, the possible formation of ionic complexes in the Me_2AlCl co-initiated dimerization system (**Scheme 3.24**) is highly feasible.

3.9 Reaction of $W(NAr)_2Me_2 \cdot THF$ (**84**) and $Mo(NAr)_2R_2$ ($R = Me$ or CH_2CMe_3) with Alkenes

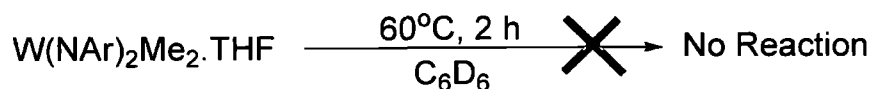
It is clear that the intramolecularly-coordinating chloride ligands of both $W(N\{Ar\}.AlMe_2\{\mu-Cl\})(NAr)Me_2$ (**67**) and $Mo(N\{Ar\}.AlMe_2\{\mu-Cl\})(NAr)Me_2$ (**76**) are not readily displaced, with both **67** and **76** being inert to reaction with ethylene (**Section 3.8.1**), undoubtedly because neither **67** nor **76** has a vacant orbital available for coordination of an σ -donor ligand. In contrast to the complexes **67** or **76**, the base-free $W(NAr)_2Me_2$ fragment, (formed in solution *via* facile dissociation of $W(NAr)_2Me_2 \cdot THF$ (**84**)), does have a vacant metal-based orbital available for ethylene coordination. Thus, **84** and related molybdenum complexes are anticipated to have a higher affinity than either **67** or **76** for reaction with alkenes. To assess if this is indeed the case, the reactivity of **84** and $Mo(NAr)_2R_2$ ($R = Me$ or CH_2CMe_3) complexes with alkenes (ethylene or propylene) was investigated.

3.9.1 Reaction of $W(NAr)_2Me_2 \cdot THF$ (**84**) with Ethylene

Initially, the reactivity of $W(NAr)_2Me_2 \cdot THF$ (**84**) with alkenes was examined. It was found that direct addition of ethylene (approximately five equivalents) to a C_6D_6 solution of complex **84** resulted in an immediate reaction to give multiple unknown reaction products (verified using 1H NMR spectroscopy). Re-analysis of the reaction solution after a 48 h period, again by NMR spectroscopy, indicated that the formation of both but-1-ene and methane (in a 4:1 molar ratio) had occurred slowly, resulting in complete consumption of ethylene (**Scheme 3.25**). The presence of the but-1-ene was confirmed by GC analysis of the volatile components of the reaction solution.

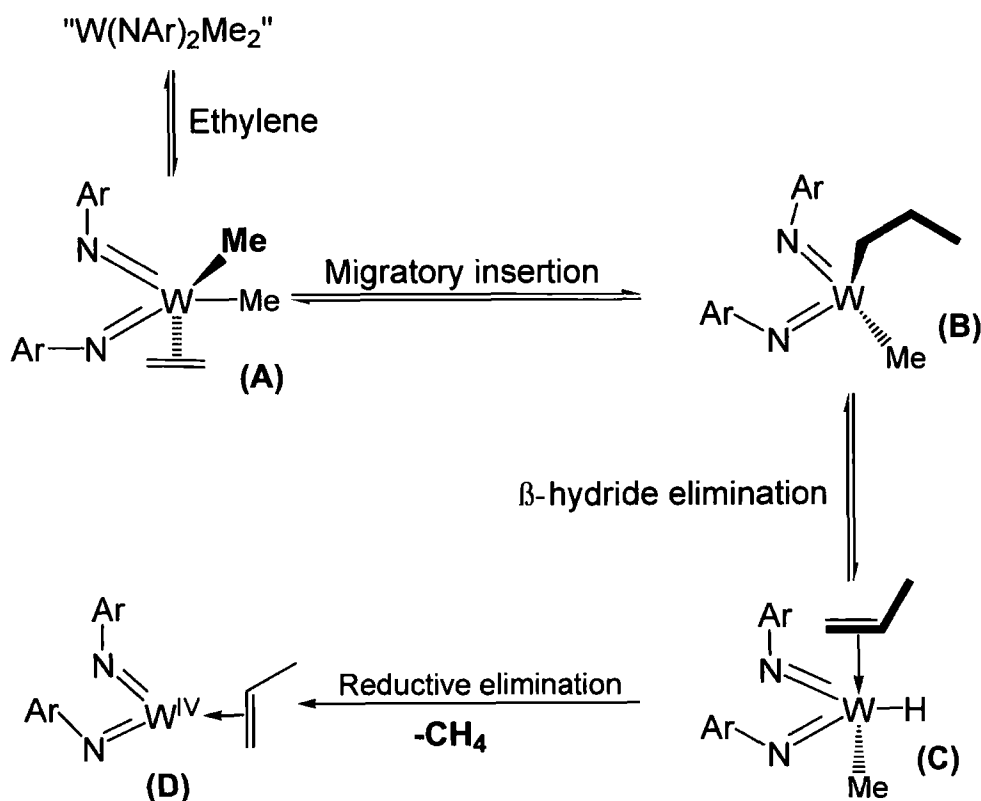
Scheme 3.25 Ethylene dimerization initiated by complex **84**

To assess the thermal stability of **84**, a sample of $\text{W(NAr)}_2\text{Me}_2\cdot\text{THF}$ (**84**) was dissolved in C_6D_6 and the solution was heated ($60\text{ }^\circ\text{C}$, 2 h). Notably no hydrolysis or thermal degradation of **84** occurred. Evidently complex **84** is stable to reductive elimination of ethane (**Scheme 3.26**).

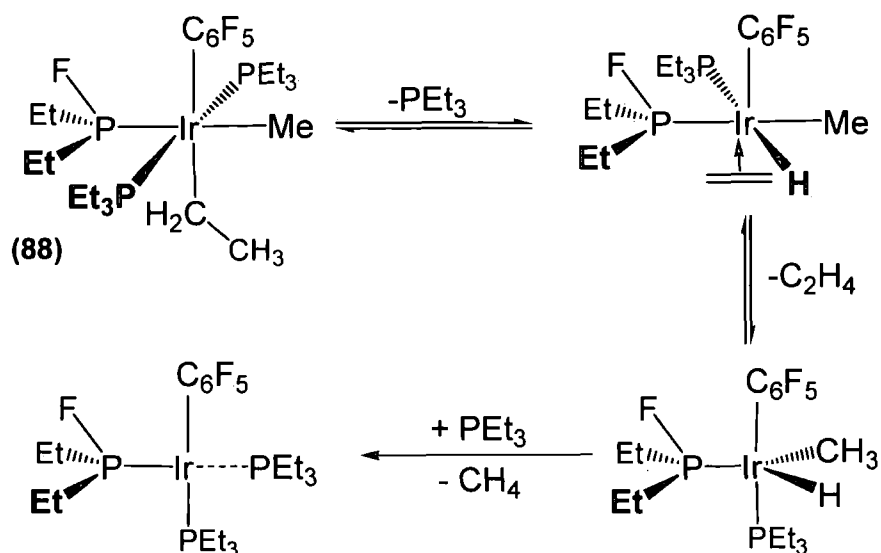
Scheme 3.26 Assessing the thermal stability of $\text{W(NAr)}_2\text{Me}_2\cdot\text{THF}$ (**84**)

It may be concluded, from the thermal stability of **84**, that activation of **84** by reductive elimination of ethane alone is not viable; instead activation of **84** is more likely to occur *via* elimination of methane (**Scheme 3.27**). As complex **84** has been shown to dissociate in solution, the first reaction step on interaction with C_2H_4 is proposed to be coordination of the alkene to give the intermediate **A**. Next, a migratory insertion reaction could take place to give a tungsten propyl complex **B**, which has the capacity to undergo β -hydride elimination to give intermediate **C**. Reductive elimination of methane from intermediate **C** would then afford the W^{V} intermediate **D**. Both the intermediates **C** or **D** of **Scheme 3.27** have the capacity to dimerize ethylene *via* a hydride cycle or cross coupling mechanism, respectively (**Chapter 1, Section 1.2**).

Scheme 3.27 Proposed mechanism for methane formation from reaction of complex **84** and ethylene



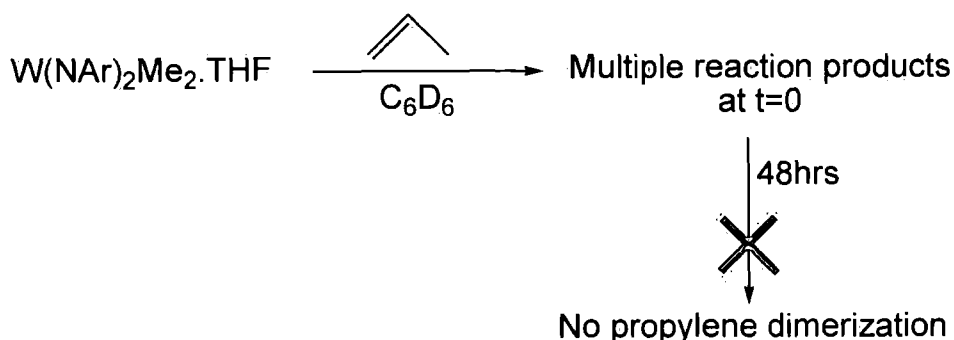
There is literature precedent for some of the steps involved in the reaction pathway outlined in **Scheme 3.27**. Macgregor *et al.* have examined the degradation of the iridium complex $Ir(C_6F_5)(Et)(Me)(PEt_2F)(PEt_3)_2$ (**88**) using DFT.⁴⁴ They established that degradation of complex **88** is initiated when a Ir-Et moiety undergoes β -hydride elimination, to give an Ir-H intermediate, from which methane is eliminated (**Scheme 3.28**). This is the same sequence of reactions to that proposed to generate methane upon reaction of **84** with ethylene (**Scheme 3.27**).

Scheme 3.28 Decomposition of $\text{Ir}(\text{C}_6\text{F}_5)(\text{Et})(\text{Me})(\text{PEt}_2\text{F})(\text{PEt}_3)_2$ (**88**)

Clearly, the formation of an active initiator species via β -hydride elimination from a *W* propyl group as outlined in **Scheme 3.27** would necessitate the formation of propylene. However, despite extensive investigation, propylene could not be detected by either ^1H NMR spectroscopic or GC analysis. It is possible that any propylene generated *in situ* reacted with ethylene to give a range of C_5 products, each in too low a concentration to be detected upon analysis of the reaction solution.

3.9.2 Reaction of $\text{W}(\text{NAr})_2\text{Me}_2\cdot\text{THF}$ (**84**) with Propylene

It has now been established that complex **84** can initiate the dimerization of ethylene. Thus, it was of interest to assess whether complex **84** would be capable of initiating dimerization of higher α -olefins. To this end, a C_6D_6 solution of **84** was treated with propylene which resulted in the formation of multiple unknown *W*-containing complexes (**Scheme 3.29**). In contrast to the ethylene system, no dimerization of propylene, occurred (as verified using ^1H NMR spectroscopy) (**Scheme 3.29**). However, the by-product methane was observed, indicating that similar reactions to those outlined in **Scheme 3.27**, **Section 3.9.1** did occur, namely migratory insertion of propylene followed by β -hydride elimination and then reductive elimination. It is unclear as to why reaction of **84** and propylene did not generate a complex *in situ* capable of initiating propylene dimerization.

Scheme 3.29 Stoichiometric Reaction of $W(NAr)_2Me_2 \cdot THF$ (**84**) with propylene**3.9.3 Reaction of $Mo(NAr)_2Me_2$ (**27**) with Ethylene**

To assess if $Mo(NAr)_2Me_2$ (**27**) would display similar reactivity with alkenes to that of the closely related tungsten complex $W(NAr)_2Me_2 \cdot THF$ (**84**), the reaction of **27** with ethylene was investigated. Addition of ethylene to a C_6D_6 solution of $Mo(NAr)_2Me_2$ (**27**) (approximately 3 equivalents) resulted in the immediate formation of multiple products the structures of which could not be determined using NMR spectroscopy. It was clear from 1H NMR analysis of the reaction solution that all of complex **27** reacted upon addition of ethylene. However, no ethylene dimerization occurred, the excess ethylene added to the reaction solution was not consumed, and no butenes were detected (1H NMR spectroscopy).

3.9.4 Rationalizing the Different Reactivity of $W(NAr)_2Me_2 \cdot THF$ (84**) and $Mo(NAr)_2Me_2$ (**27**) with Ethylene**

It has now been established that although $Mo(NAr)_2Me_2$ (**27**) reacts with ethylene, this reaction does not generate higher olefins. In contrast, but-1-ene is generated from reaction of the closely related complex $W(NAr)_2Me_2 \cdot THF$ (**84**) with ethylene. This difference in reactivity between the **27** and **84** systems is unlikely to be a steric effect, as both complexes have very similar coordination spheres. Indeed, it is unlikely that the dimethyl moiety in either complex **27** or **84** would hinder ethylene coordination. Instead the discrepancy between the Mo- and W-systems has to be attributed to electronic factors.

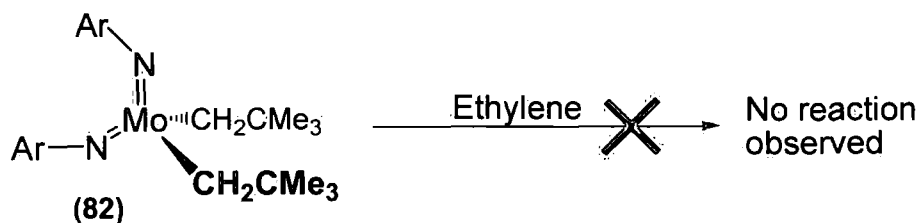
As represented in **Section 3.9.1**, **Scheme 3.27** the activation of a $W(NAr)_2Me_2$ fragment is proposed to occur *via* coordination of ethylene to the tungsten centre, followed by insertion of an ethylene ligand into a W-Me bond. It is likely that the thermodynamic penalty associated with ethylene inserting into an M-Me bond will be similar in both the molybdenum and tungsten systems. Although this feature has not been studied in detail for group 6 complexes, a DFT study has been

reported that quantifies the thermodynamic parameters associated with ethylene inserting into the M-Me bonds of a series of Ti^{VI} , Zr^{VI} and Hf^{VI} complexes.⁴⁵ This computational study found that the barrier to ethylene insertion for all three systems was similar. Thus, the observed difference in reactivity of complexes $W(NAr)_2Me_2 \cdot THF$ (**84**) and $Mo(NAr)_2Me_2$ (**27**) with ethylene is more likely to originate from the different strengths of the $Mo(\eta^2-CH_2CH_2)$ and $W(\eta^2-CH_2CH_2)$ interactions.

The relative strengths of $M(\eta^2-CH_2CH_2)$ ($M = Mo, W$) interactions have previously been examined using energy partitioning analysis.⁴⁶ It has been reported that the enthalpy of dissociation of $Mo(CO)_5(\eta^2-CH_2CH_2)$ is -20.6 kcal/mol. In contrast, for the analogous tungsten complex, $W(CO)_5(\eta^2-CH_2CH_2)$, is reported as being thermodynamically more stable, having a more negative enthalpy of dissociation, -27.9 kcal/mol. Similarly, the tungsten complex $WCl_4(\eta^2-CH_2CH_2)$ is thermodynamically more stable than the analogous complexes $MoCl_4(\eta^2-CH_2CH_2)$, with respective bond dissociation energies calculated as being -12.9 kcal/mol and $+7.8$ kcal/mol. Thus, it can be concluded that $MoCl_4(\eta^2-CH_2CH_2)$ is only kinetically not thermodynamically stable. Together, these observations suggest that molybdenum complexes seemingly have a lower affinity for ethylene than their comparable tungsten counterparts. Hence, $Mo(\eta^2-CH_2CH_2)$ species may not be thermodynamically sufficiently stable to act as catalytic intermediates, potentially hampering ethylene dimerization in the $Mo(NAr)_2Me_2$ (**27**) reaction.

3.9.5 Addition of Ethylene to $Mo(NAr)_2(CH_2CMe_3)_2$ (82**)**

Although it is unlikely that the dimethyl moieties of $W(NAr)Me_2 \cdot THF$ (**84**) and $Mo(NAr)_2Me_2$ (**27**) will inhibit ethylene coordination in either case, the same may not be true if different alkyl groups are employed. To assess the influence of steric factors upon reaction of $Mo(NAr)_2R_2$ with olefins, ethylene was added to a C_6D_6 solution of the dialkyl complex $Mo(NAr)_2(CH_2C(CH_3)_3)_2$ (**82**). Upon addition of ethylene no reaction of **82** occurred, with the 1H NMR spectrum of the reaction solution comprised exclusively of resonances assignable to free ethylene and unreacted **82** (Scheme 3.30). This demonstrates that even ethylene, a relatively small molecule, can be physically blocked by the bulk of the $CH_2C(CH_3)_3$ alkyl groups from binding to the vacant coordination site of a Mo^{VI} atom. Clearly reaction of ethylene with both $Mo(NAr)_2Me_2$ (**27**) and $W(NAr)_2Me_2 \cdot THF$ (**84**) is facilitated by the relatively low steric influence of the Mo-Me or W-Me groups.

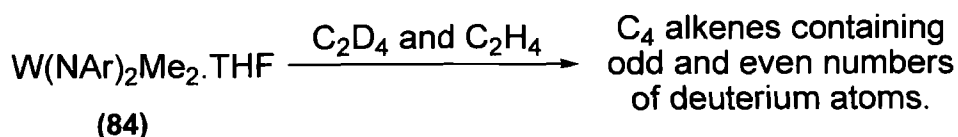
Scheme 3.30 Addition of ethylene to $\text{Mo}(\text{NAr})_2(\text{CH}_2\text{CMe}_3)_2$ (**82**)**3.10 Reaction of $\text{W}(\text{NAr})_2\text{Me}_2\cdot\text{THF}$ (**84**) with a 1:1 Mixture of C_2D_4 and C_2H_4**

As discussed in detail in **Chapter 1, Section 1.4**, Bercaw *et al.* have examined the mechanism of their chromium-initiated ethylene trimerization reaction through reaction of a 1:1 mixture of C_2D_4 and C_2H_4 .⁴⁷ The resulting C_6 products were found to contain exclusively even numbers of D and H atoms, which was cited as being proof of a metallacycle mechanism. With the aim of building upon the investigation of Bercaw, in this thesis work a $\text{C}_2\text{D}_4:\text{C}_2\text{H}_4$ mixture was reacted with a dimerization system generated *in situ* from the reaction of $\text{W}(\text{NPh})\text{Cl}_4\cdot\text{THF}$ (**32**) with $\text{Et}_3\text{Al}_2\text{Cl}_3$ (**Chapter 2 Section 2.5**). Treatment of the $\text{W}(\text{NPh})\text{Cl}_4\cdot\text{THF}/\text{Et}_3\text{Al}_2\text{Cl}_3$ solution with equimolar quantities of C_2D_4 and C_2H_4 (approximately 3 equivalents of each), resulted in the formation of a mixture of C_4 alkene products, many of which (such as $\text{C}_8\text{H}_7\text{D}$ or $\text{C}_8\text{H}_3\text{D}_5$) contained odd numbers of deuterium atoms. Furthermore, the relative abundances of the C_4 isotopomers did not fit that predicted for either a hydride or a metallacycle pathway. Thus, no information as to the mechanism of the $\text{W}(\text{NPh})\text{Cl}_4\cdot\text{THF}/\text{Et}_3\text{Al}_2\text{Cl}_3$ -based dimerization system could be ascertained.

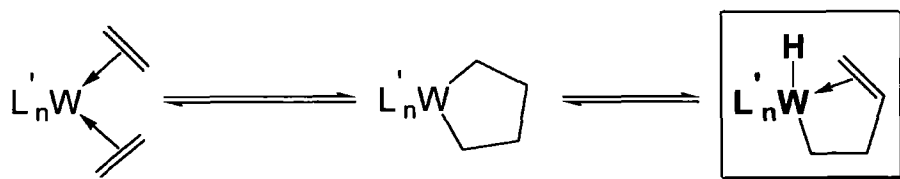
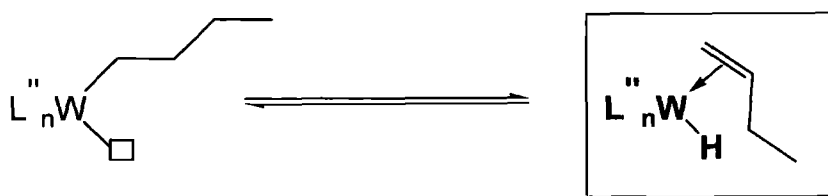
It has now been established that $\text{W}(\text{NAr})_2\text{Me}_2\cdot\text{THF}$ (**84**) can be utilized as a pre-catalyst for ethylene dimerization, generating exclusively but-1-ene (**Section 3.9.1**). Indeed, this high selectivity for but-1-ene makes the $\text{W}(\text{NAr})_2\text{Me}_2\cdot\text{THF}$ (**84**) reaction system ideally suited for mechanistic investigations. With the aim of identifying the reaction mechanism of the **84** system (hydride vs metallacycle) attention turned to examining the reactivity of **84** with a 1:1 $\text{C}_2\text{H}_4:\text{C}_2\text{D}_4$ feedstock.

Addition of C_2H_4 and then C_2D_4 to a C_6D_6 solution of $\text{W}(\text{NAr})_2\text{Me}_2\cdot\text{THF}$ (**84**) resulted in the slow formation of C_4 alkenes over a 48 h period. Analysis of the reaction solution using GC-MS determined that a multitude of C_4 products had been generated, which contained both odd and even numbers of D or H atoms (**Scheme 3.31**).^{iv}

^{iv} Ion recognition software was used to detect the presence of the products C_4H_8 , $\text{C}_4\text{H}_7\text{D}$, $\text{C}_4\text{H}_6\text{D}_2$, $\text{C}_4\text{H}_5\text{D}_3$, $\text{C}_4\text{H}_4\text{D}_4$, $\text{C}_4\text{H}_3\text{D}_5$, $\text{C}_4\text{H}_2\text{D}_6$ and C_4HD_7 .

Scheme 3.31 Dimerization of C_2D_4 and C_2H_4 initiated by $W(NAr)_2Me_2 \cdot THF$ (**84**)

Disappointingly, because C_4 olefins containing both odd and even numbers of deuterium atoms were obtained, detailed insights into the mechanism of ethylene dimerization for the **84**-based system cannot be ascertained. However, it is clear that "odd" products, such as the observed C_4H_7D , can only result from transfer of a D atom of a W-D moiety, to a C_nH_{2+n} molecule. Thus, this generation of "odd" products can be attributed to the *in situ* formation of W-H or W-D moieties. However, both the chain growth and metallacycle mechanisms of olefin dimerization have W-H (or W-D) intermediates (**Scheme 3.32**) (see **Chapter 1, Section 1.2**), which have the capacity to react with C_2D_4 or C_2H_4 , and exchange H and D atoms.

Scheme 3.32 Formation of W-H complexes in both metallacycle and hydride mechanismsMetallacycle W-H intermediateChain-growth mechanism W-H intermediate

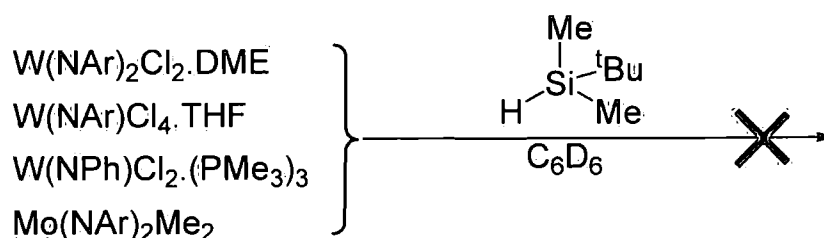
3.11 Attempts to Synthesise Tungsten and Molybdenum Hydrides From Reaction of Discrete Imido Complexes

The complex $\text{Cp}_2\text{TiH}(\text{dmpe})_2$ (**89**) has been reported by Girolami *et al.* to initiate ethylene dimerization/trimerization.⁴⁸ These researchers have also shown, using ^1H NMR spectroscopy, that insertion of ethylene into the Ti-H bond is surprisingly unfavourable, with no depletion in the ^1H NMR resonance associated with the Ti-H moiety being apparent upon ethylene dimerization. Thus, in the reaction of $\text{Cp}_2\text{TiH}(\text{dmpe})_2$ (**89**) with ethylene the hydride is viewed as being a 'spectator ligand', with dimerization of ethylene in this system being preferentially initiated *via* a metallacycle mechanism. The investigation made by Girolami and co-workers clearly demonstrates that characterization of a discrete hydride complex can ultimately lead to experimental observations that can assist in determining the mechanism of an ethylene dimerization initiator. Consequently, attention was turned to the synthesis of discrete tungsten and molybdenum imido hydride complexes.

3.11.1 Treatment of Discrete Imido Complexes with $\text{HSiMe}_2^t\text{Bu}$

It has long been established that metathesis of a Group 14 hydrides can be utilized to synthesis a transition metal hydride moiety.⁴⁹ Thus, a range of discrete Mo and W imido complexes were treated with $\text{HSiMe}_2^t\text{Bu}$ with the aim of synthesising an imido hydride complex *via* metathesis. Disappointingly, it was found that following addition of stoichiometric amounts of $\text{HSiMe}_2^t\text{Bu}$ to C_6D_6 solutions of $\text{W}(\text{NAr})_2\text{Cl}_2 \cdot \text{DME}$ (**40**), $\text{W}(\text{NAr})\text{Cl}_4 \cdot \text{THF}$ (**38**), and $\text{W}(\text{NPh})(\text{Cl})_2(\text{PMe}_3)_3$ (**34**), no reaction was observed to occur in either case (**Scheme 3.33**).

Scheme 3.33 Attempts to synthesise a M-H complex with $\text{HSiMe}_2^t\text{Bu}$



Of note is that neither of these three complexes formally has a vacant coordination site; this could block the formation of the four membered W-Cl-Si-H transitional chelate required for ligand metathesis. As such attention turned to investigating the reactivity of the complex $\text{Mo}(\text{NAr})_2\text{Me}_2$ (**27**) with $\text{HSiMe}_2^t\text{Bu}$, as **27** is coordinatively

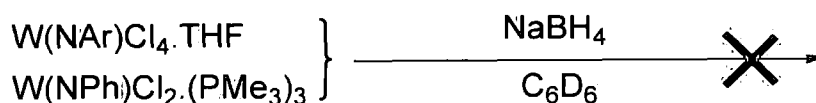
unsaturated. However, disappointingly **27** proved to be equally inert to reaction with $\text{HSiMe}_2^t\text{Bu}$ (Scheme 3.33).

3.11.2 Reaction of Discrete Imido Complexes with NaBH_4

With $\text{HSiMe}_2^t\text{Bu}$ seemingly incapable of generating an imido M-H moiety (Mo or W), efforts were made to synthesise an imido hydride complex, using alternative procedures. It has been reported that the *bis*(imido) complex $\text{Mo}(\text{NAr})_2(\text{PMe}_3)_2(\eta^2\text{-BH}_4)$ can be synthesised *via* reaction of $\text{Mo}(\text{NAr})_2\text{Cl}_2\cdot\text{DME}$ (**23**) and NaBH_4 in the presence of PMe_3 .⁵⁰ This indicates that stable tungsten hydride complexes could be produced *via* reaction of NaBH_4 .

Addition of NaBH_4 to a C_6D_6 solution of $\text{W}(\text{NAr})\text{Cl}_4\cdot\text{THF}$ (**38**) or $\text{W}(\text{NPh})(\text{Cl})_2(\text{PMe}_3)_3$ (**34**) did not result in reaction of either complex **38** or **33** (Scheme 3.34).^v In contrast to the **33** and **38** systems, addition of NaBH_4 to a C_6D_6 solution of $\text{W}(\text{NAr})_2\text{Cl}_2\cdot\text{DME}$ (**40**) did result in the partial reaction of **40**, giving unknown complexes that presented new, broad resonances at 1.40 and 3.52 ppm assignment of which has not been possible. However, no W-H moieties could be identified upon analysis of the reaction solution using NMR spectroscopy.

Scheme 3.34 Addition of NaBH_4 to the complexes **33** and **38**



3.12 Summary and Conclusions

The reaction of $\text{W}(\text{NAr})_2\text{Cl}_2\cdot\text{DME}$ (**40**) with Me_3Al has been shown to generate the dimethyl complex $\text{W}(\text{N}\{\text{Ar}\})\text{AlMe}_2\{\mu\text{-Cl}\}(\text{NAr})\text{Me}_2$ (**67**), in which a AlMe_2Cl fragment bridges the nitrogen and tungsten centres. Coordination of the Me_2AlCl Lewis acid fragment to the *bis*(imido) moiety results in a bonding motif for **67** in which one imido adopts a linear configuration and the second a bent geometry. Identical results are obtained upon reaction of the Mo complex $\text{Mo}(\text{NAr})_2\text{Cl}_2\cdot\text{DME}$ (**23**) with Me_3Al to give $\text{Mo}(\text{N}\{\text{Ar}\})\text{AlMe}_2\{\mu\text{-Cl}\}(\text{NAr})\text{Me}_2$ (**76**). Notably, complexes **67** and **70** are obtained with full conversion (verified using ^1H NMR spectroscopy). Conversely, reaction of Me_2AlCl with $\text{W}(\text{NAr})_2\text{Cl}_2\cdot\text{DME}$ (**40**) gives both $\text{W}(\text{N}\{\text{Ar}\})\text{AlMeCl}\{\mu\text{-Cl}\}(\text{NAr})\text{Me}_2$ (**77**), as well as multiple unknown complexes. The different reactivity of Me_2AlCl and

^v NaBH_4 shows an appreciable solubility in C_6D_6 , with a quartet being observed by ^1H NMR spectroscopy at 0.85 ppm (400 MHz, C_6D_6).

Me_3Al with $\text{W}(\text{NAr})_2\text{Cl}_2\cdot\text{DME}$ (**40**) has been attributed to the greater Lewis acidity of Me_2AlCl .²⁷

Addition of MeAlCl_2 to $\text{W}(\text{NAr})_2\text{Cl}_2\cdot\text{DME}$ (**40**) and $\text{Mo}(\text{NAr})_2\text{Cl}_2\cdot\text{DME}$ (**23**) gives the complexes $\text{W}(\text{N}\{\text{Ar}\}\text{AlCl}_2\{\mu\text{-Cl}\})(\text{NAr})\text{Me}_2$ (**78**) and $\text{Mo}(\text{N}\{\text{Ar}\}\text{AlCl}_2\{\mu\text{-Cl}\})(\text{NAr})\text{Me}_2$ (**79**), respectively, which were shown by single crystal X-ray diffraction analysis to be isostructural with **67**. Hence, the synthesis of complexes **67**, **78**, and **79** demonstrates that upon reaction of $\text{W}(\text{NAr})_2\text{Cl}_2\cdot\text{DME}$ (**40**) with either Me_3Al or MeAlCl_2 , the $\text{Me}_x\text{AlCl}_{3-x}$ species reacts both as an alkylating agent and as a Lewis acid. A study of **78** and **79** by multinuclear NMR spectroscopy demonstrates that this new class of complex does not undergo facile dissociation. The complexes **67** and **78** are both thermally stable. However, all the $\text{M}(\text{N}\{\text{Ar}\}\text{AlMe}_{(x-1)}\text{Cl}_{(3-x)}\{\mu\text{-Cl}\})(\text{NAr})\text{Me}_2$ complexes identified in this study were found to be highly air and moisture sensitive.

It has been shown by comparison of the molecular structures of $\text{W}(\text{N}\{\text{Ar}\}\text{AlMe}_2\{\mu\text{-Cl}\})(\text{NAr})\text{Me}_2$ (**67**) and $\text{W}(\text{N}\{\text{Ar}\}\text{AlCl}_2\{\mu\text{-Cl}\})(\text{NAr})\text{Me}_2$ (**78**) that the different Lewis acidities of the coordinating Me_2AlCl and AlCl_3 moieties can influence the relative lengths of the N-Al and Cl-W contacts. Substitution of Me_2AlCl (**67**) for AlCl_3 (**78**) results in both a lengthening of the W-Cl bond and a shortening of the N-Al contact. In contrast, variation of the group 6 metal from molybdenum (**79**), to tungsten (**78**), has no discernable effect upon the bond lengths or angles of the 4-membered chelate.

Upon reaction of the mixed imido complex $\text{Mo}(\text{NAr})(\text{N}^i\text{Bu})\text{Cl}_2\cdot\text{DME}$ (**11**) with Me_3Al and MeAlCl_2 , the difference in π -donor ability of the two imido ligands directs coordination of the $\text{Me}_x\text{AlCl}_{3-x}$ fragments to the NAr ligand exclusively. Hence, reaction of $\text{Mo}(\text{NAr})(\text{N}^i\text{Bu})\text{Cl}_2\cdot\text{DME}$ (**11**) with Me_3Al and MeAlCl_2 gives the respective complexes $\text{Mo}(\text{N}\{\text{Ar}\}\text{AlMe}_2\{\mu\text{-Cl}\})(\text{N}^i\text{Bu})\text{Me}_2$ (**80**) and $\text{Mo}(\text{N}\{\text{Ar}\}\text{AlCl}_2\{\mu\text{-Cl}\})(\text{N}^i\text{Bu})\text{Me}_2$ (**81**). Notably, the greater *trans* influence of the strongly π -donor N^iBu ligand results in a lengthening of the Mo-Cl interaction in $\text{Mo}(\text{N}\{\text{Ar}\}\text{AlCl}_2\{\mu\text{-Cl}\})(\text{N}^i\text{Bu})\text{Me}_2$ (**80**) relative to the complex $\text{Mo}(\text{N}\{\text{Ar}\}\text{AlCl}_2\{\mu\text{-Cl}\})(\text{N}^i\text{Bu})\text{Me}_2$ (**81**).

The reactivity of $\text{W}(\text{N}\{\text{Ar}\}\text{AlMe}_2\{\mu\text{-Cl}\})(\text{NAr})\text{Me}_2$ (**67**) with ethylene has been investigated. When generated *in situ* from reaction of $\text{W}(\text{NAr})_2\text{Cl}_2\cdot\text{DME}$ and Me_3Al , complex **67** has been shown to be inert towards reaction with ethylene. This demonstrates that complexes such as **67** are unlikely to react as ethylene dimerization initiators, requiring further modification in order to fulfill this role. This observation is directly relevant to the ethylene dimerization system formed upon reaction of $\text{W}(\text{NAr})_2\text{Cl}_2\cdot\text{DME}$ (**40**) with Me_2AlCl . It can be concluded that ethylene dimerization co-initiated by Me_2AlCl cannot be attributed to the complex

$W(N\{Ar\}AlMeCl(\mu-Cl))(NAr)Me_2$ (**77**), but is instead initiated by an unknown complex formed from reaction **77** and the Lewis acid Me_2AlCl .

Further investigation into the reactivity of this new class of $M(N\{Ar\}AlMe_xCl_{2-x}(\mu-Cl))(NAr)Me_2$ complex has revealed that exchange of the coordinating Me_xAlCl_{3-x} moieties is possible *via* intramolecular reactions. Hence, addition of one equivalent of $MeAlCl_2$ to complex **67** gives $W(N\{Ar\}AlMeCl(\mu-Cl))(NAr)Me_2$ (**77**). It has also been found that both $W(N\{Ar\}AlMe_2(\mu-Cl))(NAr)Me_2$ (**67**) and $Mo(N\{Ar\}AlMe_2(\mu-Cl))(NAr)Me_2$ (**76**) readily react with Lewis bases, resulting in displacement of the coordinating Me_xAlCl_{3-x} moiety. For instance, reaction of $Mo(N\{Ar\}AlMe_2(\mu-Cl))(NAr)Me_2$ (**76**) with NEt_3 and PMe_3 , generates the known complexes $Mo(NAr)_2Me_2$ (**27**) and $Mo(NAr)_2Me_2PMe_3$, respectively. Similarly addition of the Lewis bases THF and Et_3N to $W(N\{Ar\}AlMe_2(\mu-Cl))(NAr)Me_2$ (**67**) has been shown to give a base-free " $W(NAr)_2Me_2$ " species. Hence, the reactivity of complex **67** with Lewis bases has been used to synthesise the complex $W(NAr)_2Me_2.THF$ (**84**).

In the solid state the complex $W(NAr)_2Me_2.THF$ (**84**) has been shown by single crystal X-ray diffraction to adopt a highly distorted trigonal bipyramidal structure with a bound THF moiety. However, in solution (**84**) is believed to dissociate, giving free THF and a $W(NAr)_2Me_2$ species. Attempts to remove the coordinating THF fragment of **84** by drying a sample of **84** *in vacuo* resulted in degradation of the compound. This demonstrates that in the solid state THF stabilizes the WMe_2 fragment forcing the methyl groups to adopt an axial geometry and hence enhancing its stability, presumably by blocking reductive elimination. In solution the $W(NAr)_2Me_2$ fragment of **84** readily binds to the strong Lewis base PMe_3 to give $W(NAr)_2Me_2.PMe_3$, which in contrast to complex **84**, is stable *in vacuo*.

With a vacant coordination site the " $W(NAr)_2Me_2$ " species formed *in situ* through displacement of the extremely weakly-bound THF molecule, in contrast to the saturated complex $W(N\{Ar\}AlMe_2(\mu-Cl))(NAr)Me_2$ (**67**), can readily react with olefins such as propylene and ethylene. Indeed, reaction of $W(NAr)_2Me_2.THF$ (**84**) with ethylene initiates the selective formation of but-1-ene *via* dimerization over a 48 hour period. Notably reaction of **84** and ethylene has been found to generate the by-product methane. It has been observed that complex **84** is thermally stable and, upon heating is not susceptible to reductive elimination. Thus, activation of **84** is unlikely to occur *via* reductive elimination of ethane.^{vi}

^{vi} Reductive elimination of ethane could feasibly give a W^V complex capable of initiating ethylene dimerization *via* oxidative coupling.

Simultaneous reaction of **84** with equimolar quantities of C_2D_4 and C_2H_4 gives “odd” products (such as C_2H_7D) and “even” products (such as C_2H_8), according to GC-MS analysis. Hence, no detailed mechanistic information into how **84** initiates ethylene dimerization can be made. What has been established, however, is that upon reaction of **84** with ethylene, both W-H or W-D moieties are formed *in situ*, and that migratory insertion of alkenes into W-H bonds does occur in this system. Initial attempts to synthesise relevant discrete hydride complexes have been made. However, reactions of discrete molybdenum and tungsten complexes with both $HSiMe_2^tBu$ and $NaBH_4$ have failed to produce a complex with a hydride moiety.

3.13 References

- ¹ US Patents, 3,784,6(31), 30, 29 and (3,903,193), (3,897,512) to The Goodyear Tire and Rubber Company (1974-75), H.R. Menapace, G.S. Benner and N.A. Maly.
- ² World patent 2005/089940 to Sasol Technology (UK) Ltd (2005), M.J. Hanton and R.P. Tooze.
- ³ M.J. Hanton, Unpublished results.
- ⁴ H. Olivier and P.L. Gerot, *J. Mol. Cat A.*, **1999**, *148*, 43.
- ⁵ J. Kress, M. Wesolek, J.P. Le Ny and J.A. Osborn, *J.C.S. Chem. Commun.*, **1981**, 1039.
- ⁶ M.P. Coles and V.C. Gibson, *Polymer Bulletin*, **1994**, *33*, 529.
- ⁷ D.L. Thorn, W.A. Nugent and R.L. Harlow, *J. Am. Chem. Soc.*, **1981**, *103*, 357.
- ⁸ W.A. Nugent and R.L. Harlow, *J. Am. Chem. Soc.*, **1980**, *102*, 1759.
- ⁹ S.F. Pedersen and R.R. Schrock, *J. Am. Chem. Soc.*, **1982**, *104*, 7483.
- ¹⁰ N.C. Means, C.M. Means, S.G. Bott and J.L. Atwood, *Inorg. Chem.*, **1987**, *26*, 1466.
- ¹¹ V.C. Gibson, E.L. Marshall, C. Redshaw, W. Clegg and M.R.J. Elsegood, *J. Chem. Soc., Dalton Trans.*, **1996**, 4197.
- ¹² V.C. Gibson, *J. Chem. Soc., Dalton Trans.*, **1994**, 1607.
- ¹³ A search of the Cambridge Structural data base indicates that typical W-Cl bond distances are between 2.30 and 2.55 Å.
- ¹⁴ M.W. Glenny, A.J. Nielson and C.E.F. Rickard, *Polyhedron*, **1997**, *17*, 851.
- ¹⁵ i) P.W. Dyer, PhD thesis, University of Durham, **1993**; ii) Y.S. Won, Y.S. Kim, T.J. Anderson, L.L. Reifort, I. Ghiviriga and L. McElwee-White., *J. Am. Chem. Soc.*, **2006**, *128*, 13781.

- ¹⁶ i) T. Kauffman, *Angew. Chem. Int. Ed.*, **1997**, *36*, 1258; ii) T. Kauffman, M. Enk, W. Kaschube, E. Tolipoulos and D. Wingbermübler, *Angew. Chem. Int. Ed.*, **1986**, *25*, 910.
- ¹⁷ A.A. Danopoulos, G. Wilkinson, B. Hussain-Bates and M.B. Hursthouse, *J. Chem. Soc. Dalton Trans.*, **1990**, 2753.
- ¹⁸ A search of the Cambridge Structural Database for all relevant N-Al contacts (the Al was specified as having four contacts) indicates distances of between 1.86 and 2.04 Å are typical for an N-Al dative bond.
- ¹⁹ P.D. Bolton, N. Adams, E. Clot, A.R. Cowley, P.J. Wilson, M. Schröder and P. Mountford, *Organometallics*, **2006**, *25*, 5549.
- ²⁰ P.D. Bolton, E. Clot, A.R. Cowey and P. Mountford, *J. Am. Chem. Soc.*, **2006**, *128*, 15005.
- ²¹ B.D. Ward, G. Orde, E. Clot, A.R. Cowley, L.H. Gade and P. Mountford, *Organometallics*, **2004**, *23*, 4444.
- ²² P. Binger, F. Sandmeyer and C. Krüger, *Organometallics*, **1995**, *14*, 2969.
- ²³ C.J. Harlan, B.M. Bridgewater, T. Hascall and J.R. Norton, *Organometallics*, **1999**, *18*, 3827.
- ²⁴ A. Jabri, C.B. Mason, Y. Sim, S. Gambarotta, T.J. Burchell and R. Duchateau, *Angew. Chem. Int. Ed.*, **2008**, *47*, 9717.
- ²⁵ T.J. Crevier and J.M. Mayer, *Angew. Chem. Int. Ed.*, **1998**, *37*, 1891.
- ²⁶ "Organometallics: A concise Introduction" C.H. Elschenbroich and A. Salzer, VCH, Weinheim, 1992, p.82.
- ²⁷ R.F. Childs, *Can. J. Chem.*, 1982, *60*, 801.
- ²⁸ R.C.B. Copley, P.W. Dyer, V.C. Gibson, J.A.K. Howard, E.L. Marshall, W. Wang and B. Whittle, *Polyhedron*, **1996**, *15*, 3001.
- ²⁹ V.C. Gibson, C. Redshaw, G.L.P. Walker, J.A.K. Howard, V.J. Hoy, J.M. Cole, L.G. Kuzmina and D.S. De Silva, *J. Chem. Soc., Dalton Trans.*, **1999**, 161.
- ³⁰ M.P. Coles, C.I. Dalby, V.C. Gibson, I.R. Little, E.L. Marshall, M.H. Ribeiro da Costa and S. Mastroianni, *J. Organometallic Chem.*, **1999**, *591*, 78.
- ³¹ H.W. Turner, European Patent No. 277,004, **1988**.
- ³² i) X. Yang, C.L. Stern and T.J. Marks, *J. Am. Chem. Soc.*, **1994**, *116*, 10015; ii) X. Yang, C.L. Stern and T.J. Marks, *J. Am. Chem. Soc.*, **1991**, *113*, 3623.
- ³³ i) H.W. Turner, Eur. Pat. Applic., 277004, **1998**; ii) A.G. Massey and A. Park, *J. Organometallic Chem.*, **1964**, *2*, 245.
- ³⁴ Molecular structures containing W-C bond lengths of between 2.05 and 2.36 Å are currently deposited in the Cambridge Structural Database.

- ³⁵ M.H Schofield, T.P. Kee, J.T. Anhaus, R.R. Schrock, K.H. Johnson and W.M. Davis, *Inorg. Chem.*, **1991**, *30*, 3595.
- ³⁶ An authentic sample of THF.B(C₆F₅)₃ was obtained from dissolution of B(C₆F₅)₃ in THF. The ¹H NMR spectrum of THF.B(C₆F₅)₃ (C₆D₆, 400 MHz) was found to consist of two THF resonances at 3.23 and 0.94 ppm.
- ³⁷ i) H. Sinn and W. Kaminsky, *Adv. Organomet. Chem.*, **1980**, *18*, 99. ii) H. Sinn, W. Kiaminsky, H.J. Vollmer and R. Woldt, *Angew. Chem., Int. Ed. Engl.*, **1980**, *19*, 390. iii) D.E. Babushkin, C. Naundorf and H.H. Brintzinger, *Dalton Trans.*, **2006**, 4539.
- ³⁸ L. Resconi and S. Bossi, *Macromolecules.*, **1990**, *23*, 4489.
- ³⁹ W.J. van Rensburg, J.A. van den Berg and P.J. Steynberg, *Organometallics*, **2007**, *26*, 1000.
- ⁴⁰ S. Tobisch, *Dalton Trans.*, **2008**, 2120.
- ⁴¹ R.D. Broene, M. Brookhart, W.M. Lamanna and A.F. Volpe (Jr), *J. Am. Chem. Soc.*, **2005**, *127*, 17194.
- ⁴² A.J. Jiang, R.R. Schrock and P. Müller, *Organometallics*, **2008**, *27*, 4428.
- ⁴³ i) A.K. Zefirova and A.E. Shilov, *Dokl. Akad. Nauk. SSSR.*, **1961**, *136*, 599; ii) F.S. Dyachkovskii, A.K. Shilova and A.E. Shilov, *J. Polym. Sci. Part C.*, **1967**, *16*, 2333; iii) F.S. Dyachkovshii, in *Coordination Polymerisation*, ed. J.C.W. Chien, Academic Press, New York, **1975**, p 199.
- ⁴⁴ S. Erhardt and S.A. Macgregor, *J. Am. Chem. Soc.*, **2008**, *130*, 15491.
- ⁴⁵ L. Fan, D. Harrison, T.K. Woo and T. Ziegler, *Organometallics*, **1995**, *14*, 2018.
- ⁴⁶ M.S. Nechaev, V.M. Rayón and G. Frenking, *J. Phys. Chem. A.*, **2004**, *108*, 3134.
- ⁴⁷ T. Agapie, J.A. Labinger and J.E. Bercaw, *J. Am. Chem. Soc.*, **2007**, *129*, 14295.
- ⁴⁸ Y. You and G.S. Girolami, *Organometallics*, **2008**, *27*, 3172.
- ⁴⁹ E.H. Brooks and F. Glockling, *J. Chem. Soc. (A).*, **1966**, 1241.
- ⁵⁰ A.Y. Khalimon, J.P. Holland, R.M. Kowalczyk, E.J.L. McInnes, J.C. Green, P. Mountford and G.I. Nikonov, *Inorg. Chem.*, **2008**, *47*, 999.

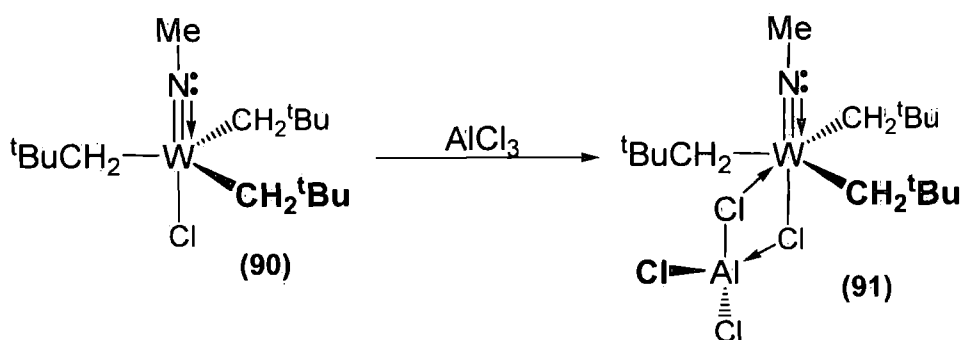
Chapter 4: Reaction of Tungsten *mono*(imido) Chloride Complexes with Methyl Aluminium Reagents

4.0 Introduction

In **Chapter 2, Section 2.8**, the relative capacities of the reagents EtMgCl and EtAlCl₂ to activate W(NAr)Cl₄.THF (**38**) for propylene dimerization were assessed. This revealed that the greater ability of EtAlCl₂ to react as a Lewis acid was crucial to the formation of an active propylene dimerization initiator. With a view to further clarifying the mode by which R_xAlCl_{3-x} reagents interact with imido chloride pre-initiators, attention turned to investigating the reactivity of discrete *mono*(imido) chloride complexes and methyl aluminium reagents such as Me₃Al or MeAlCl₂.

Previous investigations into the reactivity of *mono*(imido) complexes and Group 13 Lewis acids have been reported in the literature. For example, Osborn, *et al.* have studied the reactivity of the complexes W(NR)(X)(CH₂^tBu)₃ (X = F, Cl, Br), with GaCl₃, AlCl₃ and AlBr₃.¹ It was found that addition of AlCl₃ to a solution of W(NMe)(Cl)(CH₂^tBu)₃ (**90**) gave the single 1:1 adduct **91**, which was characterized using ¹⁴N NMR spectroscopy (**Scheme 4.1**).

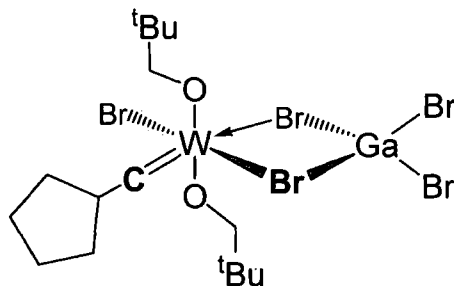
Scheme 4.1 Reaction of W(NMe)(Cl)(CH₂^tBu)₃ (**90**) with AlCl₃ affording adduct **91**



Comparison of the ¹⁴N NMR spectra of the parent complex **90** and the adduct **91**, shows that an increase in the magnitude of the ¹J_{WN} coupling is observed following AlCl₃ coordination (83 to 105 Hz). This strongly suggests that AlCl₃ binding to complex **90** actually decreases the W-N bond distance, presumably as a consequence of enhanced lone pair donation from the N-atom to the tungsten core. Significantly, a decrease in the length of the W-N contact is inconsistent with AlCl₃ binding to the imido ligand of **90** (as observed for complex **67** in **Chapter 3, Section 3.1.1**), since this would reduce the extent of π-donation from the nitrogen to the tungsten atom, which in turn would lengthen the W-N bond. Furthermore, the AlCl₃ adduct of complex **91** presented a sharp ¹⁴N resonance with a line width of 11 Hz,

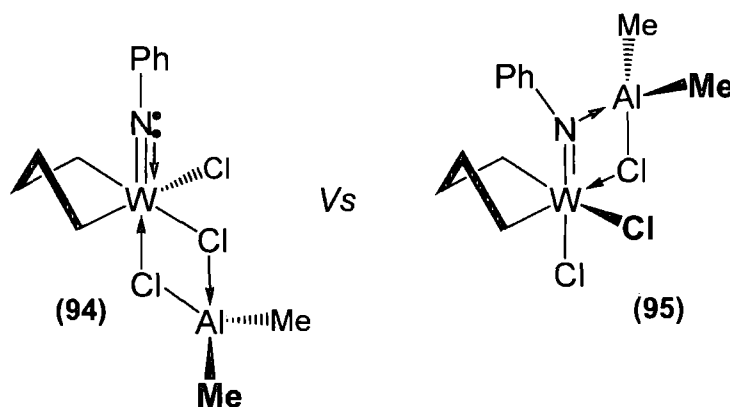
which is incompatible with a quadrupolar ^{27}Al nuclei lying adjacent to a ^{14}N atom. Instead, coordination of the Lewis acid is proposed to occur preferentially to the W-Cl ligand, giving exclusively $\text{W}(\text{NR})(\text{CH}_2^t\text{Bu})_3(\mu_2\text{-AlCl}_4)$ (**91**) (Scheme 4.1). A similar bonding mode is observed in the molecular structure of the carbene complex $\text{WBr}(\text{CH}(\text{CH}_2)_4)(\text{OCH}_2\text{C}(\text{CH}_3)_3)_2(\mu_2\text{-GaBr}_4)$ (**92**) in which a GaBr_3 fragment bridges between the tungsten and bromine ligands (Figure 4.1).²

Figure 4.1 Molecular structure adopted by complex **92**



More recently, Tobisch examined the interaction of Me_2AlCl with the complex $\text{W}(\text{NPh})\text{Cl}_2((\text{CH}_2)_4)$ (**93**) using DFT.³ He concluded that coordination of the Lewis acid (Me_2AlCl) occurs preferentially *via* a bridging chloride ligand giving the adduct $\text{W}(\text{NPh})(\text{Cl})((\text{CH}_2)_4)(\mu_2\text{-Cl}_2\text{AlMe}_2)$ (Figure 4.2, complex **94**), which has a low ΔG of association (3.4 kcal/mol). In contrast, an unfavourably high ΔG of association of 17.4 kcal/mol was found to result from Me_2AlCl binding to the *mono*(imido) ligand of complex **93** giving the adduct $\text{W}(\text{N}\{\text{Ph}\}\text{AlMe}_2\{\mu\text{-Cl}\})(\text{Cl})((\text{CH}_2)_4)$ (Figure 4.2, complex **95**). Formation of adduct **95** is postulated to be disfavoured as the lone pair of the imido N-atom is believed to be preferentially donated to the W^{VI} core, and is thus less available for donation to a MeAlCl_2 fragment.

Figure 4.2 Comparison of the structure of adducts **94** and **95**



Significantly, Tobisch also showed that coordination of Me_2AlCl to $\text{W}(\text{NPh})\text{Cl}_2((\text{CH}_2)_4)$ through a bridging chloride ligand (as in structure **94**, **Figure 4.2**) considerably reduced the energetic barrier associated with $\text{W}(\text{NPh})\text{Cl}_2((\text{CH}_2)_4)$ initiating ethylene dimerization *via* a metallacycle mechanism. In the metallacycle mechanism examined, two molecules of ethylene oxidatively couple to a W^{IV} atom giving a W^{VI} metallacycle, which decomposes first by β -hydride and then by reductive elimination to simultaneously give but-1-ene and a regenerated W^{IV} intermediate. Coordination of Me_2AlCl to **93** *via* a bridging chloride ligand, as in **94** (**Figure 4.2**), was found to lower the energetic penalty associated with reductive elimination of but-1-ene, without affecting the thermodynamics of the rate determining β -hydride elimination step.¹ Hence, the information from Tobisch's theoretical study strongly suggests that the capacity of $\text{Me}_x\text{AlCl}_{3-x}$ to react as a Lewis acid by accepting a chloride lone pair is important for the activation of *mono*(imido) pre-initiators. Similar conclusions have been made by Olivier *et al.* who found that reaction of the Lewis acid AlCl_3 with $\text{W}(\text{NPh})(\text{Cl})_2(\text{PMe}_3)_3$ (**34**) generates, *in situ*, an active ethylene dimerization initiator that is postulated to be the ionic complex $[\text{W}(\text{NPh})(\text{Cl})(\text{CH}_2)_4(\text{PMe}_3)_2][\text{AlCl}_4]$.⁴

Together, the investigations made by both Olivier and Tobisch indicate that *mono*(imido) halide pre-catalysts are activated for ethylene dimerization *via* the reaction of $\text{R}_x\text{AlCl}_{3-x}$ species as Lewis acids. To further clarify the mode by which *mono*(imido) halide complexes are activated by $\text{R}_x\text{AlCl}_{3-x}$ co-initiators, a series of model reactions using $\text{Me}_x\text{AlCl}_{3-x}$ reagents have been investigated in this thesis. Thus, in this Chapter the capacity of $\text{Me}_x\text{AlCl}_{3-x}$ groups to coordinate to and/or react with *mono*(imido) halide complexes will be discussed.

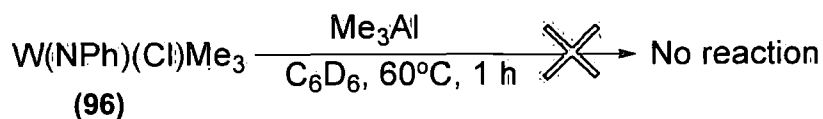
4.1 Reaction of $\text{W}(\text{NR})\text{Cl}_4 \cdot \text{THF}$ ($\text{R} = \text{Ph}$ or Ar) with Me_3Al in C_6D_6

A number of model reactivity studies using $\text{Me}_x\text{AlCl}_{3-x}$ reagents were undertaken and analyzed using NMR spectroscopy. In order to evaluate the reactivity of *mono*(imido) tetrahalide complexes with Me_3Al , a C_6D_6 solution of $\text{W}(\text{NPh})\text{Cl}_4 \cdot \text{THF}$ (**32**) was treated with six equivalents of Me_3Al (**Scheme 4.2**). This was followed by immediate analysis using ^1H NMR spectroscopy, which identified complete loss of the starting material **32** and the clean formation of $\text{W}(\text{NPh})(\text{Cl})\text{Me}_3$ (**96**) (**Figure 4.3**). Identical results are obtained from addition of Me_3Al to complex **32** in CD_2Cl_2 .

¹ See **Chapter 1, Section 1.1** for in-depth discussion of the metallacycle mechanism

with the Me_3Al in this reaction acting only as an alkylating agent. It was also found that heating (1 h, 60°C) a mixture of $\text{W}(\text{NPh})(\text{Cl})\text{Me}_3$ (**96**) and Me_3Al in C_6D_6 did not induce any additional reaction of **96** (Scheme 4.3).

Scheme 4.3 Attempted reaction of **96** with Me_3Al at 60°C

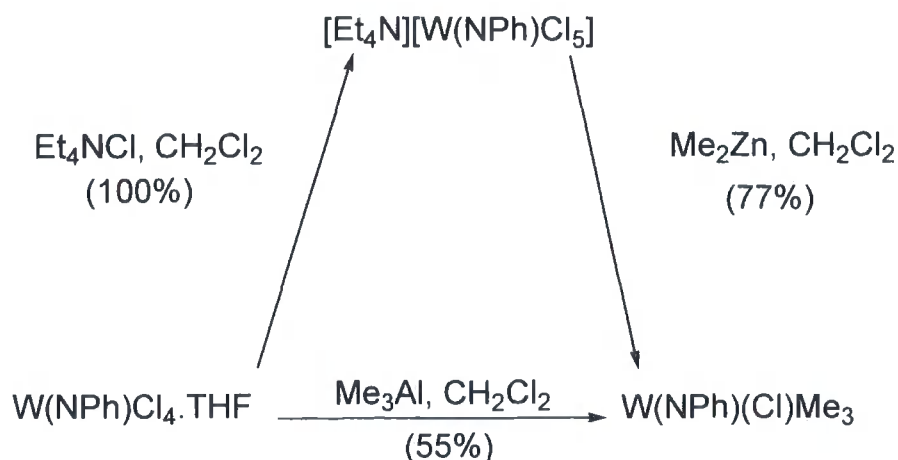
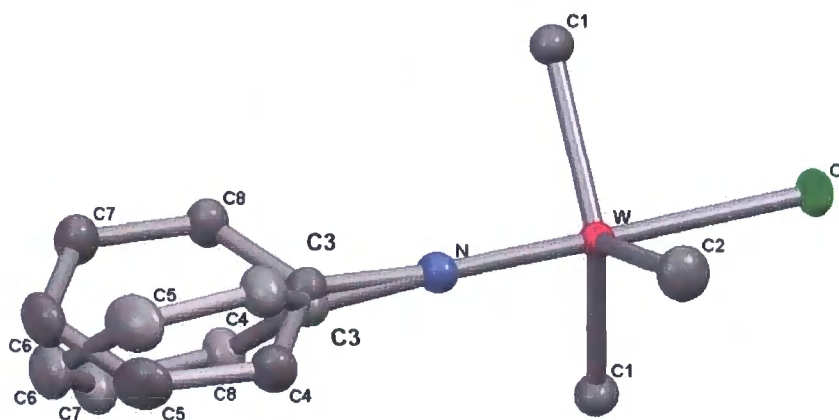


Using closely related procedures to that employed for the reaction of $\text{W}(\text{NPh})\text{Cl}_4 \cdot \text{THF}$ (**32**) and Me_3Al , it was found that the complexes $\text{W}(\text{NAr})\text{Cl}_4$ (**31**)⁹ and $\text{W}(\text{NAr})\text{Cl}_4 \cdot \text{THF}$ (**38**) when treated with Me_3Al in C_6D_6 both gave $\text{W}(\text{NAr})(\text{Cl})\text{Me}_3$ (**97**) with full conversion.ⁱⁱ

4.2 Synthesis and Characterization of $\text{W}(\text{NR})(\text{Cl})\text{Me}_3$ (96**)**

Schrock *et al.* have previously reported the synthesis of **96**, via reaction of the salt $[\text{Et}_4\text{N}][\text{W}(\text{NPh})\text{Cl}_5]$ with Me_2Zn . However, in work conducted for this thesis it has been found convenient to synthesise **96** directly from the reaction of $\text{W}(\text{NPh})\text{Cl}_4 \cdot \text{THF}$ (**32**) and Me_3Al (Scheme 4.4). Similarly, $\text{W}(\text{NAr})(\text{Cl})\text{Me}_3$ (**97**) can be readily synthesised on a preparatory scale from reaction of Me_3Al with either $\text{W}(\text{NAr})\text{Cl}_4$ (**31**) or $\text{W}(\text{NAr})\text{Cl}_4 \cdot \text{THF}$ (**38**) also in CH_2Cl_2 . Recrystallization of complex **96** from diethyl ether (-15°C) gave light yellow crystals of sufficient quality for single crystal X-ray diffraction analysis (Figure 4.4 and Table 1.1).

ⁱⁱ In contrast, reaction of the related *mono*(imido) complex $\text{Ta}(\text{NAr})\text{Cl}_3 \cdot (\text{TMEDA})$ with Me_3Al in C_6D_6 , failed to produce discrete complexes, with ^1H NMR spectroscopic analysis indicating that no alkylation of the $\text{Ta}(\text{NAr})\text{Cl}_3$ core occurs.

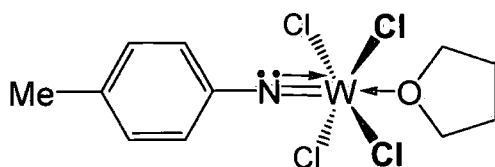
Scheme 4.4 Alternative routes for the synthesis of $W(NPh)(Cl)Me_3$ (**96**)**Figure 4.4** Solid state structure of $W(NPh)(Cl)Me_3$ (**96**) with the thermal ellipsoids set at the 50% level (rotational disorder associated with the phenyl ring is shown).**Table 4.1** Selected bond distances (Å) and bond angles (°) for $W(NPh)(Cl)Me_3$ (**96**)

W-N	1.738(3)	C1-W-C2	122.90(15)
W-C1	2.101(4)	N-W-C1	92.96(8)
W-C2	2.106(3)	Cl-W-C2	87.99(12)
W-Cl	2.4198(9)	N-W-Cl	176.87(10)
N-C3	1.396(4)	N-W-Cl	176.87(10)

A notable feature of the molecular structure of **96** is the disorder associated with the imido phenyl ring substituent. This is manifested as two possible orientations of this ring relative to a Cl-N-W mirror plane, giving two inequivalent rotamers. Despite this disorder, it is clear that complex **96** adopts *pseudo* trigonal bipyramidal geometry about the W atom, with the electronegative Cl atom lying preferentially *trans* to the

strongly π -donating imido ligand. Indeed, the high *trans* influence of the phenyl imido ligand results in a lengthening of the W-Cl bond of **96** (2.4198(9) Å), relative to the W-Cl contacts of the related *pseudo* octahedral complex $W(NC_6H_4\{p\text{-Me}\})Cl_4 \cdot THF$ (**98**) (2.338(4) Å), in which the imido and chloride ligands are *cis* (Figure 4.5).⁹

Figure 4.5 Molecular structure adopted by $W(NC_6H_4\{p\text{-Me}\})Cl_4 \cdot THF$ (**98**) in the solid state



Another significant feature of complex **96** is the W-N-C3 bond angle, which at $174.9(4)^\circ$ is close to the ideal 180° angle associated with an LX_2 donor imido ligand.¹⁰ Indeed, the short W-N bond distance of **96** at 1.738(3) Å is typical of a 4-electron donor imido ligand (neutral formalism) bound to tungsten.¹¹ The observation that the *mono*(imido) ligand of $W(NPh)(Cl)Me_3$ (**96**) is a 4-electron donor, can be used to rationalize the formation of Lewis acid-free complex **96** from reaction of $W(NPh)Cl_4 \cdot THF$ (**32**) with Me_3Al (see Section 4.3). It can be reasoned that the formation of **96** *via* reaction of **32** and Me_3Al must also generate $Me_xAlCl_{(3-x)}$ fragments *in situ*.ⁱⁱⁱ These $Me_xAlCl_{(3-x)}$ fragments are unable to coordinate to the imido moiety of complex **96** as in the *bis*(imido) $M(N\{Ar\})AlMe_xCl_{2-x}\{\mu\text{-Cl}\}(NAr)Me_2$ complexes investigated in Chapter 3, since the phenyl imido N-lone pair of **96** is preferentially donated to the electropositive W^{VI} centre.

4.3 Reaction of $W(NPh)(Cl)Me_3$ (**96**) with $LiMe$

As is evident from the molecular structure of complex **96**, the W-Cl bond is seemingly weakened by the strong *trans* influence of the phenyl imido moiety; consequently it would be expected that the chloride ligand of **96** would be relatively labile. With a view to assessing if the tungsten chloride ligand of complex **96** can indeed readily be substituted, attention turned to the reactivity of $W(NPh)(Cl)Me_3$ (**96**) with alkylating

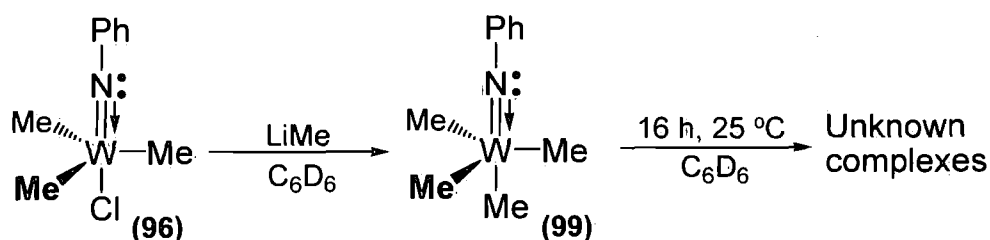
ⁱⁱⁱ Reaction of Me_3Al with $W(NPh)Cl_4 \cdot THF$ (**32**) in C_6D_6 to give $W(NPh)(Cl)Me_3$ (**96**) must also produce *in situ* either Me_2AlCl , $MeAlCl_2$ or $AlCl_3$ from ligand metathesis of W-Cl and Al-Me moieties. The 1H NMR spectra presented by the **32** reaction solution contains a single broad Al-(CH₃) resonance at -0.39 ppm (Figure 4.3), which is assignable to Me_3Al . This intense Me_3Al signal masks any Me_2AlCl resonances, as the chemical shift of Me_2AlCl in C_6D_6 is -0.44 ppm.

agents. In this regard, Schrock *et al.* have reacted $W(NPh)(Cl)Me_3$ (**96**) with $LiMe$, reporting that this gives the complex $W(NPh)Me_4$ (**99**), although no characterization of **99** was made due to the complex's reported instability.⁸ In work conducted during the preparation of this thesis, it has been observed that even after heating **96** in the presence of excess Me_3Al , no methylation of the $W-Cl$ moiety of **96** occurs, indicating that formation of complex **99** is unfavourable presumably as a result of locating a strongly *trans*-influencing methyl group *trans* to the imido moiety.

However, to further clarify if alkylation of **96** is indeed viable, $W(NPh)(Cl)Me_3$ (**96**) was reacted with $LiMe$ in C_6D_6 . This reaction was observed to result in a shift of the $W-Me$ 1H NMR resonance (1.27 to 1.34 ppm), with integration of the 1H NMR spectrum confirming the formation of $W(NPh)Me_4$ (**99**) *in situ* (Scheme 4.5). Notably, only one broad 1H NMR resonance was presented for **99**, which is suggestive of the fact that the two $W-CH_3$ environments of **99** resonate with similar frequencies, generating a single broad peak (or overlapping resonances). Alternatively complex **99** may have a fluxional structure; this again would be consistent with the broad nature of the resonance observed.

In solution, degradation of $W(NPh)Me_4$ (**99**) was found to occur over a 16 h period, generating an insoluble material that could not be characterized using NMR analysis. Of note, is that decomposition of **99** did not produce ethane,^{iv} demonstrating that the decay of **99** does not result from the reductive elimination of two *cis* $W-Me$ ligands.

Scheme 4.5 Reaction of $W(NPh)(Cl)Me_3$ (**96**) with $LiMe$



4.3.1 Reaction of $W(NPh)(Cl)Me_3$ (**96**) with $Me_3SiOSO_2CF_3$

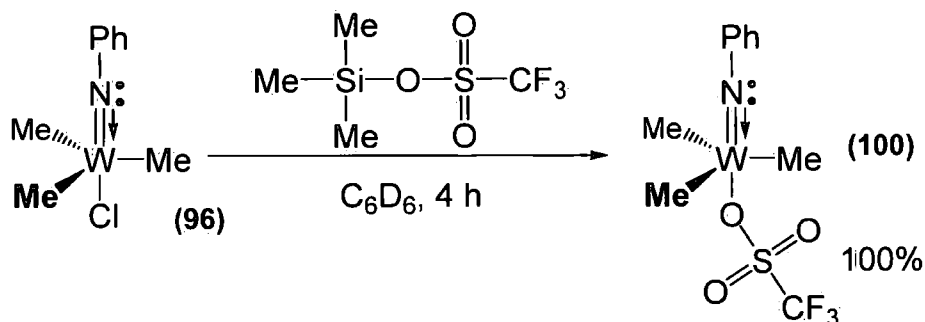
The strong *trans* influence exerted by the imido ligand in complex **96** should also correspond to the *trans* chloride atom being particularly susceptible to abstraction by a Lewis acid. Furthermore, reaction of **96** with Lewis acids is of particular interest

^{iv} The Reaction of $W(NPh)(Cl)Me_3$ (**96**) with $LiMe$, generating **99** was carried out in a sealed NMR tube.

here, as this could generate a cationic tungsten core with a vacant coordination site capable of accommodating alkene coordination. Hence, in the first instance, attention turned to investigating the reactivity of **96** with strong Lewis acids such as $\text{Me}_3\text{SiOSO}_2\text{CF}_3$.

Addition of $\text{Me}_3\text{SiOSO}_2\text{CF}_3$ to a C_6D_6 solution of $\text{W}(\text{NPh})(\text{Cl})\text{Me}_3$ (**96**) led to the formation of the complex $\text{W}(\text{NPh})\text{Me}_3(\text{OSO}_2(\text{CF}_3))$ (**100**) and the by-product ClSiMe_3 in the expected 1:1 molar ratio (verified by ^1H NMR) over a 4 h period. Complex **100** has been characterized by NMR spectroscopy and displays a single tungsten methyl resonance, indicating that **100** adopts the same *pseudo* trigonal bipyramidal geometry as the parent complex $\text{W}(\text{NPh})(\text{Cl})\text{Me}_3$ (**96**). It is presumed that the triflate moiety of **100** will coordinate to the tungsten core, as triflate counterions are known to be moderately coordinating.¹² Indeed, numerous complexes containing M-OTf bonds have been isolated and characterized.¹³ Thus, the conversion of complex (**96**) to $\text{W}(\text{NPh})\text{Me}_3(\text{OSO}_2(\text{CF}_3))$ (**100**) reveals that the chloride ligand of **96** can readily be abstracted by an appropriate Lewis acid (**Scheme 4.6**). This conclusion is of consequence when evaluating the solution structure of $\text{W}(\text{NR})(\text{Cl})\text{Me}_3 \cdot \text{AlCl}_3$ ($\text{R} = \text{Ph}$ or Ar) adducts, which will be discussed later in **Section 4.7**.

Scheme 4.6 Reaction of $\text{W}(\text{NPh})(\text{Cl})\text{Me}_3$ (**96**) with $\text{Me}_3\text{SiOSO}_2\text{CF}_3$



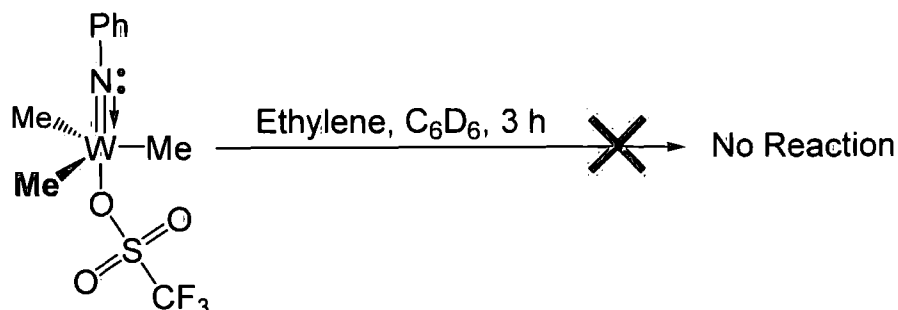
4.3.2 Reaction of $\text{W}(\text{NPh})\text{Me}_3(\text{OSO}_2(\text{CF}_3))$ (100**) with Ethylene**

A rationalization of the impact and effect of Lewis acid coordination upon the reactivity of *mono*(imido) pre-catalysts with alkenes is of general interest. In the context of this work, the way in which such coordination can modify a complexes reaction with alkenes (such as ethylene) is of particular significance. Thus, attention was turned to investigating the reactivity of **100** with ethylene.

Ethylene was added to a C_6D_6 solution of $\text{W}(\text{NPh})\text{Me}_3(\text{OSO}_2(\text{CF}_3))$ (**100**) (**Scheme 4.7**). Neither reaction of complex **100** nor the formation of higher olefins

were observed to occur by ^1H NMR spectroscopy. The inability of **100** to interact with ethylene is presumed to be attributed to the strongly coordinating triflate moiety, which blocks ethylene coordination to the W^{VI} centre.

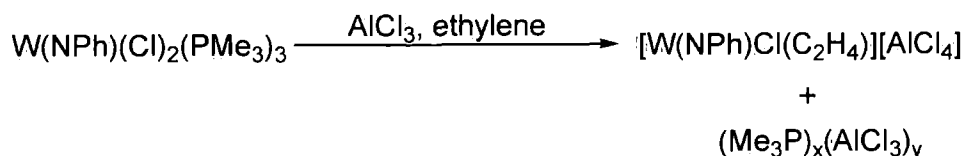
Scheme 4.7 Reaction of $\text{W}(\text{NPh})\text{Me}_3(\text{OSO}_2(\text{CF}_3))$ (**100**) and ethylene



4.4 Reaction of $\text{W}(\text{NR})(\text{Cl})\text{Me}_3$ ($\text{R} = \text{Ph}, \text{Ar}$) with $[\text{Li}(\text{OEt})_2][\text{B}(\text{C}_6\text{F}_5)_4]$ and $[\text{Na}][\text{B}(3,5\text{-}(\text{CF}_3)_2\text{C}_6\text{H}_3)_4]$

Olivier and co-workers have proposed that activation of the ethylene dimerization pre-catalyst $\text{W}(\text{NPh})(\text{Cl})_2(\text{PMe}_3)_3$ (**34**) by the Lewis acid AlCl_3 generates, *in situ*, the active ionic initiator complex $[\text{W}(\text{NPh})(\text{Cl})(\text{CH}_2)_4(\text{PMe}_3)_2][\text{AlCl}_4]$ (**Scheme 4.8**).⁴ Consequently, abstraction of tungsten chloride ligands by a Lewis acid to give a charged complex may be a viable general route to initiator formation. To evaluate if *mono(imido)* complexes can indeed react with Lewis acids to give stable salts, the complexes $\text{W}(\text{NPh})(\text{Cl})\text{Me}_3$ (**96**) and $\text{W}(\text{NAr})(\text{Cl})\text{Me}_3$ (**97**) have been reacted with both $[\text{Li}(\text{OEt})_2][\text{B}(\text{C}_6\text{F}_5)_4]$ and $[\text{Na}][\text{B}(3,5\text{-}(\text{CF}_3)_2\text{C}_6\text{H}_3)_4]$. These Lewis acids were selected because the corresponding anions $[\text{B}(\text{C}_6\text{F}_5)_4]^-$ and $[\text{B}(3,5\text{-}(\text{CF}_3)_2\text{C}_6\text{H}_3)_4]^-$ are known to be weakly-coordinating.¹⁴

Scheme 4.8 Olivier's proposed route of $\text{W}(\text{NPh})(\text{Cl})_2(\text{PMe}_3)_3$ (**34**) activation.



In the first instance, an MeCN solution of $\text{W}(\text{NPh})(\text{Cl})\text{Me}_3$ (**96**) was treated with an equimolar quantity of $[\text{Na}][\text{B}(3,5\text{-}(\text{CF}_3)_2\text{C}_6\text{H}_3)_4]$. This resulted in the rapid formation of a yellow precipitate. Disappointingly, characterization of this material by NMR spectroscopy was hampered by its lack of solubility even in polar solvents such

as CD_2Cl_2 or CD_3CN . Consequently, attention turned to the reaction of the more soluble complex $\text{W}(\text{NAr})(\text{Cl})\text{Me}_3$ (**97**), which can readily be synthesised *via* reaction of $\text{W}(\text{NAr})\text{Cl}_4 \cdot \text{THF}$ (**38**) and Me_3Al (Section 4.2).

Using a similar procedure to that described above, a CD_2Cl_2 solution of $\text{W}(\text{NAr})\text{Me}_3\text{Cl}$ (**97**) was treated with $[\text{Na}][\text{B}(3,5\text{-(CF}_3)_2\text{C}_6\text{H}_3)_4]$, which resulted in the immediate formation of a bright purple solution. Monitoring the reaction by ^1H NMR spectroscopy revealed the slow conversion of **97** to what is believed to be $[\text{W}(\text{NAr})\text{Me}_3][\text{B}(3,5\text{-(CF}_3)_2\text{C}_6\text{H}_3)_4]$ (**101**); after a period of 5 h **101** was present in approximately 30% (by integration) as the only new product. It was found that complex **101** presented a new ^1H NMR singlet resonance at 1.86 ppm (W-CH_3) and a doublet at 1.24 ppm (CH_3 , ^iPr) in a 9:12 ratio by integration. All attempts to induce further conversion of **97** to **101** by heating (2 h, 60°C) failed.

In order to try and obtain an ionic *mono(imido)* complex in higher yield, a different salt of a weakly-coordinating anion was explored. Thus, $\text{W}(\text{NAr})(\text{Cl})\text{Me}_3$ (**97**) was dissolved in $\text{C}_6\text{D}_5\text{Cl}$ and mixed with $[\text{Li}(\text{OEt})_2][\text{B}(\text{C}_6\text{F}_5)_4]$. Here, no reaction of **97** was observed to occur at ambient temperature. However, subsequent heating of the same sample (60°C , 16 h) was found to induce the formation of a new product, formulated as $[\text{W}(\text{NAr})\text{Me}_3][\text{B}(\text{C}_6\text{F}_5)_4]$ (**102**), with approximately 30% conversion by integration (Scheme 4.9), as verified by ^1H NMR analysis (Figure 4.6). Attempts to induce further conversion of **97** to **102** by additional heating (60°C , 48 h) resulted in a decomposition of both **97** and **102**.

Scheme 4.9 Reaction of $\text{W}(\text{NAr})(\text{Cl})\text{Me}_3$ (**97**) with $[\text{Li}(\text{OEt})_2][\text{B}(\text{C}_6\text{F}_5)_4]$

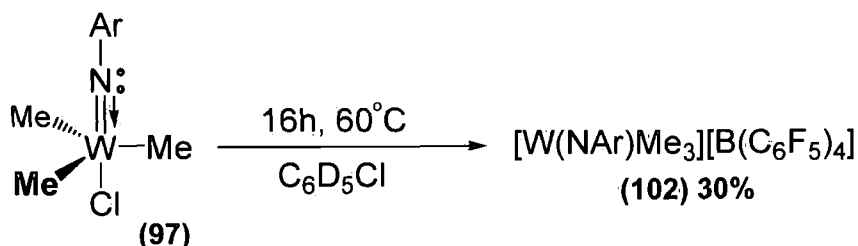
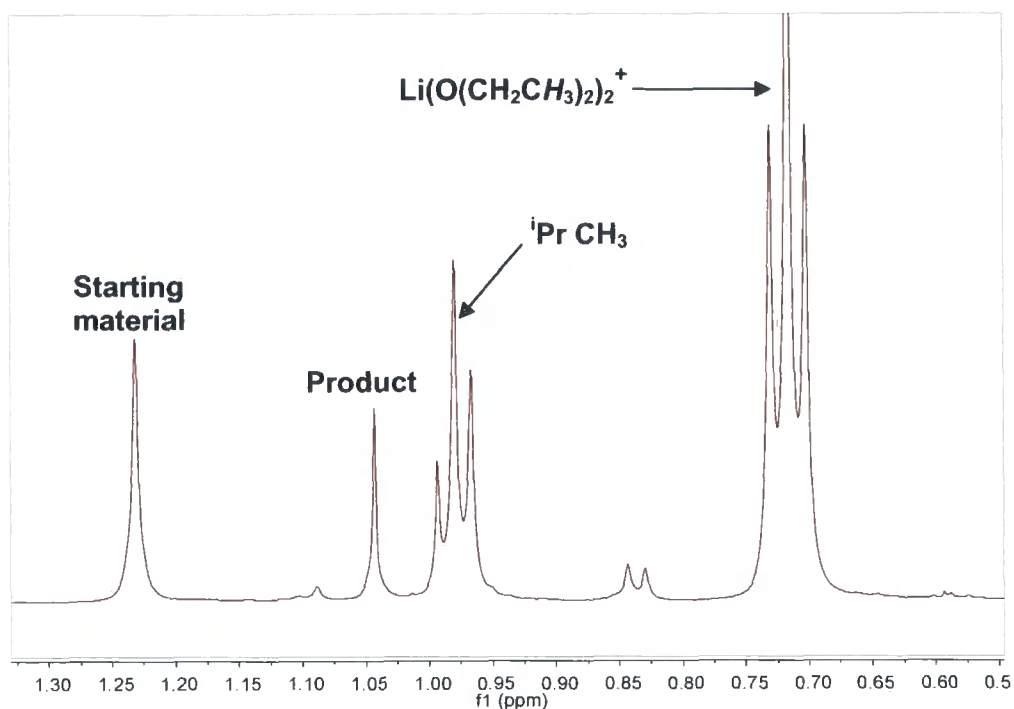


Figure 4.6 ^1H NMR ($\text{C}_6\text{D}_5\text{Cl}$, 400 MHz) spectrum obtained *in situ* from reaction of $\text{W}(\text{NAr})(\text{Cl})\text{Me}_3$ (**97**) and $[\text{Li}(\text{OEt})_2][\text{B}(\text{C}_6\text{F}_5)_4]$, (aromatic region omitted)



In the ^1H NMR spectrum of the crude reaction mixture (**Figure 4.6**), a somewhat broadened resonance was observed at 1.23 ppm ($\text{Bv}_{1/2} = 6$ Hz), which corresponds to the $\text{W}-\text{CH}_3$ signal of the precursor complex $\text{W}(\text{NAr})(\text{Cl})\text{Me}_3$ (**97**), with a second less intense resonance at 1.04 ppm being attributable to the $\text{W}-\text{CH}_3$ unit of the product $[\text{W}(\text{NAr})\text{Me}_3][\text{B}(\text{C}_6\text{F}_5)_4]$ (**102**). The CH_3 $i\text{Pr}$ groups of the complexes **97** and **102** resonate with similar chemical shifts, giving two overlapping doublets at 0.99 and 0.98 ppm.

Although investigations into the reactivity of the phenyl *mono*(imido) complex $\text{W}(\text{NPh})(\text{Cl})\text{Me}_3$ (**96**) with $[\text{Na}][\text{B}(3,5\text{-(CF}_3)_2\text{C}_6\text{H}_3)_4]$ were hampered by the insolubility of the resulting product complexes, it was found that $\text{C}_6\text{D}_5\text{Cl}$ was a sufficiently polar to permit examination of the reaction of **96** with $[\text{Na}][\text{B}(3,5\text{-(CF}_3)_2\text{C}_6\text{H}_3)_4]$. Addition of $[\text{Na}][\text{B}(3,5\text{-(CF}_3)_2\text{C}_6\text{H}_3)_4]$ to a $\text{C}_6\text{D}_5\text{Cl}$ solution of $\text{W}(\text{NPh})(\text{Cl})\text{Me}_3$ (**96**) resulted in the formation of a new, ^1H NMR, $\text{W}-\text{CH}_3$ resonance at 1.16 ppm (*c.f.* the $\text{W}-\text{Me}$ resonance of **96** is detected at 1.28 ppm). This observation is consistent with the *in situ* formation of $[\text{W}(\text{NPh})\text{Me}_3][\text{B}(3,5\text{-(CF}_3)_2\text{C}_6\text{H}_3)_4]$ (**103**) with approximately 40% conversion (by integration). The structure of **103** can be assigned as $\text{W}(\text{NPh})\text{Me}_3(\text{OSO}_2(\text{CF}_3))$ (**100**) as it also displays a $\text{W}-\text{CH}_3$ resonance at 1.16 ppm

(albeit in C_6D_6) which indicates that a similar $[W(NPh)Me_3]$ core is present in each case.

Complex **103** was observed (over a 2 h period) to convert to an unknown product, with two new resonances being observed at 1.70 and 1.20 ppm in an approximately 1:2 ratio. Of note, is the influence of the imido subsistent, with $W(NPh)(Cl)Me_3$ (**96**) reacting with $[Na][B(3,5-(CF_3)_2C_6H_3)_4]$ at room temperature in contrast to the analogous $W(NAr)(Cl)Me_3$ (**97**) system, which required heating ($60^\circ C$, 16 h) to induce any formation of $[W(NAr)Me_3][B(3,5-(CF_3)_2C_6H_3)_4]$ (**101**).

While reaction of $W(NAr)(Cl)Me_3$ (**97**) with $[Li(OEt)_2][B(C_6F_5)_4]$ and $[Na][B(3,5-(CF_3)_2C_6H_3)_4]$ did generate *in situ* the complexes $[W(NAr)Me_3][B(C_6F_5)_4]$ (**102**) and $[W(NAr)Me_3][B(3,5-(CF_3)_2C_6H_3)_4]$ (**103**), respectively, neither **102** nor **103** were obtained in full conversion despite a lengthy period of heating. It remains unclear as to why incomplete reaction of **97** with either $[Li(OEt)_2][B(C_6F_5)_4]$ or $[Na][B(3,5-(CF_3)_2C_6H_3)_4]$ was observed. However, one possibility is that the reactions between the W-Cl bond of **97** and the Lewis acid reagents are slow. This is potentially further complicated by the poor solubility of these lithium and sodium salts in the reaction solvents employed (*i.e.* C_6D_6 , CD_2Cl_2 and C_6D_5Cl).

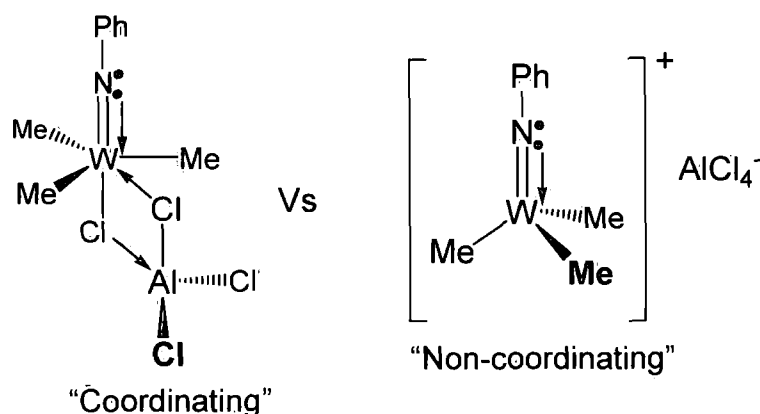
Despite the lack of complete conversion, the limited formation of $[W(NAr)Me_3][B(C_6F_5)_4]$ (**102**) and $[W(NAr)Me_3][B(3,5-(CF_3)_2C_6H_3)_4]$ (**101**) from $W(NAr)(Cl)Me_3$ (**97**) is significant as this demonstrates that abstraction of a tungsten chloride by a Lewis acid to give a stable ionic complex is indeed a viable reaction pathway. This supports Olivier's hypothesis that the active initiator complex in her $W(NPh)(Cl)_2(PMe_3)_3/AlCl_3$ ethylene dimerization system is an ionic complex, which results from abstraction of a tungsten chloride ligand by the Lewis acid $AlCl_3$, generating a weakly-coordinating $AlCl_4^-$ anion.⁷

4.5 Investigation of the Reactivity of $W(NR)(Cl)Me_3$ (R = Ph or Ar) with the Lewis Acid $MeAlCl_2$

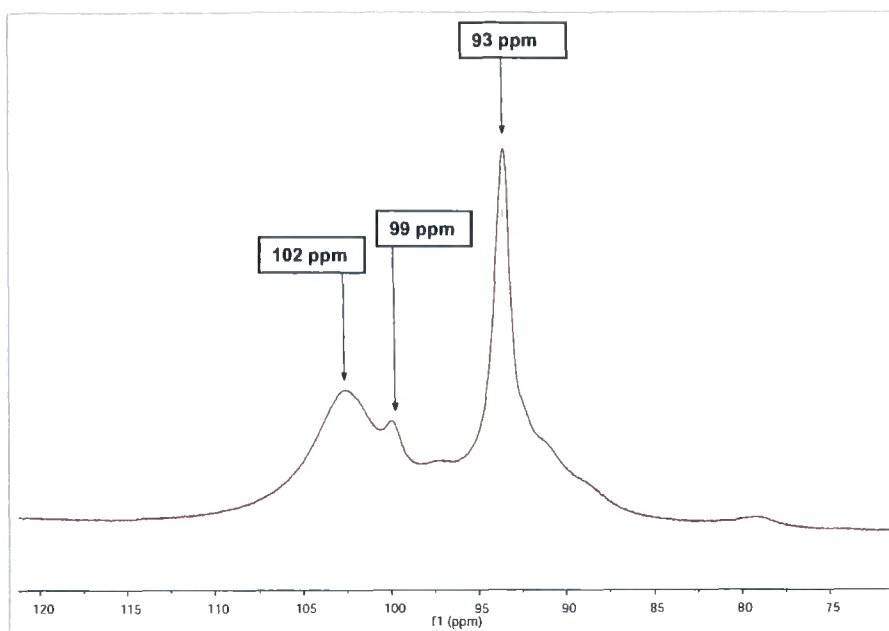
As illustrated in the preceding section, the reaction of compounds such as $[Li(OEt)_2][B(C_6F_5)_4]$ with the complexes **96** and **97** has shown that the W-Cl bond of **96** or **97** can be cleaved *via* abstraction of the chloride atom by a Lewis acid. This indicates that a similar reaction pathway, resulting from reaction of R_xAlCl_{3-x} as a Lewis acid, is viable and may be significant in the activation of *mono*(imido) halide complexes by R_xAlCl_{3-x} co-initiators (see **Chapter 2.2, Table 2.3**). To evaluate if abstraction of a tungsten chloride ligand by R_xAlCl_{3-x} species is indeed feasible, attention turned to investigating a series of model reactions between $MeAlCl_2$ and the complexes $W(NR)(Cl)Me_3$ (R = Ph or Ar).

Notably, Osborn *et al.* determined that addition of Lewis acids (such as AlCl_3) to $\text{W}(\text{NMe})(\text{Cl})(\text{CH}_2^t\text{Bu})_3$ (**90**) resulted in coordination of the AlCl_3 fragment to the tungsten halide giving $\text{W}(\text{NMe})(\text{CH}_2^t\text{Bu})_3(\mu^2\text{-AlCl}_4)$ (**91**) (Scheme 4.1).¹ These results strongly suggest that reaction of $\text{W}(\text{NR})(\text{Cl})\text{Me}_3$ ($\text{R} = \text{Ph}$ or Ar) with MeAlCl_2 could also lead to an $\text{Me}_x\text{AlCl}_{3-x}$ fragment interacting with the tungsten chloride ligand. Less clear is the mode of $\text{Me}_x\text{AlCl}_{3-x}$ association; with the aluminium-based Lewis acid fragment capable of interacting with the $\text{W}(\text{NR})(\text{Cl})\text{Me}_3$ ($\text{R} = \text{Ph}$ or Ar) framework as a coordinating or non-coordinating Lewis acid (Figure 4.7).

Figure 4.7 Possible bonding modes of AlCl_3 in the adduct $[\text{W}(\text{NPh})(\text{Cl})\text{Me}_3.\text{AlCl}_3]$ (**104**)



In order to explore the structures of the adducts **104** and **105** ^{27}Al NMR spectroscopy was employed (Figure 4.8). This technique is uniquely suited to analysis of the solution structures of **104** (and **105**), since δ ^{27}Al has been shown to be extremely sensitive to the coordination number of the aluminium centre in a given complex.¹⁵

Figure 4.8 ^{27}Al NMR (CD_2Cl_2 , 130 MHz) spectrum of $[\text{W}(\text{NPh})(\text{Cl})\text{Me}_3.\text{AlCl}_3]$ (**104**)

The ^{27}Al NMR spectrum (CD_2Cl_2) of the proposed adduct $[\text{W}(\text{NPh})(\text{Cl})\text{Me}_3.\text{AlCl}_3]$ (**104**) presents three broad resonances at δ 102, 99, and 93 ppm (**Figure 4.8**).^v The same three resonances were detected upon analysis of the proposed adduct $[\text{W}(\text{NAr})(\text{Cl})\text{Me}_3.\text{AlCl}_3]$ (**105**), although for **105** the resonance at 102 ppm was less intense. Assignment of the resonance at 102 ppm to a AlCl_4^- ion can be made. This assignment is possible as a comparable ^{27}Al NMR spectrum of an authentic sample of the ionic complex $[\text{AlCl}_4][\text{P}(\text{N}^i\text{Pr}_2)_2]$ (**107**),¹⁶ was found to comprise a single sharp resonance at 102 ppm.^{vi}

Assignment can also be made to the resonances detected at 99 and 93 ppm in the ^{27}Al NMR of both **104** and **105**. It has previously been reported that AlCl_3 presents two ^{27}Al NMR resonances at δ 99 and 91 ppm in C_6D_6 .^{17, vii} Although it is unclear as to why AlCl_3 presents two resonances, it is apparent from the similarity in the ^{27}Al NMR chemical shifts that an AlCl_3 moiety is formed from treatment of both $\text{W}(\text{NPh})(\text{Cl})\text{Me}_3$ (**96**) and $\text{W}(\text{NAr})(\text{Cl})\text{Me}_3$ (**97**) with MeAlCl_2 . One potential explanation

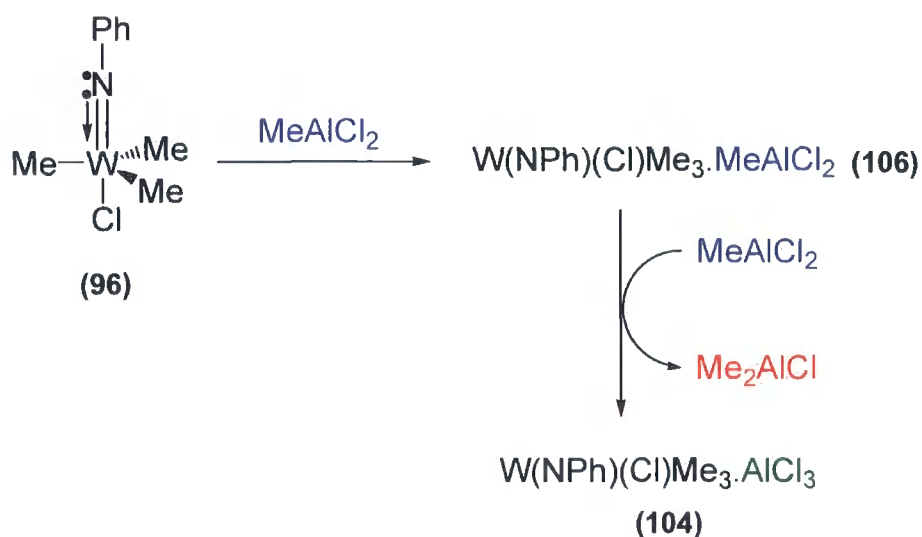
^v Analysis of an empty NMR tube gave a broad resonance at approximately 56 ppm resulting from the aluminium content of the glass. This background signal was not sufficiently intense to be detected upon analysis of **104**, **105** or **107**.

^{vi} The solution and solid state structure of $[\text{AlCl}_4][\text{P}(\text{N}^i\text{Pr}_2)_2]$ (**107**) has been extensively investigated. It is well known that **107** possesses a discrete $[\text{AlCl}_4]^-$ anion.¹⁶

^{vii} Notably, the ^{27}Al NMR chemical shifts presented by **104** in both C_6D_6 and CD_2Cl_2 were identical.

as to the origin of the AlCl_3 fragment is given in **Scheme 4.11**. It is proposed that **96** reacts initially with MeAlCl_2 to form an adduct such as **106**. Then, subsequent reaction of intermediate **106** with the excess MeAlCl_2 present in the reaction solution, initiates a methyl exchange process, which eliminates Me_2AlCl and gives the product complex **104**.

Scheme 4.11 Proposed mechanism for the formation of the AlCl_3 adduct **104** from reaction of $\text{W}(\text{NPh})(\text{Cl})\text{Me}_3$ (**96**) with MeAlCl_2

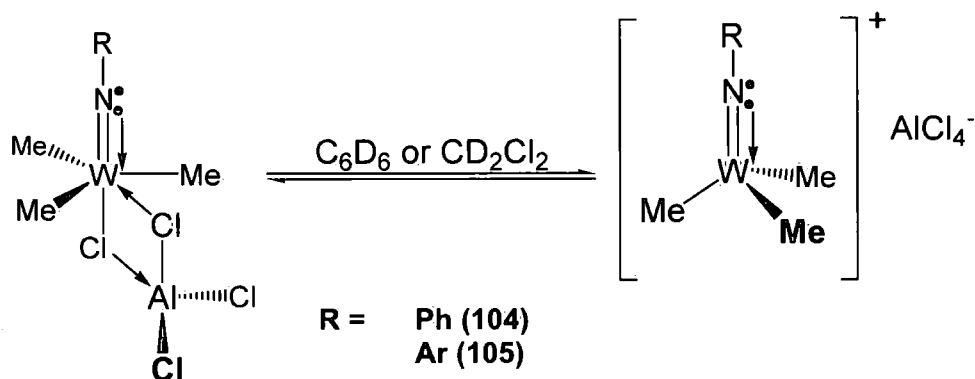


The change in the chemical shift of the W-CH_3 resonances, observed by ^1H NMR spectroscopy, following reaction of MeAlCl_2 with $\text{W}(\text{NR})(\text{Cl})\text{Me}_3$ ($\text{R} = \text{Ph}$ or Ar) (**Tables 4.2**), indicate that the ensuing AlCl_3 moiety binds to the $\text{W}(\text{NR})(\text{Cl})\text{Me}_3$ ($\text{R} = \text{Ar}$ or Ph) fragment. This conclusion is corroborated by the theoretical work of Tobisch, which showed that coordination of a $\text{Me}_x\text{AlCl}_{3-x}$ fragment to the tungsten chloride ligand of a related *mono(imido)* complex is highly favourable.³ The notion that AlCl_3 is coordinating to a $\text{W}(\text{NR})(\text{Cl})\text{Me}_3$ core has also been investigated here experimentally. It was found that addition of THF to a solution of $\text{W}(\text{NPh})(\text{Cl})\text{Me}_3 \cdot \text{AlCl}_3$ (**104**) resulted in the formation of free $\text{W}(\text{NPh})(\text{Cl})\text{Me}_3$ (**96**) and an unknown $(\text{AlCl}_3)_y(\text{THF})_x$ adduct. However, the set of ^1H NMR spectra obtained, before and after THF addition, clearly showed that displacement of the bound AlCl_3 fragment of **104** by THF resulted in a shift in the W-CH_3 resonance from 1.35 to 1.28 ppm (the ^1H NMR chemical shift associated with free **96**). This indicates that prior to THF addition, AlCl_3 was indeed interacting with a tungsten chloride ligand.

The formation of an AlCl_4^- anion upon reaction of **96** and **97** with MeAlCl_2 is also of significance. This is suggestive of an AlCl_3 fragment abstracting a W-Cl

chloride ligand to give a “non-coordinating” AlCl_4^- counter ion.^{viii} Notably the AlCl_4^- resonances detected upon analysis of **104** and **105** using ^{27}Al NMR were somewhat broader than the related signal presented by the ionic complex $[\text{AlCl}_4][\text{P}(\text{N}^i\text{Pr}_2)_2]$ (**107**) (Figure 4.8). Similarly the W-CH_3 resonances of **104** and **105** observed by ^1H NMR were broadened to the extent that no $^2J_{\text{WH}}$ satellites were observed in either case. One possible explanation for the broadening of both the ^{27}Al and ^1H NMR spectra is that an exchange process is occurring in solution between a 1:1 adduct and a charge separated salt. Notably, Osborn and co-workers determined that $\text{W}(\text{NMe})(\text{CH}_2^i\text{Bu})_3\text{Cl}$ (**90**) forms a 1:1 adduct with a range of Lewis acids, including AlCl_3 . As such, it is plausible that both $\text{W}(\text{NPh})(\text{Cl})\text{Me}_3$ (**96**) and $\text{W}(\text{NAr})(\text{Cl})\text{Me}_3$ (**97**) similarly form a 1:1 adduct with AlCl_3 in solution. The dissociation of these AlCl_3 adducts could then generate the observed AlCl_4^- anion *in situ* (Scheme 4.12).

Scheme 4.12 Proposed equilibrium between the limiting structures of the complexes $[\text{W}(\text{NR})(\text{Cl})\text{Me}_3.\text{AlCl}_3]$ ($\text{R} = \text{Ph}$ or Ar)



With a view to assessing whether complexes **104** and **105** were in fact labile, both **104** and **105** were analysed by ^1H and ^{27}Al NMR spectroscopy at -80°C (CD_2Cl_2). At -80°C the ^1H NMR spectra for both **104** and **105** were consistent with those obtained at ambient temperature (25°C), although a broadening of the W-CH_3 resonance was observed in both cases ($B_{1/2}^Y = \sim 25$ Hz). The ^{27}Al NMR spectra of both **104** and **105** at -80°C consisted of a single broad resonance centred at 95 ppm. As such, the low temperature ^{27}Al NMR spectra do not provide nor disprove the notion that either **104** or **105** dissociate in solution to give an AlCl_4^- counter ion.

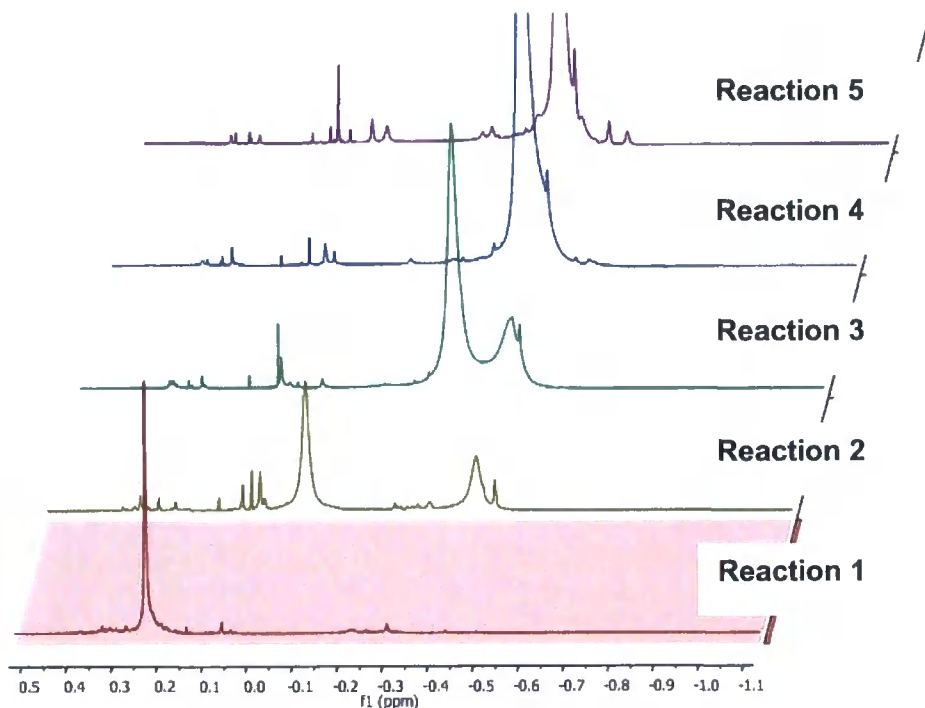
^{viii} The complete abstraction of the tungsten chloride ligand of $\text{W}(\text{NPh})\text{Me}_3\text{Cl}$ (**96**) by a strong Lewis acid has previously been shown to be viable as reaction of **96** with TMS-triflate generated $\text{W}(\text{NPh})\text{Me}_3(\text{OSO}_2(\text{CF}_3))$ (**100**) (see Section 4.3.1).

4.6 Investigating the Interaction Between MeAlCl₂ and W(NPh)(Cl)Me₃ (96) in

Solution

In Section 4.5 the adduct [W(NPh)(Cl)Me₃.AlCl₃] (**104**) was examined using ²⁷Al NMR (at ~25°C) spectroscopy. The presence of a broad AlCl₄⁻ resonance in the ensuing spectrum suggests that **104** partially dissociates in solution to give [W(NPh)Me₃][AlCl₄]. With the aim of gaining further insight into the interaction of *mono(imido)* complex and Me_xAlCl_{3-x} Lewis acids, W(NPh)(Cl)Me₃ (**96**) was reacted with varying numbers of equivalents of MeAlCl₂ in C₆D₆. This allowed direct observation of the reaction products using ¹H NMR spectroscopy (**Figure 4.9** and **Table 4.3**).

Figure 4.9 ^1H NMR (400 MHz, C_6D_6) spectra obtained from reaction of $\text{W}(\text{NPh})(\text{Cl})\text{Me}_3$ (**96**) with MeAlCl_2 (aromatic and tungsten-alkyl regions omitted).^a



a) All reactions were conducted using $\text{W}(\text{NPh})(\text{Cl})\text{Me}_3$ (**96**) (20mg, 0.056 mmol) and C_6D_6 (0.8mL).

Table 4.3 ^1H NMR (400 MHz, C_6D_6) Al- CH_3 resonances presented after reaction of $\text{W}(\text{NPh})(\text{Cl})\text{Me}_3$ (**96**) with MeAlCl_2 ^a

Reaction	Equivalents of MeAlCl_2	δ ^1H (ppm) Al- CH_3
1	1	0.23
2	2	-0.05 and -0.42
3	5	-0.30 and -0.43
4	10	-0.38
5	20	-0.39

a) A sample of MeAlCl_2 in C_6D_6 presented a single ^1H NMR resonance at 0.42 ppm

The established ^1H NMR resonance of the $\text{W}-\text{CH}_3$ moieties of $\text{W}(\text{NPh})(\text{Cl})\text{Me}_3$ (**96**) is 1.28 ppm in C_6D_6 . Addition of MeAlCl_2 to complex **96** in **Reactions 1-5** resulted in the formation of a single new ^1H NMR $\text{W}-\text{CH}_3$ resonance at 1.32 ppm, which was the only tungsten methyl signal presented by each reaction solution, even when excess MeAlCl_2 was utilized. In contrast, it is clear that that the chemical shifts of the Al- CH_3

^1H NMR resonances are highly dependent on the amount of MeAlCl_2 employed (**Table 4.3, Figure 4.9**). When one equivalent of MeAlCl_2 is utilized (**Reaction 1**) the resulting Al-CH_3 resonance at 0.23 ppm, is at considerably higher frequency than that measured for an authentic sample of MeAlCl_2 (-0.42 ppm, C_6D_6 , 400 MHz). This suggests that in this instance a MeAlCl_2 fragment closely associates to the W centre, most likely giving a 1:1 adduct of the formula $[\text{W}(\text{NPh})(\text{Cl})\text{Me}_3.\text{AlMeCl}_2]$ (**106**).^{ix}

In contrast, treatment of $\text{W}(\text{NPh})(\text{Cl})\text{Me}_3$ (**96**) with a slight excess of MeAlCl_2 (two equivalents) as in **Reaction 2**, gives two broad Al-CH_3 resonances by ^1H NMR at -0.05 and -0.42 ppm in a 1:1 ratio. This indicates that a slow exchange is occurring in solution between the MeAlCl_2 fragment of **106** and free non-associated MeAlCl_2 . A similar equilibrium is believed to be established in **Reaction 3** in which five equivalents of MeAlCl_2 are used, with two Al-CH_3 resonances again being detected by ^1H NMR. However, for **Reaction 3** the two signals are further broadened and are beginning to converge (**Figure 4.9**), possibly indicating a more rapid exchange between coordinated and non-coordinating MeAlCl_2 , resulting from the presence of MeAlCl_2 in higher concentrations. Indeed, the rate of this equilibrium is seemingly heightened further still when larger excesses of MeAlCl_2 are used. As a result, both reactions **4** and **5** present a single converged Al-CH_3 resonance with a chemical shift (-0.39 ppm) approaching that of free MeAlCl_2 (-0.42 ppm). Together all these observations are suggestive that a rapid exchange between free MeAlCl_2 and MeAlCl_2 groups bound to $\text{W}(\text{NPh})(\text{Cl})\text{Me}_3$ (**96**) occurs in solution.

4.6.1 Investigating the Interaction of $\text{W}(\text{NPh})(\text{Cl})\text{Me}_3$ (96**) with MeAlCl_2 at Low Concentrations**

In the previous sub-section **4.6.0** it was established that $\text{W}(\text{NPh})(\text{Cl})\text{Me}_3$ (**96**) reacts with MeAlCl_2 to give the 1:1 adduct $[\text{W}(\text{NPh})(\text{Cl})\text{Me}_3.\text{AlMeCl}_2]$ (**106**). Furthermore, rapid exchange occurs between the MeAlCl_2 fragment of **106** and any non-coordinated MeAlCl_2 present in solution. The rate of this exchange is clearly dictated by the concentration of MeAlCl_2 . As such, attention turned to investigating the

^{ix} ^1H NMR spectroscopic evidence is consistent with the formation of the adduct $\text{W}(\text{NPh})(\text{Cl})\text{Me}_3.\text{AlMeCl}_2$ (**106**) in reactions **1-5**. Evaporation of volatile components from **Reaction 3** gave a brown residue, which was analysed by ^1H NMR spectroscopy and was found to be the adduct $[\text{W}(\text{NPh})(\text{Cl})\text{Me}_3.\text{AlCl}_3]$ (**104**). This reinforces the hypothesis that **104** forms *via* **106** through exchange of aluminium groups, as illustrated in **Section 4.5, Scheme 4.11**.

interaction between complex **96** and MeAlCl_2 at relatively low concentrations, with the aim of establishing if interaction of **96** and MeAlCl_2 can occur in dilute solutions.

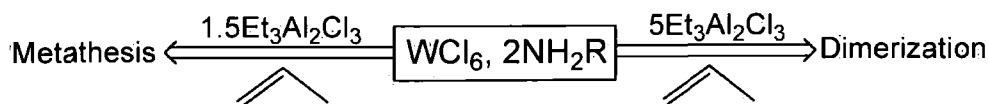
To this end, a C_6D_6 solution of $\text{W}(\text{NPh})(\text{Cl})\text{Me}_3$ (**96**) with a molarity of approximately 0.015 M was reacted with five equivalents of MeAlCl_2 and analysed using ^1H NMR spectroscopy. No interaction between **96** and MeAlCl_2 was found to occur. This contrasts with **Reaction 5** (see **Table 4.3, Section 4.6.0**) in which treatment of an approximately 0.75 M C_6D_6 solution of **96** with five equivalents of MeAlCl_2 gave the adduct $[\text{W}(\text{NPh})(\text{Cl})\text{Me}_3 \cdot \text{AlMeCl}_2]$ (**106**). Evidently, formation of the adduct **106** is disfavoured at low concentrations. Indeed, dilution of the solution from **Reaction 3**, from 0.75 M to 0.013 M, resulted in dissociation of the adduct $[\text{W}(\text{NPh})(\text{Cl})\text{Me}_3 \cdot \text{AlMeCl}_2]$ (**106**) to give free MeAlCl_2 and $\text{W}(\text{NPh})(\text{Cl})\text{Me}_3$ (**96**). This establishes that formation of the adduct **106** is a reversible process (**Scheme 4.13**).

Scheme 4.13 Reversible formation of $[\text{W}(\text{NPh})(\text{Cl})\text{Me}_3 \cdot \text{AlMeCl}_2]$ (**106**)



The tendency of the adduct $[\text{W}(\text{NPh})(\text{Cl})\text{Me}_3 \cdot \text{AlMeCl}_2]$ (**106**) to dissociate when diluted is important. This suggests that the capacity of $\text{R}_x\text{AlCl}_{3-x}$ co-initiators to bind to tungsten chloride ligands as Lewis acids can be affected by co-initiator or pre-catalyst concentration. In turn, this could rationalize the fact that the selectivity (alkene metathesis vs dimerization) of WCl_6 based initiators ($\text{WCl}_6, 2\text{NH}_2\text{R}$) is heavily dependent on the W:Al molar ratio as illustrated in **Scheme 4.14** (see **Chapter 2, Section 2.4**).¹⁸

Scheme 4.14 Alternative selectivity of WCl_6 -based initiator solutions



As it has now been established that the adduct $[\text{W}(\text{NPh})(\text{Cl})\text{Me}_3 \cdot \text{AlMeCl}_2]$ (**106**) undergoes facile dissociation in a dilute solutions, it can be proposed that at low $\text{Et}_3\text{Al}_2\text{Cl}_3$ concentrations coordination of aluminium-based Lewis acid fragments to tungsten chloride complexes will be unfavourable. In contrast, at high $\text{Et}_3\text{Al}_2\text{Cl}_3$ concentrations adduct formation *via* interaction of $\text{Et}_x\text{AlCl}_{3-x}$ Lewis acid fragments to

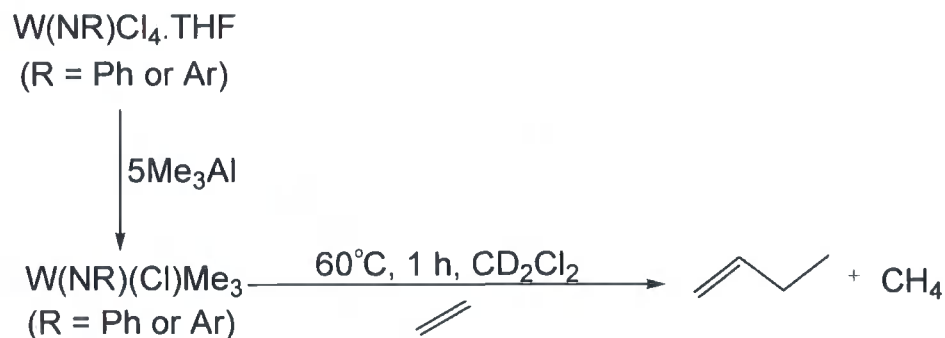
tungsten chloride ligands (in an interaction similar to that of **106**) is likely to be more feasible. Thus, it can be postulated that it is the favourability of adduct formation at high concentrations that may direct WCl_6 -based systems (WCl_6 , $2NH_2R$) to olefin dimerization.

4.7 Activation of *mono*(Imido) Tetrahalide pre-Catalysts Using Me_xAlCl_{3-x} co-Initiators

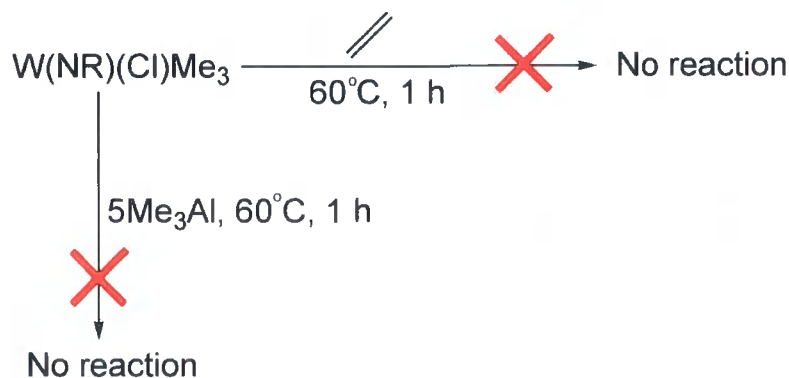
In this Chapter the reaction of discrete $W(NR)Cl_4 \cdot THF$ ($R = Ph, Ar$) complexes with methyl aluminium reagents has been examined. It has been shown that the *mono*(imido) ligands of both $W(NPh)(Cl)Me_3$ (**96**) and $W(NAr)(Cl)Me_3$ (**97**) do not readily coordinate to Lewis acids. In contrast, it has been demonstrated that Lewis acids will readily interact with the $W-Cl$ moieties of both **96** and **97**. Coordination of Me_xAlCl_{3-x} groups to complex **96** has been achieved *via* reaction of the strong Lewis acid $MeAlCl_2$, generating the adducts $[W(NPh)(Cl)Me_3 \cdot AlCl_3]$ (**104**) or $[W(NPh)(Cl)Me_3 \cdot AlMeCl_2]$ (**106**), depending on the reaction procedure. Furthermore, the detection of an $AlCl_4^-$ anion in the ^{27}Al NMR spectrum of **104**, suggests that the adduct partly dissociates in solution to potentially give $[W(NPh)Me_3][AlCl_4]$. It has also been established *via* an examination of **106** at various concentrations that adduct formation is a reversible process. Hence, the interaction of *mono*(imido) complexes and Me_xAlCl_{3-x} Lewis acids in solution is now well understood. As such, attention turned to investigating the capacity of Me_3Al , Me_2AlCl and $MeAlCl_2$ to activate *mono*(imido) pre-catalysts for ethylene dimerization.

4.8 Activation of *mono*(Imido) Tetrahalide pre-Catalysts with Me_3Al

Treatment of a CD_2Cl_2 solution of $W(NPh)Cl_4 \cdot THF$ (**32**) with Me_3Al (five equivalents) generated complex $W(NPh)(Cl)Me_3$ (**96**) *in situ* with 100% conversion (by NMR). Subsequently, this solution was placed under an atmosphere of ethylene (ten equivalents) and was then heated ($60^\circ C$, 1 h). This resulted in full conversion of ethylene to but-1-ene (as verified by 1H NMR spectroscopy and GC) (**Scheme 4.15**). Similarly, an ethylene dimerization system can be formed *via* reaction of $W(NAr)Cl_4 \cdot THF$ (**38**) using comparable conditions. Addition of Me_3Al to **38** in CD_2Cl_2 resulted in the formation of $W(NAr)(Cl)Me_3$ (**47**) *in situ*. When the reaction solution was placed under an atmosphere of ethylene, but-1-ene was again formed after the mixture was heated ($60^\circ C$, 1 h). Notably, both systems produced the by-product methane (which presented a singlet at δ 0.3 ppm), which was obtained in a 1:1 ratio with but-1-ene in both cases.

Scheme 4.15 Activation of $W(NR)Cl_4 \cdot THF$ by Me_3Al 

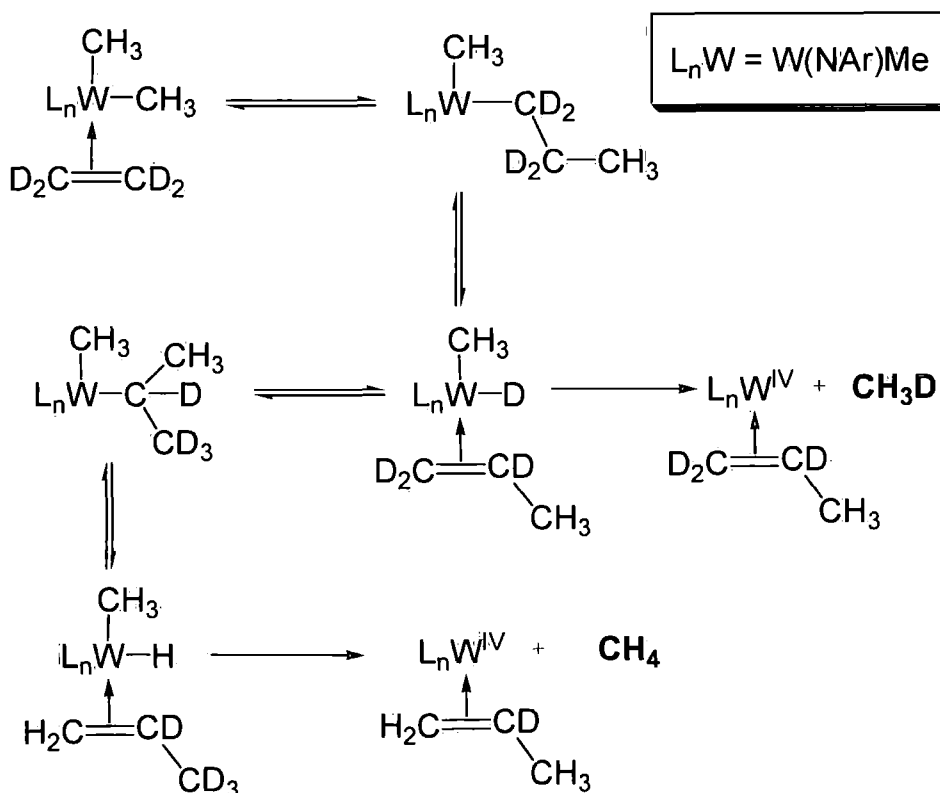
To determine the role of each component in the $W(NPh)Cl_4 \cdot THF/Me_3Al$ ethylene dimerization system a series of control reactions was undertaken. To this end, a CD_2Cl_2 solution of Me_3Al was heated ($60^\circ C$, 1 h) in the presence of ethylene (ten equivalents). No reaction occurred and no methane was observed to evolve (according to 1H NMR spectroscopy). This shows that the methane observed in the initiator systems outlined in **Scheme 4.15** is not due to any inadvertent hydrolysis of Me_3Al . Furthermore, heating a solution of $W(NPh)(Cl)Me_3$ (**96**) in the presence of either ethylene or Me_3Al alone did not induce any reaction (**Scheme 4.16**). Consequently, as no ethylene dimerization occurred in the absence of Me_3Al , it is clear that for the $W(NR)Cl_4 \cdot THF/Me_3Al$ dimerization system the presence of all three components are required for the conversion of ethylene to higher olefins.

Scheme 4.16 Treatment of $W(NPh)(Cl)Me_3$ (**96**) with Me_3Al and ethylene

4.8.1 Examining the Route of Methane Formation in the $W(NR)Cl_4 \cdot THF/Me_3Al$ Dimerization Systems

It has been established that the $W(NR)Cl_4 \cdot THF/Me_3Al$ ($R = Ph, Ar$) ethylene dimerization systems produce methane upon initiator formation. To simultaneously assess the mode by which methane and the active initiator complex are formed, a $W(NAr)Cl_4 \cdot THF/Me_3Al$ reaction solution was used to dimerize C_2D_4 (ten equivalents) in CD_2Cl_2 . Analysis of the resulting reaction mixture using 1H NMR spectroscopy both before and after dimerization had taken place, did not identify the active initiator complex. Instead broad alkyl resonances were detected, which were unassignable using 1H and ^{13}C NMR spectroscopy. Of note, is that dimerization of C_2D_4 produced both CH_4 and CH_3D , the later presenting a resonance at 0.21 ppm by 1H NMR spectroscopy (CD_2Cl_2 , 500 MHz, $^2J_{HD} = 1.5$ Hz). Together, these observations indicate that methane formation must occur *via* β -hydride elimination with transfer of a deuterium atom from a C_2D_4 molecule giving a W-D intermediate, which can then undergo reductive elimination (**Scheme 4.17**).

Scheme 4.17 Rationalizing the formation of both CH_4 and CH_3D upon dimerization of C_2D_4 by a $W(NAr)Cl_4 \cdot THF/Me_3Al$ initiator solution.



The reaction pathways outlined in **Scheme 4.17** are supported by GC-MS analysis of the volatile components obtained from the $W(NAr)Cl_4 \cdot THF/Me_3Al/C_2D_4$ reaction solution. These analyses determined that trace C_5D_{10} is produced by this system, indicating that the propylene moiety formed *via* reductive elimination of CH_4 , couples with a molecule of C_2D_4 to give C_5 products. It is conceivable that olefin dimerization by the $W(NAr)Cl_4 \cdot THF/Me_3Al$ system is induced by either W^{VI} or $W-H$ intermediates (**Scheme 4.17**) *via* an oxidative coupling or hydride cycle, respectively. A similar activation pathway to that outlined in **Scheme 4.17** is believed to be occurring in the $W(NAr)_2Me_2 \cdot THF/C_2H_4$ dimerization system outlined in **Chapter 3, Section 3.9.1**, from which methane is also observed to evolve.

4.8.2 Contrasting the Abilities of the Lewis Acids $MeAlCl_2$, Me_2AlCl , Me_3Al to co-Initiate Ethylene Dimerization

In **Section 4.8.1** an ethylene dimerization initiator solution was formed *via* reaction of $W(NPh)Cl_4 \cdot THF$ (**32**) with Me_3Al . However, it has been established that reaction of **32** with Me_3Al in the absence of olefins gives $W(NPh)(Cl)Me_3$ (**96**) as the only tungsten-containing reaction product. With both of these observations in mind, attention turned to investigating the capacity of a discrete sample of **96** to initiate ethylene dimerization when treated with Me_3Al , Me_2AlCl and $MeAlCl_2$. All of the reactions were conducted using comparable conditions, with the aim of establishing the different capacities of the Me_xAlCl_{3-x} reagents to co-initiate ethylene dimerization. It was found that Me_3Al , Me_2AlCl and $MeAlCl_2$ can all indeed activate $W(NPh)(Cl)Me_3$ (**96**) for ethylene dimerization (**Table 4.4**).

Table 4.4 Activation of $W(NPh)(Cl)Me_3$ (**96**) by various Me_xAlCl_{3-x} reagents

Co-initiator (four equivalents)	Olefin observed (1H NMR spectroscopy)	Conditions (nine equivalents of C_2H_4)
$MeAlCl_2$	But-1-ene	C_6D_6 , $25^\circ C$
Me_2AlCl	But-1-ene	C_6D_6 , $25^\circ C$
Me_3Al	No reaction of ethylene	C_6D_6 , $25^\circ C$
Me_3Al	But-1-ene	CD_2Cl_2 , ($60^\circ C$, 1 h)

Evidently the Lewis acid strength of the Me_xAlCl_{3-x} co-initiator can influence the reactivity of a given dimerization system. For instance, when $MeAlCl_2$ or Me_2AlCl are

used to activate $W(NPh)(Cl)Me_3$ (**96**) ethylene dimerization can be achieved in a non-polar solvent (e.g. C_6D_6) and without the requirement of heating. In contrast, when the weaker Lewis acid Me_3Al is used, ethylene dimerization only occurs at elevated temperatures (ca. $60^\circ C$). Furthermore, it has been found that Me_3Al can only activate **96** in polar solvents (such as CD_2Cl_2) with no dimerization being observed when C_6D_6 is utilized.^x As ethylene dimerization is co-initiated by both $MeAlCl_2$ and Me_2AlCl in C_6D_6 , this indicates that the inability of Me_3Al to co-initiate dimerization in C_6D_6 is not due to the insolubility of an initiator complex in C_6D_6 .

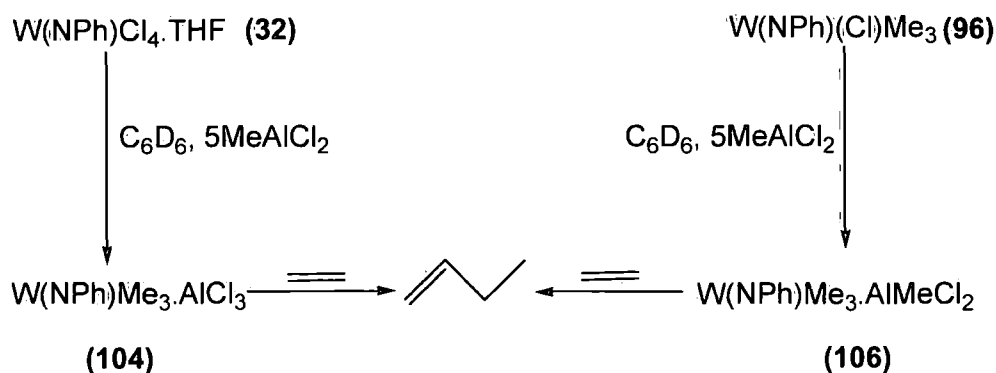
Before addition of ethylene to the $MeAlCl_2/W(NPh)(Cl)Me_3$ initiator solution, the mixture was analyzed using 1H NMR spectroscopy. This confirmed the formation of the adduct $[W(NPh)(Cl)Me_3 \cdot AlMeCl_2]$ (**106**), which was identified using 1H NMR spectroscopy (as in **Section 4.6**). Indeed, 1H NMR analysis showed that in the $W(NPh)(Cl)Me_3/MeAlCl_2$ system, **96** was fully converted to **106** before addition of ethylene. As such it can be concluded that in this $MeAlCl_2$ -based ethylene dimerization system, the active initiator complex is formed *via* modification of **106**.

4.8.3 Evaluating the Role of Adduct Formation in Me_xAlCl_{3-x} co-Initiated Dimerization Systems

In the $W(NPh)(Cl)Me_3/MeAlCl_2$ ethylene dimerization system, the adduct $[W(NPh)(Cl)Me_3 \cdot AlMeCl_2]$ (**106**) has been observed to form *in situ*. The co-initiator $MeAlCl_2$ has also been found to activate $W(NPh)Cl_4 \cdot THF$ (**32**) for ethylene dimerization (**Scheme 4.18**). Notably, reaction of $MeAlCl_2$ and **32** in C_6D_6 in the absence of ethylene is found to generate the adduct $[W(NPh)(Cl)Me_3 \cdot AlCl_3]$ (**104**) (verified by 1H NMR spectroscopy). This tendency of adducts such as **106** or **104** to form upon reaction of $MeAlCl_2$ with *mono(imido)* tungsten chloride complexes, indicates that adduct formation is crucial to the generation of the active initiator complex in the Me_xAlCl_{3-x} co-initiated ethylene dimerization systems.

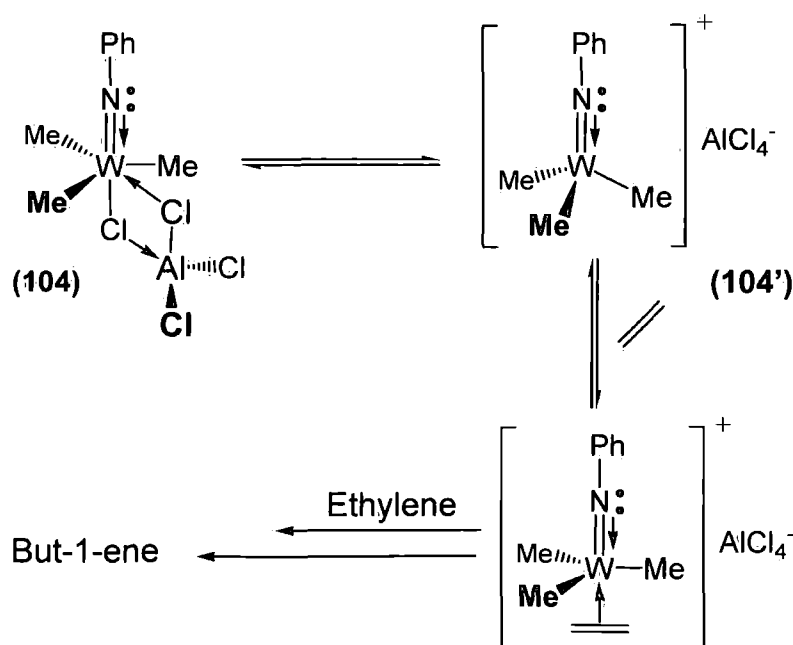
^x Heating a CD_2Cl_2 solution of Me_3Al did not result in any reaction. This indicates that in the Me_3Al dimerization system, the active initiator complex is not formed *via* reaction of Me_3Al with CD_2Cl_2 .

Scheme 4.18 Ethylene dimerization systems based on the activation of mono(imido) complexes by MeAlCl_2



In **Section 4.5** it was shown that a Lewis base (THF) can displace the coordinating AlCl_3 moiety of **104**. This suggests that ethylene as a Lewis base could displace the $\text{Me}_x\text{AlCl}_{3-x}$ fragment of $[\text{W}(\text{NPh})(\text{Cl})\text{Me}_3\cdot\text{AlCl}_3]$ (**104**) or $[\text{W}(\text{NPh})(\text{Cl})\text{Me}_3\cdot\text{AlMeCl}_2]$ (**106**). However, such a reaction is unlikely to generate an initiator complex, as removal of the MeAlCl_2 or AlCl_3 groups of **104** and **106** would generate the inactive complex **96**. Instead, it is highly probable that the ethylene dimerization observed in the $\text{MeAlCl}_2/\text{W}(\text{NPh})\text{Cl}_4\cdot\text{THF}$ (**32**) system is initiated upon coordination of ethylene to the tungsten core of $[\text{W}(\text{NPh})(\text{Cl})\text{Me}_3\cdot\text{AlCl}_3]$ (**104**) via the pathway outlined in **Scheme 4.19**.

Scheme 4.19 Proposed route by which ethylene coordinates to **104**



The computational investigation carried out by Tobisch indicates that ethylene coordination to **104** can occur when the AlCl_3 fragment is closely bound to the tungsten core as a coordinating Lewis acid.³ However, association of ethylene to the dissociated form of **104**, $[\text{W}(\text{NPh})\text{Me}_3][\text{AlCl}_4]$, as outlined in **Scheme 4.19** is arguably more viable. This is because introduction of ethylene into the coordination sphere of a $[\text{W}(\text{NPh})\text{Me}_3]^+$ fragment will be more favourable since there will be no steric constraints imposed by the bound Lewis acid fragment. Furthermore, coordination of a strong σ -donor (ethylene) to a positively charged tungsten centre (stabilized by an AlCl_4^- anion) will also be highly favourable electronically and electrostatically. Thus, it is hereby proposed that initiator formation in the $\text{W}(\text{NPh})(\text{Cl})\text{Me}_3/\text{Me}_x\text{AlCl}_{3-x}$ dimerization systems outlined in **4.9.3** occurs *via* the intermediate $[\text{W}(\text{NPh})\text{Me}_3(\eta^2\text{-C}_2\text{H}_4)][\text{Me}_x\text{AlCl}_{4-x}]$ (**Scheme 4.19**). This sequence can be used to rationalize the observation that Me_3Al can only activate $\text{W}(\text{NPh})(\text{Cl})\text{Me}_3$ (**96**) in polar solvents such as CD_2Cl_2 .

As Me_3Al is a weaker Lewis acid (relative to MeAlCl_2), it is reasonable to postulate that Me_3Al will be less able to abstract the chloride atom of **96** to give the corresponding ionic complex $[\text{W}(\text{NPh})\text{Me}_3][\text{Me}_3\text{AlCl}]$ (**108**).¹⁹ Indeed, formation of the adduct **108** *via* reaction of Me_3Al would be hampered further still by a non-polar environment such that of C_6D_6 . If indeed **108** was the precursor to the active initiator complex, then this would explain why Me_3Al cannot co-initiate ethylene dimerization in C_6D_6 . Conversely, the ionic intermediate **108** would feasibly be stabilized by a polar solvation environment such as that of CD_2Cl_2 . Thus, the use of CD_2Cl_2 would feasibly allow for greater conversion of **96** to **108**, which could explain why using CD_2Cl_2 is essential for the Me_3Al co-initiated dimerization systems identified in this study.

4.9 Summary and Conclusions

In this Chapter the association of $\text{Me}_x\text{AlCl}_{3-x}$ Lewis acids to *mono(imido)* systems has been investigated. This was undertaken with a view to clarifying the effect of aluminium coordination on the reactivity of *mono(imido)* systems with ethylene. Generation of $\text{W}(\text{NPh})(\text{Cl})\text{Me}_3$ (**96**) by treatment of $\text{W}(\text{NPh})\text{Cl}_4\cdot\text{THF}$ with Me_3Al has shown that coordination of $\text{Me}_x\text{AlCl}_{3-x}$ groups to *mono(imido)* ligands is not favourable. In contrast, it has been found that $\text{Me}_x\text{AlCl}_{3-x}$ fragments will readily coordinate to tungsten chloride ligands to give adducts such as $[\text{W}(\text{NPh})(\text{Cl})\text{Me}_3\cdot\text{AlCl}_3]$ (**104**) or $[\text{W}(\text{NPh})(\text{Cl})\text{Me}_3\cdot\text{AlMeCl}_2]$ (**106**). Indeed, adduct formation has been shown to be crucial in the activation of *mono(imido)* systems. Furthermore, the adduct **104** has been observed to dissociate in solution giving an

AlCl_4^- cation (identified by ^{27}Al NMR spectroscopy). Consequently, it is proposed that for $\text{Me}_x\text{AlCl}_{3-x}$ co-initiated systems, active initiator complexes are formed via $[\text{W}(\text{NPh})\text{Me}_3(\eta^2\text{-C}_2\text{H}_4)][\text{Me}_x\text{AlCl}_{4-x}]$ intermediates as illustrated in **Scheme 4.19**.

4.10 References

- ¹ J.P. Le Ny, J.A. Osborn, *Organometallics*, **1991**, *10*, 1546.
- ² M.T. Youinou, J. Kress, J. Fischer, A. Agüero and J.A. Osborn, *J. Am. Chem. Soc.*, **1988**, *110*, 1488.
- ³ S. Tobisch, *Organometallics*, **2007**, *26*, 6529.
- ⁴ H. Olivier and P. Laurent-Gérot, *J. Mol. Cat A.*, **1999**, *148*, 43.
- ⁵ G. Kong, G.N. Harakas and B.R. Whittlesey, *J. Am. Chem. Soc.*, **1995**, *117*, 3502.
- ⁶ i) J.W. Faller and Y. Ma, *Organometallics*, **1989**, *8*, 609; ii) J.W. Faller and Y. Ma, *Organometallics*, **1988**, *7*, 559; iii) J.W. Faller and Y. Ma, *J. Organomet. Chem.*, **1989**, *368*, 45; iv) J.W. Faller, R.R. Kucharczyk and Y. Ma, *Inorg. Chem.*, **1990**, *29*, 1662
- ⁷ S.F. Pedersen and R.R. Schrock, *J. Am. Chem. Soc.*, **1982**, *104*, 7483.
- ⁸ R.R. Schrock, R.T. DePue, J. Feldman, K.B. Yap, D.C. Yang, W.M. Davis, L. Park, M. DiMare, M. Schofield, J. Anhaus, E. Walborsky, E. Evitt, C. Krüger and P. Betz, *Organometallics*, **1990**, *9*, 2262.
- ⁹ D.C. Bradley, R.J. Errington, M.B. Hursthouse, R.L. Short, B.R. Ashcroft, G.R. Clark, A.J. Nielson and C.E.F. Rickard, *J. Chem. Soc. Dalton Trans.*, **1987**, 2067.
- ¹⁰ M.L.H. Green, *J. Organometallic Chem.*, **1995**, *500*, 127.
- ¹¹ Y.S. Won, Y.S. Kim, T.J. Anderson, L.L. Reitfort, I. Ghiviriga and L. McElwee-White, *J. Am. Chem. Soc.*, **2006**, *128*, 13781.
- ¹² T. Hayashida, H. Kondo, J. Terasawa, K. Kirchner, Y. Sunada, H. Nagashima, *J. Organomet. Chem.*, **2007**, *692*, 382.
- ¹³ i) G.A. Lawrance, *Chem. Rev.*, **1986**, *86*, 17; ii) W. Beck, K. Sünkel, *Chem. Rev.*, **1988**, *88*, 1405; iii) S.H. Strauss, *Chem. Rev.*, **1993**, *93*, 927.
- ¹⁴ W.E. Piers, *Adv. Organomet. Chem.*, **2005**, *52*, 11.
- ¹⁵ i) R. Benn, E. Janssen, H. Lekomühl and A. Rifińska, *J. Organomet. Chem.*, **1987**, *333*, 169; ii) R. Benn, E. Janssen, H. Lekomühl and A. Rifińska, *J. Organomet. Chem.*, **1987**, *333*, 181; iii) R. Benn, E. Janssen, H. Lekomühl and A. Rifińska, *J. Organomet. Chem.*, **1987**, *333*, 155.

-
- ¹⁶ A.H. Cowley, M.C. Cushner and J.S. Szobota, *J. Am. Chem. Soc.*, **1978**, *100*, 7784.
- ¹⁷ Z. Černý, J. Macháček, J. Fúsek, B. Čásenský, O. Kříž and D.G. Tuck, *Inorg. Chim. Acta*, **2000**, 300-302, 556.
- ¹⁸ H.R. Menapace, N.A. Maly, J.L. Wang and L.G. Wideman, *J. Org. Chem.*, **1975**, *40*, 2983.
- ¹⁹ R.F. Childs, D.L. Mulholland and A. Nixon, *Can. J. Chem.*, **1982**, *60*, 801.

Chapter 5: Experimental

5.0 Introduction

All operations were conducted under an atmosphere of dry nitrogen using standard Schlenk and cannula techniques, or in a nitrogen-filled glove box, unless stated otherwise. NMR-scale reactions were conducted using NMR tubes fitted with Young's tap valves. Bulk solvents were purified using an Innovative Technologies SPS facility and degassed prior to use. NMR solvents (C_6D_6 , C_6D_5Cl , CD_3CN and $CDCl_3$) were dried over P_2O_5 , distilled and degassed before use. DME was distilled under nitrogen from sodium/benzophenone. When appropriate, liquid reagents were dried, distilled and deoxygenated. Nitrogen gas was passed through a drying column (silica/ $CaCO_3/P_2O_5$) and ethylene was dried using a column of activated alumina.

The known complexes and compounds $Mo(NR)_2Cl_2 \cdot DME$ ($R = ^iBu$ (**26**), Ar (**23**)),¹ $Mo(NAr)_2(CH_2C(Me)_3)_2$ (**82**),² $Mo(NAr)(N^iBu)Cl_2 \cdot DME$ (**11**),³ $Mo(NAr)_2Me_2$ (**27**),⁴ $W(NR)Cl_4 \cdot THF$ ($R = Ph$ (**32**), Ar (**38**)),⁵ $W(NAr)Cl_4$ (**62**),⁶ $W(NPh)(Cl)_2(PMe_3)_3$ (**34**)⁷, $Ta(NAr)Cl_3(TMEDA)$ (**59**),⁸ and $[AlCl_4][P(N^iPr_2)_2]$ (**107**)⁹ were prepared using standard literature procedures. Aluminium reagents were purchased from Albermarle R and D centre and Aldrich either neat (Me_3Al , $EtAlCl_2$ and $Et_3Al_2Cl_3$) or as solutions in hexane (Me_2AlCl , $MeAlCl_2$, MAO and $EtAlCl_2$). Neat $MeAlCl_2$, Me_2AlCl and MAO were obtained by evaporation of hexane from the appropriate commercial solution. Similarly, neat samples of $EtMgCl$, $MeMgCl$ and $LiMe$ were obtained by the drying the commercially available solutions *in vacuo*. All other chemicals were obtained commercially and used as received.

Mass spectra (ES) were obtained using a Micromass Autospec instrument. GC analysis was performed on an Agilent Technologies 6890N GC system equipped with PONA (50m \times 0.020mm \times 0.50 μ m) and MDN12 (60m \times 0.025mm \times 0.25 μ m) columns. GC-MS analysis was performed on an Agilent Technologies 6890N GC system equipped with a MDN12 (60m \times 0.025mm \times 0.25 μ m) column, coupled to an Agilent Technologies 5973N MSD Mass Spectrometric instrument. Elemental analyses were performed by the Analytical Services Department of the Chemistry Department, Durham University. Full crystallographic experimental details are presented in Appendix 1.

Routine NMR spectra were collected on a Varian Unity 300 or 200, a Varian Mercury 400, Avance 400 MHz Bruker, Varian Inova 500, or a Varian 700 MHz spectrometers. Chemical shifts were referenced to residual protio impurities in the deuterated solvent (1H) or the ^{13}C shift of the solvent (^{13}C). Solvent proton shifts (ppm): $CDCl_3$, 7.26; C_6D_6 , 7.15; CD_2Cl_2 , 5.34; C_6D_5Cl , 7.13, 6.98, 6.95. Solvent carbon shifts (ppm): $CDCl_3$, 77.2; C_6D_6 , 128.3; CD_2Cl_2 , 54.0. ^{31}P NMR chemical

shifts were referenced against an external standard of 85% phosphoric acid, while ^{27}Al NMR chemical shifts were referenced against a saturated aqueous solution of aluminium nitrate. ^{13}C NMR spectra were assigned with the aid of DEPT 135 and gHMQC $^1\text{H}/^{13}\text{C}$ correlation experiments. Chemical shifts are reported in ppm and coupling constants in Hz unless otherwise stated.

5.1 General Procedure for the Testing of Ethylene Dimerization Systems Based on the Reaction of Imido Complexes

A stainless steel autoclave (250 mL) was charged with $\text{C}_6\text{H}_5\text{Cl}$ (78 mL) and the required pre-catalyst (20 μmol). The vessel was then heated (60°C), pressurized with ethylene (5 bars), and stirred (1800 rpm). Next, the autoclave was vented, which enabled addition of the desired co-initiator, EtAlCl_2 (300 μmol) or $\text{B}(\text{C}_6\text{F}_5)_3$ (80 μmol). After co-initiator addition, the vessel was pressurized with ethylene (40 bars). A constant pressure of 40 bars was maintained throughout the reaction period, with a gas-flow meter providing a measure of ethylene consumption. After gas uptake was observed to decrease, the autoclave was isolated from the ethylene supply, and was then cooled (-5°C) and slowly vented. Addition of an external standard, nonane (1 mL, 5.60 mmols), to the spent initiator solutions allowed for the calculation of a given initiator's activity and selectivity using GC analysis.

5.2 Synthesis of $\text{W}(\text{NAr})_2\text{Cl}_2\cdot\text{DME}$ (40**)**

In work conducted for this thesis, the complex $\text{W}(\text{NAr})_2\text{Cl}_2\cdot\text{DME}$ (**40**) was prepared using a slight modification of the procedure developed by Schrock *et al.* Initially, WO_2Cl_2 (3.00 g, 0.010 mols) was suspended in DME (5 mL). To this suspension was added sequentially ClSiMe_3 (15.82 mL, 0.124 mols) followed by 2,6-lutidine (7.51 mL, 0.064 mols) and then H_2NAr (4.14 mL, 0.022 mols). This mixture was heated (60°C , 24 h), which generated a bright red solution that was filtered and allowed to stand for 20 minutes. During this time dark red single crystals of **40** precipitated from solution and were then collected *via* filtration; yield 2.10 g, 28 %. The ^1H and ^{13}C NMR chemical shifts, displayed by a sample of **40** prepared by this methodology, were found to be consistent with the values previously reported by Schrock *et al.*

^1H NMR (CDCl_3 , 200 MHz): δ 7.09 (4H, d, H_{meta} , $^3J_{\text{HH}} = 6.8$ Hz), 6.89 (2H, t, $^3J_{\text{HH}} = 6.8$ Hz), 3.96 (6H, broad, CH_3OCH_2), 3.86 (12H, broad, CH_3OCH_2 and CH_3CH), 1.06 (24H, d, CH_3CH , $^3J_{\text{HH}} = 6.8$ Hz).

^{13}C $\{^1\text{H}\}$ NMR (CDCl_3 , 125.6 MHz): δ 150.1 (C_{ipso}), 144.6 (C_{ortho}), 125.5 (C_{meta}), 122.2 (C_{para}), 71.5 (CH_3OCH_2), 63.6 (CH_3OCH_2), 27.2 (CH_3CH), 24.6 (CH_3CH).

5.3 Synthesis of $\text{Mo}(\text{NAr})_2(\text{NH}^t\text{Bu})_2$ (55)

$\text{Mo}(\text{NAr})_2\text{Cl}_2\cdot\text{DME}$ (**23**) (2.0 g, 3.38 mmols) was dissolved in Et_2O (30 mL) and the solution was cooled to -78°C . A separate solution was formed *via* the dissolution of LiNH^tBu (0.52 g, 6.57 mmols) also in Et_2O (100 mL). The two solutions were combined slowly at -78°C . The resulting mixture was then allowed to warm to room temperature, before being stirred for an additional 4 h period. The reaction solution was then dried *in vacuo*, enabling $\text{Mo}(\text{NAr})_2(\text{NH}^t\text{Bu})_2$ (**55**) to be extracted from LiCl using hexane (3×30 mL). Concentration of the hexane solution and recrystallization (-35°C) gave orange cube-shaped crystals of sufficient quality for solid state analysis; Yield 0.36g (20%).

^1H NMR (CDCl_3 , 200 MHz): δ 6.96 (6H, broad, H_{meta} and H_{para}), 6.29 (2H, broad, NH), 3.57 (4H, septet, CH_3CHCH_3 , $^3J_{\text{HH}} = 6.8$ Hz), 1.29 (18H, s, CCH_3), 1.11 (24H, d, CH_3CH , $^3J_{\text{HH}} = 6.8$ Hz).

^{13}C $\{^1\text{H}\}$ NMR (CDCl_3 , 125.6 MHz): δ 153.5 (C_{ipso}), 140.5 (C_{ortho}), 123.3 (C_{meta}), 122.1 (C_{para}), 55.2 (CCH_3), 33.1 (CCH_3), 28.3 (CH_2CH_3), 23.1 (CH_2CH_3).

Anal. Calcd for $\text{C}_{35}\text{H}_{54}\text{MoN}_4$: C; 65.06, H; 9.21, N; 9.48, found C; 65.00, H; 9.34 and N; 9.58.

Mass Spectrometry (ES): $m/z = 592.2$.

5.4 Reaction of $\text{Mo}(\text{NAr})_2(\text{NH}^t\text{Bu})_2$ (55) with Me_3Al

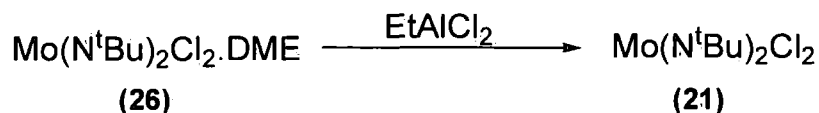
$\text{Mo}(\text{NAr})_2(\text{NH}^t\text{Bu})_2$ (**55**) (50 mg, 0.08 mmols) was dissolved in C_6D_6 (0.8 mL). To this solution was added Me_3Al (12.0 mg, 0.16 mmols). The reaction mixture was then analysed using ^1H NMR spectroscopy. This revealed resonances assignable to the known complex $\text{Mo}(\text{NAr})_2\text{Me}_2$ (**27**).

5.5 Reaction of $\text{W}(\text{NPh})(\text{Cl})_2(\text{PMe}_3)_3$ (34) with Me_3Al

$\text{W}(\text{NPh})(\text{Cl})_2(\text{PMe}_3)_3$ (**34**) (20 mg, 0.03 mmols) was dissolved in C_6D_6 (0.8 mL). To this solution was added Me_3Al (15 mg, 0.20 mmols) and the reaction mixture was analysed using ^{31}P NMR spectroscopy. The established ^{31}P NMR shifts of **34** were not detected. Instead, a broad resonance at -21.16 ppm and two sharper signals at

-29.8 and -33.5 ppm were obtained. Ethylene (0.17 mmols) was added to the reaction mixture. No consumption of ethylene was observed to occur, even after heating the reaction solution (1 h, 60°C).

5.6 Reaction of Mo(N^tBu)₂Cl₂.DME (26) with One Equivalent of EtAlCl₂

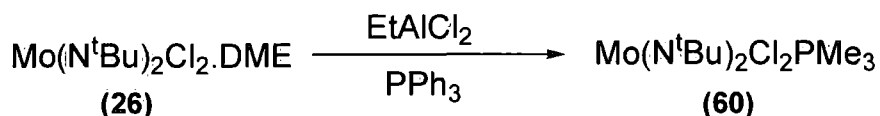


Mo(N^tBu)₂Cl₂.DME (1.0 g, 2.30 mmols) was dissolved in toluene (20 mL) and to this solution was added EtAlCl₂ (1.3 mL, 1.8 M in toluene, 2.30 mmols). The reaction solution was then dried *in vacuo* generating a dark red solid, which was extracted with hexane (3 × 30 mL). The hexane washings were collected, concentrated *in vacuo* and then cooled (-30°C). This induced the precipitation of a light red solid, which was collected *via* filtration. The ¹H and ¹³C NMR spectroscopic data presented by this material are consistent with previously reported data for the known complex Mo(N^tBu)₂Cl₂ (21).¹⁰ Yield; 0.46 g (65%).

¹H (C₆D₆, 400 MHz): δ 1.28 (s, CCH₃).

¹³C {¹H} (C₆D₆, 125.5 MHz): δ 30.06 (CCH₃) and 74.11 (CCH₃).

5.7 Synthesis of Mo(N^tBu)₂Cl₂PPh₃ (60)



Mo(N^tBu)₂Cl₂.DME (1.0 g, 2.3 mmols) was dissolved in toluene (20 mL). The solution was cooled to -78°C before addition of a solution of EtAlCl₂ (1.3 mL, 1.8 M in toluene, 2.3 mmols). Next, PPh₃ (0.8 g, 3.05 mmols) was added to the reaction mixture, also as a solution in toluene (20 mL). The reaction mixture was then allowed to warm to room temperature, and on warming, a light yellow solid precipitated from solution. This material was collected *via* filtration and recrystallized from acetonitrile (-35°C); yield 0.4 g (28%).

¹H (CDCl₃, 200 MHz): δ 7.89 (15H, b, P(C₆H₅)₃), 1.26 (18H, s, CCH₃).

^{13}C $\{^1\text{H}\}$ (CDCl_3 , 125.6 MHz): δ 134.8 (C_{ortho}), 131.3 (C_{meta}), 129.0 (C_{para}), 74.6 (CCH_3), 30.3 (CCH_3). The C_{ipso} resonance was not detected.

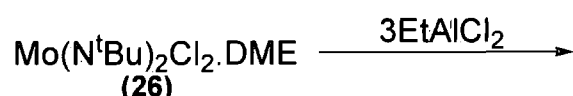
^{31}P $\{^1\text{H}\}$ (CDCl_3 , 81 MHz): δ 33.8.

Anal. Calcd for $\text{C}_{26}\text{H}_{33}\text{Cl}_2\text{MoN}_2\text{P}$: C; 54.65, H; 5.82, N; 4.90. Found: C; 54.52, H; 5.74, N; 4.80%.

5.8 Reaction of $\text{Mo}(\text{N}^t\text{Bu})_2\text{Cl}_2\cdot\text{DME}$ (**26**) with PPh_3

$\text{Mo}(\text{N}^t\text{Bu})_2\text{Cl}_2\cdot\text{DME}$ (**26**) (30 mg, 0.07 mmols) was dissolved in CDCl_3 (0.8 mL) and to this solution was added PPh_3 (20 mg, 0.07 mmols). The mixture was then analysed using ^1H NMR spectroscopy. After a 2 h period the ^tBu ^1H NMR resonance of $\text{Mo}(\text{N}^t\text{Bu})_2\text{Cl}_2\cdot\text{PPh}_3$ (**60**) was observed at 1.26 ppm (see Section 5.8). Furthermore, the known ^tBu resonance of the starting complex **26** was also detected at 1.48 ppm.¹¹ Integration of the ^1H NMR spectra showed that 60% of complex **26** had converted to **60**.

5.9 Reaction of $\text{Mo}(\text{N}^t\text{Bu})_2\text{Cl}_2$ (**26**) and Excess EtAlCl_2



$\text{Mo}(\text{N}^t\text{Bu})_2\text{Cl}_2\cdot\text{DME}$ (**26**) (1.0 g, 2.40 mmols) was dissolved in toluene (20 mL) before addition of a solution of EtAlCl_2 (3.9 mL, 1.8 M in toluene, 7.02 mmols). The reaction mixture was then dried *in vacuo* producing a dark red oil, which was analysed using ^1H and ^{13}C NMR spectroscopy. This revealed that reaction of **26** and EtAlCl_2 gave multiple products, unassignable by ^1H and ^{13}C NMR spectroscopy.

5.10 Reaction of $\text{W}(\text{NAr})_2\text{Cl}_2\cdot\text{DME}$ (**40**) with EtAlCl_2

$\text{W}(\text{NAr})_2\text{Cl}_2\cdot\text{DME}$ (**40**) (50 mg, 0.07 mmols) was dissolved in C_6D_6 (0.8 mL). To this solution was added EtAlCl_2 (53 mg, 0.42 mmols) and the reaction mixture was analysed immediately using ^1H NMR spectroscopy. This showed that the reaction gave multiple products unassignable by ^1H NMR spectroscopy, although ethane was detected at δ 0.79 ppm.¹² Next, ethylene (0.17 mmols) was added to this C_6D_6

solution. No reaction of ethylene occurred and no higher olefins were detected by ^1H NMR spectroscopy.

5.11 Reaction of $\text{W}(\text{NAr})_2\text{Cl}_2\cdot\text{DME}$ (40) with $\text{Et}_3\text{Al}_2\text{Cl}_3$

The procedure outlined in **Section 5.11** was repeated, but with replacement of EtAlCl_2 with $\text{Et}_3\text{Al}_2\text{Cl}_3$ (27 mg, 0.10 mmols). Ethane was again observed in the ^1H NMR spectrum presented by the reaction mixture. However, the reaction also gave multiple products unassignable by ^1H NMR spectroscopy. After addition of ethylene (0.17 mmols) to the $\text{Et}_3\text{Al}_2\text{Cl}_3$ reaction solution, the mixture was again analysed using ^1H NMR spectroscopy. It was clear from the resulting spectrum that no consumption of ethylene occurred and no higher olefins were detected.

5.12 Synthesis of $\text{EtAlCl}_2\cdot(\text{THF})_2$

A toluene solution of EtAlCl_2 (1 mL, 1.8 M in toluene, 1.8 mmols) was dissolved in excess THF (5 mL). The resulting mixture was stirred for 30 minutes, before being dried *in vacuo*. This generated $\text{EtAlCl}_2\cdot(\text{THF})_2$, which was found to be a highly air sensitive, clear and colourless liquid.

^1H (C_6D_6 , 300 MHz): δ 3.46 (8H, m, OCH_2CH_2), 1.25 (3H, CH_2CH_3 , t, $^3J_{\text{HH}} = 8.1$ Hz), 0.80 (8H, m, OCH_2CH_3), 0.25 (2H, q, $^3J_{\text{HH}} = 8.1$ CH_2CH_3).

^{13}C $\{^1\text{H}\}$ (C_6D_6 , 125.6 MHz): δ 73.76 (OCH_2CH_2), 25.65 (OCH_2CH_2), 9.17 (CH_2CH_3).

The CH_2 (ethyl) resonance was not detected.

Mass Spectroscopy (ES): $m/z = 242.8$ ($\text{Al}(\text{THF})_2\text{Cl}_2^+$).

5.13 Reaction of $\text{W}(\text{NPh})\text{Cl}_4\cdot\text{THF}$ (32) with One Equivalent of EtAlCl_2

$\text{W}(\text{NPh})\text{Cl}_4\cdot\text{THF}$ (32) (64 mg, 0.13 mmols) was dissolved in toluene (5 mL) before addition of a solution of EtAlCl_2 (0.07 mL, 1.8 M in toluene, 0.13 mmols). The resulting solution was allowed to stir for 5 minutes during which time a light brown precipitate developed. This material was collected *via* filtration and was analysed using ^1H NMR spectroscopy. This analysis detected two ^1H NMR resonances at δ 3.46 and 0.80 ppm, consistent with the formation of the adduct $\text{EtAlCl}_2\cdot(\text{THF})_2$ *in situ* (**Section 5.14**).

5.14 Reaction of W(NPh)Cl₄.THF (32) with Et₃Al₂Cl₃

W(NPh)Cl₄.THF (**32**) (30 mg, 0.06 mmols) was dissolved in C₆D₆ (0.8 mL). To this solution was added Et₃Al₂Cl₃ (38 mg, 0.15 mmols); the reaction mixture was then analysed using ¹H NMR spectroscopy. This showed that **32** reacted with Et₃Al₂Cl₃ to give multiple unassignable products as well as the by-product ethane.¹²

5.15 Reaction of W(NPh)Cl₄.THF (32) with EtAlCl₂

W(NPh)Cl₄.THF (**32**) (30 mg, 0.06 mmols) was dissolved in C₆D₆ (0.8 mL). To this solution was added EtAlCl₂ (39 mg, 0.30 mmols) and the reaction mixture was analysed using ¹H NMR spectroscopy. This confirmed the formation of ethane, as well as multiple, unassignable products. Next, to the reaction solution was added excess PMe₃ (0.06 mL, 0.61 mmols) and the solution was re-analysed using ¹H NMR spectroscopy. This confirmed the formation of but-1-ene.¹³

5.15.1 Reaction of Ta(NAr)Cl₃(TMEDA) (59) with EtAlCl₂

Ta(NAr)Cl₃(TMEDA) (**59**) (50 mg, 0.10 mmols) was dissolved in C₆D₆ (0.8 mL). To this solution was added EtAlCl₂ (55 mg, 0.43 mmols) and the mixture was analyzed using ¹H NMR spectroscopy. This confirmed the formation of ethane as well as multiple unassignable reaction products.¹²

5.16 Activation of W(NAr)Cl₄ (62) using Et₃Al₂Cl₃ and Subsequent Propylene Dimerization

W(NAr)Cl₄ (**62**) (20 mg, 0.04 mmols) was dissolved in C₆D₆ (0.8 mL). To this solution was added Et₃Al₂Cl₃ (20 mg, 0.08 mmols) and the mixture then charged into a Young's NMR tube, which was then placed under an atmosphere of propylene (0.17 mmols). After propylene addition, a spontaneous and exothermic reaction occurred. Next, the reaction solution was analysed by GC-MS. The GC-MS trace contained a peak with a retention time of 2.65 mins (m/z = 83, C₆H₁₁⁺), consistent with the formation of 2,3-dimethylbut-1-ene.¹⁴ No other alkenes were detected using GC-MS.

5.17 Activation of W(NAr)Cl₄.THF (38) using Et₃Al₂Cl₃ and EtAlCl₂ and Subsequent Ethylene Dimerization/Oligomerization

W(NAr)Cl₄.THF (**38**) (30 mg, 0.05 mmols) was dissolved in C₆D₆ (0.8 mL). To this solution was added Et₃Al₂Cl₃ (32 mg, 0.13 mmols) and the reaction mixture charged to a Young's NMR tube, which was placed under an atmosphere of ethylene (0.17 mmols). The solution was analysed by both ¹H NMR spectroscopy and GC-MS.

These analyses confirmed the formation of a range of C₄, C₅, and C₆ olefins (see **Chapter 2, Section 2.4**).

The above procedure was repeated but Et₃Al₂Cl₃ was replaced with EtAlCl₂ (53 mg, 0.40 mmols). After addition of ethylene, the reaction mixture was analysed using GC. This analysis confirmed the formation of C₄, C₆ and C₈ alkenes (see **Chapter 2, Section 2.4**).¹⁵

5.18 Dimerization of C₂D₄ and C₂H₄ (1:1) using W(NAr)Cl₄.THF (38)

W(NAr)Cl₄.THF (**38**) (30 mg, 0.05 mmols) was dissolved in C₆D₆. To this solution was added Et₃Al₂Cl₃ (32 mg, 0.25 mmols) and the reaction mixture charged into a Young's NMR tube. The reaction solution was then frozen (-78°C), allowing for the addition of first C₂H₄ (0.17 mmols) and then C₂D₄ (0.17 mmols). Next, the solution was allowed to warm to room temperature, which induced an exothermic reaction. After this reaction had ceased, the solution was sampled by GC and GC-MS (see **Chapter 2, Section 2.6** for C₄ product isotopmer distributions which were determined using Agilent ion recognition software).

5.19 Activation of W(NAr)Cl₄ (62) using EtMgCl and Subsequent Ethylene Dimerization

W(NAr)Cl₄ (**62**) (20 mg, 0.04 mmols) was dissolved in C₆D₆ (0.8 mL) and the solution then mixed with solid EtMgCl (25 mg, 0.28 mmols) and charged into a Young's NMR tube. The solution was then placed under an atmosphere of ethylene (0.15 mmols) and analysed using ¹H NMR spectroscopy. This ¹H NMR analysis indicated that full conversion of ethylene to but-1-ene had occurred in a 2 h reaction period. The formation of but-1-ene was verified by analysis of the reaction solution using GC.¹⁶

5.20 Attempts to Activate W(NAr)Cl₄ (62) for Ethylene Dimerization using MeMgCl and Mg

W(NAr)Cl₄ (**62**) (40 mg, 0.08 mmols) was dissolved in C₆D₆ (0.8 mL). To this solution was added solid MeMgCl (39 mg, 0.32 mmols) and the mixture charged into a Young's NMR tube. Next, the solution was placed under an atmosphere of ethylene (0.15 mmols) and then analysed using ¹H NMR spectroscopy. No higher olefins were detected using ¹H NMR spectroscopy.

This procedure was repeated as above, but replacing of MeMgCl with Mg turnings (8 mg, 0.33 mmols). Again, no higher olefins were formed after addition of ethylene to the reaction solution.

5.21 Activation of W(NAr)Cl₄.THF (38) with Et₃Al₂Cl₃ and Subsequent C₂D₄ Dimerization

W(NAr)Cl₄.THF (38) (30 mg, 0.05 mmols) was dissolved in C₆D₆ (0.8 mL). To this solution was added Et₃Al₂Cl₃ (33 mg, 0.13 mmols) and the mixture charged into a Young's NMR tube. The solution was then placed under an atmosphere of C₂D₄ (0.15 mmols) and allowed to react for a 1 h period. The reaction was then analysed using ¹H NMR spectroscopy; no alkene ¹H NMR resonances were detected. The initiator solution was also analysed using GC-MS, which showed that reaction of C₂D₄ had generated C₄ (~23%), C₅ (~6%) and C₆ (~67%) products, which contained exclusively deuterium atoms (verified by the mass spectrum obtained from each fraction).

The procedure outlined above was repeated, but replacing Et₃Al₂Cl₃ by EtMgCl (28 mg, 0.31 mmols). The ensuing reaction was analysed using GC-MS, which identified both C₄ (~90%) and C₆ (~10%) products. Again the mass spectrum of each fraction confirmed that alkenes containing deuterium atoms were formed exclusively in each case.

5.22 Activation of W(NAr)Cl₄.THF (38) for Propylene Dimerization

W(NAr)Cl₄.THF (38) (30 mg, 0.05 mmols) was dissolved in C₆D₆ (0.8 mL). To this solution was added EtAlCl₂ (53 mg, 0.42 mmols). The reaction was then placed under an atmosphere of propylene (0.15 mmols). This resulted in an exothermic reaction converting all of the propylene present to C₆, C₉ and C₁₂ alkenes (verified using GC).¹⁷

The procedure outlined above was repeated, but EtAlCl₂ was replaced with EtMgCl (38 mg, 0.43 mmols). No higher olefins were detected upon analysis of the EtMgCl reaction solution using ¹H NMR, even after the mixture was heated (60°C, 2 h).

5.23 Addition of Ethylene and Propylene to EtAlCl₂

EtAlCl₂ (53 mg, 0.42 mmols) was dissolved in C₆D₆. To this solution was added ethylene (0.15 mmols). The ensuing mixture was analysed using ¹H NMR

spectroscopy, which indicated no reaction had taken place. Identical results were obtained when ethylene was replaced with propylene (0.15 mmols).

5.24 Reaction of WCl_6 with Et_3N and H_2NR (R = Ph or Ar)

WCl_6 (40mg, 0.10 mmols) was dissolved in chlorobenzene (5.0 mL). To this solution was added Et_3N (41 mg, 40.1 μ L, 0.40 mmols) and then H_2NAr (42.7 μ L, 0.22 mmols). This mixture was then heated at 60°C for 1 hour. Next, the reaction solution was dried *in vacuo*, which gave a residue that was analysed using 1H NMR spectroscopy. The resulting spectra presented multiple resonances, the assignment of which has not been possible. Identical results were obtained when this procedure was repeated replacing H_2NAr for H_2NPh (18.2 μ L, 0.19 mmols).

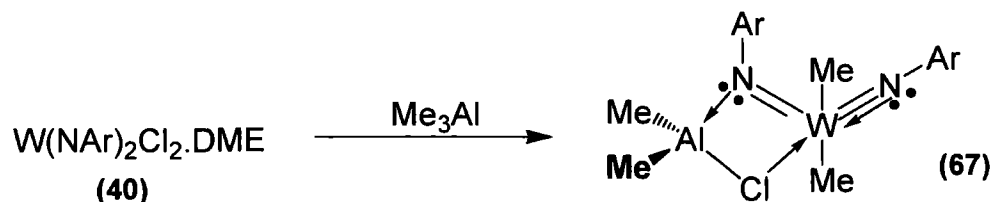
5.25 Reaction of $W(NPh)Cl_4 \cdot THF$ (32) with H_2NAr

$W(NPh)Cl_4 \cdot THF$ (32) (50 mg, 0.10 mmols) was dissolved in C_6D_6 (0.8 mL) and mixed with H_2NPh (12 mg, 0.12 mmols). This solution was analysed using 1H NMR spectroscopy, which presented multiple broad resonances, the assignment of which has not been possible.

5.26 Reaction of $W(NAr)Cl_4 \cdot THF$ (38) with Et_3N and H_2NAr

$W(NAr)Cl_4 \cdot THF$ (38) (50 mg, 0.08 mmols) was dissolved in C_6D_6 (0.8 mL) and to this solution was added first NEt_3 (17.7 mg, 0.17 mmols), and then H_2NAr (16 mg, 0.09 mmols). The reaction mixture was then analysed using 1H NMR spectroscopy, which presented multiple broad resonance, the assignment of which cannot be made.

5.27 Reaction of $W(NAr)_2Cl_2 \cdot DME$ with Me_3Al in C_6D_6 : Generation of $W(N\{Ar\}AlMe_2\{\mu-Cl\})(NAr)Me_2$ (67**) *in situ***



To a solution of $W(NAr)_2Cl_2 \cdot DME$ (**40**) (50 mg, 0.07 mmol) in C_6D_6 (0.8 mL) was added Me_3Al (64 mg, 0.88 mmol),ⁱ which resulted in an immediate color change. This solution was analyzed using multinuclear NMR spectroscopy, after which the mixture was heated (60°C, 1 h); this did not result in any additional reaction between **40** and Me_3Al . Repetition of this procedure using lower Me_3Al loadings (25 mg, 0.34 mmol) gave an identical 1H NMR spectrum.

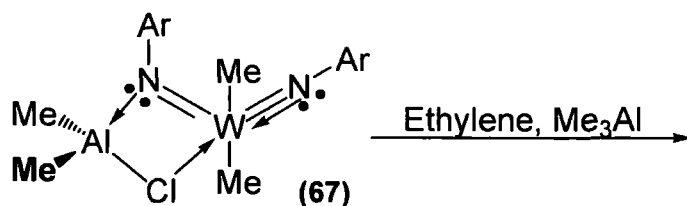
Removal of volatile components from the C_6D_6 solution *in vacuo* gave a small quantity of a tan brown solid. This material was recrystallized from the minimal amount of hexane (−5°C) to give single crystals of $W(N\{Ar\}AlMe_2\{\mu-Cl\})(NAr)Me_2$ (**67**) of sufficient quality for X-ray diffraction analysis.

1H (C_6D_6 , 200 MHz): δ 6.96 (6H, b, H_{meta} and H_{para}), 3.50 (2H, septet, CH_3CH , $^3J_{HH} = 6.8$ Hz), 2.65 (2H, septet, CH_3CH , $^3J_{HH} = 6.6$ Hz), 1.56 (6H, s, $W(CH_3)_2$), 1.17 (6H, d, CH_3CH , $^3J_{HH} = 6.8$ Hz), 1.03 (6H, d, CH_3CH , $^3J_{HH} = 6.8$ Hz), 0.89 (12H, d, CH_3CH , $^3J_{HH} = 6.6$ Hz), 0.15 (6H, s, $Al(CH_3)_2Cl$).

^{13}C $\{^1H\}$ (C_6D_6 , 125.6 MHz): δ 151.3 (C_{ipso}), 149.2 (C_{ortho}), 140.8 (C_{meta}), 124.8 (C_{para}), 71.1 (CH_3OCH_2), 61.3 (CH_3OCH_2), 50.9 ($W(CH_3)_2$), 29.4 (CH_3CH), 28.6 (CH_3CH), 26.3 (CH_3CH), 24.2 (CH_3CH), −6.80 ($Al(CH_3)_3$).

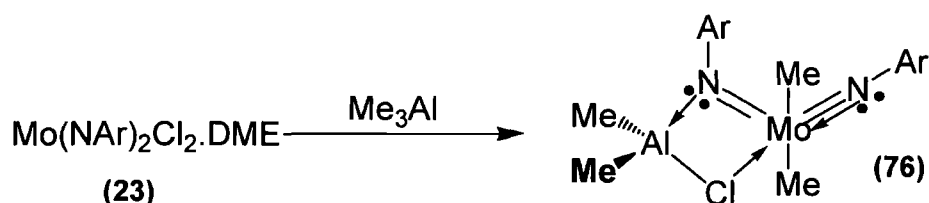
Satisfactory elemental analyses of **67** could not be obtained, despite repeated attempts, presumably due to the complex's high sensitivity to air and moisture.

ⁱ Large Me_3Al loadings were used in this procedure in order to assess if at high Me_3Al concentrations any additional reaction between $W(N\{Ar\}AlMe_2\{\mu-Cl\})(NAr)Me_2$ (**67**) and Me_3Al occurs.

5.28 Addition of Ethylene to $W(N\{Ar\}AlMe_2\{\mu\text{-Cl}\})(NAr)Me_2$ (67)

i) In a variation to the procedure for the preparation of **67**, $W(NAr)_2Cl_2 \cdot DME$ (**40**) (50 mg, 0.07 mmol) was dissolved in C_6D_6 (0.8 mL). Following addition of Me_3Al (25 mg, 0.34 mmols), 1H NMR spectroscopic analysis confirmed the formation of **67** *in situ*. The reaction mixture was then placed under an atmosphere of ethylene (0.15 mmols). The presence of ethylene in solution was confirmed by 1H NMR spectroscopy, and the sample heated ($60^\circ C$, 1 h). No reaction between ethylene and **67** was observed to occur.

ii) Reaction of $W(NAr)_2Cl_2 \cdot DME$ (**40**) (50 mg, 0.07 mmol) and Me_3Al (25 mg, 0.34 mmols) in C_6D_5Cl (0.8 mL) generated **67** *in situ*. Addition of ethylene (0.15 mmols) followed by heating ($60^\circ C$, 1 h), did not result in the occurrence of any observable interaction or reaction between **67** and ethylene (verified using 1H NMR spectroscopy).

5.29 Synthesis of $Mo(N\{Ar\}AlMe_2\{\mu\text{-Cl}\})(NAr)Me_2$ (76)

$Mo(NAr)_2Cl_2 \cdot DME$ (**23**) (1.0 g, 1.64 mmols) was dissolved in hexane (30 mL) and a solution of Me_3Al (0.80 g, 11.11 mmols) in hexane (30 mL) was added. This resulted in the immediate formation of a dark brown solution. The reaction was allowed to proceed for 16 hours, after which time the solution was filtered to remove insoluble Me_3Al/DME adducts. The resulting solution was then cooled ($-35^\circ C$), which led to the formation of a small quantity of brown precipitate (Me_3Al/DME by-product), which was again removed *via* filtration. Further concentration of the hexane solution

resulted in precipitation of **76** as a yellow solid, which was collected by filtration and recrystallized from hexane; Yield 230 mg (24%):

¹H NMR (C₆D₆, 200 MHz): δ 6.93 (6H, s, H_{meta} and H_{para}), 3.53 (2H, CH₃CH, septet ³J_{HH} = 6.8 Hz), 2.59 (2H, CH₃CH, septet ³J_{HH} = 6.6 Hz), 1.64 (6H, s, Mo(CH₃)₂), 1.17 (6H, d, CH₃CH, ³J_{HH} = 6.8 Hz), 1.02 (6H, d, CH₃CH, ³J_{HH} = 6.8 Hz), 0.87 (12H, d, CH₃CH, ³J_{HH} = 6.6 Hz), -0.09 (6H, s, Al(CH₃)₂Cl).

¹³C {¹H} NMR (C₆D₆, 125.6 MHz): δ 154.0 (C_{ipso}), 150.0 (C_{ortho}), 140.6 (C_{meta}), 125.0 (C_{para}), 124.9 (C_o), 41.5 (Mo(CH₃)₂), 30.1 (CH₃CH), 28.7 (CH₃CH), 28.7 (CH₃CH), 26.2 (CH₃CH), 24.2 (CH₃CH), - 7.0 (Al(CH₃)₃).

Anal. Calcd for C₂₈H₄₆AlClMoN₂: C; 59.10, H; 8.15, N; 4.92 Found C; 59.28, H; 8.14, N; 5.10.

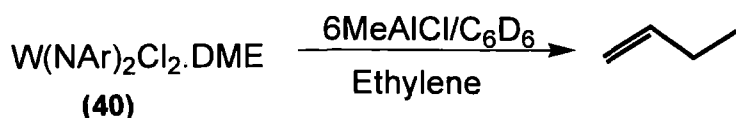
5.30 Attempted Reaction of Mo(N{Ar}AlMe₂{μ-Cl})(NAr)Me₂ (76) with Ethylene

Mo(NAr)₂Cl₂.DME (50 mg, 0.08 mmols) was dissolved in C₆D₆ (0.8 mL) and Me₃Al (40 mg, 0.55 mmols) was added giving a dark brown solution. ¹H NMR analysis was consistent with the formation of **76** *in situ*. The reaction mixture was then placed under an atmosphere of ethylene (0.15 mmols) and then heated (60°C, 1 h). No reaction of ethylene or **76** was observed to take place by ¹H NMR spectroscopy.

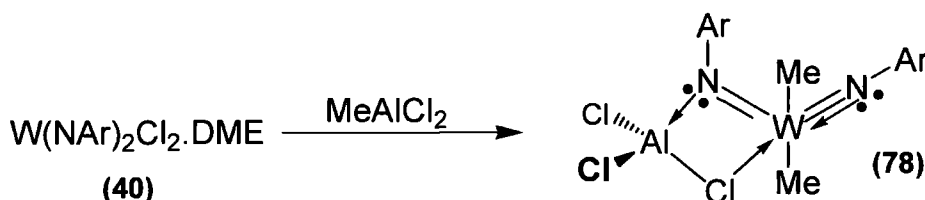
5.31 Reaction of W(NAr)₂Cl₂.DME (40) with Me₂AlCl in C₆D₆: Generation of W(N{Ar}AlMeCl{μ-Cl})(NAr)Me₂ (77) and Additional Products *in situ*

W(NAr)₂Cl₂.DME (**40**) (30 mg, 0.04 mmols) was dissolved in C₆D₆ (0.8 mL) and Me₂AlCl (31 mg, 0.33 mmols) added. ¹H NMR spectroscopic analysis indicated the formation of multiple reaction products, the identity of which could not be established. However, it has been possible to assign the ¹H NMR resonances presented by W(N{Ar}AlMeCl{μ-Cl})(NAr)Me₂ (**77**) (see below), which was present in the reaction mixture.

¹H NMR (C₆D₆, 400MHz): δ 6.95 (6H, b, H_{meta} and H_{para}), 3.58 (2H, CH₃CH, septet ³J_{HH} = 6.8 Hz), 2.59 (2H, CH₃CH, septet ³J_{HH} = 6.8 Hz), 1.60 (6H, s, W(CH₃)₂), 1.26 (6H, d, CH₃CH, ³J_{HH} = 6.4 Hz), 1.01 (6H, d, CH₃CH, ³J_{HH} = 6.8 Hz), 0.87 (12H, d, CH₃CH, ³J_{HH} = 6.8 Hz), 0.14 and 0.13 (6H, s, Al(CH₃)₂Cl).

5.32 Activation of $W(NAr)_2Cl_2 \cdot DME$ (40) by $MeAlCl_2$ for Ethylene Dimerization

Addition of ethylene (0.15 mmols) to a solution of $W(NAr)_2Cl_2 \cdot DME$ (30 mg, 0.04 mmols) and Me_2AlCl (31 mg, 0.33 mmols) resulted in ethylene dimerization, over a 1 h period at room temperature. The identity of the olefin product but-1-ene was confirmed by a COSY $^1H/^1H$ correlation experiment. After dimerization, volatile components were removed *in vacuo* and the sample reanalysed using 1H NMR spectroscopy. No information as to the connectivity of the active initiator complex could be ascertained from this NMR analysis.

5.33 Reaction of $W(NAr)_2Cl_2 \cdot DME$ (40) with $MeAlCl_2$ in C_6D_6 : Generation of $W(N\{Ar\}AlCl_2\{\mu-Cl\})(NAr)Me_2$ (78) *in situ*

$W(NAr)_2Cl_2 \cdot DME$ (40) (40 mg 0.05 mmols) was dissolved in C_6D_6 (0.8 mL). To this solution was added $MeAlCl_2$ (52 mg, 0.46 mmols) giving a light brown reaction mixture, which was then charged to a recrystallization tube. Over a 16 h period, single crystals of sufficient quality for X-ray diffraction analysis formed. These crystals were then collected, washed with hexane (3×2 mL), and allowed to dry over a 24 h period.

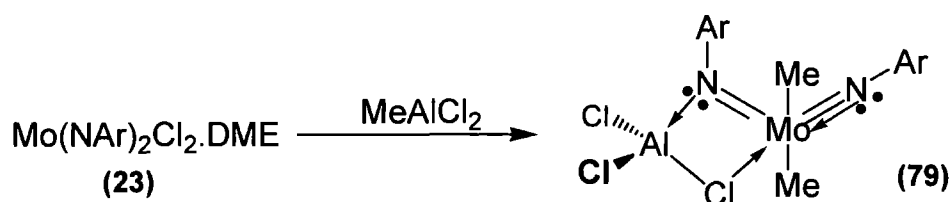
Satisfactory elemental analyses were not obtained due to the high sensitivity of complex **78** to air and moisture. To assess the thermal stability of **78**, a C_6D_6 solution of **78** was heated (1 h, 60°C); no change in the 1H NMR spectrum was observed.

1H NMR (C_6D_6 , 500 MHz): δ 6.95 (6H, b, H_{meta} and H_{para}), 3.67 (2H, septet, CH_3CH , $^3J_{HH} = 6.5$ Hz), 2.47 (2H, septet, CH_3CH , $^3J_{HH} = 6.5$ Hz), 1.57 (6H, s, $W(CH_3)_2$), 1.33 (6H, d, CH_3CH , 6.5 Hz), 0.98 (6H, d, CH_3CH , $^3J_{HH} = 6.5$ Hz), 0.83 (12H, d, CH_3CH , $^3J_{HH} = 6.5$ Hz).

^{13}C $\{^1\text{H}\}$ NMR (C_6D_6 , 125.6 Hz): δ 149.0 (C_{ipso}), 141.2 (C_{ortho}), 129.8 (C_{meta}), 125.2 and 124.8 (C_{para}), 56.8 ($\text{W}(\text{CH}_3)_2$), 29.6 and 29.2 (CH_3CH), 26.1 and 24.5 (CH_3CH).

Repetition of the above procedure, but with the use of a higher MeAlCl_2 (91 mg, 0.81 mmols) loadings, resulted in the formation of multiple complexes, assignment of which was not possible using ^1H NMR spectroscopy.

5.34 Synthesis of $\text{Mo}(\text{N}\{\text{Ar}\}\text{AlCl}_2\{\mu\text{-Cl}\})(\text{NAr})\text{Me}_2$ (**79**) from Reaction of MeAlCl_2 and $\text{Mo}(\text{NAr})_2\text{Cl}_2\cdot\text{DME}$



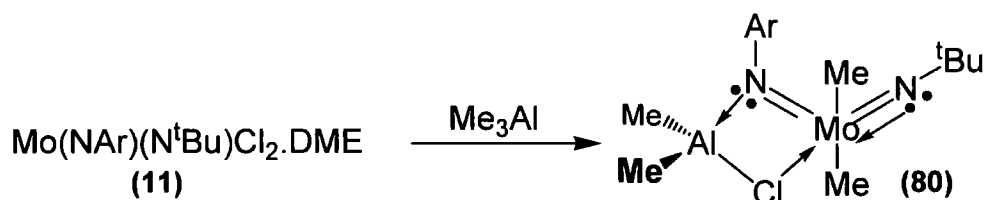
i) $\text{Mo}(\text{NAr})_2\text{Cl}_2\cdot\text{DME}$ (**23**) (400 mg, 0.65 mmols) was dissolved in a minimal amount of toluene (20 mL), before addition of a solution of MeAlCl_2 (1.9 mL, 1.0 M in hexanes, 1.90 mmols). The reaction mixture was allowed to stir (16 h) before being filtered and the volatile components removed *in vacuo*. Recrystallization from CH_2Cl_2 gave brown micro crystals of complex **79** of sufficient quality for single crystal X-ray diffraction analysis. However, ^1H NMR spectroscopy of the bulk reaction material consistently indicated the formation of multiple reaction products. Furthermore, all attempts to purify the bulk of the material by recrystallization repeatedly failed. Repetition of this procedure using a larger amount of $\text{Mo}(\text{NAr})_2\text{Cl}_2\cdot\text{DME}$ (3.0 g, 4.93 mmols) also failed to produce material of sufficient purity for full micro analysis.

ii) Addition of solid MeAlCl_2 (30 mg, 0.26 mmols) to a toluene solution (0.8 mL) of $\text{Mo}(\text{NAr})_2\text{Cl}_2\cdot\text{DME}$ (**23**) (50 mg, 0.08 mmols) resulted in an immediate color change to give a dark brown solution; this solution was then charged to a recrystallization tube. Over a 24 h period several large red crystals of **79** evolved in the tube and were collected *via* filtration and then washed with hexane (3×2 mL). Dissolution of a sample of these crystals in C_6D_6 allowed **79** to be characterized using ^1H NMR spectroscopy.

^1H NMR (C_6D_6 , 200 MHz): δ 6.90 and 6.79 (6H, aromatic), 3.70 (2H, septet, CH_3CH , $^3\text{J} = 6.8$ Hz), 2.37 (2H, septet, CH_3CH , $^3\text{J} = 6.8$ Hz), 1.67 (6H, s, $\text{Mo}(\text{CH}_3)_2$), 1.33 (6H, d, CH_3CH , $^3\text{J} = 6.8$ Hz), 0.98 (6H, d, CH_3CH , $^3\text{J} = 7$ Hz), 0.82 (12H, d, CH_3CH , $^3\text{J} = 6.6$ Hz).

Heating (1 h, 60°C) a C₆D₆ solution of complex **79** did not alter its ¹H NMR spectrum. However, complex **79** was not sufficiently stable in solution to enable characterization using ¹³C NMR spectroscopy. Attempts to obtain elemental analysis of **79** have also proven unsuccessful on repeated occasions due to the sensitivity of complex **79** to air and moisture.

5.35 Reaction of Mo(NAr)(N^tBu)Cl₂.DME (**11**) with Me₃Al: Generation of MoN{Ar}AlMe₂{μ-Cl}(N^tBu)Me₂ (**80**) *in situ*

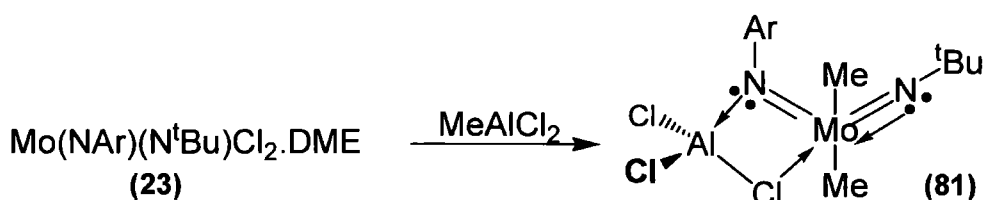


Mo(NAr)(N^tBu)Cl₂.DME (**11**) (75 mg, 0.14 mmols) was dissolved in C₆D₆ (0.8 mL) and to this solution was added Me₃Al (64 mg, 0.88 mmols). The C₆D₆ solution was then analyzed using multinuclear NMR spectroscopy.

¹H (C₆D₆, 500 MHz): δ 6.92 (3H, s, aromatic), 3.45 (2H, septet, CH₃CH, ³J_{HH} = 6.5 Hz), 3.19 (4H, s, CH₃OCH₂), 1.39 (6H, s, Mo(CH₃)₂), 1.19 (12H, b, CH₃CH), 0.84 (6H, s, Al(CH₂)₂Cl), -0.42 (45H, s, Al(CH₃)₃).

In a ¹H/¹H NOESY spectrum of the reaction solution revealed a correlation between the CH₃CH resonances and Al(CH₃)₂Cl resonances. This verifies, that in solution, the Me₂AlCl fragment of **80** coordinates at the site of the 2,6-diisopropyl phenyl imido (NAr) ligand.

¹³C {¹H} NMR (C₆D₆, 125.6 MHz): δ 156.0 (C_{ipso}), 140.4 (C_{ortho}), 127.2 (C_{meta}), 124.5 (C_{para}), 74.2 (CCH₃), 71.2 (CH₃OCH₂), 61.4 (CH₃OCH₂), 39.3 (Mo(CH₃)₂), 28.6 (C(CH₃)₃), 28.2 (CH₃CH), 25.8 (CH₃CH), 25.0 (CH₃CH), -6.74 (AlCH₃)₃ and Al(CH₃)₂Cl.

5.36 Synthesis of MoN{Ar}AlCl₂{μ-Cl}(N^tBu)Me₂ (81)

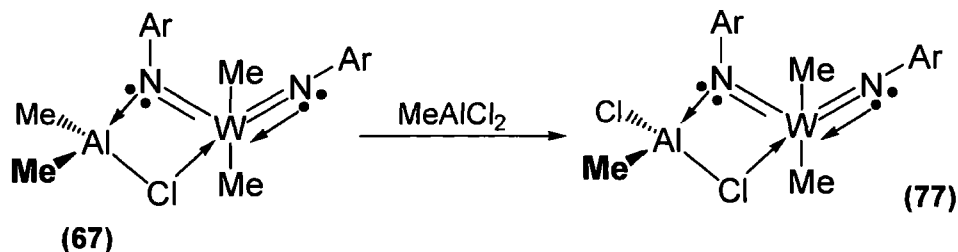
Mo(NAr)(N^tBu)Cl₂.DME (800 mg, 1.58 mmols) was dissolved in toluene (30 mL) and a hexane solution of MeAlCl₂ (4.76 mL, 1M in hexanes, 4.76 mmols) was added. The reaction was allowed to stir for 16 h, after which time the solution was filtered. Concentration of the toluene solution followed by cooling (−5°C) gave an initial crop of yellow micro crystals of complex **81** that were of sufficient quality for X-ray diffraction. After collection of the micro crystals the toluene washings were concentrated *in vacuo* resulting in further precipitation of complex **81**, which was collected *via* filtration and washed with hexane (3 × 5 mL). This material was then recrystallized from CH₂Cl₂ to give a yellow powder; Yield 330 mg (40%):

¹H NMR (C₆D₆, 500 MHz): δ 6.90 (3H, s, H_{meta} and H_{para}), 3.63 (2H, septet, CH₃CH, ³J_{HH} = 7.0 Hz), 1.38 (6H, s, Mo(CH₃)₂), 1.32 (6H, d, CH₃CH, ³J_{HH} = 7.0 Hz), 1.11 (6H, d, CH₃CH, ³J = 7.0 Hz), 0.68 (9H, s, C(CH₃)₃).

¹³C {¹H} NMR (C₆D₆, 125.6 MHz): δ 154.5 (C_{ipso}), 140.9 (C_{ortho}), 128.1 (C_{meta}), 124.9 (C_{para}), 76.3 (C(CH₃)₃), 45.1 (Mo(CH₃)₂), 28.6 (CH₃CH), 28.1 (C(CH₃)₃), 25.7 (CH₃CH), 25.3 (CH₃CH).

Anal. Calcd for C₁₈H₃₃AlCl₃MoN₂: C; 42.66, H; 6.56, N; 5.53. Found: C; 42.87, H; 6.47, N; 5.56.

5.37 Reaction of $W(NAr)AlMe_2(\mu-Cl)(N^tBu)Me_2$ (67) with $MeAlCl_2$: Generation of $W(NAr)AlMeCl(\mu-Cl)(N^tBu)Me_2$ (77) *in situ*



As in **Section 5.27**, $W(NAr)_2Cl_2 \cdot DME$ (**40**) (30 mg, 0.04 mmols) was reacted with Me_3Al (18 mg, 0.25 mmols) in C_6D_6 . Analysis by 1H NMR spectroscopy confirmed the formation of complex **67** *in situ*. The C_6D_6 solution was then transferred to a Schlenk before addition of a solution of $MeAlCl_2$ (0.14 mmols, 1 M in hexanes, 0.14 mL). After a period of 30 minutes volatile components were removed *in vacuo* giving a light brown solid. This material was analyzed using 1H NMR spectroscopy; the resulting spectrum presented signals assignable to complex **77** (**Section 5.31**). The 1H NMR spectrum also contained resonances attributable to an unknown $Me_xAlCl_{3-x} \cdot DME$ adduct, a by-product of the reaction of $W(NAr)_2Cl_2 \cdot DME$ (**40**) and Me_3Al . Further reaction of **77** with an additional portion of $MeAlCl_2$ (0.14 mmols, 1 M in hexanes, 0.14 mL) resulted in the formation of multiple reaction products, the connectivity of which cannot be established by NMR spectroscopic analysis.

5.38 Reaction of $Mo(NAr)_2(CH_2C(CH_3)_3)_2$ (82) with $MeAlCl_2$

$Mo(NAr)_2(CH_2C(CH_3)_3)_2$ (**82**) (400 mg, 0.67 mmols) was dissolved in hexane (40 mL) and $MeAlCl_2$ (1.43 mL, 1M in hexanes, 1.43 mmols) was added, resulting in the immediate formation of a small amount of precipitate. This material was separated by filtration. Concentration of the hexane solution and cooling to ($-35^\circ C$), gave a dark brown precipitate that was isolated by filtration and analysed using 1H NMR spectroscopy. The resulting spectra contained multiple, overlapping alkyl resonances, the assignment of which was not possible. Further attempts at separation and purification were unsuccessful.

5.39 Addition of Me_3Al to $Mo(NAr)_2(CH_2C(CH_3)_3)_2$ (82)

$Mo(NAr)_2(CH_2C(CH_3)_3)_2$ (**82**) (400 mg, 0.67 mmols) was dissolved in hexane (40 mL) and a solution of Me_3Al (103 mg, 1.43 mmols) in hexane (20 mL) was added. After 30 mins the mixture was filtered to remove trace precipitates. The filtrate was then concentrated, which resulted in the development of a precipitate that was analysed

using ^1H NMR spectroscopy. The resulting spectrum was consistent with that of the starting material, complex **82**.²

5.40 Attempted Reaction of $\text{Mo}(\text{NAr})_2\text{Me}_2$ (27**) with Me_3Al**

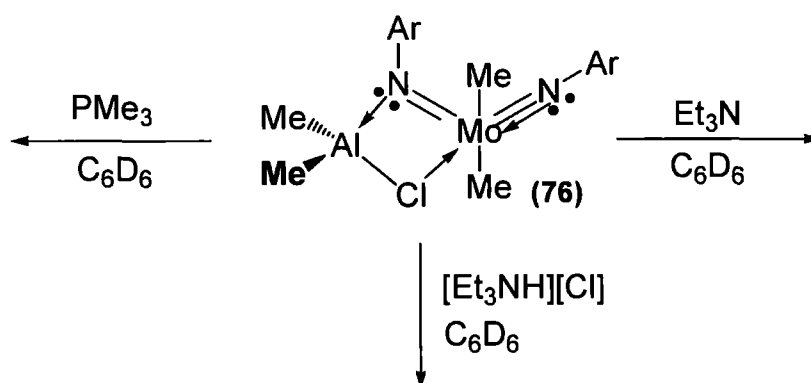
$\text{Mo}(\text{NAr})_2\text{Me}_2$ (**27**) (47 mg, 0.12 mmols) was dissolved in C_6D_6 (0.8 mL) and to this solution was added Me_3Al (14 mg, 0.19 mmols). Subsequent ^1H NMR spectroscopic analysis revealed that no reaction had occurred, with only resonances corresponding to each of the starting materials being present.

5.41 Reaction of $\text{Mo}(\text{NAr})_2\text{Me}_2$ (27**) with MeAlCl_2 : Formation of $\text{Mo}(\text{N}\{\text{Ar}\}\text{AlMeCl}\{\mu\text{-Cl}\})(\text{NAr})\text{Me}_2$ (**83**) *in situ***

$\text{Mo}(\text{NAr})_2\text{Me}_2$ (**27**) (350 mg, 0.71 mmols) was dissolved in the minimal amount of hexane before addition of MeAlCl_2 (0.73 mL, 1M in hexanes, 0.73 mmols), which immediately caused an orange precipitate to develop. This solid was collected *via* filtration and recrystallized from the minimal amount of toluene. It was shown by ^1H NMR spectroscopy that the desired product $\text{Mo}(\text{N}\{\text{Ar}\}\text{AlMeCl}\{\mu\text{-Cl}\})(\text{NAr})\text{Me}_2$ (**83**) was formed, but in conjunction with significant quantities of various impurities. Repeated attempts to remove these impurities by recrystallization proved unsuccessful.

^1H (C_6D_6 , 300 MHz): δ 6.92 (6H, b, H_{meta} and H_{para}), 3.61 (4H, septet, CH_3CH , $^3J_{\text{HH}} = 6.6$ Hz), 2.51 (4H, septet, CH_3CH , $^3J_{\text{HH}} = 6.6$ Hz), 1.69 (6H, s, $\text{Mo}(\text{CH}_3)_2$), 1.24 (6H, d, CH_3CH , $^3J_{\text{HH}} = 6.6$ Hz), 0.99 (6H, d, CH_3CH , $^3J_{\text{HH}} = 6.6$ Hz), 0.84 (12H, d, CH_3CH , $^3J_{\text{HH}} = 6.6$ Hz) -0.017 (3H, s, $\text{Al}(\text{CH}_3)\text{Cl}_2$).

5.42 Reaction of $\text{Mo}(\text{N}\{\text{Ar}\}\text{AlMe}_2\{\mu\text{-Cl}\})(\text{NAr})\text{Me}_2$ (**76**) with PMe_3 , NEt_3 , and HNEt_3Cl



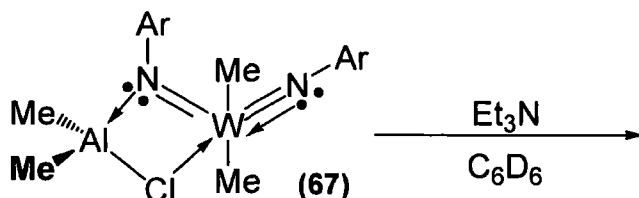
$\text{Mo}(\text{NAr})_2\text{Cl}_2 \cdot \text{DME}$ (1 g, 1.64 mmols) was dissolved in CH_2Cl_2 (40 mL) and then Me_3Al (800 mg, 11.10 mmols) diluted in CH_2Cl_2 (20 mL) was added. Next the solution was dried *in vacuo*, to give a light brown solid. Subsequent ^1H NMR spectroscopic analysis showed that this crude reaction mixture comprised a 1:1 mixture of $\text{Mo}(\text{N}\{\text{Ar}\}\text{AlMe}_2\{\mu\text{-Cl}\})(\text{NAr})\text{Me}_2$ (**76**) and a $\text{Me}_2\text{AlCl} \cdot \text{DME}$ adduct. This 1:1 mixture was then reacted with PMe_3 , NEt_3 , and HNEt_3Cl in C_6D_6 without further purification, as outlined below.

Reaction of $\text{Mo}(\text{N}\{\text{Ar}\}\text{AlMe}_2\{\mu\text{-Cl}\})(\text{NAr})\text{Me}_2$ (76**) with PMe_3 :** A crude sample of **76** (50 mg, 0.06 mmols) was dissolved in C_6D_6 and the solution degassed *via* freeze-pump-thaw, before the addition of an excess of PMe_3 (0.034 mL, 0.32 mmols) by *vac*-transfer. The subsequent ^1H and ^{31}P NMR spectra were consistent with the data previously reported for the known complex $\text{Mo}(\text{NAr})_2\text{Me}_2 \cdot \text{PMe}_3$.⁴

Reaction of $\text{Mo}(\text{N}\{\text{Ar}\}\text{AlMe}_2\{\mu\text{-Cl}\})(\text{NAr})\text{Me}_2$ (76**) with NEt_3 :** A crude sample of (**76**) (50 mg, 0.06 mmols) was dissolved in C_6D_6 . Next, to this solution was added Et_3N (13 mg, 0.12 mmols). Subsequent ^1H NMR spectroscopic analysis was consistent with the formation of the known complex $\text{Mo}(\text{NAr})_2\text{Me}_2$ *in situ*.

Reaction of $\text{Mo}(\text{N}\{\text{Ar}\}\text{AlMe}_2\{\mu\text{-Cl}\})(\text{NAr})\text{Me}_2$ (76**) with HNEt_3Cl :** A crude sample of **76** (50 mg, 0.06 mmols) was dissolved in C_6D_6 . Next, to this solution was added HNEt_3Cl (9 mg, 0.06 mmols). Ensuing ^1H NMR spectroscopic analysis indicated the formation of multiple products, assignment of which could not be made.

5.43 Reaction of $\text{W}(\text{N}\{\text{Ar}\}\text{AlMe}_2\{\mu\text{-Cl}\})(\text{NAr})\text{Me}_2$ (**67**) with NEt_3

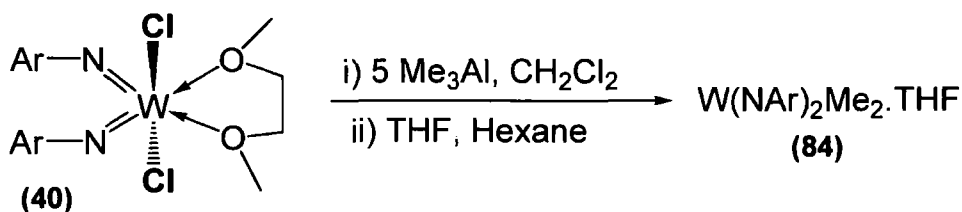


Complex **67** was formed *in situ* from reaction of $W(NAr)_2Cl_2 \cdot DME$ (**40**) (50 mg, 0.07 mmols) with Me_3Al (25 mg, 0.34 mmols) in C_6D_6 (0.8 mL). Next, the reaction mixture was dried *in vacuo*, giving a tan brown solid. This material was then redissolved in C_6D_6 (0.8 mL) containing NEt_3 (8 mg, 0.08 mmols) and the reaction re-analysed using 1H NMR spectroscopy. The resulting spectrum was consistent with the formation of a $W(NAr)_2Me_2$ fragment *in situ*. The 1H NMR spectrum also contained resonances attributable to aluminium adducts of both DME and Et_3N , formed as reaction by-products in this procedure. Only the 1H NMR data for the $W(NAr)_2Me_2$ fragment are reported:

1H (C_6D_6 , 400 MHz): δ 7.08 (6H, b, H_{para} and H_{meta}), 3.62 (4H, septet, CH_3CH , $^3J_{HH} = 6.8$ Hz), 1.24 (6H, s, $W(CH_3)_2$), 1.16 (24H, d, CH_3CH , $^3J_{HH} = 6.8$ Hz).

5.44 Reaction of $W(NAr)_2Cl_2 \cdot DME$ (40**) with $MeMgBr$**

$W(NAr)_2Cl_2 \cdot DME$ (**40**) (1.0 g, 1.44 mmols) was dissolved in diethyl ether (40 mL) and the solution then cooled ($-35^\circ C$) before the drop-wise addition of an $MeMgCl$ solution (1.05 mL, 3M in hexanes, 3.15 mmols) in diethyl ether (20 mL). After 16 h the solution was dried *in vacuo* giving a light brown precipitate, which was extracted with pentane (3×20 mL). Concentration of the pentane solution followed by cooling ($-15^\circ C$) gave a crystalline yellow solid, which was collected *via* filtration. 1H NMR spectroscopic analysis revealed the presence of multiple tungsten-containing complexes, the connectivity of which could not be ascertained.

5.45 Synthesis of $W(NAr)_2Me_2.THF$ (84**)**

$W(NAr)_2Cl_2.DME$ (**40**) (0.80 g, 1.15 mmols) was dissolved in CH_2Cl_2 (30 mL) and Me_3Al (414 mg, 5.75 mmols) dissolved in CH_2Cl_2 (10 mL) was added. The solution was allowed to stir for approximately five minutes before the volatile components were then removed *in vacuo* to give a dark brown solid, which was then re-dissolved in hexane (40 mL). To this hexane solution was added THF (0.41 mL, 5.76 mmols) and, after 5 minutes, the mixture was concentrated *in vacuo*. This resulted in the immediate formation of a yellow precipitate that was collected *via* filtration and recrystallized from diethyl ether ($-15^\circ C$), giving light brown crystals of sufficient quality for X-ray diffraction analysis; yield 200 mg (27%).

1H (C_6D_6 , 400 MHz): δ 7.07 (6H, b, H_{meta} and H_{para}), 3.62 (4H, septet, CH_3CH , $^3J_{HH} = 7.2$ Hz), 3.57 (4H, m, OCH_2CH_2), 1.39 (4H, m, OCH_2CH_2), 1.25 (6H, s, $W(CH_3)_2$, $^2J_{WH} = 7.6$ Hz), 1.17 (24H, d, CH_3CH , $^3J_{HH} = 7.2$ Hz).

^{13}C { 1H } (C_6D_6 , 175.9 MHz): δ 152.8 (C_{ipso}), 143.1 (C_{ortho}), 126.0 (C_{meta}), 123.0 (C_{para}), 68.6 (OCH_2CH_2), 48.6 ($W(CH_3)_2$), 29.3 (CH_3CH), 26.3 (OCH_2CH_2), 23.9 (CH_3CH).

Anal. Calcd for $C_{30}H_{48}N_2OW$: C; 56.60, H; 7.60, N; 4.40. Found: C; 55.80, H; 7.52 N; 4.70.

$W(NAr)_2Me_2.THF$ (**84**) has also been analysed by 1H NMR spectroscopy (C_6D_5Cl) at both room temperature ($\sim 20^\circ C$) and at $-40^\circ C$. No difference between the two 1H NMR spectra are apparent.

On subjecting a solid sample of $W(NAr)_2Me_2.THF$ (**84**) (20mg, 0.03 mmols) to vacuum for a period of 1 h, removal of the THF moiety of **84** took place (as shown by 1H NMR spectroscopy). This leads to the decomposition of **84**, again verified using 1H NMR spectroscopy. In contrast, heating a C_6D_6 solution of **84** for 1 h ($60^\circ C$) did not result in any apparent changes to the 1H NMR spectra presented by complex **84**.

5.46 Synthesis of $W(NAr)_2Me_2.PMe_3$ from reaction of $W(NAr)_2Me_2.THF$ (84) and PMe_3

A solution of $W(NAr)_2Me_2.THF$ (40 mg, 0.06 mmols) in C_6D_6 was degassed *via* freeze-pump-thaw in a Young's NMR tube, followed by the addition of PMe_3 (0.19 mmols) by vacuum transfer. After 20 min, the volatile components were removed *in vacuo*, giving a light brown solid. Dissolution of this solid in C_6D_6 (0.8 mL) enabled the product complex $W(NAr)_2Me_2.PMe_3$ to be characterized using NMR spectroscopy.

1H (C_6D_6 , 700 MHz): δ 7.12 (4H, d, H_{meta} , $^3J_{HH} = 7.7$ Hz), 7.02 (2H, t, H_{para} , $^3J_{HH} = 7.7$ Hz), 3.88 (4H, septet, CH_3CH , $^3J_{HH} = 7.7$ Hz), 1.25 (24H, d, CH_3CH , 7.7 Hz), 1.08 (6H, s, $W(CH_3)_2$, $^2J_{WH} = 5.2$ Hz), 0.93 (9H, d, $P(CH_3)_3$, $^2J_{PH} = 7.7$ Hz).

^{13}C { 1H } (C_6D_6 , 175.9 MHz): δ 154.1 (C_{ipso}), 144.2 (C_{ortho}), 125.1 (C_{meta}), 123.0 (C_{para}), 28.8 (CH_3CH), 24.4 (CH_3CH), 21.9 ($W(CH_3)_2$), 13.4 ($P(CH_3)_3$, $^1J_{WP} = 18$ Hz).

^{31}P { 1H } (C_6D_6 , 283.2 MHz): δ -25.03 ppm.

5.47 Reaction of $B(C_6F_5)_3$ with $W(NAr)_2Me_2.THF$ (84)

i) $W(NAr)_2Me_2.THF$ (84) (20 mg, 0.03 mmols) was dissolved in C_6D_6 (0.8 mL) and $B(C_6F_5)_3$ (18 mg, 0.03 mmols) added. Later 1H NMR (400 MHz, C_6D_6) analysis of the reaction solution indicated no modification of the signals assigned to the $W(NAr)_2Me_2$ fragment. However, a downfield shift of both CH_2 resonances of the THF moiety was observed (from 3.57 and 1.39 ppm to 3.21 and 0.91 ppm), suggesting the formation of the adduct $THF.B(C_6F_5)_3$.ⁱⁱ

This procedure was repeated using excess $B(C_6F_5)_3$ (54 mg, 0.10 mmols). Ensuing 1H NMR spectroscopic did not indicate any change in the resonances of the $W(NAr)_2Me_2$ fragment within a 16 h period.

ⁱⁱ To verify this a sample of $B(C_6F_5)_3$ (20mg, 0.039 mmols) was dissolved in THF (5 mL). The mixture was then dried *in vacuo* to give a solid which was then analyzed using 1H NMR spectroscopy (C_6D_6 , 400 MHz). The resulting spectrum consisted of two THF resonances at 3.20 and 0.92 ppm, consistent with the formation of a $B(C_6F_5)_3/THF$ adduct observed to form upon reaction of $W(NAr)_2Me_2.THF$ (84).

5.48 Reaction of [Ph₃C][B(C₆F₅)₄] with W(NAr)₂Me₂.THF (84)

W(NAr)₂Me₂.THF (**84**) (20 mg, 0.03 mmols) was dissolved in C₆D₆ (0.8 mL) and to this solution was added [Ph₃C][B(C₆F₅)₄] (29 mg, 0.04 mmols). ¹H NMR spectroscopy revealed that multiple products had formed, unassignable by ¹H NMR.

5.49 Addition of [PhNMe₂H][B(C₆F₅)₄] to W(NAr)₂Me₂.THF (84)

W(NAr)₂Me₂.THF (**84**) (20 mg, 0.03 mmols) was dissolved in C₆D₅Cl (0.8 mL) and [PhNMe₂H][B(C₆F₅)₄] (127 mg, 0.16 mmols) added. Later ¹H NMR spectroscopic analysis (in a sealed Young's NMR tube) indicated that no methane formation occurred. In addition, no depletion in the ¹H NMR resonances assigned to the W(NAr)₂Me₂ fragment of **84** was observable, even after heating (1 h, 60°C) the C₆D₅Cl solution.

5.50 Reaction of W(NAr)₂Cl₂.DME (40) with MAO

W(NAr)₂Cl₂.DME (**40**) (15 mg, 0.02 mmols) was dissolved in C₆D₅Cl (0.8 mL) and solid MAO (267 mg, 3.24 mmols) added. The mixture was then analysed using ¹H NMR spectroscopy, which confirmed the formation of a W(NAr)₂Me₂ fragment *in situ*. Heating (2 h, 60°C) of the reaction mixture did not result in any apparent changes to the W(NAr)₂Me₂ fragment.

¹H (C₆D₅Cl, 400 MHz): δ 7.07 (6H, b, H_{meta} and H_{para}), 3.21 (4H, b, CH₃CH, ¹J_{HH} = 6.8 Hz), 1.16 (6H, s, W-CH₃), 1.07 (24H, d, CH₃CH, ¹J_{HH} = 6.8 Hz).

5.51 Reaction of W(NAr)₂Me₂.THF (84) with Ethylene and Propylene

A solution of W(NAr)₂Me₂.THF (**84**) (20 mg, 0.03 mmols) was prepared in C₆D₆ (0.8 mL), which was then charged into a Young's NMR tube and placed under an atmosphere of ethylene (0.17 mmols). The reaction solution was immediately then analysed using ¹H NMR spectroscopy, which demonstrated methane evolution had taken place.¹⁸ After a 48 h reaction period but-1-ene (confirmed by a ¹H/¹H NMR COESY correlation) was observable in the ¹H NMR spectrum. This was verified by analysis of the volatile component of the reaction solution using GC.

The same procedure was repeated using propylene (0.17 mmols) instead of ethylene. Addition of propylene to **84** generated multiple and unassignable products (verified using ¹H NMR spectroscopy) and methane. However, re-analysis of the reaction solution after a 48 h period indicated that the excess propylene was not

consumed. Furthermore, no higher olefins were detected using ^1H NMR spectroscopy.

5.52 Reaction of $\text{Mo}(\text{NAr})_2\text{Me}_2$ (27) and $\text{Mo}(\text{NAr})_2(\text{CH}_2\text{C}(\text{CH}_3)_3)_2$ (82) with Ethylene

$\text{Mo}(\text{NAr})_2\text{Me}_2$ (**27**) (20 mg, 0.04 mmols) was dissolved in C_6D_6 (0.8 mL) and this solution charged into a Young's NMR tube. The sample was then placed under an atmosphere of ethylene (0.11 mmols) and the reaction mixture analysed by ^1H NMR spectroscopy. The resulting spectrum contained multiple, overlapping and unassignable resonances. After a 48 h period the sample was re-analyzed using ^1H NMR; no resonances assignable to higher olefins were detected.

This procedure was repeated with ethylene (0.17 mmols) added to a C_6D_6 solution of $\text{Mo}(\text{NAr})_2(\text{CH}_2\text{C}(\text{CH}_3)_3)_2$ (**82**) (20 mg, 0.03 mmols). ^1H NMR spectroscopy showed that no reaction of $\text{Mo}(\text{NAr})_2(\text{CH}_2\text{C}(\text{CH}_3)_3)_2$ (**82**) occurred.

5.53 Reaction of $\text{W}(\text{NAr})_2\text{Me}_2\cdot\text{THF}$ (84) with C_2D_4 and C_2H_4

A C_6D_6 solution of $\text{W}(\text{NAr})_2\text{Me}_2\cdot\text{THF}$ (**84**) (20 mg, 0.03 mmols) was charged to a Young's NMR tube. The solution was then frozen (liquid N_2) and to the sample was added equal quantities of C_2D_4 and then C_2H_4 (0.17 mmols). Next, the solution was warmed to room temperature and left for 48 h. At this point higher olefins were detected using ^1H NMR spectroscopy. This was verified by analysis of the volatile components of the reaction solution by GC and GC-MS, which highlighted the presence of C_4 olefin products. Ion recognition software, supplied by *Agilent Technologies* was used to identify isotopomers, C_4H_8 , $\text{C}_4\text{H}_7\text{D}$, $\text{C}_4\text{H}_6\text{D}_2$, $\text{C}_4\text{H}_5\text{D}_3$, $\text{C}_4\text{H}_4\text{D}_4$, $\text{C}_4\text{H}_3\text{D}_5$, $\text{C}_4\text{H}_2\text{D}_6$ and C_4HD_7 , the ions of which were present in the mass-spectrum of the but-1-ene fraction.

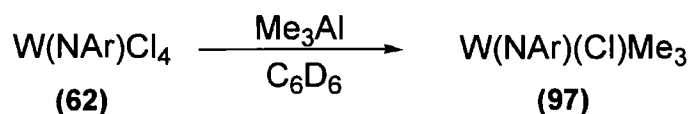
5.54 Addition of $\text{HSiMe}_2^t\text{Bu}$ to Discrete Imido Complexes

$\text{HSiMe}_2^t\text{Bu}$ (14 mg, 0.12 mmols) was mixed with a solution of $\text{W}(\text{NAr})_2\text{Cl}_2\cdot\text{DME}$ (**40**) (40mg, 0.06 mmols) in C_6D_6 . This mixture was then analyzed using ^1H NMR spectroscopy. No reaction was observed, even after heating (1 h, 60°C).

A variation of this experimental procedure was used to study the reactivity of $\text{HSiMe}_2^t\text{Bu}$ with the complexes $\text{Mo}(\text{NAr})_2\text{Cl}_2\cdot\text{DME}$ (**23**), $\text{W}(\text{NPh})\text{Cl}_4\cdot\text{THF}$ (**32**), $\text{W}(\text{NAr})\text{Cl}_4\cdot\text{THF}$ (**38**), $\text{W}(\text{NPh})(\text{Cl})_2(\text{PMe}_3)_3$ (**34**), $\text{Mo}(\text{NAr})_2(\text{NH}^t\text{Bu})_2$ (**55**), and $\text{Mo}(\text{N}^t\text{Bu})_2\text{Cl}_2\cdot\text{PPh}_3$ (**60**). In no case was reaction observed to have taken place (^1H NMR spectroscopy), even after heating (1 h, 60°C).

The procedure outlined above was repeated using CD₂Cl₂ (0.8 mL) as a reaction solvent. Later ¹H NMR spectroscopic analysis was again consistent with the formation of W(NPh)(Cl)Me₃ (**96**) in full conversion.

5.58 Reactions of W(NAr)Cl₄ (62**) and W(NAr)Cl₄.THF (**38**) with Me₃Al in C₆D₆**



W(NAr)Cl₄ (**62**) (25 mg, 0.05 mmols) was dissolved in C₆D₆ (0.8 mL) and mixed with Me₃Al (21 mg, 0.29 mmols). Analysis of the resulting solution by both ¹H and ¹³C NMR spectroscopy was consistent with full conversion of **62** to W(NAr)(Cl)Me₃ (**97**).

¹H (C₆D₆, 500 MHz): δ 7.03 (2H, d, H_{meta}, ³J_{HH} = 8.0 Hz), 6.95 (1H, t, H_{para}, ³J_{HH} = 8.0 Hz), 3.38 (2H, septet, CH₃CH, ³J_{HH} = 6.8 Hz), 1.38 (6H, s, W(CH₃)₃, ²J_{WH} = 6.4 Hz), 1.04 (12H, d, CH₃CH, ³J_{HH} = 6.8 Hz).

¹³C {¹H} (C₆D₆, 125.6 MHz): δ 150.9 (C_{ipso}), 147.6 (C_{ortho}), 123.7 (C_{para}), 57.1 (W(CH₃)₂, ¹J_{WC} = 309 Hz), 29.3 (CH₃CH), 24.8 (CH₃CH). No resonance assignable to the C_{meta} were detected.

The procedure outlined above was repeated replacing W(NAr)Cl₄ (**62**) with W(NAr)Cl₄.THF (**38**) (28 mg, 0.05 mmols). Complex **97** was again obtained in full conversion, presenting identical ¹H and ¹³C NMR chemical shifts to that reported above

5.59 Synthesis of W(NPh)(Cl)Me₃ (96**) via Reaction of Me₃Al**

W(NPh)Cl₄.THF (**38**) (260 mg, 0.53 mmols) was dissolved in CH₂Cl₂ (20 mL) and Me₃Al (80mg, 1.11 mmols) dissolved in CH₂Cl₂ (15 mL) was added. The reaction was allowed to stir for a 20 minutes and then the volatile components were removed *in vacuo*, giving a light brown solid. This material was then extracted with ether (3 x 20 mL) and the ether washings were collected and concentrated. This gave a solution that yielded, upon cooling (-5°C), golden needle-shaped crystals of complex **96** of sufficient quality for single crystal X-ray diffraction analysis; Yield 150 mg (65%).

A sample of **96** prepared by the above methodology was dissolved in C₆D₆; both the ¹H and ¹³C NMR spectroscopic data were consistent with those reported previously by Schrock *et al.*

¹H (C₆D₆, 200 MHz): δ 6.96 (5H, multiplet, H_{meta}, H_{para}, H_{ortho}), 1.28 (9H, s, W(CH₃)₃), ²J_{WH} = 7.2 Hz).

¹³C {¹H} (C₆D₆, 400 MHz): δ 156.3 (C_{ipso}), 128.5 (C_{ortho}), 126.9 (C_{meta}), 124.7 (C_{para}), 56.9 (W(CH₃)₃).

5.60 Synthesis of W(NAr)(Cl)Me₃ (97) via Reaction of Me₃Al with W(NAr)Cl₄ (62)

W(NAr)Cl₄ (**62**) (400 mg, 0.80 mmols) was dissolved in CH₂Cl₂ (30 mL) and a solution of Me₃Al (69 mg, 0.96 mmols) in CH₂Cl₂ (10 mL) added. After 15 mins the solution was filtered and the volatile components removed *in vacuo* giving W(NAr)(Cl)Me₃ (**97**), which was isolated as a red-orange solid; yield 262 mg, (75 %). The ¹H and ¹³C NMR chemical shifts presented by a sample of **97** prepared by this methodology were identical to those reported for **97** in Section 5.58.

Anal. Calcd for C₁₅H₂₆ClN₂W: C; 40.98, H; 5.96, N; 3.19. Found: C; 40.70, H; 5.80, N; 3.25.

5.61 Synthesis of Complex (97) via Reaction of W(NAr)Cl₄.THF (38) and Me₃Al

W(NAr)Cl₄.THF (**38**) (400 mg, 0.70 mmols) was dissolved in CH₂Cl₂ (20 mL) and a solution of Me₃Al (101 mg, 1.40 mmols) dissolved in CH₂Cl₂ (10 mL) added. After 15 minutes the volatile components of the reaction were removed *in vacuo*, affording a dark brown solid, which was extracted with hexane (3 x 20 mL). The hexane washings were then collected and dried *in vacuo* giving a sample of W(NAr)(Cl)Me₃ (**97**) of sufficient purity for further reaction; yield (214 mg, 70%). The ¹H and ¹³C NMR chemical shifts presented by a sample of **97** prepared by this methodology were identical to those reported for **97** in Section 5.58.

5.62 Reaction of Ta(NAr)Cl₃(TMEDA) (59) with Me₃Al

Ta(NAr)Cl₃(TMEDA) (**59**) (50mg, 0.11 mmols) was dissolved in C₆D₆ (0.8 mL) and then mixed with Me₃Al (12 mg, 0.17 mmols). Multiple, unassignable signals were observed by ¹H NMR spectroscopy; no resonance could clearly be assigned as being that of a Ta-(CH₃) moiety.

5.63 Reaction of W(NPh)(Cl)Me₃ (96) with LiMe

Complex **(96)** (50 mg, 0.14 mmols) was dissolved in C₆D₆ and then mixed with solid LiMe (8 mg, 0.36 mmols). Subsequent ¹H NMR spectroscopic analysis revealed the quantitative formation of W(NPh)Me₄ (**99**). Furthermore, complex **99** was observed to decay over a 16 h period (verified by ¹H NMR spectroscopy). However, it has been possible to assign the ¹H NMR chemical shifts of W(NPh)(Cl)Me₃ (**96**):

¹H (C₆D₆, 200 MHz): δ 7.02 (5H, b, H_{ortho}, H_{meta} and H_{para}), 1.33 (12H, s, W(CH₃)₄).

5.64 Reaction of W(NPh)(Cl)Me₃ (96) with Me₃SiOS(O)₂CF₃: Generation of W(NPh)Me₃(OSO₂(CF₃)) (100)

W(NPh)(Cl)Me₃ (**100**) (30 mg, 0.08 mmols) was dissolved in C₆D₆ and mixed with Me₃SiOS(O)₂CF₃ (30 mg, 0.13 mmols). After 4 h, the solution was analysed by ¹H and ¹³C NMR spectroscopy, which revealed complete conversion of **96** to complex **100**. The new complex **100** was characterised spectroscopically;

¹H (C₆D₆, 500 MHz): δ 6.97 (2H, t, H_{meta}, ³J_{HH} = 8.0 Hz), 6.88 (1H, t, H_{para}, ³J_{HH} = 8.0 Hz), 6.83 (2H, d, H_{ortho}, ³J_{HH} = 8.0 Hz), 1.17 (9H, s, W(CH₃)₃, ²J_{HH} = 6.8 Hz).

¹³C {¹H} (C₆D₆, 125.5 Hz): δ 129.5 (C_{ipso}), 129.4 (C_{ortho}), 127.4 (C_{para}), 57.2 (W(CH₃)₃, ¹J_{WC} = 87.8 Hz), 54.0 (CF₃).

Next, the reaction solution was placed under an atmosphere of ethylene (0.11 mmols). No reaction of **100** occurred and no higher olefins were detected using ¹H NMR spectroscopy.

5.65 Reaction of W(NPh)(Cl)Me₃ (96) with [Na][B(3,5-(CF₃)₂-C₆H₃)₄] in MeCN

W(NPh)(Cl)Me₃ (75mg, 0.21 mmols) (**96**) was dissolved in MeCN (20 mL) and [Na][B(3,5-(CF₃)₂-C₆H₃)] (188 mg, 0.21 mmols) added; the resulting mixture was stirred for 2 h. During this period a yellow precipitate developed which was collected *via* filtration and dried *in vacuo*. The insolubility of this solid in D₃CCN, CD₂Cl₂, and C₆D₅Cl precluded characterization using NMR spectroscopy.

5.66 Reaction of W(NAr)(Cl)Me₃ (97) with [Li(OEt)₂][B(C₆F₅)₄]

W(NAr)(Cl)Me₃ (**97**) (30 mg, 0.07 mmols) was dissolved in C₆D₅Cl (0.8 mL) and to this solution was added [Li(OEt)₂][B(C₆F₅)₄] (72 mg, 0.08 mmols). The reaction was then heated (16 h, 60°C) and the solution re-analyzed using ¹H NMR spectroscopy (400 MHz). The resulting spectra contained a new singlet at 1.04 ppm with ²J_{WH} satellites (²J_{WH} = 6.8 Hz) and a new doublet at 0.99 ppm (³J_{HH} = 6.8 Hz). These resonances have been assigned to the W(CH₃)₃ and ⁱPr moieties of [W(NAr)Me₃][B(C₆F₅)₄] (**102**) which was formed in 30% conversion.

¹H NMR (C₆D₅Cl, 400 MHz): δ 3.17 (2H, septet, CH₃CH, ³J_{HH} = 7.0 Hz), 1.04 (6H, s, W-CH₃), 0.99 (12H, d, CH₃CH, ³J_{HH} = 7.0 Hz).

¹³C {¹H} NMR (C₆D₅Cl, 125.5 MHz): δ 62.7 Hz (W-CH₃), 29.6 (CH₃CH), 24.5 (CH₃CH).

The ¹³C and ¹H NMR resonances of the phenyl ring of complex **102** could not be assigned, as these were obscured by the related resonances of the starting material. Similarly the ¹³C resonances of the B(C₆F₅)₄⁻ anion of **102** were also obscured.

5.67 Reaction of W(NAr)(Cl)Me₃ (97) with [Na][B(3,5-(CF₃)₂-C₆H₃)₄]

W(NAr)(Cl)Me₃ (**97**) (30 mg, 0.07 mmols) was dissolved in CD₂Cl₂ (0.8 mL) and to this solution was added [Na][B(3,5-(CF₃)₂-C₆H₃)₄] (146 mg, 0.16 mmols). After 5 h the mixture was analysed using ¹H NMR spectroscopy (400 MHz). The resulting spectra contained a new singlet at 1.86 ppm with ²J_{WH} satellites (²J_{WH} = 6.8 Hz) and a new doublet at 1.24 ppm (³J_{HH} = 6.8 Hz). These resonances have been assigned to the W(CH₃)₃ and ⁱPr moieties of [W(NAr)Me₃][B(C₆H₃-*m*-(CF₃)₂)₄] (**103**) which was formed in 30% conversion after 5 h. Heating of the reaction solution (2h, 60°C) did not induce further formation of **103**.

¹H NMR (CD₂Cl₂, 400 MHz): δ 1.89 (6H, s, W-CH₃, ²J_{WH} = 6.8 Hz), 1.24 (12H, CH₃CH, d, ³J_{HH} = 6.8 Hz). The H_{meta}, H_{para} and CH₃CH (ⁱPr) resonances of **103** were obscured by those of the starting complex **97**.

Attempts to obtain meaningful ¹³C NMR data for complex **103** failed. This was hampered by the low concentration of **103** in solution.

5.68 Reaction of W(NPh)(Cl)Me₃ (96) with [Na][B(3,5-(CF₃)₂-C₆H₃)₄]

W(NPh)(Cl)Me₃ (**96**) (20 mg, 0.05 mmols) was dissolved in C₆D₅Cl (0.8 mL) and to this solution was added [Na][B(3,5-(CF₃)₂-C₆H₃)₄] (49 mg, 0.05 mmols). The mixture was analyzed using ¹H NMR spectroscopy (400 MHz), with the resulting spectrum containing a new singlet at 1.16 ppm. This has been assigned to the W-Me moieties of the product [W(NAr)Me₃][B(3,5-(CF₃)₂-C₆H₃)₄] (**103**).^{iv} Integration of the spectrum is consistent with 40% of **96** converting to **103**. The 3:2 reaction mixture of **96** and **103** was re-analyzed after a 2 h reaction period, at which point it was apparent that **103** had decomposed.

¹H NMR (C₆D₅Cl, 400 MHz): 1.16 (6H, s, W-CH₃, ²J_{WH} = 6.8 Hz). The H_{ortho}, H_{meta} and H_{para} resonances of **103** were obscured by those of the starting complex.

5.69 Synthesis and Characterization of [W(NPh)(Cl)Me₃.AlCl₃] (104)

W(NPh)(Cl)Me₃ (**96**) (75 mg, 0.21 mmols) was dissolved in CH₂Cl₂ (10 mL) and MeAlCl₂ (1.05 mL, 1M in hexanes, 1.05 mmols) added. After 15 minutes, the volatile components were removed *in vacuo*, generating a brown residue, which was dissolved in C₆D₆ (0.8 mL). Subsequent analysis of this solution by ¹H and ¹³C NMR spectroscopy are consistent with the formation of the product [W(NPh)(Cl)Me₃.AlCl₃] (**104**).

¹H NMR (C₆D₆, 500 MHz): δ 7.03 (2H, m, H_{ortho}), 6.98 (1H, m, H_{para}), 6.84 (2H, m, H_{meta}), 1.35 (9H, s, W(CH₃)₃).

¹³C {¹H} (C₆D₆, 125.6 MHz): δ 152.9 (C_{ipso}), 131.1 (C_{ortho}), 129.7 (C_{meta}), 127.2 (C_{para}), 65.0 (W(CH₃)₃, ¹J_{WC} = 87.8 Hz).

The procedure outlined above was repeated replacing C₆D₆ with CD₂Cl₂ (0.8 mL). This has enabled the ²⁷Al and ¹H NMR spectrum of **104** to be measured in CD₂Cl₂.

²⁷Al (CD₂Cl₂, 130.2 MHz, ~ 20°C): δ 102.6, 99.5 and 93.6.

²⁷Al (CD₂Cl₂, 130.2 MHz, ~ 80°C): δ 94.3 (ν_{1/2} = 6.5 MHz).

^{iv} An identical ¹H NMR chemical shift is found for the W-(CH₃) moieties of W(NPh)Me₃(OSO₂(CF₃)) (**100**).

The ^1H NMR spectrum of **104** acquired at -80°C was consistent with that obtained at ambient temperature.

5.70 Synthesis and Characterization of $[\text{W}(\text{NAr})(\text{Cl})\text{Me}_3.\text{AlCl}_3]$ (105**)**

$\text{W}(\text{NAr})(\text{Cl})\text{Me}_3$ (**97**) (75 mg, 0.17 mmols) was dissolved in CH_2Cl_2 (10 mL) and to this solution was added MeAlCl_2 (0.85 mL, 1 M in hexanes, 0.85 mmols). After 15 minutes volatile components were removed *in vacuo* giving a dark brown residue, which was dissolved in C_6D_6 (0.8 mL). Subsequent analysis of this solution by ^1H and ^{13}C NMR spectroscopy revealed the product to be $[\text{W}(\text{NAr})(\text{Cl})\text{Me}_3.\text{AlCl}_3]$ (**105**).

^1H NMR (C_6D_6 , 500 MHz): δ 6.91 (3H, s, H_{meta} and H_{para}), 3.16 (2H, septet, CH_3CH , $^3J_{\text{HH}} = 6.5$ Hz), 1.46 (6H, s, $\text{W}(\text{CH}_3)_3$), 0.97 (12H, d, CH_3CH , $^1J_{\text{HH}} = 6.5$ Hz).

^{13}C $\{^1\text{H}\}$ NMR (C_6D_6 , 125.5 MHz): δ 150.4 (C_{ipso}), 131.1 (C_{ortho}), 124.1 (C_{para}), 67.0 ($\text{W}(\text{CH}_3)_3$), 29.6 (CH_3CH), 24.5 (CH_3CH). No resonances assignable to the C_{meta} were detected.

The procedure outlined above was repeated replacing C_6D_6 with CD_2Cl_2 (0.8 mL), enabling the ^{27}Al NMR spectrum of **105** to be determined in CD_2Cl_2 .

^{27}Al (CD_2Cl_2 , 130.2 MHz): δ 102.8, 99.9 and 93.5.

^{27}Al (CD_2Cl_2 , 130.2 MHz, -80°C): δ 95.0 ($\nu_{1/2} = 6.5$ MHz).

The ^1H NMR spectrum of **105** acquired at -80°C was consistent with that obtained at ambient temperature.

5.71 Characterization of $[\text{AlCl}_4][\text{P}(\text{N}^i\text{Pr}_2)_2]$ (107**) using ^{27}Al NMR Spectroscopy**

The known salt $[\text{AlCl}_4][\text{P}(\text{N}^i\text{Pr}_2)_2]$ (**107**) (50 mg, 0.12 mmols) was dissolved in CD_2Cl_2 (0.8 mL) and analysed by ^{27}Al NMR spectroscopy.

^{27}Al (CD_2Cl_2 , 130.2 MHz): δ 102.0 ($\nu_{1/2} = 455$ Hz)

5.72 Reaction of $\text{W}(\text{NPh})(\text{Cl})\text{Me}_3$ (96**) with MeAlCl_2 in C_6D_6**

$\text{W}(\text{NPh})(\text{Cl})\text{Me}_3$ (**96**) (20mg, 0.05 mmols) was dissolved in C_6D_6 (0.8 mL) and to this solution was added MeAlCl_2 (7 mg, 0.06 mmols). The mixture was then analyzed using ^1H NMR spectroscopy. This procedure was repeated using varying amounts of

MeAlCl₂. The amount of MeAlCl₂ used in a given reaction and the resulting Al-CH₃ ¹H NMR chemical shifts are reported in **Table 5.1**.

Table 5.1 Reaction of W(NPh)(Cl)Me₃ (**96**) with MeAlCl₂^{a,b,c}

Amount of MeAlCl ₂	δ ¹ H (ppm) Al-CH ₃
7 mg, 0.06 mmols	0.23
26 mg, 0.23 mmols	-0.05 and -0.42
51 mg, 0.45 mmols	-0.30 and -0.43
102 mg, 0.91 mmols	-0.38

a) For all solutions a single W-CH₃ ¹H NMR resonance was detected at 1.32 ppm. b) All ¹H NMR spectra were acquired using a 400 MHz instrument. c) All solutions were prepared using C₆D₆ (0.8 mL).

To establish the ¹H NMR spectrum of MeAlCl₂ in C₆D₆, MeAlCl₂ (102 mg, 0.91 mmols) was dissolved in C₆D₆ (0.8 mL). This solution presented a single ¹H NMR resonance at 0.42 ppm.

5.72.1 Reaction of W(NPh)(Cl)Me₃ (96**) with MeAlCl₂ in C₆D₆ at Low Dilutions**

W(NPh)(Cl)Me₃ (**96**) (4 mg, 0.01 mmols) was dissolved in C₆D₆ (0.8 mL) and MeAlCl₂ (6 mg, 0.05 mmols) was added. The resulting mixture was analysed using ¹H NMR spectroscopy (400 MHz), with the ensuing ¹H NMR chemical shifts consistent with only the presence of unreacted **96** and MeAlCl₂.

5.72.2 Dilution of a W(NPh)(Cl)Me₃/MeAlCl₂ Reaction Solution

W(NPh)(Cl)Me₃ (**96**) (20 mg, 0.05 mmols) was dissolved in C₆D₆ (0.8 mL) and to this solution was added MeAlCl₂ (26 mg, 0.23 mmols). The resulting mixture was analysed using ¹H NMR spectroscopy. A single W-CH₃ ¹H resonance was detected at 1.32 ppm along with two Al-Me resonances, which were detected at -0.05 and -0.42 ppm. Next, a 0.1 mL aliquot of the reaction solution was diluted in C₆D₆ (5.2 mL). A sample of this newly diluted solution was then charged to a Young's NMR tube and the mixture was again analyzed using ¹H NMR spectroscopy. The resulting spectra contained exclusively resonances assignable to **96** and free MeAlCl₂.

5.73 Catalytic Ethylene Dimerization Testing using W(NR)Cl₄.THF (R = Ph, Ar) and Me₃Al

W(NPh)Cl₄.THF (**32**) (75 mg, 0.15 mmols) was dissolved in CD₂Cl₂ (0.8 mL) and mixed with Me₃Al (55 mg, 0.76 mmols). Analysis of the reaction mixture using ¹H NMR spectroscopy was consistent with W(NPh)(Cl)Me₃ (**96**) having been formed *in situ* with full conversion. The reaction solution was then placed under an atmosphere of ethylene (0.15 mmols) and the mixture heated (60°C, 1 h) prior to analysis by ¹H NMR spectroscopy. The resulting spectra presented signals assignable to both methane and but-1-ene in a 1:1 ratio.^{13,18} Addition of a second portion of ethylene (0.15 mmols), followed by additional heating (60°C, 2 h), resulted in further but-1-ene formation.

This procedure outlined above was repeated replacing complex **38** by W(NAr)Cl₄.THF (**38**) (50 mg, 0.09 mmols). After heating, both but-1-ene and methane were observed using ¹H NMR spectroscopy in a 1:1 ratio.^{13,18} Reaction of either **32** or **38** with Me₃Al and then ethylene in C₆D₆ (0.8 mL) did not result in the production of any higher olefins.

5.73.1 Addition of Ethylene to Me₃Al

Me₃Al (55 mg, 0.76 mmols) was dissolved in CD₂Cl₂ (0.8 mL) in a Young's NMR tube and placed under an atmosphere of ethylene (0.15 mmols). The solution was heated (2 h, 60°C) and then analysed using ¹H NMR spectroscopy; no reaction between ethylene and Me₃Al was observed to have occurred.

5.73.2 Addition of Ethylene to W(NPh)(Cl)Me₃ (96**)**

W(NPh)(Cl)Me₃ (**96**) (25 mg, 0.07 mmols) was diluted in CD₂Cl₂ (0.8 mL). This solution was charged into a young's NMR tube and placed under an atmosphere of ethylene (0.15 mmols). The sample was then heated (2 h, 60°C) and then analyzed using ¹H NMR spectroscopy; no reaction between complex **96** and ethylene had occurred.

5.73.3 Analysis of Me₃Al in CD₂Cl₂

Me₃Al (55 mg, 0.76 mmols) was dissolved in CD₂Cl₂ (0.8 mL) and the solution heated (2 h, 60°C). Subsequent analysis using ¹H NMR spectroscopy showed that no reaction of Me₃Al had occurred, with a single resonance detected at 0.42 ppm, which is assignable to free Me₃Al.

5.74 Reaction of W(NAr)Cl₄.THF (38), Me₃Al and C₂D₄

W(NAr)Cl₄.THF (**38**) (30 mg, 0.05 mmols) was dissolved in CD₂Cl₂ (0.8 mL) and Me₃Al (20 mg, 0.27 mmols) was added. The mixture was then charged to a Young's NMR tube, placed under an atmosphere of C₂D₄ (0.15 mmols) and heated (2 h, 60°C). Subsequent analysis using ¹H NMR spectroscopy (500 MHz) revealed a singlet at 0.23 ppm resulting from methane formation and a triplet at 0.21 ppm, which can be assigned to CH₃D (²J_{DH} = 2.0 Hz).

The C₂D₄ reaction solution was analyzed using GC-MS. Peaks were detected with retention times of 3.62, 3.91 and 4.48. The MS of these fractions contained signals with an m/z of 62 (C₄D₇⁺). Furthermore a peak was detected at 5.49 mins, the MS of this fraction had an m/z of 79 (C₅D₉⁺). The relative GC counts of each peak indicate that the C₄ and C₅ products were produced in the molar ratio of 16:1.

5.75 Activation of W(NPh)(Cl)Me₃ (96) for Ethylene Dimerization using Me₃Al

W(NPh)(Cl)Me₃ (**96**) (20 mg, 0.05 mmols) was dissolved in CD₂Cl₂ (0.8 mL) and to this solution was added Me₃Al (17 mg, 0.24 mmols). The mixture was placed under an atmosphere of ethylene (0.15 mmols) and then heated (2 h, 60°C). Subsequent ¹H NMR spectroscopic and GC analysis of this reaction solution confirmed the formation of but-1-ene.^{13,16}

The above procedure was repeated, but CD₂Cl₂ was replaced with C₆D₆ (0.8 mL). No higher olefins were detected using ¹H NMR spectroscopy and the ethylene added was not consumed.

5.76 Activation of W(NPh)(Cl)Me₃ (96) for Ethylene Dimerization using Me₂AlCl or MeAlCl₂

W(NPh)(Cl)Me₃ (**96**) (20 mg, 0.05 mmols) was dissolved in C₆D₆ (0.8 mL) and to this solution was added MeAlCl₂ (26 mg, 0.23 mmols). The mixture was placed under an atmosphere of ethylene (0.15 mmols) and analyzed using ¹H NMR spectroscopy. This analysis indicated that complete conversion of ethylene to but-1-ene occurred over a 2 h period.¹³

The above procedure was repeated but MeAlCl₂ was replaced with Me₂AlCl (21 mg, 0.23 mmols). Again ethylene dimerization had occurred at room temperature giving but-1-ene.

5.77 Using MeAlCl₂ to activate W(NPh)Cl₄.THF (32) for Ethylene Dimerization

W(NPh)Cl₄.THF (**32**) (30 mg, 0.05 mmols) was dissolved in C₆D₆ and to this solution was added MeAlCl₂ (24 mg, 0.21 mmols). The mixture was then analyzed using ¹H NMR spectroscopy (200 MHz). A single W-CH₃ resonance was detected at 1.34 ppm consistent with the formation of [W(NPh)(Cl)Me₃.AlCl₃] (**104**). Ethylene (0.15 mmols) was added to the solution, which was converted to but-1-ene over a 2 h period.

5.78 References

- ¹ P.W. Dyer, V.C. Gibson and W. Clegg, *J. Chem. Soc., Dalton Trans.*, **1995**, 3313.
- ² H.H. Fox, K.B. Yap, J. Robbins, S. Cai and R.R. Schrock, *Inorg. Chem.*, **1992**, *31*, 2287.
- ³ R.C.B. Copley, P.W. Dyer, V.C. Gibson, J.A.K. Howard, E.L. Marshall, W. Wang and B. Whittle, *Polyhedron*, **1996**, *15*, 3001.
- ⁴ V.C. Gibson, C. Redshaw, G.L.P. Walker, J.A.K. Howard, V.J. Hoy, J.M. Cole, L.G. Kuzmina and D.S. De Silva, *J. Chem. Soc., Dalton Trans.*, **1999**, 161.
- ⁵ D.C. Bradley, M.B. Hursthouse, K.M. Abdul Malik, A.J. Nielson and R.L. Short, *J. Chem. Soc. Dalton Trans.*, **1983**, 2651.
- ⁶ R.R. Schrock, R.T. DePue, J. Feldman, K.B. Yap, D.C. Yang, W. M. Davis, L. Park, M. DiMare, M. Schofield, J.T. Anhaus, E. Walborsky, E. Evitt, C. Kruger and P. Betz, *Organometallics*, **1990**, *9*, 2262.
- ⁷ D.C. Bradley, M.B. Hursthouse, K.M. Abdul Malik, A.J. Nielson and R.L. Short, *J. Chem. Soc. Dalton Trans.*, **1983**, 2651.
- ⁸ K.S. Heinselman, V.M. Miskowski, S.J. Geib, L.C. Wang, M.D. Hopkins, *J. Am. Chem. Soc.*, **1997**, *36*, 5530.
- ⁹ A.H. Cowley, M.C. Cushner and J.S. Szobota, *J. Am. Chem. Soc.*, **1978**, *100*, 7784.
- ¹⁰ G. Schoettel, J. Kress and J.A. Osborn, *Chem. Commun.*, **1989**, 1062.
- ¹¹ H.H. Fox, K.B. Yap, J. Robbins, S. Cai and R.R. Schrock, *Inorg. Chem.*, **1992**, *31*, 2287.
- ¹² An authentic sample of ethane in C₆D₆ presented a single ¹H NMR resonance at 0.79 ppm.
- ¹³ An authentic sample of but-1-ene was analysed using ¹H NMR spectroscopy. **¹H NMR (CD₂Cl₂, 500 MHz):** δ 5.88 (1H, multiplet, CH₂CH), 5.02 (1H, d, *cis*CH₂, ³J_{HH} = 13 Hz), 4.93 (1H, doublet, *trans*CH₂, ³J_{HH} = 10Hz), 2.07 (2H, quartet,

$\text{CH}_2\text{CHCH}_2\text{CH}_3$, $^3J_{\text{HH}} = 7.0$ Hz), 1.01 (2H, t, $\text{CH}_2\text{CHCH}_2\text{CH}_3$, $^3J_{\text{HH}} = 7.0$ Hz). Similar ^1H NMR resonances were detected when but-1-ene was analyzed in C_6D_6 .

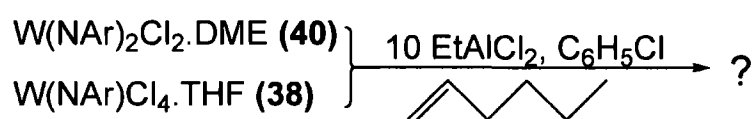
- ¹⁴ The fragmentation pattern obtained here experimentally was identical to that found for an authentic sample of 2,3-dimethyl but-1-ene.
- ¹⁵ GC analysis of a range of authentic samples of C_4 -, C_6 -, C_8 - alkenes established the retention times associated with each type of alkene. It was found that C_4 alkenes had a retention time of between 2.96 and 3.03 mins. Conversely the retention times associated with C_6 -alkenes were between 4.08 and 5.37 mins and C_8 -alkenes were detected between 10.38 and 10.33 mins. This knowledge was used to establish the product distribution obtained in the $\text{EtAlCl}_2/\text{W}(\text{NAr})\text{Cl}_4$.THF (**38**) ethylene dimerization/oligomerization system outlined in **Section 5.18**.
- ¹⁶ Identification of but-1-ene was possible using GC as a peak was detected with a retention time of 2.96 minutes. This is the same retention time found for an authentic sample of but-1-ene analyzed using the same conditions.
- ¹⁷ This assignment was enabled by the knowledge that authentic samples of hex-1-ene, Non-1-ene and Dodec-1-ene have established retention times of 5.59, 13.52 and 18.86 mins.
- ¹⁸ A ^1H NMR spectrum of an authentic sample of methane gives rise to a singlet resonance at 0.30 ppm.
- ¹⁹ S.F. Pedersen and R.R. Schrock, *J. Am. Chem. Soc.*, **1982**, *104*, 7483.

Chapter 6: Further Work

6.1 Hex-1-ene Dimerization

Notably, there has been a recent interest in using WCl_6 -based systems for the dimerization of higher olefins such as hex-1-ene.¹ As such, repeating the comparative ethylene dimerization study outlined in **Chapter 2, Section 2.2** using hex-1-ene instead of ethylene is of interest. Furthermore, the use of hex-1-ene for dimerization studies has the advantage of not requiring high pressure reaction vessels. Ideally a range of *bis* and *mono*(imido) pre-catalysts would be activated using $EtAlCl_2$ and subsequently screened (**Scheme 6.1**).

Scheme 6.1 Potential hex-1-ene dimerization investigation



The complexes $Mo(NAr)_2Cl_2 \cdot DME$ (**23**), $Mo(NAr)_2(NH^iBu)_2$ (**56**), $W(NPh)(Cl)Me_3$ (**96**) and $W(NPh)Cl_4 \cdot THF$ (**32**) could also be used as pre-catalysts, with emphasis placed on comparing the different TOF and selectivity obtained from each pre-catalyst. This would establish whether or not similar active initiator complexes were forming in each system.

6.2 Further Ethylene Dimerization Studies

In **Chapter 4, Section 4.8.2**, a range of ethylene dimerization systems were described based upon the reaction of $W(NPh)(Cl)Me_3$ (**96**) with $MeAlCl_2$, Me_2AlCl and Me_3Al . Notably, these studies were conducted at low ethylene pressures (~ 1 bar) in C_6D_6 . It would be of interest to conduct similar investigations using higher ethylene pressures (40 bars) and the same reaction conditions to those employed in the comparative ethylene dimerization system outlined in **Chapter 2, Section 2**. Furthermore, the relative capacities of $MeAlCl_2$ or $EtAlCl_2$ to activate complex **96** for ethylene dimerization could be examined. This could provide further clarification as to the role of β -hydride elimination reactions in initiator formation.

6.3 Potential DFT Calculations

6.3.1 Examining the Reaction of $M(\text{NAr})_2\text{Me}_2$ ($M = \text{Mo}$ or W) Complexes With Ethylene

This thesis has revealed a number of cases in which theoretical studies could enhance understanding of a given reaction pathway. For instance, it is unclear as to why reaction of $\text{W}(\text{NAr})_2\text{Me}_2\cdot\text{THF}$ (**84**) with ethylene results in but-1-ene formation, while reaction of $\text{Mo}(\text{NAr})_2\text{Me}_2$ (**27**) using similar procedures does not. This discrepancy could potentially be rationalized by a DFT investigation. Of particular interest is determining the relative capacity of ethylene to coordinate to a $M(\text{NAr})_2\text{Me}_2$ ($M = \text{Mo}$ or W) fragment. Also of curiosity would be the relative energy penalties associated with ethylene inserting into the $M\text{-Me}$ ($M = \text{W}$ or Mo) bonds. It is hoped that quantifying these key parameters could give an indication as to the relative favourability of initiator formation in each system.

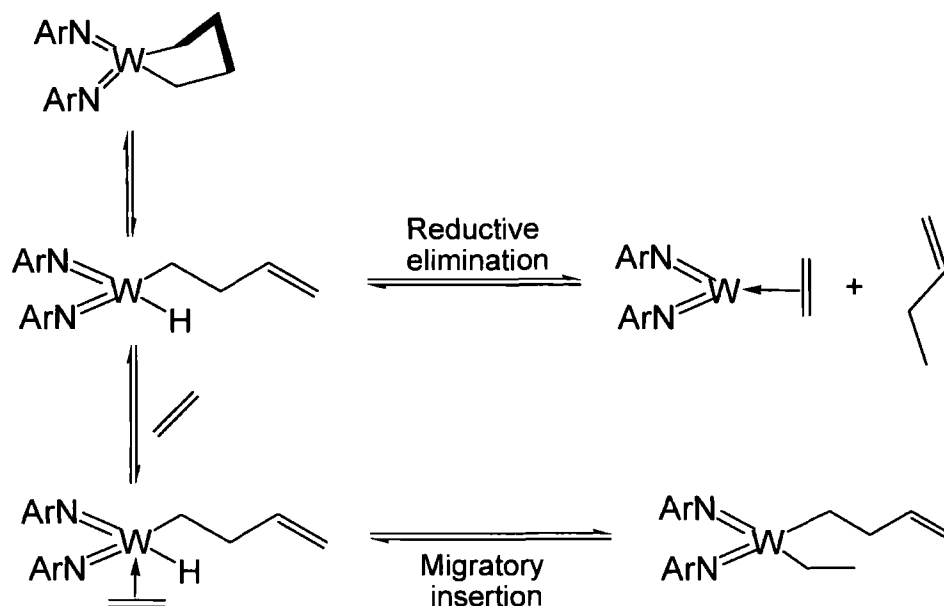
6.3.2 Examining the $\text{W}(\text{NAr})_2\text{Me}_2\cdot\text{THF}$ (84**) $\text{C}_2\text{D}_4/\text{C}_2\text{H}_4$ Reaction**

Another situation in which DFT calculations could be helpful lies in the reaction of $\text{W}(\text{NAr})_2\text{Me}_2\cdot\text{THF}$ (**84**) with C_2D_4 and C_2H_4 (**Chapter 3, Section 3.10**). Following reaction of complex **84**, olefins containing odd numbers of deuterium atoms, such as $\text{C}_4\text{H}_7\text{D}$ were produced. Such products can only result from transfer of a deuterium atom to a molecule of C_2H_4 or C_4H_8 via insertion of the alkene into the W-D bond. As W-D or W-H intermediates could be present in either a hydride or an metallacycle mechanism, disappointingly this reaction could not be used to draw firm conclusions regarding the mechanism of the $\text{W}(\text{NAr})_2\text{Me}_2\cdot\text{THF}$ (**84**) ethylene dimerization system.

Of interest would be assessing the viability of an ethylene moiety inserting into the W-H bond of an intermediate originating from a tungsten metallacycle, using a theoretical approach. It may be that such a species preferentially undergoes rapid reductive elimination, to give but-1-ene (**Scheme 6.2**). If this was indeed the case, then a metallacycle mechanism would not be compatible with the formation of products such as $\text{C}_4\text{H}_7\text{D}$, as the hydride moiety would not be “available” for ethylene insertion. Alternatively, the hydride intermediate may be sufficiently stable to allow insertion of ethylene into the W-H bond (**Scheme 6.2**). If such insertions were possible, then a metallacycle mechanism would be compatible with the observed transfer of W-D or W-H atoms in the $\text{C}_2\text{D}_4/\text{C}_2\text{H}_4$ reaction. Thus, calculating the kinetic and thermodynamic parameters associated with the migratory insertion and/or reductive elimination pathways outlined in **Scheme 6.2**, could allow assessment as

to the viability of a metallacycle mechanism operating in the $W(NAr)_2Me_2 \cdot THF$ (**84**) ethylene dimerization system.

Scheme 6.2 Possible reactions of a tungsten hydride species with ethylene



6.3.3 Examining the Solution Structure of $[W(NR)(Cl)Me_3 \cdot AlCl_3]$ $R = Ph$ or Ar

Adducts

In Chapter 4, Section 4.7 the adducts $[W(NPh)(Cl)Me_3 \cdot AlCl_3]$ (**104**) and $[W(NAr)(Cl)Me_3 \cdot AlCl_3]$ (**105**) were characterized using ^{27}Al NMR spectroscopy. This strongly indicated that both **105** and **104** partly dissociated in solution to give an $AlCl_4^-$ anion. Of interest would be to use theoretical calculations to determine the thermodynamic parameters associated with this dissociation. This would provide further clarification as to the stability of a $[W(NPh)Me_3]^+$ cation. This is of particular interest as it is believed that coordination of ethylene to a $[W(NPh)Me_3]^+$ fragment is the prerequisite step for the formation of the active initiator complexes in the $W(NPh)(Cl)Me_3/Me_xAlCl_{3-x}$ ethylene dimerization systems outlined in Chapter 4, Section 4.8.2.

6.4 References

- ¹ World patent 2005/089940 to Sasol Technology (UK) Ltd (2005), M.J. Hanton and R.P. Tooze.

Appendix 1 – Crystallographic data

All collections were conducted using graphite-monochromated Mo-K α radiation ($\lambda = 0.71073 \text{ \AA}$) on a Bruker Smart 1K or a 6K CCD area diffractometer at 120K. Cell parameters were determined and refined using SMART¹ software and raw frame data were integrated using SAINT² programs. Structures were refined using SHELXL-97.³

Parameters from X-Ray Diffraction Experiments

Complex	Mo(NAr) ₂ (NH ^t Bu) ₂ (55)	W(NAr) ₂ Cl ₂ .DME (40)
Empirical formula	C ₃₂ H ₅₄ MoN ₄	C ₅₆ H ₈₈ N ₄ W ₂ Cl ₄ O ₄
Formula weight	590.73	695.40
Temperature/K	120(2)	120(2)
Crystal system	Orthorhombic	Triclinic
Space group	Pbca	P-1
a/ \AA	10.463(1)	10.5913(14)
b/ \AA	19.225(2)	16.009(2)
c/ \AA	33.429(3)	18.714(3)
$\alpha/^\circ$	90.00	80.84(3)
$\beta/^\circ$	90.00	87.75(3)
$\gamma/^\circ$	90.00	76.79(2)
Volume/ \AA^3	6724(1)	3049.5(7)
Z	8	4
ρ_{calc} mg/mm ³	1.167	1.515
m/mm ⁻¹	0.414	3.989
F(000)	2528	1400
Crystal size	0.22 × 0.22 × 0.10	0.35 × 0.30 × 0.20
Theta range for data collection	2.44 to 28.99°	1.59 to 30.00°
Index ranges	-14 ≤ h ≤ 14, -26 ≤ k ≤ 26, -45 ≤ l ≤ 45	-14 ≤ h ≤ 14 -22 ≤ k ≤ 22 -26 ≤ l ≤ 26
Reflections collected	71726	43557
Independent reflections	8928 [R(int) = 0.0469]	17064 [R(int) = 0.0235]
Data/restraints/parameters	8928/0/370	17064/0/671
Goodness-of-fit on F ²	0.978	1.056
Final R indexes [$ I > 2\sigma(I)$]	R ₁ = 0.0334, wR ₂ = 0.0750	R ₁ = 0.0197 wR ₂ = 0.0432
Final R indexes [all data]	R ₁ = 0.0502, wR ₂ = 0.0790	R ₁ = 0.0266 wR ₂ = 0.0460
Largest diff. peak/hole	0.456/-0.768	0.990/-0.478

¹ SMART – NT, Data Collection Software, version 6.1. Bruker Analytical X-ray Instruments Inc, Madison, WI, USA, 2000.

² SAINT – NT, Data Collection Software, version 6.1. Bruker Analytical X-ray Instruments Inc, Madison, WI, USA, 2000.

³ SHELX – G.M. Sheldrick, *Acta Cryst.*, 2008, A64, 112.

Complex	W(N{Ar}.AlMe ₂ {μ-Cl})(NAr)Me ₂ (67)	W(N{Ar}.AlCl ₂ {μ-Cl})(NAr)Me ₂ (78)
Empirical formula	C ₂₈ H ₄₆ N ₂ WClAl	C ₄₄ H ₄₀ D ₁₈ N ₂ WAlCl ₃
Formula weight	656.95	866.07
Temperature	120(2)	120(2)
Crystal system	Monoclinic	Triclinic
Space group	P2 ₁ /n	P-1
a/Å	11.691(2)	11.534(1)
b/Å	17.983(3)	11.695(1)
c/Å	14.342(2)	15.474(2)
α/°	90.00	93.87(1)
β/°	92.64(1)	92.80(1)
γ/°	90.00	109.58(1)
Volume/Å ³	3012.1(8)	1956.4(3)
Z	4	2
ρ _{calc} /mg/mm ³	1.449	1.470
m/mm ⁻¹	3.970	3.207
F(000)	1328	864
Crystal size	0.34 × 0.26 × 0.11	0.32 × 0.23 × 0.10
Theta range for data collection	1.82 to 29.06°	1.32 to 30.00°
Index ranges	-15 ≤ h ≤ 15 -24 ≤ k ≤ 23 -19 ≤ l ≤ 18	-16 ≤ h ≤ 16 -16 ≤ k ≤ 16 -21 ≤ l ≤ 21
Reflections collected	35373	27232
Independent reflections	8025 [R(int) = 0.0282]	11397 [R(int) = 0.0462]
Data/restraints/parameters	8025/0/362	11397/28/432
Goodness-of-fit on F ²	1.055	1.030
Final R indexes [I > 2σ(I)]	R ₁ = 0.0176 wR ₂ = 0.0363	R ₁ = 0.0196 wR ₂ = 0.0451
Final R indexes [all data]	R ₁ = 0.0228 wR ₂ = 0.0380	R ₁ = 0.0232 wR ₂ = 0.0461
Largest diff. peak/hole	0.934/-0.464	1.455/-0.568

Complex	Mo(N{Ar}.AlCl ₂ {μ-Cl})(NAr)Me ₂ (79)	Mo(N{Ar}AlMe ₂ {μ-Cl})(N ^t Bu)Me ₂ (81)
Empirical formula	C ₁₀₈ H ₁₆₅ N ₈ Mo ₄ Cl ₂₀ Al ₄	C ₁₈ H ₃₂ N ₂ MoCl ₃ Al
Formula weight	652.33	505.73
Temperature	120(2)	125(2)
Crystal system	Monoclinic	Monoclinic
Space group	P2 ₁ /n	P2 ₁ /c
a/Å	16.424(2)	9.046(1)
b/Å	19.713(2)	16.3938(18)
c/Å	39.485(4)	16.6047(19)
α/°	90.00	90.00
β/°	97.22(1)	101.757(10)
γ/°	90.00	90.00
Volume/Å ³	12683(2)	2410.8(5)
Z	16	4
ρ _{calc} /mg/mm ³	1.367	1.393
m/mm ⁻¹	0.796	0.917
F(000)	5392	1040
Crystal size	0.14 × 0.08 × 0.06	0.30 × 0.26 × 0.11
Theta range for data collection	1.04 to 25.01°	1.76 to 29.00°
	-18 ≤ h ≤ 19	-12 ≤ h ≤ 12
Index ranges	-16 ≤ k ≤ 23	-22 ≤ k ≤ 22
	-46 ≤ l ≤ 44	-22 ≤ l ≤ 22
Reflections collected	68336	28594
Independent reflections	22279[R(int) = 0.1405]	6418 [R(int) = 0.0351]
Data/restraints/parameters	22279/0/1255	6418/0/244
Goodness-of-fit on F ²	0.977	0.848
Final R indexes [I > 2σ(I)]	R ₁ = 0.0697 wR ₂ = 0.1056	R ₁ = 0.0245 wR ₂ = 0.0612
Final R indexes [all data]	R ₁ = 0.1634 wR ₂ = 0.1313	R ₁ = 0.0337 wR ₂ = 0.0662
Largest diff. peak/hole	0.733/-0.679	0.381/-0.340

Complex	W(NAr) ₂ Me ₂ .THF (84)	W(NPh)(Cl)Me ₃ (96)
Empirical formula	C ₉₀ H ₁₄₄ N ₆ W ₃ O ₃	C ₈ H ₁₀ NWCl
Formula weight	636.55	355.51
Temperature	120(2)	120(2)
Crystal system	Monoclinic	Monoclinic
Space group	P2 ₁ /c	P2 ₁ /m
a/Å	19.506(2)	6.3483(10)
b/Å	16.994(2)	7.2804(11)
c/Å	26.404(3)	11.9671(18)
α/°	90.00	90.00
β/°	95.20(2)	93.604(10)
γ/°	90.00	90.00
Volume/Å ³	8716.4(18)	552.00(15)
Z	12	2
ρ _{calc} /mg/mm ³	1.455	2.139
m/mm ⁻¹	3.999	10.656
F(000)	3888	332
Crystal size	0.26 × 0.23 × 0.15	0.28 × 0.27 × 0.14
Theta range for data collection	1.05 to 30.03°	1.71 to 29.01°
Index ranges	-27 ≤ h ≤ 27 -23 ≤ k ≤ 23 -36 ≤ l ≤ 37	-8 ≤ h ≤ 8 -9 ≤ k ≤ 9 -16 ≤ l ≤ 16
Reflections collected	121256	6499
Independent reflections	25037 [R(int) = 0.0456]	1561 [R(int) = 0.0236]
Data/restraints/parameters	25037/0/979	1561/0/87
Goodness-of-fit on F ²	1.113	1.232
Final R indexes [I > 2σ (I)]	R ₁ = 0.0447 wR ₂ = 0.1032	R ₁ = 0.0141 wR ₂ = 0.0339
Final R indexes [all data]	R ₁ = 0.0721 wR ₂ = 0.1189	R ₁ = 0.0145 wR ₂ = 0.0341
Largest diff. peak/hole	3.876/-3.908	0.739/-0.883

Appendix 2 – Postgraduate First Year Modules

All first year postgraduates are required to pass a compulsory module in their first year.

Functional Materials – 56% (pass).

Appendix 3 – Chemistry Colloquia Attended at Durham University Chemistry

Prof. RH Grubbs, Caltech, Tuesday 20 June 2006.

"The Design and Synthesis of new Selective Olefin Metathesis Catalysts"

Dr. Simon Aldridge, Dept of Chem, Cardiff University, Monday 17 July 2006.

"Transition Metal - Group 13 Element Multiple Bonds"

Dr Patrick Toy, University of Hong Kong, Monday 4 September 2006.

"Multipolymer Reactions and Organocatalytic Mitsunobu Reactions"

Prof. Odile Eisenstein, University of Montpellier, Wednesday 15 November 2006. "Simple Ideas for d(0) Olefin Metathesis Catalyst Design from a DFT Perspective"

Dr Michael Whittlesey, Department of Chemistry, University of Bath, Wednesday 14 February 2007. "N-Heterocyclic Carbenes: Far From Inert Ligands"

Prof. Keith Pannell, University of Texas at El Paso, USA, Tuesday 24 April 2007. "Recent Advances in the Transition Metal Organometallic Chemistry of Tin, Germanium and Silicon"

Prof. Guy Bertrand, Joint Research Laboratory, University of California, Riverside, USA, Wednesday 30 May 2007. "New Families of Stable Cyclic Carbenes for the Preparation of Low Ligated Transition Metals, and Highly Active Catalysts. Can a Carbene do the Job of a Metal?"

Ian Manners, School of Chemistry, University of Bristol, Wednesday 30 May 2007. "Functional Metallized Supramolecular Materials *via* Block Copolymer Self-assembly and Living Supramolecular Polymerisations"

Prof. CNR Rao, Friday 22 June 2007. "Materials at the Liquid-liquid Interface"

Prof. Régis Réau, Université de Rennes 1, France, Friday 3 August 2007.
"Organophosphorus pi-Conjugated Systems: From Model Molecules to Functional Materials"

Prof. Malcolm Chisholm, Ohio State University, USA, Wednesday 31 October 2007. "Linking MM Quadruple Bonds (M = Mo or W) with Organic p-Systems: Studies of Mixed Valency and M2d-p Conjugation"

Dr. Richard Layfield, University of Manchester, Wednesday 14 November 2007.
"Organometallic Chemistry with Manganese(II): a Transition Metal Masquerading as a Main Group Element"

Prof. Kalman Szabo, Stockholm University, Sweden, Wednesday 5 December 2007. "One-Pot Transformations Involving Catalytic Generation of Allyl Boronates"

Prof. T. Don Tilley, University of California, Berkeley, USA, Friday 9 May 2008.
"New Bond Activations at Transition Metal Centres: Fundamental Studies and Applications to Catalysis"

Prof. Penny Brothers, University of Auckland, New Zealand, Friday 9 May 2008.
"Diboron Porphyrins and Corroles: Unexpected Chemistry for Both Boron and the Ligands"

Prof. Christian Amatore, Ecole Normale Supérieure, France, Friday 20 June 2008. "Neurotransmission and Auto Regulation of Blood Delivery in the Brain."

Appendix 4 – External Inorganic Conferences Attended and Presentations

Given

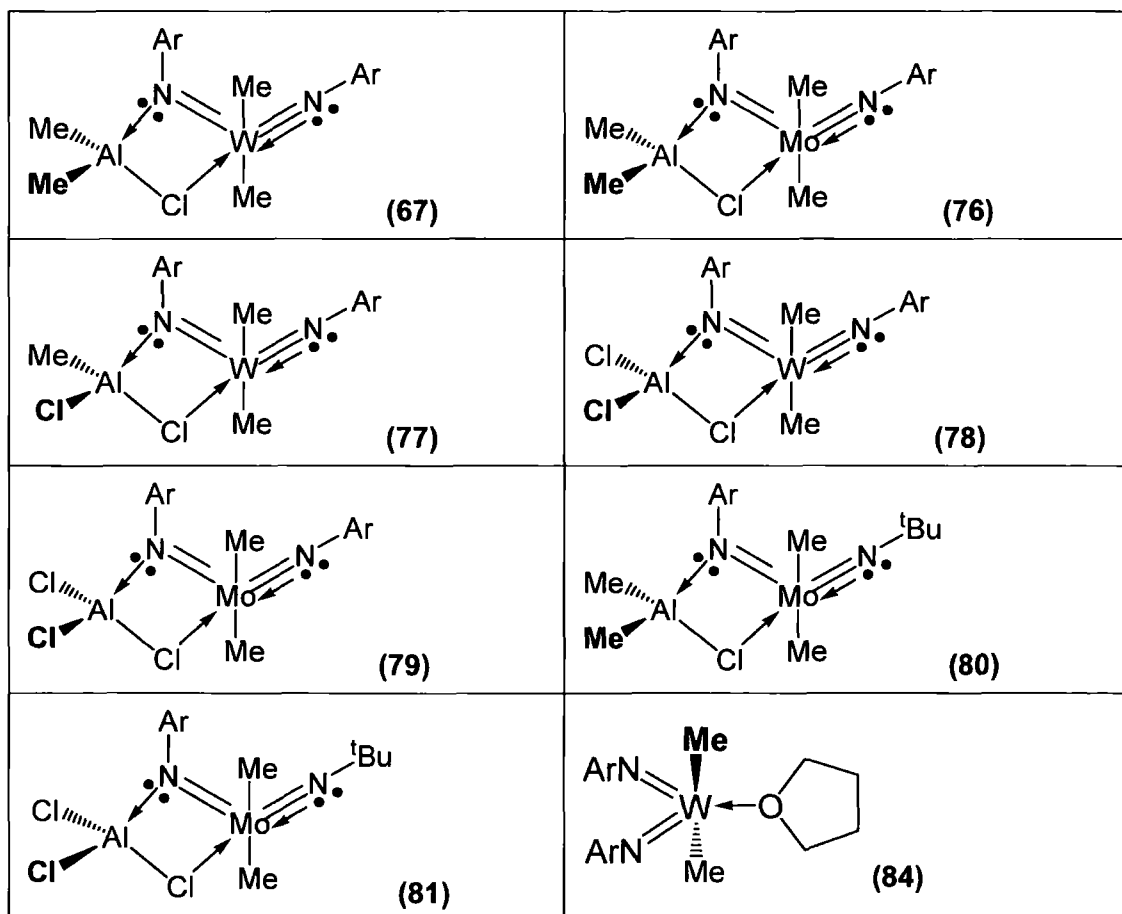
- *September 2007* – Catalysis Summer School, Liverpool University, poster presentation.
- *May 2008* – Postgraduate Symposium, University of Durham, oral presentation (25 minutes).
- *July 2008* - Final Year Postgraduate Symposium on "Catalysis enabled synthetic methodology for pharmaceuticals and fine chemicals," oral presentation (20 minutes).
- *July 2008* – International Conference on Organometallic Chemistry, poster presentation.
- *September 2008* - Universities of Scotland Inorganic Chemistry Conference, oral presentation (20 minutes)

Appendix 5 – Numbering Scheme for Key Complexes Referred to in the Text

Key pre-cursor complexes

Mo(NAr)(N ^t Bu)Cl ₂ .DME (11)	Mo(NAr) ₂ Cl ₂ .DME (23)
Mo(N ^t Bu) ₂ Cl ₂ .DME (26)	Mo(NAr) ₂ Me ₂ (27)
W(NPh)Cl ₄ .THF (32)	W(NPh)(Cl) ₂ (PMe ₃) ₃ (34)
W(NAr)Cl ₄ .THF (38)	W(NAr) ₂ Cl ₂ .DME (40)

Synthesised bis(imido) complexes



Synthesised *mono(imido)* complexes

$W(NPh)(Cl)Me_3$ (96)	$W(NAr)(Cl)Me_3$ (97)
$[W(NAr)Me_3][B(3,5-(CF_3)_2C_6H_3)_4]$ (101)	$[W(NAr)Me_3][B(C_6F_5)_4]$ (102)
$[W(NPh)(Cl)Me_3 \cdot AlCl_3]$ (104)	$[W(NAr)(Cl)Me_3 \cdot AlCl_3]$ (105)
$[W(NPh)(Cl)Me_3 \cdot AlMeCl_2]$ (106)	

